

Innovations and new technology in spine surgery

Edited by

G. Bryan Cornwall, William Robert Walsh
and Ralph Jasper Mobbs

Published in

Frontiers in Surgery



FRONTIERS EBOOK COPYRIGHT STATEMENT

The copyright in the text of individual articles in this ebook is the property of their respective authors or their respective institutions or funders. The copyright in graphics and images within each article may be subject to copyright of other parties. In both cases this is subject to a license granted to Frontiers.

The compilation of articles constituting this ebook is the property of Frontiers.

Each article within this ebook, and the ebook itself, are published under the most recent version of the Creative Commons CC-BY licence. The version current at the date of publication of this ebook is CC-BY 4.0. If the CC-BY licence is updated, the licence granted by Frontiers is automatically updated to the new version.

When exercising any right under the CC-BY licence, Frontiers must be attributed as the original publisher of the article or ebook, as applicable.

Authors have the responsibility of ensuring that any graphics or other materials which are the property of others may be included in the CC-BY licence, but this should be checked before relying on the CC-BY licence to reproduce those materials. Any copyright notices relating to those materials must be complied with.

Copyright and source acknowledgement notices may not be removed and must be displayed in any copy, derivative work or partial copy which includes the elements in question.

All copyright, and all rights therein, are protected by national and international copyright laws. The above represents a summary only. For further information please read Frontiers' Conditions for Website Use and Copyright Statement, and the applicable CC-BY licence.

ISSN 1664-8714
ISBN 978-2-8325-3857-9
DOI 10.3389/978-2-8325-3857-9

About Frontiers

Frontiers is more than just an open access publisher of scholarly articles: it is a pioneering approach to the world of academia, radically improving the way scholarly research is managed. The grand vision of Frontiers is a world where all people have an equal opportunity to seek, share and generate knowledge. Frontiers provides immediate and permanent online open access to all its publications, but this alone is not enough to realize our grand goals.

Frontiers journal series

The Frontiers journal series is a multi-tier and interdisciplinary set of open-access, online journals, promising a paradigm shift from the current review, selection and dissemination processes in academic publishing. All Frontiers journals are driven by researchers for researchers; therefore, they constitute a service to the scholarly community. At the same time, the *Frontiers journal series* operates on a revolutionary invention, the tiered publishing system, initially addressing specific communities of scholars, and gradually climbing up to broader public understanding, thus serving the interests of the lay society, too.

Dedication to quality

Each Frontiers article is a landmark of the highest quality, thanks to genuinely collaborative interactions between authors and review editors, who include some of the world's best academicians. Research must be certified by peers before entering a stream of knowledge that may eventually reach the public - and shape society; therefore, Frontiers only applies the most rigorous and unbiased reviews. Frontiers revolutionizes research publishing by freely delivering the most outstanding research, evaluated with no bias from both the academic and social point of view. By applying the most advanced information technologies, Frontiers is catapulting scholarly publishing into a new generation.

What are Frontiers Research Topics?

Frontiers Research Topics are very popular trademarks of the *Frontiers journals series*: they are collections of at least ten articles, all centered on a particular subject. With their unique mix of varied contributions from Original Research to Review Articles, Frontiers Research Topics unify the most influential researchers, the latest key findings and historical advances in a hot research area.

Find out more on how to host your own Frontiers Research Topic or contribute to one as an author by contacting the Frontiers editorial office: frontiersin.org/about/contact

Innovations and new technology in spine surgery

Topic editors

G. Bryan Cornwall — University of San Diego, United States

William Robert Walsh — University of New South Wales, Australia

Ralph Jasper Mobbs — University of New South Wales, Australia

Citation

Cornwall, G. B., Walsh, W. R., Mobbs, R. J., eds. (2023). *Innovations and new technology in spine surgery*. Lausanne: Frontiers Media SA.

doi: 10.3389/978-2-8325-3857-9

Table of contents

- 05 ***In-vivo* Performance of Seven Commercially Available Demineralized Bone Matrix Fiber and Putty Products in a Rat Posterolateral Fusion Model**
Nicholas Russell, William R. Walsh, Vedran Lovric, Peter Kim, Jennifer H. Chen, Michael J. Larson and Frank Vizesi
- 16 **The Role of Machine Learning in Spine Surgery: The Future Is Now**
Michael Chang, Jose A. Canseco, Kristen J. Nicholson, Neil Patel and Alexander R. Vaccaro
- 31 **mHealth Apps for Enhanced Management of Spinal Surgery Patients: A Review**
Michael Y. Bai, Ralph J. Mobbs, William R. Walsh and Callum Betteridge
- 36 **Innovative Technology System to Prevent Wrong Site Surgery and Capture Near Misses: A Multi-Center Review of 487 Cases**
David M. Gloystein, Bradley A. Heiges, David G. Schwartz, John G. DeVine and Deborah Spratt
- 43 **Innovation and New Technologies in Spine Surgery, Circa 2020: A Fifty-Year Review**
G. Bryan Cornwall, Andrea Davis, William R. Walsh, Ralph J. Mobbs and Alexander Vaccaro
- 50 **Complete Osseointegration of a Retrieved 3-D Printed Porous Titanium Cervical Cage**
Wimar van den Brink and Nancy Lamerigts
- 57 **Perspectives on the Treatment of Lumbar Disc Degeneration: The Value Proposition for a Cell-Based Therapy, Immunomodulatory Properties of Discogenic Cells and the Associated Clinical Evaluation Strategy**
Lara Ionescu Silverman, Will Heaton, Niloofar Farhang, Lindsey Hart Saxon, Galina Dulatova, Daniel Rodriguez-Granrose, Flagg Flanagan and Kevin T. Foley
- 65 **Development of a Computer-Aided Design and Finite Element Analysis Combined Method for Affordable Spine Surgical Navigation With 3D-Printed Customized Template**
Peter Endre Eltes, Marton Bartos, Benjamin Hajnal, Agoston Jakab Pokorni, Laszlo Kiss, Damien Lacroix, Peter Pal Varga and Aron Lazary
- 75 **Robotics in Spine Surgery: A Technical Overview and Review of Key Concepts**
S. Harrison Farber, Mark A. Pacult, Jakub Godzik, Corey T. Walker, Jay D. Turner, Randall W. Porter and Juan S. Uribe
- 81 **Therapeutic Effect of Large Channel Endoscopic Decompression in Lumbar Spinal Stenosis**
Fei-Long Wei, Ming-Rui Du, Tian Li, Kai-Long Zhu, Yi-Li Zhu, Xiao-Dong Yan, Yi-Fang Yuan, Sheng-Da Wu, Bo An, Hao-Ran Gao, Ji-Xian Qian and Cheng-Pei Zhou

- 88 **Establishment and Verification of a Perioperative Blood Transfusion Model After Posterior Lumbar Interbody Fusion: A Retrospective Study Based on Data From a Local Hospital**
Bo Liu, Junpeng Pan, Hui Zong and Zhijie Wang
- 97 **Clinical Features and Efficacy Analysis of Redundant Nerve Roots**
Jianzhong Xu and Yong Hu
- 104 **Comparison of C2-3 Pedicle Screw Fixation With C2 Spinous Muscle Complex and Iliac Bone Graft for Instable Hangman Fracture**
Dingli Xu, Kaifeng Gan, Yang Wang, Yulong Wang and Weihu Ma
- 111 **A Novel Three-Dimensional Computational Method to Assess Rod Contour Deformation and to Map Bony Fusion in a Lumbopelvic Reconstruction After En-Bloc Sacrectomy**
Peter Endre Eltes, Mate Turbucz, Jennifer Fayad, Ferenc Bereczki, György Szőke, Tamás Terebessy, Damien Lacroix, Peter Pal Varga and Aron Lazary
- 124 **Surgical Process Modeling for Open Spinal Surgeries**
Fabio Carrillo, Hooman Esfandiari, Sandro Müller, Marco von Atzigen, Aidana Massalimova, Daniel Suter, Christoph J. Laux, José M. Spirig, Mazda Farshad and Philipp Färnstahl
- 137 **An Innovative Prone Position Using a Body-Shape Plaster Bed and Skull Traction for Posterior Cervical Spine Fracture Surgeries**
Zhiyu Ding, Yijun Ren, Hongqing Cao, Yuezhan Li, Shijie Chen, Jinglei Miao and Jinsong Li



In-vivo Performance of Seven Commercially Available Demineralized Bone Matrix Fiber and Putty Products in a Rat Posterolateral Fusion Model

Nicholas Russell¹, William R. Walsh², Vedran Lovric², Peter Kim¹, Jennifer H. Chen¹, Michael J. Larson³ and Frank Vizesi^{1*}

¹ SeaSpine Inc., Carlsbad, CA, United States, ² Surgical and Orthopaedic Research Laboratories, Prince of Wales Clinical School, University of New South Wales, Sydney, NSW, Australia, ³ Ibex Preclinical Research Inc., Logan, UT, United States

OPEN ACCESS

Edited by:

Ajay Puri,
Tata Memorial Hospital, India

Reviewed by:

Konstantinos Markatos,
Biomedical Research Foundation of
the Academy of Athens, Greece
Paul Simon Unwin,
Independent Researcher, Ludlow,
United Kingdom

*Correspondence:

Frank Vizesi
frank.vizesi@seaspine.com

Specialty section:

This article was submitted to
Orthopedic Surgery,
a section of the journal
Frontiers in Surgery

Received: 12 December 2019

Accepted: 28 February 2020

Published: 20 March 2020

Citation:

Russell N, Walsh WR, Lovric V, Kim P,
Chen JH, Larson MJ and Vizesi F
(2020) In-vivo Performance of Seven
Commercially Available Demineralized
Bone Matrix Fiber and Putty Products
in a Rat Posterolateral Fusion Model.
Front. Surg. 7:10.
doi: 10.3389/fsurg.2020.00010

Introduction: Demineralized bone matrix (DBM) is a widely used bone graft in spinal fusion. Most commercial DBMs are composed of demineralized bone particles (~125–800 microns) suspended in a carrier that provides improved handling but dilutes the osteoinductive component. DBM fibers (DBF) provide improved osteoconductivity and do not require a carrier. It has been suggested that 100% DBF may offer improved performance over particulate-based DBMs with carrier.

Study Design: Seven commercially available DBM products were tested in an athymic rat posterolateral fusion model. There were four 100% DBFs, two DBFs containing a carrier, and one particulate-based DBM containing carrier.

Objective: The study objectives were to evaluate the *in vivo* performance: (1) compare fusion rate and fusion maturity of six commercially available DBFs and one particulate-based DBM, and (2) assess the effect of carrier on fusion outcomes for DBFs in a posterolateral fusion model.

Methods: The DBF/DBM products evaluated were: Strand™ Family, Propel® DBM Fibers, Vesuvius® Demineralized Fibers, Optium® DBM Putty, Grafton® DBF, Grafton Flex, and DBX® Putty. Single-level posterolateral fusion was performed in 69 athymic rats. Fusion was assessed bilaterally after 4 weeks by manual palpation, radiograph and CT for bridging bone. Fusion mass maturity was assessed with a CT maturity grading scale and by histology. Statistical analysis was performed using Fishers Exact Test for categorical data and Kruskal-Wallis Test for non-parametric data.

Results: Strand Family achieved 100% fusion (18/18) by manual palpation, radiographic and CT evaluation, significantly higher than Propel Fibers, Vesuvius Fibers, Optium Putty, and DBX Putty, and not statistically higher than Grafton DBF and Grafton Flex. Strand Family provided the highest fusion maturity, with CT maturity grade of 2.3/3.0 and 89% mature fusion rate. Fusion results suggest a detrimental effect of carrier on fusion performance.

Conclusions: There were large variations in fusion performance for seven commercially available DBM products in an established preclinical fusion model. There were even significant differences between different 100% DBF products, suggesting that composition alone does not guarantee *in vivo* performance. In the absence of definitive clinical evidence, surgeons should carefully consider available data in valid animal models when selecting demineralized allograft options.

Keywords: demineralized bone fiber, demineralized bone matrix, bone graft, spinal fusion, carrier, posterolateral spinal fusion, athymic rat

INTRODUCTION

Spinal arthrodesis is a widely performed surgical procedure used to treat numerous spinal pathologies. Autologous bone harvested from the iliac crest is often considered the gold-standard graft for spinal fusion procedures. However, supply is often limited, and its harvest is associated with increased surgery time, blood loss and risk of infection. Additionally, chronic donor site pain or morbidity has been reported in 8–26% of patients (1–3). There continues to be demand for alternative bone graft materials that can replace autograft bone harvested from the iliac crest and/or augment local autograft bone for spinal fusion procedures.

Demineralized Bone Matrix (DBM) is a type of bone graft alternative that is processed from human allograft bone. DBM is processed by removing the mineral component of bone with acid, leaving behind the extracellular matrix composed of collagen and non-collagenous proteins, including the endogenous growth factors. The presence of these endogenous growth factors, particularly BMPs, imparts osteoinductive properties, while the geometry of the collagen matrix has the potential to impart varying degrees of osteoconductivity to the graft (4). DBM has become one of the most widely used bone graft alternatives in spinal fusion surgery. DBM possesses several qualities that make it an attractive graft option. It is readily available, cost-effective, and requires little or no preparation.

Clinical studies have reported the safety and efficacy of DBM as a bone graft extender in lumbar spine fusion (5–8). One study in 120 patients undergoing 1–2 level instrumented posterolateral fusion (PLF) used a DBM gel (Grafton®) mixed with local autograft bone implanted on one side, compared to iliac crest autograft implanted on the contralateral side in the same patient (9). Fusion rates at 24 months were 52% for the DBM composite group and 54% for the iliac crest group. Another study in 59 patients undergoing 1–2 level instrumented PLF evaluated a DBM putty (Accell Connexus®) mixed with iliac crest or local autograft, compared to iliac crest or local autograft alone (10). Radiographic fusion rates after 12 months were similar between the two groups, with 70% fusion for the DBM composite group and 77% for autograft alone. Other studies report similar findings of comparable fusion rates and clinical outcomes for local autograft-DBM composites compared to iliac crest alone (11, 12). Overall, the clinical evidence supports DBM as an effective bone extender when used to augment a smaller quantity of autograft, offering similar clinical performance to autograft in posterolateral spinal fusion.

There are currently numerous DBM products commercially available for use in spinal fusion surgeries. These are available in different forms including powders, putties, gels, pre-filled syringes, pouches, strips, fibers, and others. However, the bone-forming capacity of these products has been reported to vary considerably (13–18). This may be attributed to several factors. Since commercially available DBMs are processed by different manufacturers or tissue banks, there is variability in its production from allograft bone. Sources of variability include quality of the donor bone, bone geometry, demineralization methods, sterilization method, and use of a carrier, which can result in inconsistent biologic responses (19).

The purpose of the carrier medium in DBM products is to improve the handling characteristics, but its use comes at the expense of active DBM component, diluting the osteoinductive performance of the product. Traditionally, the active DBM component extracted from bone is a fine particulate powder that is difficult to handle and deliver in surgery. The addition of inert, biocompatible carriers is intended to turn the DBM powder into a putty or paste to make it easier to localize to the fusion site. Examples of DBM carriers used in commercially available products include glycerol, hyaluronic acid, poloxamer reverse phase medium, gelatin, and others. Unfortunately, for many commercial DBM putty-type products, a major portion of the final DBM complex is the carrier (e.g., up to ~85% carrier and 15% active DBM), which decreases the amount of active DBM component that can be incorporated (6). Furthermore, upon dissolution of the carrier material, the graft volume may decrease and leave voids in the implantation site. Due to the drawbacks of carrier materials, there has been an increase in demand for DBM products composed of 100% active DBM.

Demineralized bone fibers (DBF) are a formulation of demineralized bone matrix that can provide favorable handling without the need of a carrier. To manufacture DBF, allograft bone is demineralized in the form of long fibers or ribbons, rather than fine particulate, so the resulting DBF product is cohesive on its own. However, different fiber geometry and product configurations can result in variable handling and biologic properties. One commercially available DBF (OsteoStrand™ Plus) is composed of 100% DBM in the form of long fibers that exhibit controlled expansion after implantation to maximize implant fill. In contrast, there are other commercial preparations of DBF that do still include a carrier and may be compressed into different shapes (e.g., strips).

In addition to improved handling as well as being osteoinductive, DBF has also demonstrated an osteoconductive advantage over DBM particulate in a rabbit model of posterolateral spine fusion (4). In a study by Martin et al. (4), two fiber-based formulations of DBM (Grafton Flex and Putty) were compared to a particle-based formulation (Grafton gel). All three DBMs had the same osteoinductivity, but the fiber-based DBMs demonstrated a higher fusion rate at 92% compared to the particle-based DBM fusion rate of 58%. When osteoinductivity was removed from the DBMs using guanidine extraction to remove the inductive protein pool, leaving behind only osteoconductive properties, the fiber-based DBM fusion rate decreased to 36%, whereas the particle-based DBM dropped to 0%. This suggests that the fiber-based versions of DBM provide greater osteoconductivity than particulate-based DBMs to aid in new bone formation.

There is an increasing variety of DBF products being released commercially, with variable fiber geometries and product configurations. While there may be benefits to the fiber-based DBM format, there is a need for greater understanding of the factors affecting bone-forming capacity and fusion performance of DBFs. The main objective of this study was to compare the fusion performance of different commercially available DBM fiber and putty products in a single-level posterolateral fusion model. The second objective of this study was to assess the effect of carrier on *in vivo* fusion outcomes of DBF in a posterolateral fusion model.

MATERIALS AND METHODS

Study Design

Seven different commercially available demineralized bone fiber and putty products were tested in a single-level athymic rat posterolateral fusion model (13–18). **Table 1** summarizes the product information for each DBM tested in this study. Four of the groups are 100% demineralized bone fibers: Strand™ Family DBM Fibers (SeaSpine, Carlsbad, CA), Propel® DBM Fibers (NuVasive, San Diego, CA), Vesuvius™ Demineralized Fibers (LifeNet, Virginia Beach, VA), and Grafton® DBM DBF

(Osteotech, Eatontown, NJ). Two of the DBF products contain glycerol carrier: Optium® DBM Putty (LifeNet, Virginia Beach, VA, also distributed as Vesuvius DBM putty), and Grafton® Flex (OsteoTech, Eatontown, NJ). A traditional particle-based DBM putty containing sodium hyaluronate carrier: DBX® Putty (MTF, Edison, NJ) was included as a control group. DBF and DBM products were selected for being in current widespread clinical use and/or for being manufactured by different AATB-accredited musculoskeletal tissue banks in the United States. Furthermore, two of the DBF product families were selected to enable the comparison of fibers with or without carrier: the Vesuvius family and Grafton family, which each have one product formulation with glycerol carrier (Vesuvius/Optium Putty and Grafton Flex, respectively) and another product formulation that is 100% DBF (Vesuvius Demineralized Fibers and Grafton DBF, respectively).

All DBM products were obtained in sterile, factory-sealed packaging for use in humans with at least 6 months shelf life before expiration. Multiple lots (1–3 lots) were obtained for each product. All groups were assessed using the same *in vitro* characterization, *in vivo* implantations, and fusion assessments at 4 weeks post-implantation.

Surgery and Fusion Assessment

Sixty-nine mature male athymic rats (10–11 weeks) were used following ethical approval. A single-level posterolateral fusion procedure was performed between the L4–L5 vertebra. The transverse processes were exposed by paramedian incision and the dorsal surfaces were gently decorticated with a motorized burr. An aliquot of graft material equal to 0.3 cm³ was placed bilaterally in the prepared posterolateral gutters bridging the decorticated transverse processes for a total of 0.6 cm³ of graft material for each animal. The Strand Family, Propel Fibers, Vesuvius Fibers, Optium Putty, and Grafton DBF, and DBX Putty implants were prepared by packing 0.3 cm³ of graft material into a 1cc open bore syringe for delivery to the surgical site. Grafton Flex was cut into rectangular strips equaling 0.3 cm³ by volume. Strand family, Vesuvius Fibers, Grafton DBF DBM, and Grafton Flex were hydrated with sterile saline prior to implantation. After implantation was complete, all wounds were closed with

TABLE 1 | DBM Fiber and putty products tested.

Product name	Distributor/manufacturer	DBM format	Carrier	Product composition by weight (%)		DBM dry weight (g/cc)	Sample size N
				DBM	Carrier		
Strand™ Family	SeaSpine	Fibers	N/A	100	0	0.302	18
Propel® DBM Fibers	NuVasive (AlloSource)	Fibers	N/A	100	0	*	9
Vesuvius™ Demineralized Fibers	K2M (LifeNet)	Fibers	N/A	100	0	0.164	9
Optium® / Vesuvius DBM Putty	LifeNet/K2M (LifeNet)	Fibers	Glycerol	18	82	0.304	8
Grafton® DBM DBF	Medtronic (OsteoTech)	Fibers	N/A	100	0	0.209	9
Grafton Flex	Medtronic (OsteoTech)	Fibers	Glycerol	43	57	0.353	8
DBX Putty®	DePuy Synthes (MTF)	Particles	Sodium hyaluronate	28	72	0.339	8

*Not obtained due to product being packaged wet in saline.

suture in two layers and an anterior-posterior radiograph of the lumbar spine was taken. All rats were euthanized 4 weeks post-operatively via CO₂ overdose, and the lumbar spines were harvested en bloc for analysis.

Immediately after harvest, explanted lumbar spines were manually tested for intersegmental motion by two independent trained observers blinded to treatment groups. Any motion detected between the facets or transverse processes of L4 and L5 by manual palpation was considered a failure of fusion. The absence of motion (both right and left) was considered successful fusion. Anterior-posterior Faxitron radiographs (Faxitron, Wheeling, IL) and digital plates (AGFA CR MD4.0 Cassette) were taken of each spine and evaluated in a blinded fashion by 2 independent observers. Fusion was determined by radiographic evidence of bone bridging the transverse processes, with left and right fusion masses evaluated independently.

Qualitative Fusion Maturity μ CT Grading Scale

Microcomputed tomography (μ CT) (Siemens Medical Solutions, Knoxville, Tennessee) scanning was performed on all animals to obtain high resolution radiographic images of the spinal fusions in three planes. Image analysis software, Inveon Research Workplace [IRW] (Siemens Medical Solutions, Knoxville, Tennessee) was used to reconstruct the μ CT image data and evaluate the fusions between the treated levels in the coronal and sagittal planes. Fusion was assessed using a qualitative fusion maturity grading scale to score each fusion mass on a scale of 0 to 3 (Figure 1). Grade 0 corresponds to an incomplete or lack of bridging bone spanning the transverse processes and is considered not fused. Grade 1 demonstrates continuous bone

formation spanning the transverse processes, but without a defined cortex, and is considered an immature fusion. Grade 2 demonstrates bone formation between transverse processes with discontinuous cortex formation (cortex surrounding >50% of fusion mass in at least one plane). It is considered fused and progressing toward mature fusion. Grade 3 demonstrates complete bridging between transverse processes with continuous (>90%) cortex formation in all planes and extensive trabecular remodeling. It is considered a mature fusion.

The spines were fixed in 10% phosphate buffered formalin and processed for routine Hematoxylin and Eosin (H&E) decalcified in 10% formic acid for paraffin histology. Sagittal histology sections from each side of the fusion were qualitatively assessed to evaluate the maturity of the fusion in each group. Graders were blinded to the treatment group and the results of fusion evaluation from other endpoints.

In vitro Product Characterization

Product characteristics measured were overall product composition (% DBM, % carrier) and DBM content (dry weight of DBM component). A portion of samples from each lot was set aside for *in vitro* analysis. Samples were prepared according to manufacturer's instructions and weighed before and after rinsing out the carrier (if applicable), and lyophilization.

Statistical Analysis

Statistical analysis was performed using Fishers Exact Test for categorical data and Kruskal-Wallis ANOVA for non-parametric data. A *p*-value < 0.05 was considered statistically significant. Linear regression was used to assess the relationship between fusion rate and percentage composition of carrier, for the carrier-containing products.

Fusion Mass Maturity μ CT Grading Scale

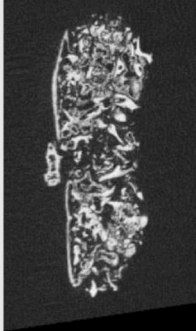
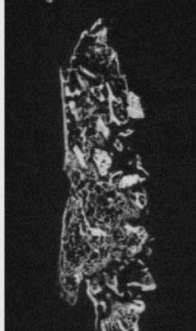
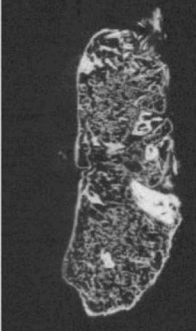
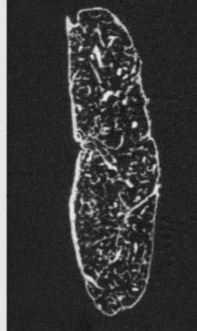
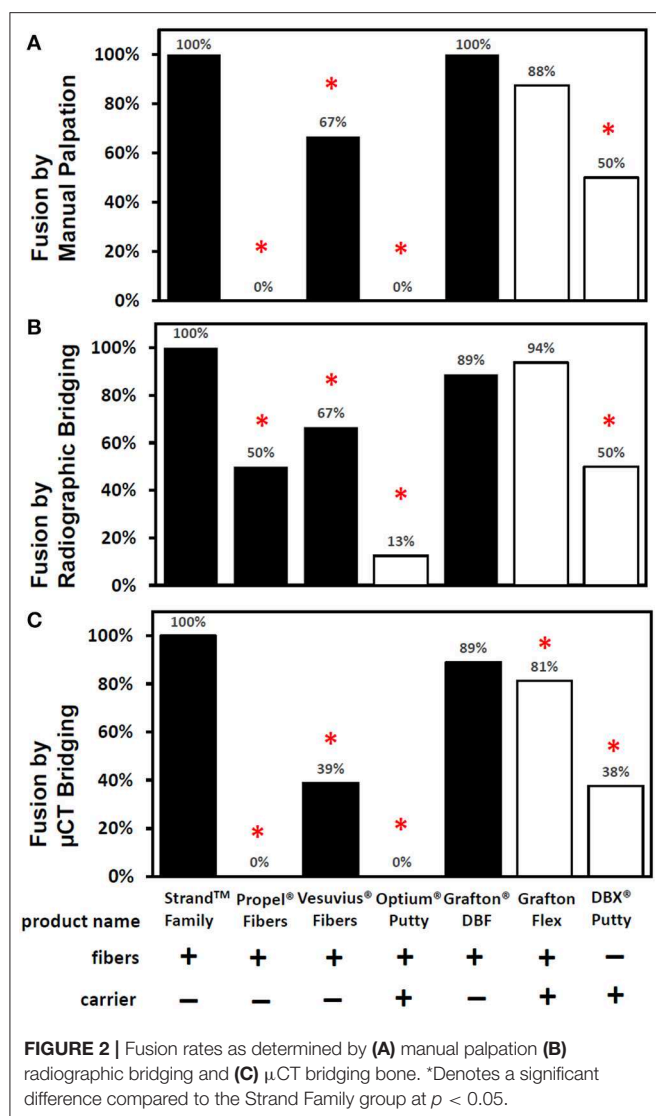
Grade	0	1	2	3
Description	Lack of bridging between the TPs. Bone localized adjacent to TPs.	Bone formation between TPs, but without a defined cortex	Bone formation between TPs with discontinuous cortex formation (>50% in at least one plane)	Complete bridging between TPs with continuous (>90%) cortex in all planes and extensive trabecular remodeling
Example				

FIGURE 1 | Qualitative fusion mass maturity μ CT grading scale with description and representative μ CT image of each grade.



RESULTS

The *in vivo* phase of the study was uneventful with all animals recovering well following surgery and no adverse reactions noted. The results of the fusion assessments from manual palpation, radiography and μ CT are presented in **Figure 2** and **Table 2**. All study endpoints were closely concordant in terms of fusion rates. Strand Family demonstrated a fusion rate of 100% (9/9), significantly higher than the 0% (0/8 fused by manual palpation) for Propel Fibers, 67% (6/9) for Vesuvius Fibers, 0% (0/8) for Optium Putty, and 50% (4/8) for DBX Putty ($p < 0.05$). Strand Family fusion rates were not statistically higher than Grafton DBF (100% by manual palpation, 89% by radiograph assessment) or Grafton Flex (88% by manual palpation, 94% by radiograph).

Radiographic and μ CT imaging illustrated substantial differences in the amount and quality of bone formation in the fusion masses between the groups (**Figures 3, 4**). Faxitron radiographs and μ CT reconstructions of the Strand Family

TABLE 2 | Fusion rates assessed by manual palpation, X-ray, and CT bridging bone.

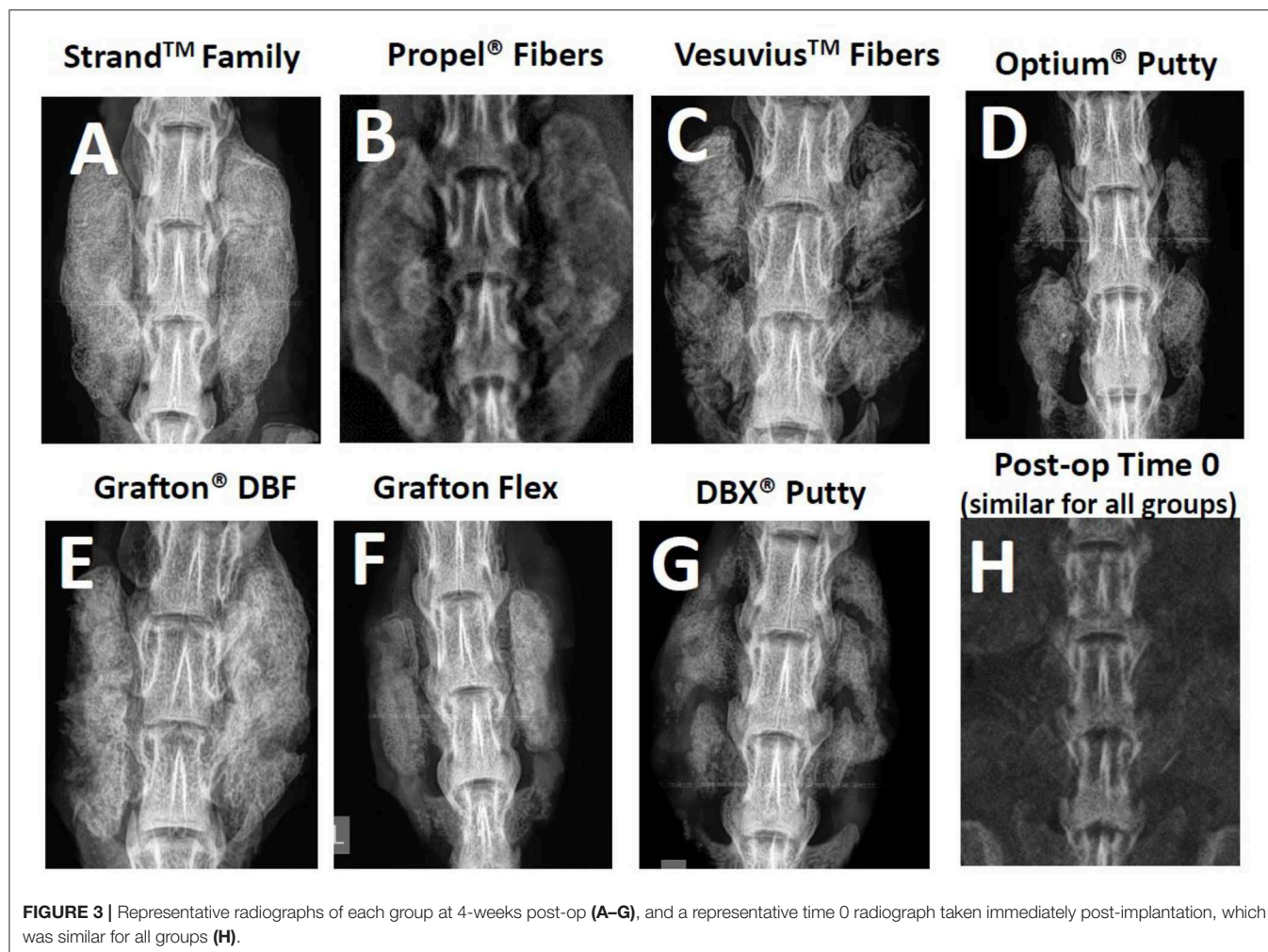
Group	MP fusion	X-ray bridging	CT bridging
Strand™ Family	100%	100%	100%
Propel® DBM Fibers	0%*	50%*	0%*
Vesuvius™ Demineralized Fibers	67%*	67%*	39%*
Optium® DBM Putty	0%*	13%*	0%*
Grafton® DBM DBF	100%	89%	89%
Grafton Flex	88%	94%	81%*
DBX Putty®	50%*	50%*	38%*

*Statistically significant vs. Strand Family, $p < 0.05$.

and Grafton DBF groups displayed large bilateral fusions with contiguous bone masses bridging between the L4-L5 transverse processes in all animals (**Figures 3A,E, 4A,E**). In contrast, bone formation for Vesuvius Fibers, Optium Putty, and DBX Putty groups was typically localized around the host transverse processes and in disparate islands between the transverse processes, (**Figures 3C,D,G, 4C,D,G**). Likewise, although bone formation was evident in the Propel Fibers and Grafton Flex groups, the fusion mass often possessed a large central void (**Figures 4D,F**).

Qualitative grading of fusion revealed significant differences in fusion bone maturity even among groups with similar fusion rates (**Figure 5**). Strand Family achieved a μ CT fusion maturity grade of 2.3 out of 3.0, significantly higher than Propel Fibers, Vesuvius Fibers, Optium Putty, and DBX Putty (**Figure 5**). Although Grafton DBF and Grafton Flex had lower maturity grades of 1.78 and 1.19 compared to Strand, the differences did not reach statistical significance. Correspondingly, Strand Family had an 89% mature fusion rate, where mature fusion is defined as Grade 2 or Grade 3 on the μ CT fusion maturity grading scale (**Table 3**). Strand Family fusion maturity was 89%, compared to 61% for Grafton DBF and 38% for Grafton Flex, but differences were not statistically significant. Strand Family was statistically higher than Propel Fibers, Vesuvius Fibers, Optium Putty, and DBX Putty which all had 0% mature fusions.

Histological evaluation supported the radiographic observations in terms of both bridging bone from transverse process to transverse process and the formation of new cortex. The Strand Family specimens demonstrated clear trabeculae bridging from one transverse process to the next, incorporating the DBM fibers within a bone marrow remodeled fusion mass (**Figure 6A**). There was little interposed fibrous tissue in these specimens. In contrast, the Propel Fibers, Vesuvius Fibers, Optium Putty, and DBX Putty groups showed bone formation adjacent to the transverse processes, but with predominantly fibrous tissue interposed between them (**Figures 6B–G**). In these four groups the DBM material in the center of the fusion mass was infiltrated with hypocellular fibrous tissue, with minimal new woven bone formation. The DBM particulate in the DBX fusions were clearly visible with minimal resorption and remodeling noted (**Figure 6G**). The Grafton DBF group demonstrated



trabecular bone and marrow spaces like the Strand Family group, but also had long fibers of residual DBM within the fusion mass (Figure 6E). The Grafton Flex group was characterized by bone formation and small bone marrow cavities at the periphery of the implanted material (Figure 6F). In the center, there was fibrous tissue infiltration with no trabecular remodeling, and a general hypocellular characteristic, resulting in a “hollow” fusion mass. There was no evidence of inflammatory cell population for all groups.

The *in vitro* product characterization revealed significant differences in product composition (% DBM vs. % carrier) and DBM content by dry weight (Table 1). For the carrier-containing groups, Optium Putty had the lowest % DBM content at 18% DBM (82% carrier), followed by DBX Putty at 28% DBM (72% carrier), and Grafton Flex at 43% DBM (57% carrier). For products containing carrier, there was a linear inverse correlation between percentage carrier in the product and the fusion rate ($R^2 = 0.99$). DBM content was slightly higher in the carrier-containing DBMs with an average DBM content of 0.33 g/cc, compared to 100% DBF groups which averaged 0.24 g DBM/cc, but the difference was not statistically significant.

DISCUSSION

There were large variations in fusion performance for seven commercially available DBF and DBM products in an established preclinical fusion model. These data agree well with previous reports using the athymic rat spinal fusion model (13–18, 20–24). Among different 100% DBF products with no carrier present, there were significant differences in fusion outcomes, suggesting that composition alone does not guarantee performance. For the carrier-containing DBF/DBM groups, the results suggest a detrimental effect of carrier on fusion outcomes. The current study did not investigate whether this detrimental effect was due to direct adverse effects of the carrier material or to indirect effects of displacing or diluting the active DBM component.

There were several limitations of this study. A relatively small number of donor lots was tested for each product due to lack of product availability and a single time point at 4 weeks. Furthermore, because the control group of the particle-based DBM had carrier, we were unable to separate the benefit of DBM fibers over particulate from the effect of having no carrier. In this study the DBM and DBF grafts were used alone, whereas in the

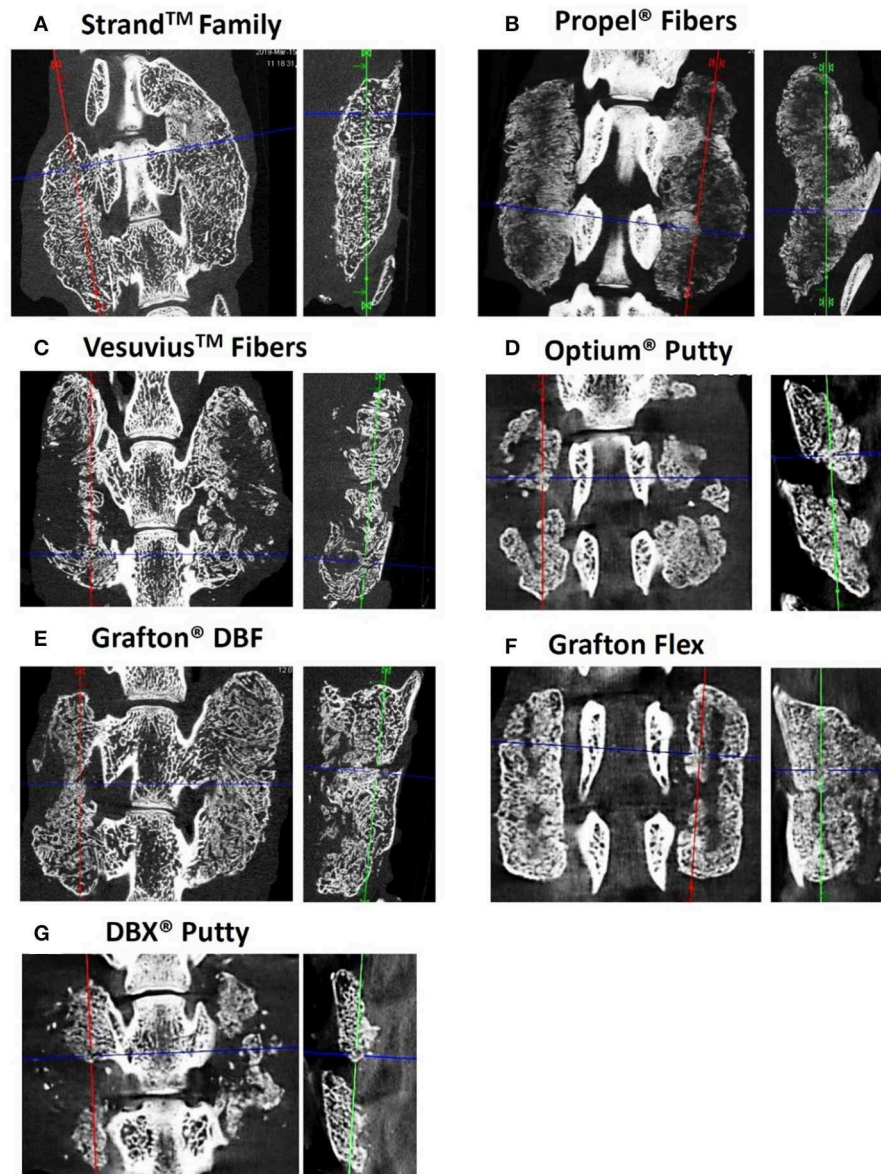
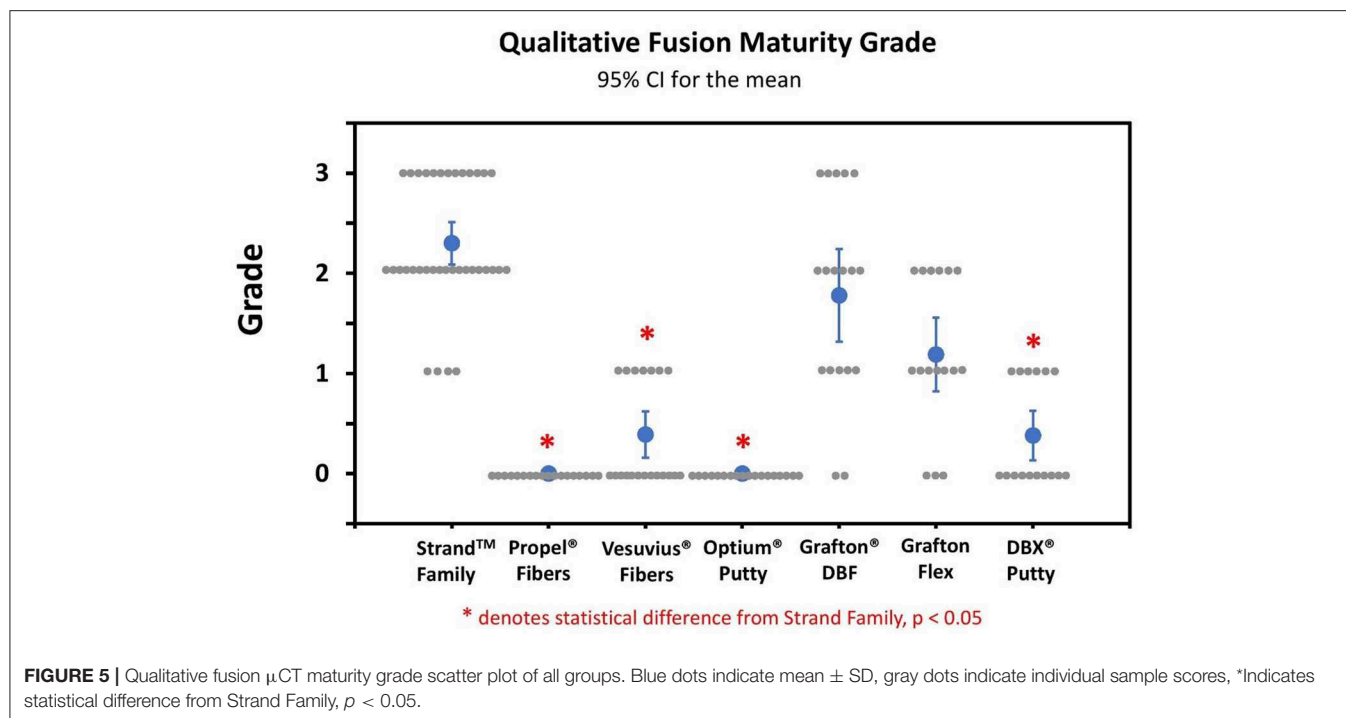


FIGURE 4 | Representative μ CTs of each group at 4 weeks demonstrating the differences in bone formation and fusion maturity between groups. Strand Family (**A**) and Grafton DBF (**E**) had large bilateral fusions bridging the transverse processes (TPs) with trabecular remodeling and the presence of a defined cortex; Vesuvius Fibers (**C**) and Grafton Flex (**F**) had centralized voids in the fusion masses; Both putties (**D,G**) were characterized by bone formation localized to the TPs with minimal bridging bone; Propel Fibers (**B**) had soft radiolucent fusion masses with no defined mineralization bridging the TPs.

clinical setting these bone grafts are often mixed with autograft and/or bone marrow aspirate.

The athymic rat spinal fusion model is well-characterized and has been used extensively to test human DBM products (13–24). In this model, DBM and DBF grafts can be tested in an unaltered “off-the-shelf” form, as would be available for use in human spine surgery. In addition, the athymic rat posterolateral fusion is a challenging model that requires the graft to possess both significant osteoinductive and osteoconductive abilities to induce a solid arthrodesis (4). Because of this challenging environment,

the reported fusion rates for DBM products tested in this model at 4 weeks vary considerably, which makes it a robust model to discern differences in product performance. Previous studies have evaluated fusion performance of commercial DBM putties and/or gels composed of different carriers and reported fusion rates of 0–100% in the same preclinical fusion model as the current study (13–18, 20–24). In studies by the Wang group (14, 15), substantial variability in performance was measured between different DBM products from different manufacturers, while Bae et al. (17), further showed substantial variability between various

**TABLE 3 |** Fusion mass maturity assessed by μ CT.

Group	CT maturity grade (0–3)	Mature fusion mass by CT (%)
Strand™ Family	2.3 ± 0.6	89%
Propel® DBM Fibers	$0 \pm 0^*$	0%*
Vesuvius™ Fibers	$0.39 \pm 0.5^*$	0%*
Optium®/Vesuvius DBM Putty	$0 \pm 0^*$	0%*
Grafton® DBM DBF	1.78 ± 1.0	61%
Grafton® Flex	1.19 ± 0.8	38%
DBX Putty®	$0.38 \pm 0.5^*$	0%*

*Statistically significant vs. Strand Family, $p < 0.05$.

lots of the same DBM material. Indeed, in the current study, the full range of fusion rates from 0 to 100% was observed for different groups, as well as corresponding differences in the quality and maturity of bone formation among different DBF and DBM products.

Fusion endpoint evaluated by multiple techniques in the current study were generally concordant, with a tendency for higher fusion rates assessed by manual palpation and for lower fusion rates assessed by μ CT. This is consistent with previous studies demonstrating that biomechanically solid fusion occurs prior to radiographic appearance of solid fusion (25). Histologically, the fusion mass initially consists predominantly of woven bone, which provides biomechanical stability, and then becomes gradually trabeculated as the bone remodels. This was evident in the current study, where different groups had distinct qualitative differences in histological appearance. For example, although Grafton Flex had a high fusion rate of 88% by

manual palpation, μ CT imaging and histology of the fusion mass revealed the presence of a hypocellular central void filled with fibrous tissue. In contrast, in the Strand Family and Grafton DBF groups, the fusion bone was a solid mass with extensive trabecular remodeling surrounded by a cortex. This indicated that different DBF or DBM grafts which were both evaluated as solidly fused could be at different stages of bone maturity. Hence, it is valuable to develop more stringent criteria to distinguish fusion performance beyond the initial phase of biomechanical stability.

A novel μ CT fusion maturity grading scale was useful and complementary with histological analysis for evaluating the fusion bone quality and maturity in the current study. The μ CT grading scale is distinguished by its ability to semi-quantitatively assess the trabecular remodeling and cortex encompassing the entire three-dimensional fusion mass. However, histological analysis is still necessary to evaluate the cellular and tissue remodeling response in the fusion mass, including any presence of marrow elements, fibrous infiltration, and residual implant material. The distribution and position of these components relative to the host transverse processes and to the newly forming fusion mass bone can help reveal the mechanisms and quality of bone formation. For example, Strand Family displayed newly formed trabecular bone with marrow spaces throughout the fusion mass, including the center of the fusion mass. This is indicative of an osteoinductive response which has resulted in new bone formation and functional bony remodeling. In contrast, Propel Fibers, Vesuvius Fibers, Optium Putty, and DBX Putty groups demonstrated central regions consisting of residual fibers surrounded by fibrous infiltration. This reflects the challenging nature of the posterolateral fusion environment, which requires both strong osteoinductive signal and a favorable osteoconductive scaffold to induce bone formation away from

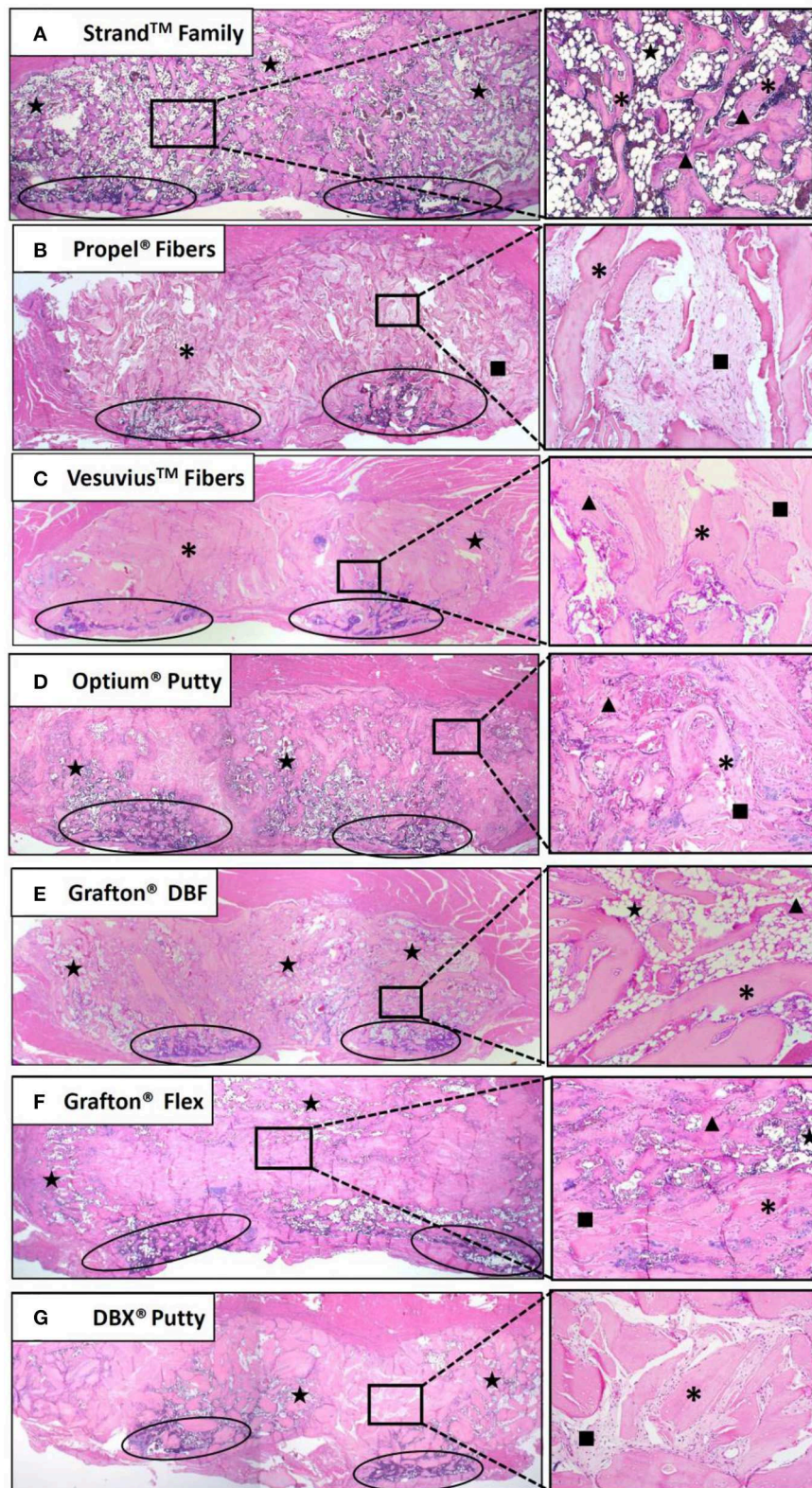


FIGURE 6 | Representative H&E histology images of fusion masses in each group. Strand Family (A) and Grafton DBF (E) had DBM fibers incorporated into bone marrow-filled bridging bone. Propel Fibers (B), Vesuvius Fibers (C), Optium Putty (D), and DBX Putty (G) had residual DBM surrounded by fibrous tissue with little bone remodeling. Grafton Flex (F) had bone formation at the periphery of the fusion mass and fibrous tissue in the center. Ovals indicate transverse processes, star indicates marrow, * indicates residual DBM, ▲ indicates new bone, ■ indicates fibrous tissue. Image magnification 1.25x objective (left) and 10x objective (right).

the adjacent host bone. Time is another important variable to consider in the overall paradigm of bone healing.

The variability in fusion performance between 100% DBF products is likely driven by variations in allograft bone processing conditions between different tissue banks. Indeed, an anonymous survey of four AATB accredited tissue banks reported four completely different chemical processing methods were used to ensure the sterility of demineralized bone products (26). While the effect of these different chemical processing methods has not been investigated, it demonstrates the inherent variability in manufacturing of DBM products across different tissue banks. Furthermore, other studies have reported variability in DBM performance arising from processing variables such as differences in donor quality (17, 27, 28), demineralization (29), storage (30, 31), and sterilization procedures (32–34). Qiu et al. (31) investigated the effect of e-beam sterilization on DBM in a hydrous (wet) state compared to an anhydrous (dry) state and reported a 22% reduction in osteoinductivity in the wet DBM. Similarly, Han et al. (30) reported time- and temperature-dependent reductions in osteoinductivity for DBM stored in a wet state for as little as 5 weeks. While these factors were not directly investigated in this study, the results of the products containing moisture (Propel Fibers, Optium Putty, and DBX Putty) in the current study had inferior fusion performance.

Results from preclinical models may not necessarily translate directly to clinical outcomes. However, the relative performance

between materials may be of importance for clinical decision making. Further preclinical investigation utilizing well-designed studies that isolate processing variables and product characteristics are required to provide clinicians with the tools to make informed decisions regarding their DBM graft selection. In the absence of definitive clinical evidence, surgeons should carefully consider available data in valid animal models when selecting their demineralized bone-based products.

DATA AVAILABILITY STATEMENT

The datasets generated for this study are available on request to the corresponding author.

ETHICS STATEMENT

The animal study was reviewed and approved by UNSW Animal Care and Ethics Committee.

AUTHOR CONTRIBUTIONS

NR, WW, VL, PK, ML, and FV contributed conception and design of the study. FV, WW, and JC performed the statistical analysis. JC wrote the first draft of the manuscript. NR, WW, and FV wrote sections of the manuscript. All authors contributed to manuscript revision, read and approved the submitted version.

REFERENCES

- Silber JS, Anderson GD, Daffner SD, Brislin BT, Leland JM, Hilibrand AS, et al. Donor site morbidity after anterior iliac crest bone harvest for single-level anterior cervical discectomy and fusion. *Spine*. (2003) 28:134–9. doi: 10.1097/00007632-200301150-00008
- Sawin PD, Traynelis VS, Menezes AH. A comparative analysis of fusion rates and donor-site morbidity for autogeneic rib and iliac crest bone grafts in posterior cervical fusions. *J Neurosurg*. (1998) 88:255–65. doi: 10.3171/jns.1998.88.2.0255
- Younger EM, Chapman MW. Morbidity at bone graft donor sites. *J Orthop Trauma*. (1989) 3:192–5. doi: 10.1097/00005131-198909000-00002
- Martin GJ, Boden SD, Titus L, Scarborough NL. New formulations of demineralized bone matrix as a more effective graft alternative in experimental posterolateral lumbar spine arthrodesis. *Spine*. (1999) 24:637–45. doi: 10.1097/00007632-199904010-00005
- Kadam A, Millhouse PW, Kepler CK, Radcliff KE, Fehlings MG, Janssen ME, et al. Bone substitutes and expanders in spine surgery: a review of their fusion efficacies. *Int J Spine Surg*. (2016) 10:33. doi: 10.14444/3033
- Lee KJH, Roper JG, Wang JC. Demineralized bone matrix and spinal arthrodesis. *Spine J*. (2005) 5:S217–23. doi: 10.1016/j.spinee.2005.02.006
- Tilkeridis K, Touzopoulos P, Ververidis A, Christodoulou S, Kazakos K, Drosos GI. Use of demineralized bone matrix in spinal fusion. *World J Orthop*. (2014) 5:30–7. doi: 10.5312/wjo.v5.i1.30
- Vaccaro AR, Block JE, Stubbs HA. Demineralized bone matrix composite grafting for posterolateral spinal fusion. *Orthopedics*. (2007) 30:567–70. doi: 10.3928/01477447-20070701-06
- Cammisa FP, Lowery G, Garfin SR, Geisler FH, Klara PM, McGuire RA, et al. Two-year fusion rate equivalency between Grafton DBM gel and autograft in posterolateral spine fusion. *Spine*. (2004) 29:660–6. doi: 10.1097/01.BRS.0000116588.17129.B9
- Schizas C, Triantafyllopoulos D, Kosmopoulos V, Tzinieris N, Stafylas K. Posterolateral lumbar spine fusion using a novel demineralized bone matrix: a controlled case pilot study. *Arch Orthop Trauma Surg*. (2008) 128:621–5. doi: 10.1007/s00402-007-0495-4
- Kang J, An H, Hilibrand A, Yoon ST, Kavanagh E, Boden S. Grafton and local bone have comparable outcomes to iliac crest bone in instrumented single-level lumbar fusions. *Spine*. (2012) 37:1083–91. doi: 10.1097/BRS.0b013e31823ed817
- Girardi FP, Cammisa FP Jr. The effect of bone graft extenders to enhance the performance of iliac crest bone grafts in instrumented lumbar spine fusion. *Orthopedics*. (2003) 26:S545–8. doi: 10.3928/0147-7447-20030502-03
- Hayashi T, Lord EL, Suzuki A, Takahashi S, Scott TP, Phan K, et al. A comparison of commercially available demineralized bone matrices with and without human mesenchymal stem cells in a rodent spinal fusion model. *J Neurosurg Spine*. (2016) 25:133–7. doi: 10.3171/2015.12.SPINE15737
- Lee YP, Jo M, Luna M, Chien B, Lieberman JR, Wang JC. The efficacy of different commercially available demineralized bone matrix substances in an Athymic rat model. *J Spinal Disord Tech*. (2005) 18:439–44. doi: 10.1097/01.bsd.0000175696.66049.f7
- Wang JC, Alanay A, Mark D, Kanim LEA, Campbell PA, Dawson EG, et al. A comparison of commercially available demineralized bone matrix for spinal fusion. *Eur Spine J*. (2007) 16:1233–40. doi: 10.1007/s00586-006-0282-x
- Bae HW, Zhao L, Kanim LEA, Wong P, Delamarter RB, Dawson EG. Intervariability and intravariability of bone morphogenetic proteins in commercially available demineralized bone matrix products. *Spine*. (2006) 31:1299–306. doi: 10.1097/01.brs.0000218581.92992.b7
- Bae H, Zhao L, Zhu D, Kanim LEA, Wang JC, Delamarter RB. Variability across ten production lots of a single demineralized bone matrix product. *J Bone Joint Surg Am*. (2010) 92:427–35. doi: 10.2106/JBJS.H.01400
- Brechevich, AT, Kiely PD, Yoon BV, Nguyen JT, Cammisa FP, Abjornson C. Efficacy comparison of Accell Evo3 and Grafton demineralized bone matrix

- putties against autologous bone in a rat posterolateral spine fusion model. *Spine J.* (2017) 17:855–62. doi: 10.1016/j.spinee.2017.01.012
19. Hsu WK Wang JC. Demineralized bone matrix for spinal arthrodesis. *Semin Spine Surg.* (2006) 18:22–5. doi: 10.1053/j.semss.2006.01.004
 20. Grauer JN, Bomback DA, Lugo R, Troiano NW, Patel TC, Friedlaender GE. Posterolateral lumbar fusions in athymic rats: characterization of a model. *Spine J.* (2004) 4:281–86. doi: 10.1016/j.spinee.2003.10.001
 21. Chung CG, James AW, Asatrian G, Chang L, Nguyen A, Le K, et al. Human perivascular stem cell-based bone graft substitute induces rat spinal fusion. *Stem Cells Transl Med.* (2014) 3:1231–41. doi: 10.5966/sctm.2014-0027
 22. Lee S, Zhang X, Shen J, James AW, Chung CG, Hardy R, et al. Brief report: human perivascular stem cells and nel-like protein-1 synergistically enhance spinal fusion in osteoporotic rats. *Stem Cells.* (2015) 33:3158–63. doi: 10.1002/stem.2103
 23. Bhamb N, Kanim LEA, Drapeau S, Mohan S, Vasquez E, Shimko D, et al. Comparative efficacy of commonly available human bone graft substitutes as tested for posterolateral fusion in an athymic rat model. *Int J Spine Surg.* (2019) 13:437–58. doi: 10.14444/6059
 24. Peterson B, Whang PG, Iglesias R, Wang JC, Lieberman JR. Osteoinductivity of commercially available demineralized bone matrix. Preparations in a spine fusion model. *J Bone Joint Surg.* (2004) 86:2243–50. doi: 10.2106/00004623-200410000-00016
 25. Kanayama M, Cunningham BW, Weis JC, Parker LM, Kaneda K, McAfee PC. Maturation of the posterolateral spinal fusion and its effect on load-sharing of spinal instrumentation. An *in vivo* sheep model. *J Bone Joint Surg.* (1997) 79:1710–20. doi: 10.2106/00004623-199711000-00013
 26. Glowacki J. A review of osteoinductive testing methods and sterilization processes for demineralized bone. *Cell Tissue Bank.* (2005) 6:3–12. doi: 10.1007/s10561-005-4252-z
 27. Traianedes K, Russell JL, Edwards JT, Stubbs HA, Shanahan IR, Knaack D. Donor age and gender effects on osteoinductivity of demineralized bone matrix. *J Biomed Mater Res B Appl Biomater.* (2004) 70:21–9. doi: 10.1002/jbm.b.30015
 28. Schwartz Z, Somers A, Mellonig JT, Carnes DL Jr, Dean DD, Cochran DL, et al. Ability of commercial demineralized freeze-dried bone allograft to induce new bone formation is dependent on donor age but not gender. *J Periodontol.* (1998) 69:470–8. doi: 10.1902/jop.1998.69.4.470
 29. Zhang M, Powers RM Jr, Wolfinbarger L Jr. Effect(s) of the demineralization process on the osteoinductivity of demineralized bone matrix. *J Periodontol.* (1997) 68:1085–92. doi: 10.1902/jop.1997.68.11.1085
 30. Han B, Yang Z, Nimni M. Effects of moisture and temperature on the osteoinductivity of demineralized bone matrix. *J Orthop Res.* (2005) 23:855–61. doi: 10.1016/j.orthres.2004.11.007
 31. Qiu QQ, Liu XH, Connor J. Effects of e-beam radiation, storage, and hydration on osteoinductivity of DBM/AM composite. *J Biomed Mater Res B Appl Biomater.* (2009) 91:401–8. doi: 10.1002/jbm.b.31415
 32. Alanay A, Wang JC, Shamie AN, Napoli A, Chen C, Tsou P. A novel application of high-dose (50kGy) gamma irradiation for demineralized bone matrix: effects on fusion rate in a rat spinal fusion model. *Spine J.* (2008) 8:789–95. doi: 10.1016/j.spinee.2007.06.009
 33. Qiu QQ Connor J. Effects of gamma-irradiation, storage and hydration on osteoinductivity of DBM and DBM/AM composite. *J Biomed Mater Res A.* (2008) 87:373–9. doi: 10.1002/jbm.a.31790
 34. Wong MY, Yu Y, Yang JL, Woolford T, Morgan DAF, Walsh WR. 11 kGy gamma irradiated demineralized bone matrix enhances osteoclast activity. *Eur J Orthop Surg Traumatol.* (2014) 24:655–61. doi: 10.1007/s00590-013-1238-6

Conflict of Interest: NR, PK, JC, and FV are employed by SeaSpine, Inc. ML is employed by Ibex Preclinical Research, Inc. WW is on the editorial board for this journal.

The remaining author declares that the research was conducted in the absence of any commercial or financial relationships that could be construed as a potential conflict of interest.

Copyright © 2020 Russell, Walsh, Lovric, Kim, Chen, Larson and Vizesi. This is an open-access article distributed under the terms of the Creative Commons Attribution License (CC BY). The use, distribution or reproduction in other forums is permitted, provided the original author(s) and the copyright owner(s) are credited and that the original publication in this journal is cited, in accordance with accepted academic practice. No use, distribution or reproduction is permitted which does not comply with these terms.



The Role of Machine Learning in Spine Surgery: The Future Is Now

Michael Chang^{1,2}, Jose A. Canseco^{1,2*}, Kristen J. Nicholson², Neil Patel^{1,2} and Alexander R. Vaccaro^{1,2}

¹ Department of Orthopaedic Surgery, Thomas Jefferson University, Philadelphia, PA, United States, ² Rothman Orthopaedic Institute, Philadelphia, PA, United States

OPEN ACCESS

Edited by:

Vassilios S. Nikolaou,
National and Kapodistrian University
of Athens, Greece

Reviewed by:

Alberto Di Martino,
University of Bologna, Italy
Konstantinos Markatos,
Biomedical Research Foundation of
the Academy of Athens
(BRFAA), Greece

*Correspondence:

Jose A. Canseco
jose.canseco@rothmanortho.com

Specialty section:

This article was submitted to
Orthopedic Surgery,
a section of the journal
Frontiers in Surgery

Received: 14 April 2020

Accepted: 13 July 2020

Published: 21 August 2020

Citation:

Chang M, Canseco JA, Nicholson KJ,
Patel N and Vaccaro AR (2020) The
Role of Machine Learning in Spine
Surgery: The Future Is Now.
Front. Surg. 7:54.
doi: 10.3389/fsurg.2020.00054

The recent influx of machine learning centered investigations in the spine surgery literature has led to increased enthusiasm as to the prospect of using artificial intelligence to create clinical decision support tools, optimize postoperative outcomes, and improve technologies used in the operating room. However, the methodology underlying machine learning in spine research is often overlooked as the subject matter is quite novel and may be foreign to practicing spine surgeons. Improper application of machine learning is a significant bioethics challenge, given the potential consequences of over- or underestimating the results of such studies for clinical decision-making processes. Proper peer review of these publications requires a baseline familiarity of the language associated with machine learning, and how it differs from classical statistical analyses. This narrative review first introduces the overall field of machine learning and its role in artificial intelligence, and defines basic terminology. In addition, common modalities for applying machine learning, including classification and regression decision trees, support vector machines, and artificial neural networks are examined in the context of examples gathered from the spine literature. Lastly, the ethical challenges associated with adapting machine learning for research related to patient care, as well as future perspectives on the potential use of machine learning in spine surgery, are discussed specifically.

Keywords: machine learning, deep learning, artificial intelligence, spine surgery, orthopedic surgery

INTRODUCTION

In clinical medicine, the rise of machine learning applications represents a new era of solving healthcare problems. This is particularly true in spine surgery where algorithmic decision support tools, computer assisted navigation, and surgical robots are already being used in the clinic and operating room. While the appetite for machine learning and its role in artificial intelligence has grown amongst spine surgeons, very little discussion has revolved around how to evaluate these applications and their contributions to patient care. In 2019 alone, 82 publications (more than twice the previous year) were PubMed indexed when searching for the terms “machine,” “learning,” and “spine” together. A core component of proper peer-review requires familiarity with machine learning methodology among clinicians. Until this can be achieved, machine learning in the spine literature will either foster skepticism or flawed enthusiasm. The intricacies and real patient-safety concerns when dealing with the spine necessitates that clinicians familiarize themselves with the terminology and guiding principles of machine learning. This review will introduce the origins of the artificial intelligence field and provide an organic discussion on how to practically synthesize machine learning modalities in spine surgery. A glossary of key terms in this review can be referred to in **Table 1**.

TABLE 1 | Glossary of key machine learning terminology.

Terminology	Definition
Artificial neural networks:	Deep machine learning inspired by the biological neural network of an animal brain and Hebbian learning (1).
Black box:	A short-term ethical challenge in machine learning where the process by which the computer reaches an outcome is not easily interpretable and is hidden from consumers and engineers alike (2).
Decision tree learning:	A supervised machine that visually resembles a tree with nodes, branches, and leaves. Trees are adept at identifying clusters of homogenous variables and predicting outcomes. Most commonly a classification and regression tree (3).
Deep learning:	Computers that utilize representation learning or hidden layers to characterize unlabeled input variables without much manual human engineering. Commonly used for natural language processing, self-driving automobiles, pharmaceutical drug research, among others (1).
Distributional shift:	A short-term ethical challenge in machine learning where the training dataset poorly represents the true test set, secondary to racial or socioeconomic biases, or outdated information (4).
Feature values:	Individual characteristics or variables that are associated with the outcome of interest. Feature engineering can either be manually conducted or automated (5).
Hebbian theory:	Based on neuropsychology work by Dr. Donald O. Hebb from his book, <i>The Organization of Behavior</i> . Dr. Hebb's work on neuronal plasticity contributed greatly to the initial architecture of artificial neurons and networks (6).
Insensitivity to impact:	An ethical challenge in machine learning where the algorithm is unaware of the consequences of a false-positive or false-negative test (4).
Linear classification:	A task that involves predicting categorical outcomes (i.e., type of fruit or species of animal).
Linear regression	A task that involves predicting discrete or numeric outcomes that are integers or serial numbers (i.e., patient reported outcome scores).
Machine learning:	The study of using algorithms and mathematics to predict outcomes or accomplish tasks with little instruction or explicit programming. A subset of artificial intelligence (7).
Reward hacking:	A long-term ethical challenge of machine learning where algorithms self-learn how to maximize favorable outcomes but do so by circumventing rules or cheating the system (4).
Supervised learning:	Learner attempts to describe the input-output relationship based on input variables that are labeled and have a grounded truth (5).
Support vector machine:	A machine learning modality that can either solve classification tasks by creating a maximum margin hyperplane between two outcomes, or regression tasks by plotting a best-fit plane. Involves significant human engineering through kernel functions to transform data into higher dimensions (8).
Unsupervised learning:	Learner attempts to describe the input-output relationship based on input variables that are unlabeled. Typically associated with deep learning (9).

A BRIEF HISTORY OF ARTIFICIAL INTELLIGENCE AND DATA SCIENCE

The study of artificial intelligence (AI) originated back in the summer of 1956 when Dr. John McCarthy and contemporaries gathered at Dartmouth College. They “proceeded on the basis of the conjecture that every aspect of learning or any other feature of intelligence could in principle be so precisely described that a machine could be made to simulate it (10, 11).” While this meeting of great minds was significant, progress within AI has been undulating, with great successes followed by even greater failures. Notwithstanding, the recent establishment of larger data sets (or Big Data) has enabled scientists to overcome previous obstacles. During the advent of popularized AI in the 1980's, ~1% of humankind's information was available digitally. Presently, digital information technology accounts for 99% of data, which is estimated to be 5 zettabytes (5×10^{21} bytes) (12, 13). This amount of information is greater than the sum total if one were to store genomes from every person on Earth (1×10^{19} bytes) (14). At an individual level, one can appreciate the abundance of data stored in the cloud and the expansion of stored memory on a smartphone. Over the last decade, the United States healthcare system has also benefited from the Health Information Technology for Economic and Clinical Health (HITECH) Act, which spurred the adoption of electronic medical records (15). Experts have speculated that society is rapidly approaching a

point where the totality of data eclipses what can be extracted from nature itself (12). This massive amount of data has also been bolstered by large-scale commercialization of computing hardware, particularly graphics processing units or GPU (16). This increased accessibility of GPUs has allowed researchers to complete largescale machine learning tasks even at home, a feat unachievable in previous decades. Modern society is at a crossroads where we have access to inordinate amounts of data and hardware, but little guidance on how to extract meaningful information that is applicable to everyday life.

OVERVIEW OF MACHINE LEARNING

Machine Learning (ML) is a subset of AI that focuses on developing automated computer systems (*learners*) that predict outputs through algorithms and mathematics (7). The output represents the machine's interpretation of complex relationships that may be either linear or non-linear. Performance is graded according to its level of *discrimination* (probability of predicting outcomes accurately) and *calibration* (degree of over- or underestimating the predicted vs. true outcome) (17). Examples of ML applications encountered by spine surgeons include image classification [i.e., automated detection of vertebral body compression fractures on CT or MRI (18–20)], preoperative risk stratification models, clinical decision support tools (21–25), among others. The purpose of this review is to define basic

TABLE 2 | Summary of machine learning applications in this review.

Authors	Model(s)	Cohort	Type of outcome	Results
Burns et al. (18)	SVM	150 CT scans	Vertebral compression fractures	SVM achieved sensitivity of 98.7% with a false-positive rate of 0.29.
Hoffman et al. (26)	SVM	27 cervical myelopathy patients	Postoperative ODI score (regression)	SVM was more accurate than multivariate linear regression for postoperative ODI.
Hopkins et al. (27)	DNN	4,046 posterior spinal fusions	Surgical site infections	Neural network employed 35 input variables with a model AUC of 0.79.
Hopkins et al. (28)	DNN	23,264 posterior spinal fusions	30-day readmissions	Neural network AUC of 0.81. ACS NSQIP database study.
Karhade et al. (23)	ANN, BPM [†] , CART, SVM	1,790 cases of spinal metastatic disease	30-day postoperative mortality	Although the neural network had superior discrimination, the Bayes Point Machine was more calibrated and accurate overall.
Khan et al. (29)	CART, GAM [†] , MARS [†] , PLS [†] , RF, SVM	173 cervical myelopathy patients	SF-36	GBM and Earth models achieved AUC between 0.74 and 0.77 for predicting improvement in PCS-36 over the MCID.
Mehta and Sebro (30)	SVM	370 DEXA scans	Lumbar fracture	SVM detected incidental lumbar fractures on DEXA with an AUC of 0.93 and over 94% sensitivity and specificity.
Ogink et al. (22)	ANN, BDT [†] , BPM [†] , SVM	28,600 lumbar surgery patients	Non-home discharge	Neural network had the highest degree of discrimination and calibration. ACS NSQIP database study.
Seoud et al. (31)	SVM	97 adolescents with scoliosis	Scoliosis classification (C1, C2 C3)	100 surface topography measurements per patient. SVM with one-against-all strategy predicted 72% of cases.
Stopa et al. (21)	ANN	144 lumbar surgery patients	Non-home discharge	External validation of ANN developed by Ogink et al. validation AUC was 0.89 with 0.50 PPV and 0.97 NPV.
Tee et al. (32)	CART	806 traumatic spinal cord injury patients	Cluster analysis	Internal nodes included AIS grade, AOSpine injury morphology, anatomical region, and age. Six clusters were identified.
Vania et al. (33)	CNN	32 CT scans	Spine segmentation	Outcomes included spine, background, and two masking or redundant classifications. Sensitivity and specificity of the algorithm were above 96%.
Varghese et al. (34)	CART	27 pedicle screw pullout conditions	Pedicle screw pullout failure	Three input variables included foam density, screw depth, and screw angle. Correlation between observed and predicted pullout events was 0.99.

ANN, artificial neural networks; BPM, Bayes point machines; BDT, boosted decision trees; CART, classification and regression decision trees; CNN, convolutional neural networks; DNN, deep neural networks; GAM, generalized additive models; MARS, multivariable adaptive regression splines; PLS, partial least squares; RF, random forests; SVM, support vector machines. [†]Indicates machine learning modalities not discussed in this review.

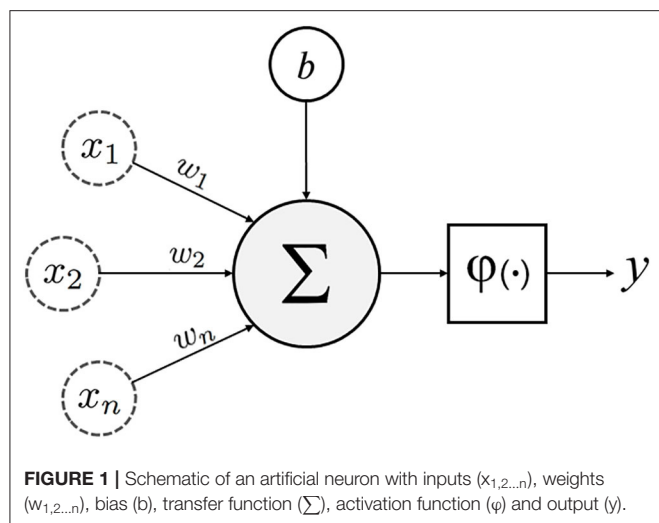
ML terminology, discuss the difference between ML and classical statistics, detail common ML models, and introduce examples in spine research. A summary of included references to machine learning applications in spine surgery and research are shown in **Table 2**.

Machine Learning Terminology

The two major forms of ML are supervised and unsupervised learning. **Supervised learning** entails labeled data based on a grounded truth (1, 5). For example, a database of lateral x-rays has films prelabeled as either “fracture” or “no fracture.” A portion of this data (**training dataset**) is analyzed to build a model that synthesizes the pattern between independent variables (i.e., pixel in an image) and dependent variables (presence or absence of pathology). Individual radiograph pixels in this example are known as **feature values** or **vectors** (1, 5). The remainder of the x-ray films (**untrained dataset**) are fed to the machine, which is then assessed based on its ability to accurately predict a fracture or otherwise. As such, supervised learning excels in

exercises of *linear classification* (where the outputs are discretely defined categories) or *linear regression* (where the outputs are continuous values).

Unsupervised learning, on the other hand, involves the analysis of unlabeled datasets, and stems from neuropsychology research conducted by Dr. Donald Olding Hebb (1, 9). **Hebbian theory** describes the general framework (**Figure 1**) of neurons and their synapses, which enable humans and other animals to learn relationships and store memories (6). The proposition being that among the multitudes of neurons in the brain, it is the distinct synaptic connections between neurons and their repetitive firing that enable learning (6). Unsupervised machines (like humans) can appreciate non-linear relationships and do so without presumptions related to the data. Unsupervised learners are particularly adept at identifying clusters of related variables, detecting anomalies, and constructing **artificial neural networks** (detailed later) (1, 35). While unsupervised learning is thought to be the standard for the future, most current ML examples in spine surgery and clinical medicine are of the supervised variety.

**TABLE 3 |** Classical Statistics vs. Machine Learning.

Classical statistics	Machine learning
(1) Originates from mathematics	(1) Originates from computer science
(2) Inferring relationships	(2) Building algorithms
(3) Quantifying uncertainty	(3) Predicting outcomes
(4) High degree of manual programming	(4) Learns from experience - less programming
(5) One model at a time	(5) Multiple models in parallel

Machine Learning vs. Classical Statistics

The delineation between machine learning and classical statistics is quite nebulous because learners are built upon statistical modeling (Table 3). Both modalities also rely on robust preprocessing of data that is representative of the general population. However, whereas statistics emerged from the field of mathematics, ML emerged from computer science. For purposes of simplification, the two concepts can be differentiated by the type of question needed to be answered. Classical statistics *infers* relationships between variables, while ML attempts to *predict* these relationships (36, 37). Inference (or statistics) involves testing the null vs. alternative hypothesis for an effect with a measurement of confidence. Prediction (or machine learning) involves forecasting outcomes without demanding as to why resultant relationships exist. It is also essential to highlight that while ML may appear to be more advanced than statistical analysis, neither is superior and both should be considered for predictive modeling.

To illustrate this further, a research question might ask, “What risk factors are associated with non-routine discharge after lumbar decompression and/or fusion?” In fact, multiple studies using classical statistics have already implicated that patients’ age, diabetes status, cardiovascular comorbidities, functional status, among others, all contribute to non-routine discharge (38–40). And with the expertise from practicing physicians, we can reason and clarify these findings. But translating these results in a clinical setting is complex, because it is unclear how one

weighs the importance of each variable when optimizing patients preoperatively. ML enables the development of tools that allow surgeons to plug-in variables and generate probabilities of a non-routine discharge. Ogink et al. recently developed learners to predict discharge to a rehabilitation or skilled nursing facility after surgery for lumbar stenosis using the American College of Surgeons National Surgical Quality Improvement Program (ACS-NSQIP) database (22). They built multiple models in parallel and ultimately arrived at a neural network that achieved high levels of discrimination and calibration with an Area Under the Curve (AUC) of 0.74 from a Receiver Operating Characteristics curve (22). This tool has since been externally validated in a smaller cohort, where 97% of patients were accurately predicted to return to home after elective lumbar surgery (21). Such algorithms warrant further independent validation, but they allow for synthesizing unwieldy large datasets in a practical way. Above all, the purpose of machine learning is *performance* based on indiscriminate analysis. But when practicing medicine, the ability of a learner to predict outcomes accurately must also take into consideration *how* and *why* it reaches such conclusions. This controversy of applying ML clinically is colloquially termed the *black box*, which will be discussed at the end of this review.

POPULAR MODELS FOR MACHINE LEARNING

With some basic ML terminology outlined, it is imperative that practicing physicians understand the architecture of learners encountered in peer-reviewed journals. Using examples from the spine literature, three ML modalities applicable to medicine will be discussed: (1) decision tree learning, (2) support vector machines, and (3) artificial neural networks. It is important to consider that while the following descriptions attempt to neatly categorize each model, they are flexible and can be adapted according to their needs. For example, support vector machines are often described as supervised models for linear classification, but there are many examples of them being used for unsupervised learning and non-linear classification exercises.

Decision Tree Learning

Decision tree learning, or more specifically, **Classification and Regression Trees (CART)** is one of the more straightforward modalities because it is better appreciated visually, rather than mathematically (3, 37, 41). By definition, a CART can analyze variables that are either categorical (classification) or continuous (regression). As shown in Figure 2, a CART is an upside-down tree with three major components (1) internal nodes, (2) branches, and (3) leaves (3, 41). **Internal nodes** are conditions by which the learner evaluates or measures variables. **Branches** are the decisions derived from each node. And **leaves** (or **terminal nodes**) represent ends of the tree where an output is finalized. The figure depicted is simplistic, and in a real-world application would only represent a branch of a much larger CART. But decision trees have a habit of becoming unnecessarily *deep* or involving too many layers of complexity. Trees with

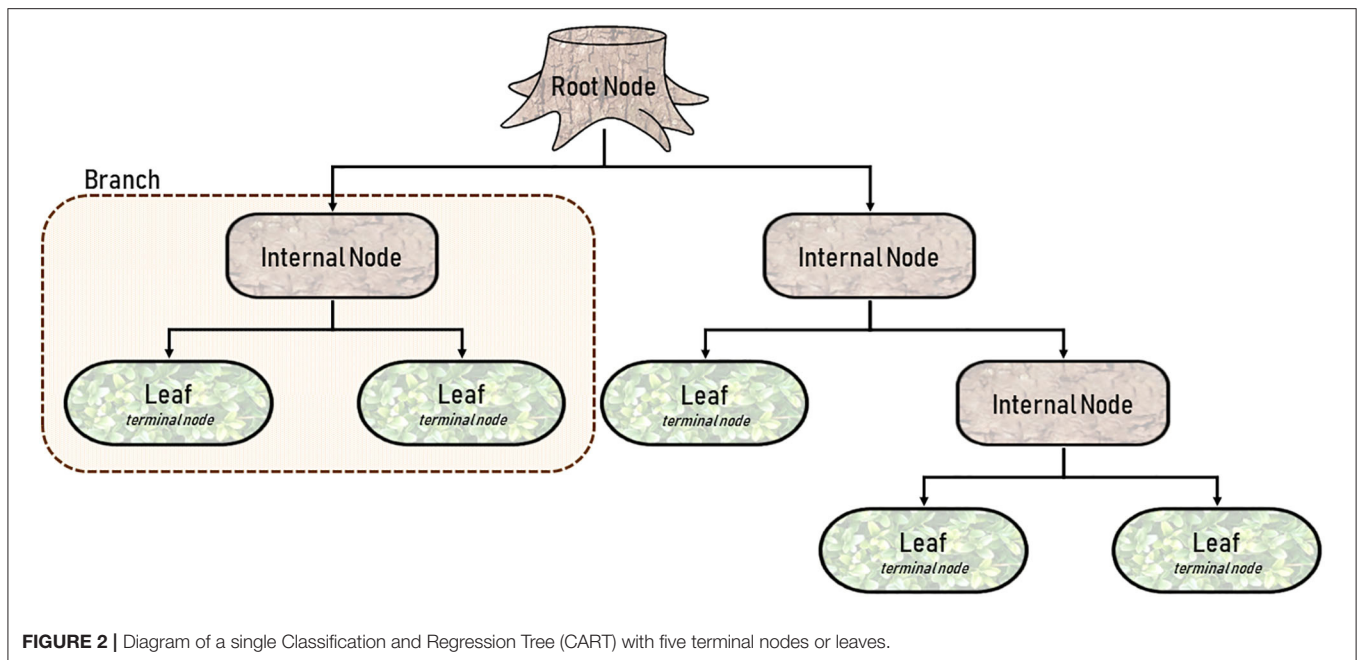


FIGURE 2 | Diagram of a single Classification and Regression Tree (CART) with five terminal nodes or leaves.

excessive internal nodes sub-divide data into too many small clusters, such that the outcomes are grouped in a way that are practically meaningless. A CART is a fundamentally *greedy algorithm* because it naturally satisfies the condition at each node, rather than optimizing conditions across the length of the tree (3). **Pruning**, as the name suggests, allows for incremental improvements in the tree by eliminating conditions that are less important. It is relevant here to discuss the concept of *fit* in both classical statistics and machine learning (42). An **underfitting** model has no utility because it poorly approximates potential relationships (Figure 5F). On the other hand, an **overfitting** model attempts to observe the smallest of associations making the model relevant only to the training dataset, and by consequence, poorly generalizable (Figure 5E) (42). In other words, overfitting learners pay too much attention to the noise in the dataset. Pruning and other adjustments are necessary to minimize overfitting and to limit the complexity of the tree, all the while optimizing accuracy.

Tee et al. application of decision tree learning for optimizing patient risk stratification after spinal cord injury provides a framework for understanding this modality (32). They combined different methods of assessing spinal cord function after trauma, including the American Spinal Injury Association (ASIA) Impairment Scale, total motor score (TMS) and the AOSpine classification system, to allow a decision tree to identify patient *clusters* that respond differently to treatment. As show in Figure 3, the cohort was first divided based on “ASIA grading (A-D)” (root node) and then evaluated at the first internal node, “AOSpine: A (compression), B (tension-band), or C (translational).” Interestingly, the learner concluded that it would be more worthwhile for the branches to keep A and B classifications together and C separate. The next internal node for each branch was binary, “cervical or thoracic injuries.” At this

level in the tree, three leaves (nodes 4, 5, and 6) were finalized as these clusters were considered homogenous enough and not worth sub-dividing further. For example, node 5 represents AOSpine C injuries in the cervical region, whereas node 6 represents AOSpine C injuries in the thoracic region. Finally, the branch containing AOSpine A and B injuries in the cervical spine were passed through another internal node for “age,” generating another three leaves or clusters. The final six clusters are detailed in Table 4 (32). The results of this study provide a platform for external validation studies with other patient cohorts to compare this unique classification system with current ones. Tee et al. findings exemplify machine learning’s ability to synthesize a multitude of variables that may associate non-linearly into a more easily digestible format. It is especially noteworthy that the investigators assembled a relatively large cohort of 806 patients for model building, a practice that is inconsistently applied in the spine literature.

The need for substantial patient datasets in spine surgery is particularly noticeable when exploring ML applications for predicting patient-reported outcomes. Exploratory investigations using decision tree learning have been pursued in spine research. Khan et al. utilized seven different supervised learners to predict improvement in SF-36 (PCS/MCS) scores after surgery for degenerative cervical myelopathy (29). The architecture of their model included multiple comorbidities, physical exam findings, imaging, baseline characteristics, among others. They set the minimal clinically important difference or MCID at +4.0 points for both PCS and MCS components of the SF-36. All seven learners were similarly accurate for predicting MCS improvement postoperatively, including their CART with an AUC of 0.74. However, no learner was particularly better than logistic regression (AUC 0.71), and the performance of the PCS model was by comparison poor. Moving forward, it is likely that

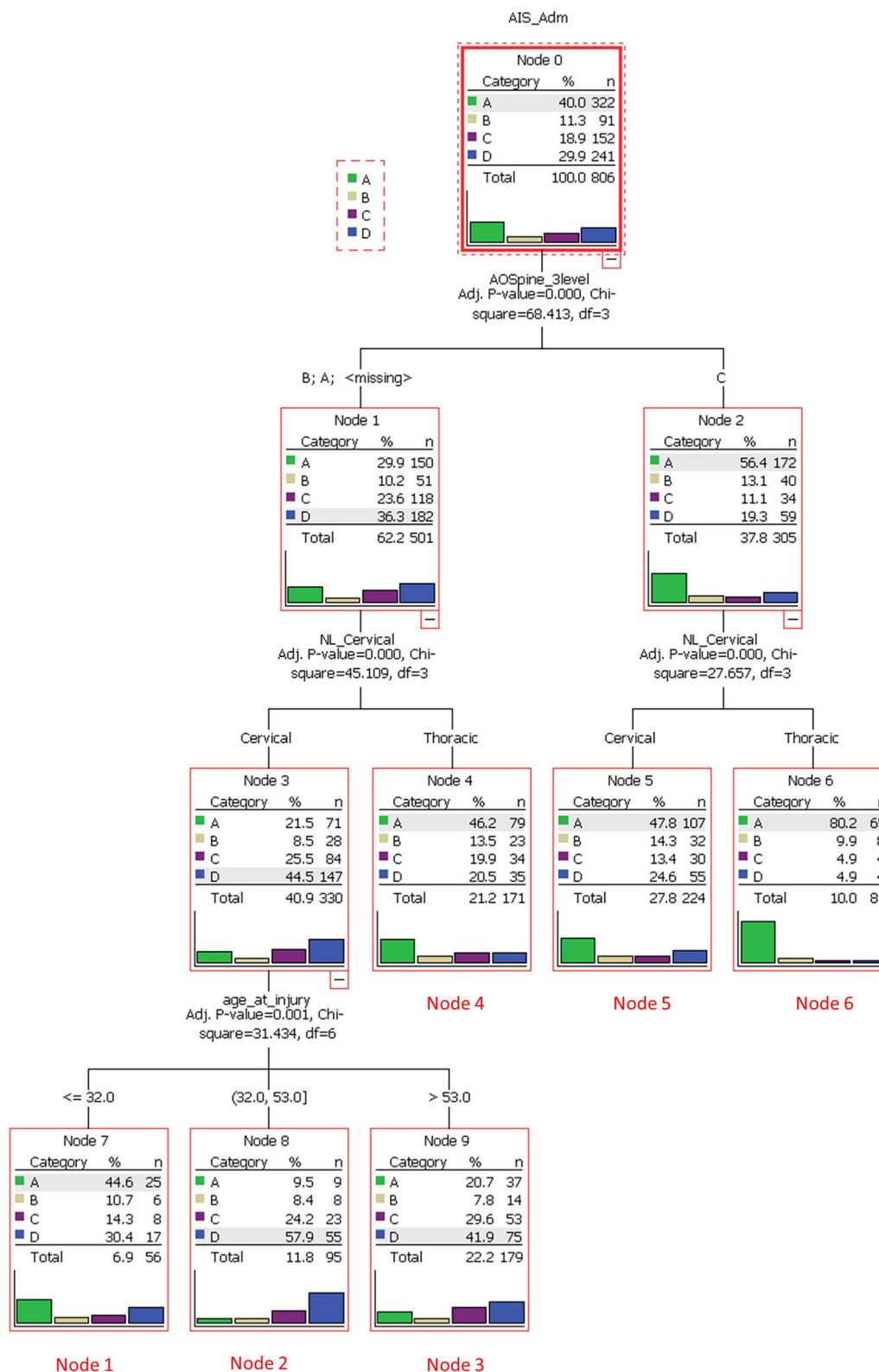


FIGURE 3 | A decision tree analysis to stratify spinal cord injury cases and to identify clusters of homogeneous patients that would respond similarly to treatment. The root node was based on the American Spinal Injury Association Impairment Scale (AIS), which ranged from grade A through D. The subsequent internal node was based on AOSpine injury classification (class A/B or C). Each branch then underwent another node based on anatomical region (cervical or thoracic). Class A/B cervical injuries were divided further based on age. Six unique terminal nodes or clusters were identified. Reproduced with permission by Tee et al. (32).

TABLE 4 | Final cluster analysis of spinal cord injury classifications based on decision tree learning.

Node	AOSC type	Level of injury	Age at injury (years)
1	A or B	Cervical	≤32
2	A or B	Cervical	>32–53
3	A or B	Cervical	>53
4	A or B	Thoracic	NA
5	C	Cervical	NA
6	C	Thoracic	NA

Reproduced with permission by Tee et al. (32).

AOSC, AOSpine injury morphology classification; NA, not applicable.

the spine literature will be inundated with publications running multiple statistical and ML models in parallel for comparative analysis. And while Khan et al. pilot investigation provides a framework for understanding machine learning, their sample size (130 training, 43 testing) leaves some concern as to the generalizability of the findings. The relationship between the natural history of spinal pathology, surgical interventions, and postoperative outcomes is delicate; and the proper use of ML for describing these relationships will require a multicenter and multidisciplinary effort to coalesce massive patient databases.

Lastly, decision tree learning can also help with characterizing medical device performance. Varghese and colleagues, using their own pedicle screw pullout strength protocol, showed that ML could be used to synthesize problems that have a large number of input permutations (34, 43). Their investigation involved the use of differing foam densities to mimic normal, osteoporotic, and extremely osteoporotic bone (**Figure 4A**). An actuator apparatus would then insert pedicle screws into the foam at three insertion angles, and three insertion depths (**Figure 4B**) (43). In total, 27 (3³) permutations of these variables were analyzed using four separate models to determine pullout failure (<650 Newtons of force) or success (≥650 Newtons of force) (**Figure 4C**). Varghese et al. produced a promising model with very low error rates and an AUC of 1.00 for predicting pedicle screw failure, which was internally validated against a separate set of novel permutations (i.e., different pedicle screw insertion angles and foam densities) (**Figure 6**) (34). Their best learner was actually a **random forest regression**, which like a CART, is a subtype of decision tree analysis (41). As the name suggests, random forests sample random batches of the data, form multiple trees, and then combine the findings to construct a singular tree. Random forests minimize overfitting and other biases by employing the *Law of Large Numbers*, such that the average of multiple trees is more accurate than a single tree. The final decision tree constructed for pedicle screw pullout failure is shown in **Figure 4E**.

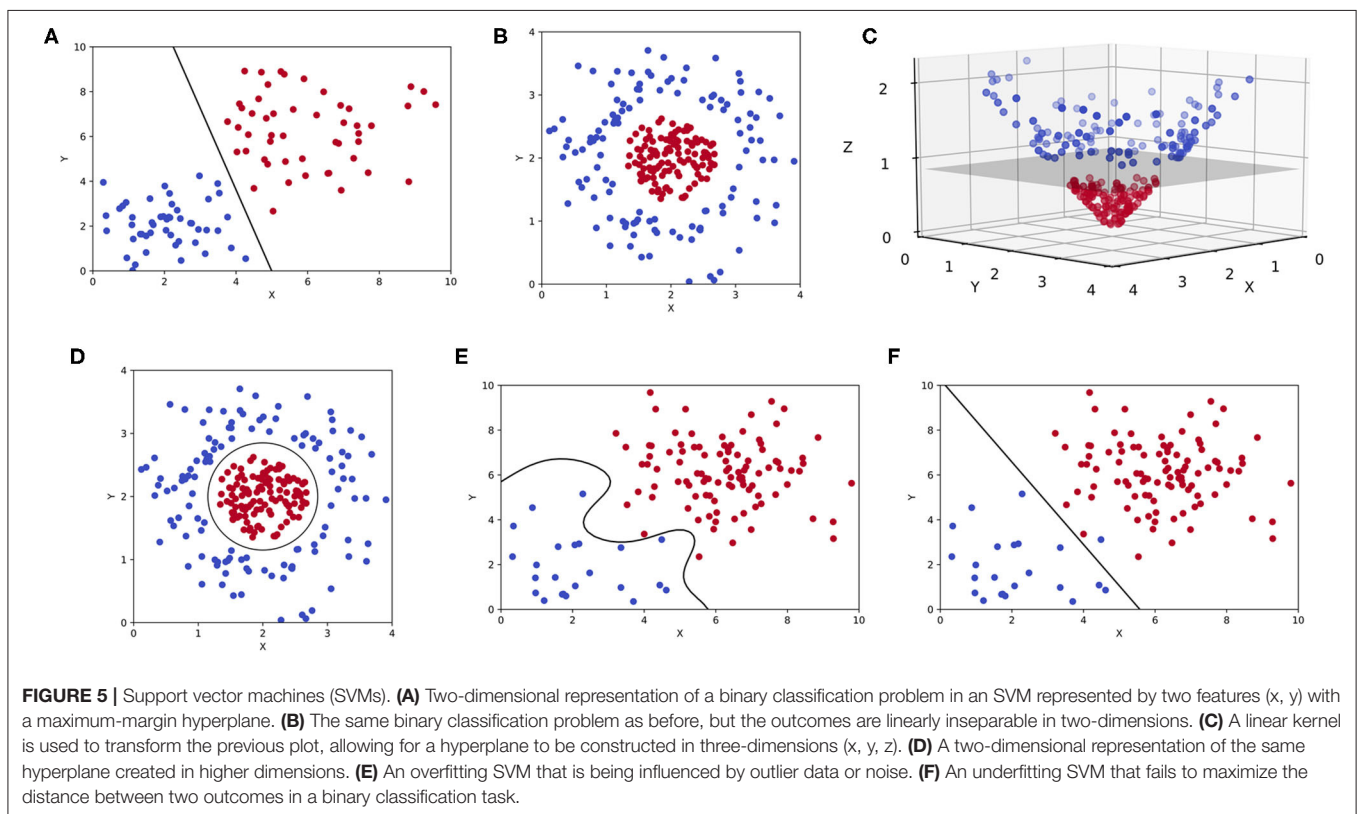
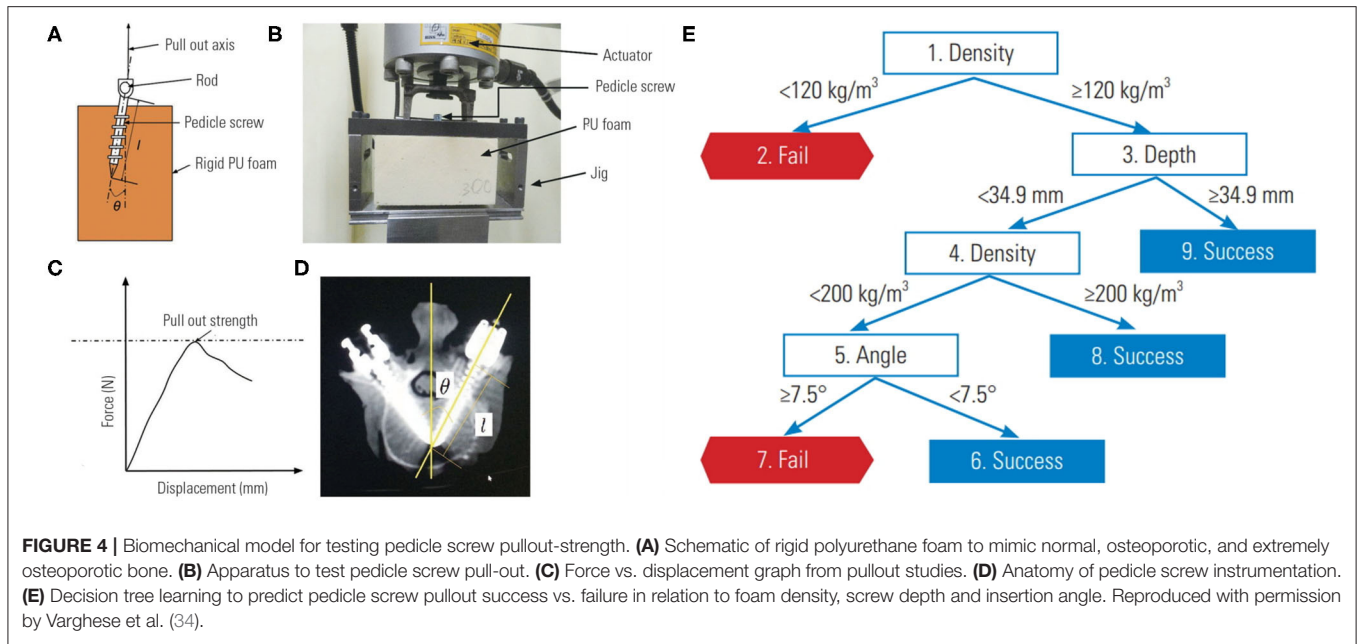
Support Vector Machines

Support vector machines (SVMs) are also a commonly encountered ML modality in clinical literature. SVMs are intuitive and best appreciated graphically as shown in **Figure 5**. Although comparable to CARTs in exercises of linear classification or regression, SVMs accomplish such goals by

constructing a **hyperplane** (8, 44). For a classification exercise, the hyperplane represents a line (or plane) that maximizes the distance between two categorical outcomes, which is also known as a *maximum-margin* hyperplane (**Figure 5A**). But as one can appreciate in **Figure 5B**, not all two-dimensional representations of data (only “x” and “y” coordinates) can be separated linearly with a hyperplane in that same dimension. Often, mathematical transformations or **kernel functions** are needed to transform the data into a *higher* dimension (44). As shown in **Figure 5C**, the same dataset plotted in three dimensions (3D) can be easily separated by a hyperplane. This transformation is prototypical and involves the inclusion of a “z” coordinate that equates the product of x and y, such that each outcome is plotted in 3D as (x,y,z) or (x,y,x*y). This is also known as a *linear kernel*. The byproduct of an SVM for an otherwise linearly inseparable dataset is shown in **Figure 5D**, where higher dimensional hyperplanes are represented as a circle in lower dimensions. However, like pruning, kernels can be overly extrapolated leading to overfitting and generating sub-clusters of outcomes that are incidental and practically meaningless (**Figure 5E**).

Delving into the literature, SVMs are popular for classifying and detecting the presence of spine pathology on imaging. For example, a common problem when managing patients with osteoporosis arises from missed fractures on routine DEXA (Dual-Energy X-Ray Absorptiometry) scans (30). Given separate management guidelines for osteoporotic patients with and without fractures, Mehta and Sebro developed a model to detect incidental lumbar spine fractures from a large cohort of routine DEXA scans (30). The two outcomes or classifiers were “control” and “fracture.” The input variables to characterize the model included baseline demographics and ancillary data from the DEXA scan (i.e., bone mineral density, Z-scores, T-scores, among others). They conducted four SVMs in parallel, using different types of kernel functions, but ultimately arrived at a linear kernel with a high AUC of 0.93 against the training set, and an AUC of 0.90 against the test set (30). Their investigation exemplifies the potential of ML for automated detection of pathology. Such innovation can minimize missed diagnoses that are critical to quality care, especially in this case for incidental lumbar fractures on routine DEXA, where the error rate has been reported to be as high as 15.8% (45).

Another example of an image classification task achieved through SVMs was conducted by Seoud et al. The investigators attempted to determine scoliosis curve based on a modified Lenke classification system (C1, C2, or C3) for adolescents by analyzing surface topography data captured by multiple cameras (31). As a learning point, this is an example of applying SVMs with 3 outcomes (or classifications) instead of two. Seoud and colleagues addressed this problem by opting for a “one-against-all” approach, where the model compares C1 scoliosis curves to C2/C3 curves (46). And as discussed previously, the learner finds the ideal dimension where the outcomes can be linearly separated with the largest margin of distance between points. In this example, an overfitting model would be one where the SVM describes sub-clusters of scoliosis classifications that are clinically irrelevant. Seoud et al. model for classification based on topography alone accurately predicted over 72% of cases (31).



In addition to image classification tasks, SVMs have also been applied for predicting outcomes after spine surgery. Hoffman et al. prospectively evaluated patients undergoing surgery for degenerative cervical myelopathy, and attempted to predict postoperative outcomes including Oswestry Disability Index (ODI), modified Japanese Orthopedic Association scale (mJOA),

and handgrip pressure (26). Their model illustrated how SVMs can also be used for regression. In contrast to classification, support vector *regressions* involve hyperplanes that *minimize* the distance between variables because the goal is to predict a continuous variable rather than a discrete one. Hoffman and colleagues also constrained the model to three input variables

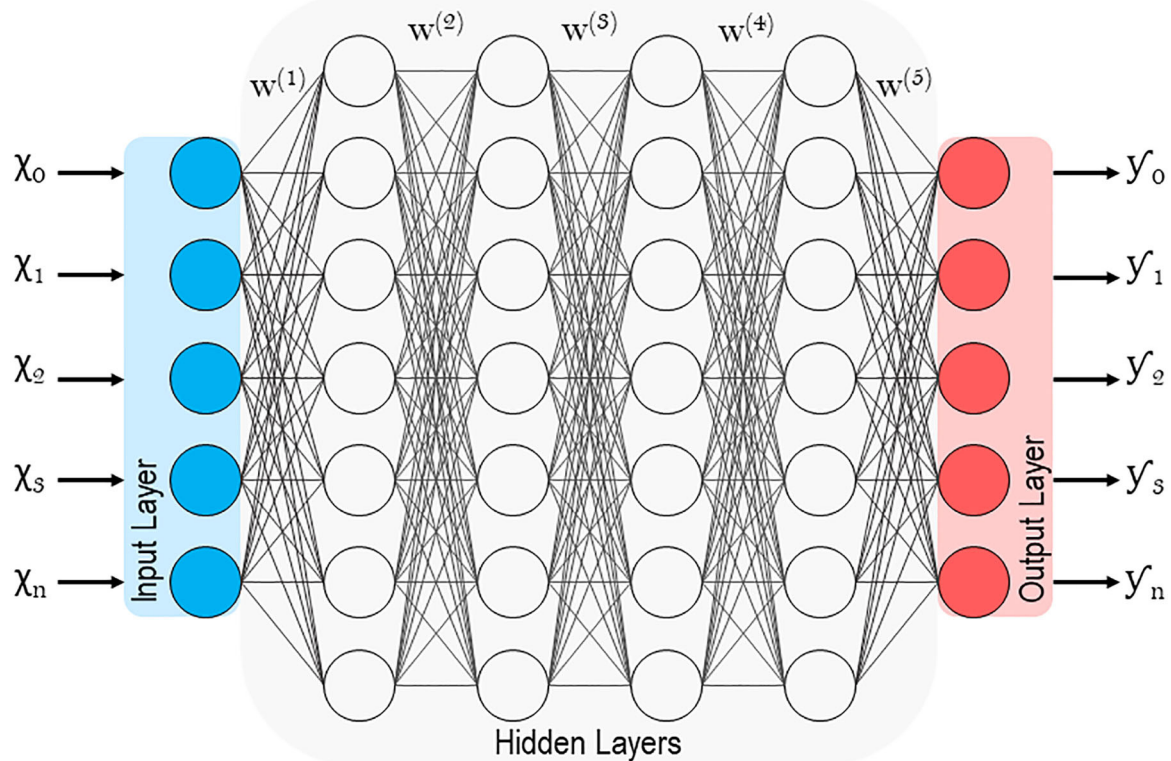


FIGURE 6 | Schematic of a deep artificial neural network with multiple hidden layers.

in order to curtail overfitting, which included preoperative ODI, symptom duration, and handgrip pressure. When compared to a traditional multiple linear regression, they achieved a higher goodness-of-fit or R^2 of 0.93 via the SVM (26). While the prospective study design was a strength, the cohort was limited to only 20 patients. Herein lies the perpetual conflict between statistical power and generalizability when using ML. Models for predicting risk necessitate prospective data, but the feasibility of large datasets is limited to national databases, which are likely heterogeneous and retrospective.

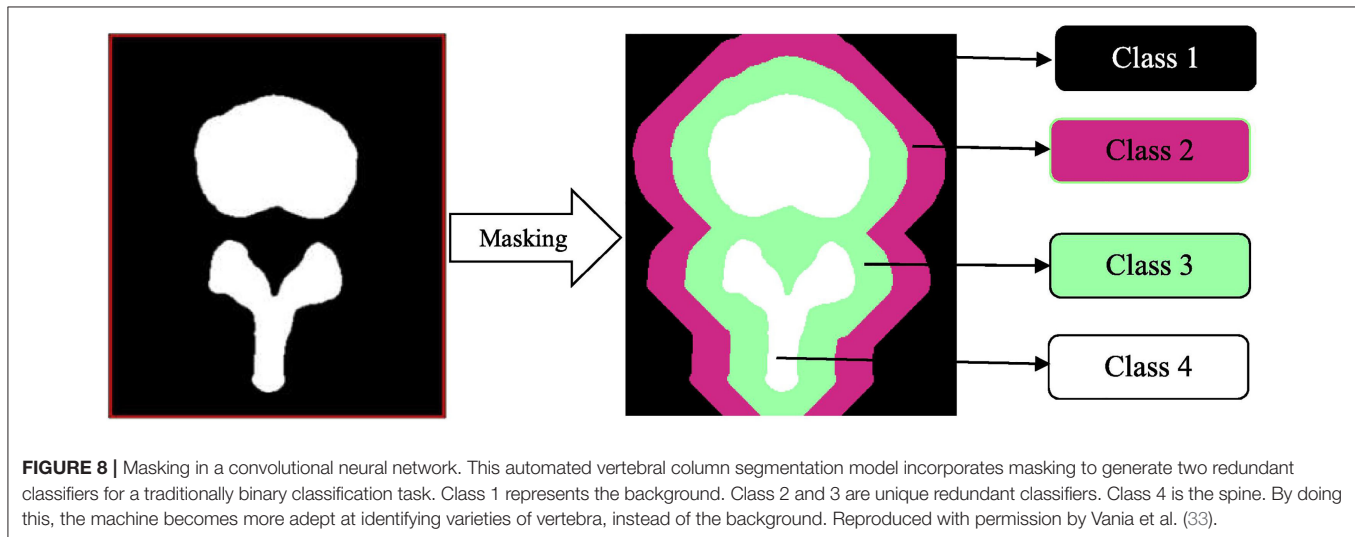
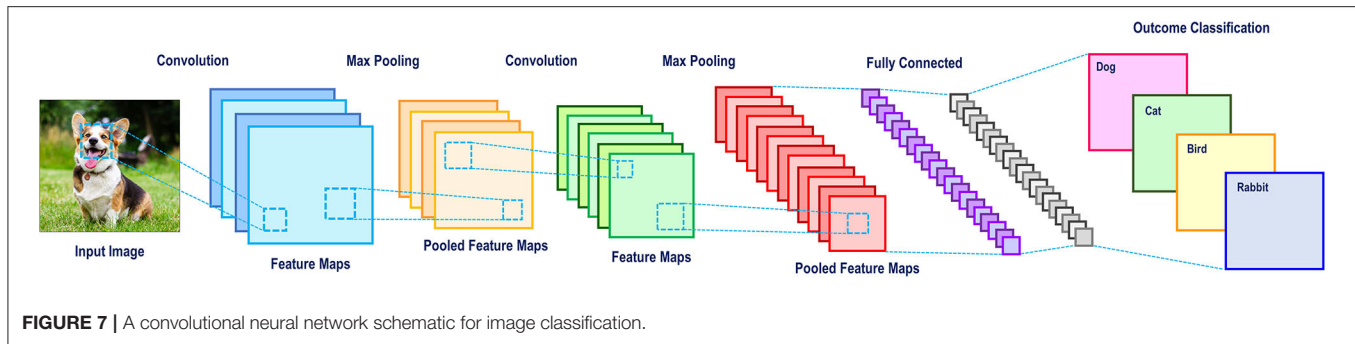
Overall, SVMs are well-suited for general purpose machine learning (particularly in medicine) because tuning kernels allows for clinicians to assign appropriate weights according to their knowledge in that field (8). SVMs are also excellent tools for problems dealing with *high dimensional* data where the number of features far exceeds the number of observations or samples (47). Common examples of high dimensional data in clinical medicine include baseline demographics, preoperative risk factors, or gene expression levels. However, if the separation between two outcomes is unclear within a reasonable number of dimensions, SVMs struggle. And because SVMs are overly reliant on finely tuned kernels, the resultant models are only applicable to solving single problems (i.e., tools for predicting outcomes for cervical vs. lumbar surgery have to be separately and manually engineered). Counterintuitive to what has been discussed, SVMs are not proficient with very large data sets where the number of observations far exceed features (opposite of high dimensional

data). As the number of points or samples increase, so does the noise, generating far too many outliers above and below the hyperplane (48).

Artificial Neural Networks

Lastly, **Artificial neural networks (ANNs)** are of particular interest because they are associated with **deep learning**, which has been traditionally unsupervised (1, 49, 50). Supervised models, as discussed previously, involve feature values that are highly discriminatory because they have been meticulously engineered with intricate knowledge of the subject matter (in this case spine surgery) (48). Deep learning circumvents this through **representation learning**, where the learner automatically classifies raw unlabeled data (51). With minimal human engineering, these unsupervised learners generate highly discriminatory feature extractors that characterize the input-output relationship, while ignoring irrelevant variations. Like in **Figure 6**, ANNs extrapolate the single neuron construct in Hebbian learning into an entire network where **hidden layers** or *intermediate representations* help refine the network of input-output synapses between artificial neurons (1). For a more technical and in-depth review of deep learning and ANNs please refer to the work by Emmert-Streib et al. (52)

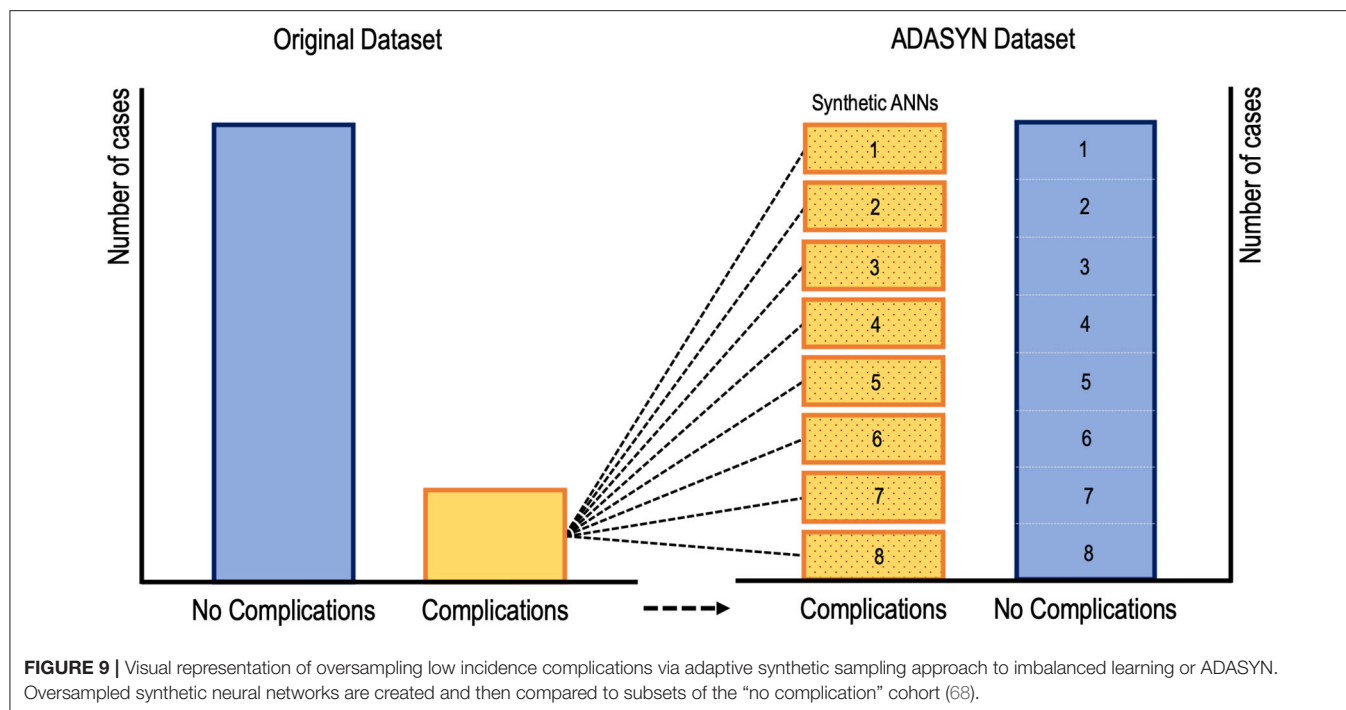
ANNs are adept in computer vision (53–56), natural language processing (51, 57), and predicting downstream effects of genetic mutations (58–60). Computer vision is of interest to spine surgeons as it may potentially increase the efficiency and accuracy



of reporting patient imaging. The classical computer vision task is identifying a “dog” in a photo (**Figure 9**). Manually extracting features is near impossible because no two photos of dogs are the same. Practically, humans recognize dogs in photos despite variations in their pose, environment, lighting or orientation of the photo, among others. However, machines can only interpret pixels in an image, none of which are specific to a dog. **Convolutional neural networks (CNNs)**, with the help of multiple hidden layers, are particularly adept at computer vision tasks and can be visualized graphically in **Figure 7**. The first hidden layer in a CNN *convolves* or filters the native input, extracting the “important” information and generates a **feature map** (a representation of the input). Subsequent **max-pooling** reduces complexity and minimizes overfitting by creating a more abstract form of the previous feature map and thus more applicable to generic pictures of dogs. This process can be repeated for the desired number of hidden layers. Once all feature maps have been considered, the images are *flattened* and the desired output (dog or otherwise) can be generated. In many ways, CNNs are more so learning to identify small arrangements or *motifs* that resemble dogs. This concept is known as **local connectivity**, meaning two neighboring pixels are considered more relevant than two distant pixels (61). Interestingly, CNNs structurally resemble the hierarchy and

pathway used by the human visual cortex found in the occipital lobe (62). Multilayer neural networks like these are also essential for the development of fully automated robots and self-driving automobiles (57).

In spine surgery, computer vision technology has risen in parallel with the use of computer assisted navigation, robotic surgery, and augmented reality in the operating room, all of which require high fidelity 3D reconstructions of the spinal column from computed tomography or magnetic resonance imaging scans (33, 63–67). This is achieved through automated segmentation and detection of vertebrae via ANNs. Vania et al. recently reported the results of their CNN for automated vertebral column segmentation with a unique classification system (33). Instead of the traditional classifiers of “vertebrae” vs. “not vertebrae,” they implemented four classifications (background, spine, and two redundant classifiers) as show in **Figure 8** (33). They did this in order to minimize overfitting so that the learner could consider variabilities in vertebral width and length outside of the training dataset. Their model generated a sensitivity and specificity of 0.97 and 0.99, respectively, both of which were either better or comparable to other commonly applied methods (33). In addition to spinal segmentation, significant strides have also been made in automated detection of vertebral compression and posterior element fractures, as well



as the grading of lumbar stenosis (18–20, 54). The potential for successful translation for preoperative and intraoperative care is promising in spine surgery. For example, automation would allow for consistent application of sagittal deformity parameters by minimizing manual measurements and displaying associated risk factors all in one software ecosystem.

While supervised learners, including CARTs and SVMs, have been used to predict postoperative outcomes, there is evidence to suggest that ANNs may be the preferred method for such tasks going forward (22, 23, 27, 28, 68). Kim et al. utilized an ANN to predict cardiac and wound complications, venous thromboembolism (VTE), and mortality rates after posterior lumbar fusion from an ACS-NSQIP cohort (68). Their learner was rather informative because they addressed the problem of low complication incidence by applying ADASYN (adaptive synthetic sampling approach to imbalanced learning). As shown in **Figure 9**, ADASYN generates multiple synthetic cohorts with positive complications that can be compared with controls, essentially creating multiple ANNs with different weights. The final ANN achieved an AUC of 0.71 for predicting cardiac complications postoperatively, which was superior to both logistic regression and American Society of Anesthesiologists (ASA) score (68). However, the regression model proved to be superior to the ANN for predicting VTE, mortality, and wound complications. In another investigation, Hopkins et al. applied an ANN with 35 input variables on over 4,000 cases of posterior spinal fusions to predict surgical site infections (27). Their model reliably predicted both infected and non-infected cases with an AUC of 0.79 across all their neural network iterations. However, the model unexpectedly demonstrated that intensive care unit admission and increasing Charlson Comorbidity Score were *protective* against surgical site infections, both findings of

which are contradictory to the literature (27). The inability to interpret what seems like inconsistent findings is a key dilemma when applying ML in clinical medicine. Though, it is possible that such associations exist in a non-linear fashion that cannot be appreciated intuitively. And while surgeon’s acumen and experience must be integrated with decision support tools, there is still significant deficits in these models before they can be safely (and without hesitancy) applied when patient lives are at stake.

FUTURE PERSPECTIVES ON MACHINE LEARNING AND SPINE SURGERY

Machine learning and artificial intelligence are progressively becoming more commonplace in modern society. We all in some ways either actively or passively contribute to Big Data through the use of smartphones, online shopping, wearables, among other activities even unbeknown to us. Moreover, the average physician is even more “plugged-in” to the modern technological ecosystem, given the use of electronic medical records, decision support tools, and imaging software. In spine surgery specifically, the nature of dealing with vital anatomic structures in the operating room instills an eagerness for innovations that might balance operative efficiency, patient safety, and surgical outcomes. Machine learning is at the core of AI advancement in healthcare and there are definite reasons for optimism.

As discussed previously, machine learning applications for computer vision will continue to optimize computer assisted navigation systems used by spine surgeons. AI implementation in the operating room has begun to transcend beyond what was previously possible through the use of augmented or

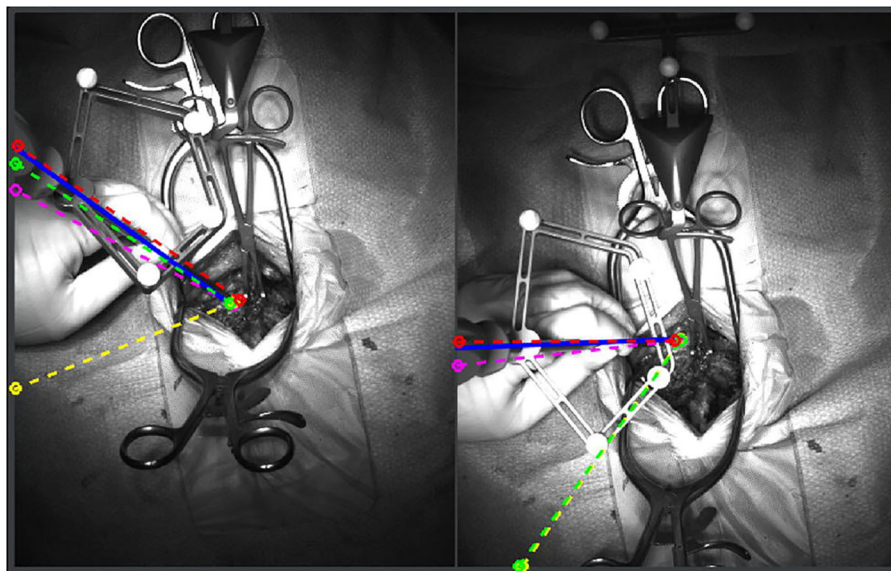


FIGURE 10 | Augmented reality system that superimposes pedicle screw trajectories from computer assisted navigation onto the operating field. By minimizing the need to memorize trajectories from a separate screen, the surgeon is more readily able to identify safe zones. The blue, red, pink, yellow, and green lines represent correct, medial, lateral, superior and inferior breaches, respectively. Reproduced with permission by Nguyen et al. (69).

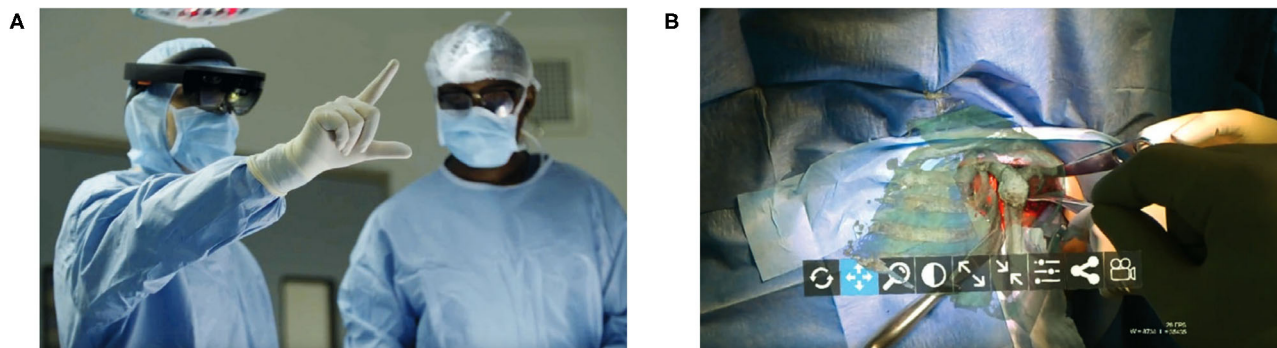


FIGURE 11 | A proof of concept application of *Microsoft HoloLens* for reverse total shoulder arthroplasty. **(A)** The surgeon is able to view in real-time and place in space a 3D hologram from a CT of the patient's scapula. **(B)** A 3D hologram of the patient's scapula is superimposed intraoperatively in order to fully visualize the glenoid and other relevant anatomy. Reproduced with permission by Gregory et al. (74).

mixed reality (69–72). Nguyen et al. in a trial of augmented reality for pedicle screw insertion with navigation, designed a virtual road map that was superimposed on the surgical site of patients undergoing spinal fusion (69). Their intention was to address the underlying obstacle of surgeons memorizing optimal screw trajectory provided by navigation, which is typically displayed away from the surgical site. By installing two overhead stereoscopic cameras, they coordinated intraoperative video with data sourced from the navigation's infrared tracking system. A representation of their innovative design is shown in **Figure 10** (69). While they did not attempt to display their augmented reality system through a headset, other investigators have undertaken pilot studies as proof of concept with devices such as the *Microsoft HoloLens* (71–75). In the shoulder arthroplasty

literature, Gregory et al. presented a proof of concept study using the *HoloLens* to superimpose a 3D hologram of a patient's scapula in real time during a shoulder replacement (74). This application of mixed reality in the operating room was impressive because the headset did not need to be synced to a navigation system, the hologram could be adjusted in space, and the surgeon's point-of-view could be teleconferenced to others (**Figure 11**). Looking forward, these innovations in computer vision for the spine may also pave the way for significant improvements for surgical robots. Spine surgery robots presently appear rudimentary when compared to those utilized for minimally invasive gastrointestinal, urologic, and gynecologic surgeries. And while there is little reported on even a semi-automated robot for the spine, machine learning advancements may change

this trajectory as it has for self-driving cars. However, spine surgeons (for patient safety concerns) may purposefully interact with robots in a *slave-and-master* paradigm in order to maintain total control over the machine. Using the five levels of autonomy described by the Society of Automotive Engineers, ranging from “no” to “full” automation, experts have postulated that clinical medicine may only ever incorporate up to “conditional” automation, where the machine both drives and monitors the circumstances, but humans are available for backup (9, 76).

Finally, as foreshadowed in the *Overview of Machine Learning* section, a major component of artificial intelligence research involves the ethical challenges of implementing machine learning for clinical practice (2, 4, 77–79). This has colloquially been termed the **black box**, which is the near impossible task of interpreting or explaining as to how a learner reaches the conclusions that it does, no matter how accurate it is (2, 4). And though the black box is typically attributed to ANNs and deep learning, it is also problematic for supervised learning. If a machine is learning non-linear associations in a manner that is hidden from both the engineer and the consumer, there will undoubtedly be apprehension toward the safety of an otherwise promising tool. As described by Dr. Alex John London, a professor of philosophy and artificial intelligence at Carnegie Mellon University, “the most powerful machine learning techniques seem woefully incomplete because they are atheoretical, associantist, and opaque.” As mentioned earlier in the study by Hopkins et al. for predicting surgical site infections, their neural network operated according to associations that oppose what spine surgeons consider grounded truths (27). To characterize this further, Caruana and colleagues published an infamous and equally informative machine learning model for predicting mortality after inpatient admission for pneumonia. While their learner was accurate, it reasoned that asthmatic patients with pneumonia should receive *less aggressive* care because on average they do better than non-asthmatics with pneumonia (80). This suggested course of action was in direct opposition to modern management guidelines for asthmatics, who are regularly provided the *most aggressive* care. However, Caruana et al. learner was not attuned to such contextual guidelines. Thus, from a prediction standpoint, asthmatics with pneumonia in an intensive care unit were observed (by the model) as experiencing better outcomes relative to the general

population that is treated more conservatively. This harkens back to the point previously discussed regarding the importance of understanding exactly which question the model is being asked to answer. Beyond the black box, other ethical and logistical obstacles in machine learning in medicine include **distributional shift** (training datasets that may be biased toward race or socioeconomic status or simply outdated), **insensitivity to impact** (predictive tools that underestimate the consequences of a false positive or false negative outcome), and **reward hacking** (the machine learns unexpected means of achieving an outcome that cheat the system) (4).

While the challenge of explaining machine learning’s method for reasoning persists, it draws some similarities to the way clinical medicine is practiced in the present. Physicians, much like deep learners, often treat patients using some component of their clinical experience or *gestalt* (difficult to explain) in addition to their technical knowledge (easy to explain). And the solution to this problem may involve a combination of (1) accepting the black box of machine learning, and (2) testing them rigorously against multiple patient cohorts (79). Altogether, these examples from the literature suggest the need for a healthy level of skepticism toward machine learning, and a willingness to appreciate its methodology.

AUTHOR CONTRIBUTIONS

MC and NP were responsible for reviewing publications for inclusion in the review, drafting of the manuscript, and creating table and figures for the manuscript. JC and KN were responsible for critical revision of the manuscript for important intellectual content related to machine learning methodology and spine surgery research. AV was responsible for the conception of the review, supervision, and critical revision of the manuscript for important intellectual content. All authors contributed to the article and approved the submitted version.

FUNDING

This study was funded internally by the Rothman Orthopaedic Institute and the Department of Orthopaedic Surgery at Thomas Jefferson University.

REFERENCES

1. LeCun Y, Bengio Y, Hinton G. Deep learning. *Nature*. (2015) 521:436. doi: 10.1038/nature14539
2. Watson DS, Krutzinna J, Bruce IN, Griffiths CE, McInnes IB, Barnes MR, et al. Clinical applications of machine learning algorithms: beyond the black box. *BMJ Clin Res Ed*. (2019) 364:l886. doi: 10.1136/bmj.l886
3. Krzywinski M, Altman N. Classification and regression trees. *Nat Methods*. (2017) 14:757–8. doi: 10.1038/nmeth.4370
4. Challen R, Denny J, Pitt M, Gompels L, Edwards T, Tsaneva-Atanasova K. Artificial intelligence, bias and clinical safety. *BMJ Qual Saf*. (2019) 28:231–7. doi: 10.1136/bmjqs-2018-008370
5. Panchmatia JR, Visenio MR, Panch T. The role of artificial intelligence in orthopaedic surgery. *Brit J Hosp Med*. (2018) 79:676–81. doi: 10.12968/hmed.2018.79.12.676
6. Munakata Y, Pfaffly J. Hebbian learning and development. *Developmental Sci*. (2004) 7:141–8. doi: 10.1111/j.1467-7687.2004.00331.x
7. Jordan MI, Mitchell TM. Machine learning: trends, perspectives, and prospects. *Science*. (2015) 349:255–60. doi: 10.1126/science.aaa8415
8. Noble WS. What is a support vector machine? *Nat Biotechnol*. (2006) 24:1565–7. doi: 10.1038/nbt1206-1565
9. Topol EJ. High-performance medicine: the convergence of human and artificial intelligence. *Nat Med*. (2019) 25:44–56. doi: 10.1038/s41591-018-0300-7
10. Russell SJ, Norvig P. *Artificial Intelligence: A Modern Approach*. 3rd ed. NJ: Pearson Education (2010).
11. McCarthy J, Minsky ML, Rochester N, Shannon CE. A proposal for the dartmouth summer research project on artificial intelligence. *AI Magazine*, Palo Alto, CA (2006) 27:12.

12. Gillings MR, Hilbert M, Kemp DJ. Information in the Biosphere: Biological and Digital Worlds. *Trends Ecol Evol.* (2016) 31:180–9. doi: 10.1016/j.tree.2015.12.013
13. Hilbert M, López P. The World's Technological Capacity to Store, Communicate, and Compute Information. *Science.* (2011) 332:60–5. doi: 10.1126/science.1200970
14. Landenmark HKE, Forgan DH, Cockell CS. An Estimate of the Total DNA in the Biosphere. *PLoS Biol.* (2015) 13:e1002168. doi: 10.1371/journal.pbio.1002168
15. Ratwani RM, Reider J, Singh H. A decade of health information technology usability challenges and the path forward. *JAMA.* (2019) 321:743. doi: 10.1001/jama.2019.0161
16. Mittal S, Vaishay S. A survey of techniques for optimizing deep learning on GPUs. *J Syst Architect.* (2019) 99:101635. doi: 10.1016/j.sysarc.2019.101635
17. Alba AC, Agoritsas T, Walsh M, Hanna S, Iorio A, Devereaux PJ, et al. Discrimination and calibration of clinical prediction models. *JAMA.* (2017) 318:1377. doi: 10.1001/jama.2017.12126
18. Burns JE, Yao J, Summers RM. Vertebral body compression fractures and bone density: automated detection and classification on CT images. *Radiology.* (2017) 284:788–97. doi: 10.1148/radiol.2017162100
19. Bar A, Wolf L, Amitai OB, Toledano E, Elnekave E. Compression fractures detection on CT. *Proceeding.* (2017) 10134:40–8. doi: 10.1117/12.2249635
20. Frighetto-Pereira L, Rangayyan RM, Metzner GA, Azevedo-Marques PM de, Nogueira-Barbosa MH. Shape, texture and statistical features for classification of benign and malignant vertebral compression fractures in magnetic resonance images. *Comput Biol Med.* (2016) 73:147–56. doi: 10.1016/j.combiomed.2016.04.006
21. Stopa BM, Robertson FC, Karhade AV, Chua M, Broekman MLD, Schwab JH, et al. Predicting nonroutine discharge after elective spine surgery: external validation of machine learning algorithms. *J Neurosurg Spine.* (2019) 26:1–6. doi: 10.3171/2019.5.SPINE1987
22. Ogink PT, Karhade AV, Thio QCBS, Gormley WB, Oner FC, Verlaan JJ, et al. Predicting discharge placement after elective surgery for lumbar spinal stenosis using machine learning methods. *Eur Spine J.* (2019) 28:1433–40. doi: 10.1007/s00586-019-05928-z
23. Karhade AV, Thio QCBS, Ogink PT, Shah AA, Bono CM, Oh KS, et al. Development of machine learning algorithms for prediction of 30-day mortality after surgery for spinal metastasis. *Neurosurgery.* (2018) 85:E83–91. doi: 10.1093/neuros/nyy469
24. Thio QCBS, Karhade AV, Ogink PT, Raskin KA, Bernstein KDA, Calderon SAL, et al. Can machine-learning techniques be used for 5-year survival prediction of patients with chondrosarcoma? *Clin Orthop Relat R.* (2018) 476:2040–8. doi: 10.1097/CORR.0000000000000433
25. Ramkumar PN, Karnuta JM, Navarro SM, Haeblerle HS, Iorio R, Mont MA, et al. Preoperative prediction of value metrics and a patient-specific payment model for primary total hip arthroplasty: development and validation of a deep learning model. *J Arthroplast.* (2019) 34:2228–34.e1. doi: 10.1016/j.arth.2019.04.055
26. Hoffman H, Lee SI, Garst JH, Lu DS, Li CH, Nagasawa DT, et al. Use of multivariate linear regression and support vector regression to predict functional outcome after surgery for cervical spondylotic myelopathy. *J Clin Neurosci.* (2015) 22:1444–9. doi: 10.1016/j.jocn.2015.04.002
27. Hopkins BS, Mazmudar A, Driscoll C, Svet M, Goergen J, Kelsten M, et al. Using artificial intelligence (AI) to predict postoperative surgical site infection: a retrospective cohort of 4046 posterior spinal fusions. *Clin Neurol Neurosurg.* (2020) 192:105718. doi: 10.1016/j.clineuro.2020.105718
28. Hopkins BS, Yamaguchi JT, Garcia R, Kesavabhotla K, Weiss H, Hsu WK, et al. Using machine learning to predict 30-day readmissions after posterior lumbar fusion: an NSQIP study involving 23,264 patients. *J Neurosurg Spine.* (2019) 32:1–8. doi: 10.3171/2019.9.SPINE19860
29. Khan O, Badhiwala JH, Witwi CD, Wilson JR, Fehlings MG. Machine learning algorithms for prediction of health-related quality-of-life after surgery for mild degenerative cervical myelopathy. *Spine J Official J North Am Spine Soc.* (2020) 1–11. doi: 10.1016/j.spinee.2020.02.003. [Epub ahead of print].
30. Mehta SD, Sebros R. Computer-aided detection of incidental lumbar spine fractures from routine dual-energy X-ray absorptiometry (DEXA) studies using a support vector machine (SVM) classifier. *J Digit Imaging.* (2019) 33:1–7. doi: 10.1007/s10278-019-00224-0
31. Seoud L, Adankon MM, Labelle H, Dansereau J, Cheriet F. Prediction of scoliosis curve type based on the analysis of trunk surface topography. In: *2010 IEEE Int Symposium Biomed Imaging Nano Macro.* Rotterdam (2010) p. 408–11. doi: 10.1109/ISBI.2010.5490322
32. Tee JW, Rivers CS, Fallah N, Noonan VK, Kwon BK, Fisher CG, et al. Decision tree analysis to better control treatment effects in spinal cord injury clinical research. *J Neurosurg Spine.* (2019) 31:1–9. doi: 10.3171/2019.3.SPINE18993
33. Vania M, Mureja D, Lee D. Automatic spine segmentation from CT images using convolutional neural network via redundant generation of class labels. *J Comput Des Eng.* (2019) 6:224–32. doi: 10.1016/j.jcde.2018.05.002
34. Varghese V, Krishnan V, Kumar GS. Evaluating Pedicle-Screw Instrumentation Using Decision-Tree Analysis Based on Pullout Strength. *Asian Spine J.* (2018) 12:611–21. doi: 10.31616/asj.2018.12.4.611
35. Galbusera F, Casaroli G, Bassani T. Artificial intelligence and machine learning in spine research. *Jor Spine.* (2019) 2:e1044. doi: 10.1002/jsp.2.1044
36. Bzdok D, Altman N, Krzywinski M. Statistics versus machine learning. *Nat Methods.* (2018) 15:233–4. doi: 10.1038/nmeth.4642
37. Bzdok D, Krzywinski M, Altman N. Machine learning: a primer. *Nat Methods.* (2017) 14:1119–20. doi: 10.1038/nmeth.4526
38. Soffin EM, Beckman JD, Beathe JC, Girardi FP, Liguori GA, Liu J. Trends in ambulatory laminectomy in the USA and key factors associated with successful same-day discharge: a retrospective cohort study. *Hss J.* (2019) 16:72–80. doi: 10.1007/s11420-019-09703-0
39. Best MJ, Buller LT, Falakassa J, Vecchione D. Risk factors for nonroutine discharge in patients undergoing spinal fusion for intervertebral disc disorders. *Iowa Orthop J.* (2015) 35:147–55.
40. Morcos MW, Jiang F, McIntosh G, Ahn H, Dea N, Abraham E, et al. Predictive Factors for Discharge Destination Following Posterior Lumbar Spinal Fusion: A Canadian Spine Outcome and Research Network (CSORN) Study. *Global Spine J.* (2018) 9:219256821879709. doi: 10.1177/2192568218797090
41. Breiman L, Friedman JH, Olshen RA, Stone CJ. Classification and regression trees. *Nat Methods.* (2017) 14:318–41. doi: 10.1201/9781315139470-12
42. Lever J, Krzywinski M, Altman N. Model selection and overfitting. *Nat Methods.* (2016) 13:703–4. doi: 10.1038/nmeth.3968
43. Varghese V, Kumar GS, Krishnan V. Effect of various factors on pull out strength of pedicle screw in normal and osteoporotic cancellous bone models. *Med Eng Phys.* (2016) 40:28–38. doi: 10.1016/j.medengphys.2016.11.012
44. Sidey-Gibbons JAM, Sidey-Gibbons CJ. Machine learning in medicine: a practical introduction. *BMC Med Res Methodol.* (2019) 19:64. doi: 10.1186/s12874-019-0681-4
45. Bazzocchi A, Ferrari F, Diano D, Albinini U, Battista G, Rossi C, et al. Incidental findings with dual-energy X-ray absorptiometry: spectrum of possible diagnoses. *Calcified Tissue Int.* (2012) 91:149–56. doi: 10.1007/s00223-012-9609-2
46. Hsu C-W, Lin C-J. A comparison of methods for multiclass support vector machines. *IEE Trans Neural Netw.* (2002) 13:415–25. doi: 10.1109/72.991427
47. Fu H, Archer KJ. High-dimensional variable selection for ordinal outcomes with error control. *Brief Bioinform.* (2020). doi: 10.1093/bib/bba007. [Epub ahead of print].
48. Domingos P. A few useful things to know about machine learning. *Commun Acm.* (2012) 55:78. doi: 10.1145/2347736.2347755
49. LeCun Y. Deep learning hardware: past, present, and future. In: *2019 International Solid-State Circuits Conference (ISSCC).* San Francisco, CA (2019). p. 12–9. doi: 10.1109/ISSCC.2019.8662396
50. LeCun Y. The power and limits of deep learning. *Res Technol Manage.* (2018) 61:22–7. doi: 10.1080/08956308.2018.1516928
51. Bengio Y, Courville A, Vincent P. Representation learning: a review and new perspectives. *IEEE Trans Pattern Anal.* (2013) 35:1798–828. doi: 10.1109/TPAMI.2013.50
52. Emmert-Streib F, Yang Z, Feng H, Tripathi S, Dehmer M. An introductory review of deep learning for prediction models with big data. *Front Artif Intell.* (2020) 3:4. doi: 10.3389/frai.2020.00004
53. Michelson JD. CORR insights®: what are the applications and limitations of artificial intelligence for fracture detection and classification in orthopaedic trauma imaging? A systematic review. *Clin Orthop Relat Res.* (2019) 477:2492–4. doi: 10.1097/CORR.0000000000000912

54. Roth HR, Wang Y, Yao J, Lu L, Burns JE, Summers RM. Deep convolutional networks for automated detection of posterior-element fractures on spine CT. In: *SPIE Medical Imaging*. San Diego, CA (2016). doi: 10.1117/12.2217146
55. Lindsey R, Daluiski A, Chopra S, Lachapelle A, Mozer M, Sicular S, et al. Deep neural network improves fracture detection by clinicians. *Proc National Acad Sci USA*. (2018) 115:11591–6. doi: 10.1073/pnas.1806905115
56. Gale W, Oakden-Rayner L, Carneiro G, Bradley AP, Palmer LJ. Detecting hip fractures with radiologist-level performance using deep neural networks. *arXiv [Preprint]*. (2017). *arXiv:1711.06504*.
57. Yu K-H, Beam AL, Kohane IS. Artificial intelligence in healthcare. *Nat Biomed Eng*. (2018) 2:719–31. doi: 10.1038/s41551-018-0305-z
58. Quang D, Chen Y, Xie X. DANN: a deep learning approach for annotating the pathogenicity of genetic variants. *Bioinformatics*. (2014) 31:761–3. doi: 10.1093/bioinformatics/btu703
59. Quang D, Xie X. DanQ: a hybrid convolutional and recurrent deep neural network for quantifying the function of DNA sequences. *Nucleic Acids Res*. (2016) 44:e107. doi: 10.1093/nar/gkw226
60. Kamps R, Brandão R, Bosch B, Paulussen A, Xanthouleas S, Blok M, et al. Next-generation sequencing in oncology: genetic diagnosis, risk prediction and cancer classification. *Int J Mol Sci*. (2017) 18:308. doi: 10.3390/ijms18020308
61. Krizhevsky A, Sutskever I, Hinton GE. ImageNet classification with deep convolutional neural networks. *Adv Neural Inform Process Syst*. (2012) 25:1097–105. doi: 10.1145/3065386
62. Yazdan-Shahmorad A, Silversmith DB, Kharazia V, Sabes PN. Targeted cortical reorganization using optogenetics in non-human primates. *Elife*. (2018) 7:e31034. doi: 10.7554/eLife.31034
63. Lessmann N, van Ginneken B, de Jong PA, Išgum I. Iterative fully convolutional neural networks for automatic vertebra segmentation and identification. *Med Image Anal*. (2018) 53:142–55. doi: 10.1016/j.media.2019.02.005
64. Chen H, Dou Q, Wang X, Qin J, Cheng JCY, Heng P-A. 3D fully convolutional networks for intervertebral disc localization and segmentation. In: *International Conference on Medical Imaging and Augmented Reality*. Hong Kong (2016). p. 375–82. doi: 10.1007/978-3-319-43775-0_34
65. Kim YJ, Ganbold B, Kim KG. Web-based spine segmentation using deep learning in computed tomography images. *Healthc Inform Res*. (2020) 26:61–7. doi: 10.4258/hir.2020.26.1.61
66. Alsofy SZ, Stroop R, Fusek I, Saravia HW, Sakellariopoulou I, Yavuz M, et al. Virtual reality-based evaluation of surgical planning and outcome of monosegmental, unilateral cervical foraminal stenosis. *World Neurosurg*. (2019) 129:e857–65. doi: 10.1016/j.wneu.2019.06.057
67. Alsofy SZ, Nakamura M, Ewelt C, Kafchitsas K, Fortmann T, Schipmann S, et al. Comparison of stand-alone cage and cage-with-plate for monosegmental cervical fusion and impact of virtual reality in evaluating surgical results. *Clin Neurol Neurosurg*. (2020) 191:105685. doi: 10.1016/j.clineuro.2020.105685
68. Kim JS, Merrill RK, Arvind V, Kaji D, Pasik SD, Nwachukwu CC, et al. Examining the ability of artificial neural networks machine learning models to accurately predict complications following posterior lumbar spine fusion. *Spine*. (2018) 43:853–60. doi: 10.1097/BRS.0000000000002442
69. Nguyen NQ, Priola SM, Ramjist JM, Guha D, Dobashi Y, Lee K, et al. Machine vision augmented reality for pedicle screw insertion during spine surgery. *J Clin Neurosci*. (2020) 72:350–6. doi: 10.1016/j.jocn.2019.12.067
70. Burström G, Nachabe R, Persson O, Edström E, Terander AE. Augmented and virtual reality instrument tracking for minimally invasive spine surgery: a feasibility and accuracy study. *Spine*. (2019) 44:1097–104. doi: 10.1097/BRS.0000000000003006
71. Gibby JT, Swenson SA, Cvetko S, Rao R, Javan R. Head-mounted display augmented reality to guide pedicle screw placement utilizing computed tomography. *Int J Comput Ass Rad*. (2018) 14:525–35. doi: 10.1007/s11548-018-1814-7
72. Deib G, Johnson A, Unberath M, Yu K, Andress S, Qian L, et al. Image guided percutaneous spine procedures using an optical see-through head mounted display: proof of concept and rationale. *J Neurointerv Surg*. (2018) 10:1187–91. doi: 10.1136/neurintsurg-2017-013649
73. Elmi-Terander A, Skulason H, Söderman M, Racadio J, Homan R, Babic D, et al. Surgical navigation technology based on augmented reality and integrated 3D intraoperative imaging. *Spine*. (2016) 41:E1303–11. doi: 10.1097/BRS.0000000000001830
74. Gregory TM, Gregory J, Sledge J, Allard R, Mir O. Surgery guided by mixed reality: presentation of a proof of concept. *Acta Orthop*. (2018) 89:480–3. doi: 10.1080/17453674.2018.1506974
75. Tepper OM, Rudy HL, Lefkowitz A, Weimer KA, Marks SM, Stern CS, et al. Mixed reality with hololens. *Plast Reconstr Surg*. (2017) 140:1066–70. doi: 10.1097/PRS.0000000000003802
76. Wen W, Kuroki Y, Asama H. The sense of agency in driving automation. *Front Psychol*. (2019) 10:2691. doi: 10.3389/fpsyg.2019.02691
77. Vayena E, Blasimme A, Cohen IG. Machine learning in medicine: addressing ethical challenges. *PLoS Med*. (2018) 15:e1002689. doi: 10.1371/journal.pmed.1002689
78. Char DS, Shah NH, Magnus D. Implementing machine learning in health care — addressing ethical challenges. *New Engl J Med*. (2018) 378:981–3. doi: 10.1056/NEJMp1714229
79. London AJ. Artificial intelligence and black-box medical decisions: accuracy versus explainability. *Hast Cent Rep*. (2019) 49:15–21. doi: 10.1002/hast.973
80. Caruana R, Lou Y, Gehrke J, Koch P, Sturm M, Elhadad N. Intelligible models for healthCare. In: *The 21th ACM SIGKDD International Conference*. Sydney, NSW (2015). p. 1721–30. doi: 10.1145/2783258.2788613

Conflict of Interest: The authors declare that the research was conducted in the absence of any commercial or financial relationships that could be construed as a potential conflict of interest.

Copyright © 2020 Chang, Canseco, Nicholson, Patel and Vaccaro. This is an open-access article distributed under the terms of the Creative Commons Attribution License (CC BY). The use, distribution or reproduction in other forums is permitted, provided the original author(s) and the copyright owner(s) are credited and that the original publication in this journal is cited, in accordance with accepted academic practice. No use, distribution or reproduction is permitted which does not comply with these terms.



mHealth Apps for Enhanced Management of Spinal Surgery Patients: A Review

Michael Y. Bai^{1,2}, Ralph J. Mobbs^{1,2,3,4,5*}, William R. Walsh^{1,5} and Callum Betteridge^{1,2,3,4}

¹ NeuroSpine Surgery Research Group (NSURG), Sydney, NSW, Australia, ² Neuro Spine Clinic, Prince of Wales Private Hospital, Randwick, NSW, Australia, ³ Faculty of Medicine, University of New South Wales (UNSW), Sydney, NSW, Australia, ⁴ Wearables and Gait Assessment Research (WAGAR) Group, Prince of Wales Private Hospital, Randwick, NSW, Australia, ⁵ Surgical Orthopedic Research Labs (SORL), University of New South Wales (UNSW), Sydney, NSW, Australia

mHealth (mobile health) refers to mobile technologies that aid medical and public health practices. As of February 2019, 81% of Americans own a smartphone, and mHealth applications (apps) have become increasingly common with more than 400,000 mHealth applications currently available. Advancements in mobile technology now allow us to provide personalized up-to-date information, track personal health data, remind and engage patients, and communicate in a cost-effective way. There are new opportunities for healthcare providers to integrate mHealth into clinical practice. We discuss the current scientific evidence, and research into mHealth technology.

OPEN ACCESS

Edited by:

Vassilios S. Nikolaou,
National and Kapodistrian University
of Athens, Greece

Reviewed by:

Konstantinos Markatos,
Salamina Medical Center, Greece
Dimitrios Chytas,
European University Cyprus, Cyprus

*Correspondence:

Ralph J. Mobbs
Ralphmobbs@hotmail.com

Specialty section:

This article was submitted to
Orthopedic Surgery,
a section of the journal
Frontiers in Surgery

Received: 16 June 2020

Accepted: 16 September 2020

Published: 23 October 2020

Citation:

Bai MY, Mobbs RJ, Walsh WR and
Betteridge C (2020) mHealth Apps for
Enhanced Management of Spinal
Surgery Patients: A Review.
Front. Surg. 7:573398.
doi: 10.3389/fsurg.2020.573398

Keywords: surgery, spine, mHealth, smartphone, apps

INTRODUCTION

mHealth (mobile health) refers to mobile technologies that aid medical and public health practices (1). As of February 2019, 81% of Americans own a smartphone (2), and mHealth applications (apps) have become increasingly common with over 400,000 mHealth applications currently available to download on the Google Play Store and Apple App Store (3). Advancements in mobile technology allow us to provide personalized up-to-date information, track personal health data, remind and engage patients, and communicate in a cost-effective way. This has created new opportunities for healthcare providers to integrate mHealth into clinical practice. However, most mHealth apps are not based on scientific evidence, and there are calls for further research to enhance the scope and utilization of mHealth technology (4).

Post-operative communication with patients is a desirable part of safe and effective clinical care. However, effective pathways for communication may be difficult and may result in patients making unplanned and potentially unnecessary visits to their general practitioner or local emergency department. They may also take up more resources in terms of time spent on screening phone calls and emails by administrative staff (5). The use of smartphone technology provides secure methods to link patients directly with care providers to streamline the patient experience and optimize the use of limited resources.

The use of mHealth in neurosurgery is becoming a hot topic, with many researchers from around the world publishing their successes regarding the use of apps with spinal surgery patients. Spinal surgery patients face important challenges in post-op rehabilitation, pain management, and complications. Any advancement in a positive direction has the benefit of increasing quality of life and patient satisfaction. A survey conducted in 2017 has shown that three-quarters of spinal surgery patients would be interested in using a mHealth app to track their post-operative progress and communicate with their care team (6).

The aim of this review is to summarize the current literature regarding mHealth in the field of spinal surgery and discuss the benefits of this useful technology.

REVIEW

Enhanced Information Delivery

Smartphone technology can be used to solve the major issues of inconsistent information, difficulty accessing information, and delayed communication, which are faced by many surgical patients (7). Compared to large, generic, printed patient information booklets, mHealth apps make it easier for patients to find important information related to their surgery and provide them with a convenient way to revisit personalized information provided to them at their clinic visit. Studies have shown that patients have poor retention of medical information, and an app can improve the patients' understanding of their diagnosis, proposed surgery, required investigations, and changes they need to make to their medications (8). mHealth apps also help remind patients of crucial tasks they must complete in preparation for their surgery, such as stopping anticoagulants (7).

The Amie™ app by FavorHealth was studied by Stewart et al., who showed that preventable surgical cancellations due to poor compliance with pre-operative instructions could be reduced by using personalized push notifications to a group of neurosurgical patients (8). Push notifications also help remind patients to follow pre-operative instructions on the correct days. An app that requires patients to acknowledge notifications can also relay information back to care providers and give them a chance to contact the patient directly to remind them of pre-operative instructions if necessary (9).

Patients are also more likely to adhere to post-operative and discharge instructions when using mHealth apps (10). Those who engage with mHealth apps show greater patient satisfaction, better medication adherence, improved clinic attendance, lower readmission, and emergency department visits post-operatively (11). One study found that in the absence of an mHealth application, up to 55% of patients would have returned to the hospital for assessment of their wounds (12).

Behavior and Activity Modification

The proof of concept for mHealth apps has been demonstrated in many other specialties, and these give insight into what makes mHealth apps successful and worthwhile. mHealth apps have been successful in behavior modification for secondary prevention of cardiovascular disease (13), substance misuse (14), and medication compliance (15). It is clear that interventions for behaviors such as physical activity, smoking, and opioid misuse would benefit patients undergoing spinal surgery. The experience of other mHealth apps can help inform the development of an application made specifically for spinal surgery patients, which can be as simple as scheduled reminders to complete a symptomatic questionnaire. Encouraging these behaviors adds diagnostic value for conditions that are partially diagnosed by symptom profile, like Lumbar Spinal Stenosis (16), and provides a longitudinal view of the symptom progression for clinical assessment of disease status.

Penn Medicine's NeuroPath app is one such mHealth app that has been piloted in spinal surgery patients (17). This app utilizes principles from enhanced recovery after surgery (ERAS) to encourage patients to do daily tasks, provide instructions and education, allow them to track and share their activity levels and medication usage and communicate directly with their care team (17). This app presented patients with daily to-do lists that included specific instructions depending on the time since their surgery, such as exercise, diet, wound care instructions, and requested patients to input their symptoms daily. Care providers can then interact with patients and provide feedback based on the information they uploaded to the app.

Postural and walking stability is an important objective gait metric for patients with spinal pathology. Changes in posture and walking stability, including falls, correlates with recovery following any spinal intervention. Yoong and authors noted, however, that mHealth apps and wearable devices to assist with the monitoring of relevant metrics following spinal interventions is still in its infancy with further device and app development to be done (18).

Improved Follow-Up

mHealth apps offer a cost-effective way to safely allow earlier discharge while maintaining close follow-up with patients post-operatively (19, 20). It can save time for care providers and patients and reduce unnecessary transfers. A French study which looked at the use of an mHealth app for the post-operative follow up of patients who underwent outpatient microdiscectomy found that 94% of issues could be handled remotely. This allows the patient to have direct access to their care team and avoid unnecessary visits to their primary care physician or return to the hospital (21). The costs associated with implementing the app and maintaining a team to respond to alerts can be offset by a reduction in length of hospital stay (22).

There is also the potential that certain patients who communicate good progress via their mHealth app may not need to return for an in-person follow-up appointment. This could reduce the costs associated with running clinics and allow health care providers to focus their resources on other activities (7).

Improved Outcomes

mHealth is an extremely promising modality for improving patient care and outcomes. It has been shown to improve patient experiences by involving patients in their own management which provides more confidence to patients after they have been discharged. Patients engage more with mHealth apps that have personalized content, a higher frequency of text messages, and two-way communication (13).

mHealth apps are extremely useful in the post-operative period for wound monitoring. Surgical site infections, if recognized early, can be safely managed as an outpatient, whereas delays in recognition can lead to readmission, patient stress, and an increased burden on the healthcare system (7). The technology exists to allow secure transfer of photographs of surgical wounds from patients to care providers via an encrypted smartphone app. This solution would decrease complication rates and increase patient satisfaction.

A randomized controlled trial of patients in China post lumbar spinal surgery explored the use of an mHealth app to deliver rehabilitation (23). The app allowed patients to view personalized rehabilitation plans made by their physicians and provided daily reports and prompts to encourage continued use of the app. Patients could also communicate with their doctors through the app, and they could make changes to their rehabilitation plans. This resulted in a significant improvement in their disability index and pain scores after 2 years compared to traditional rehabilitation (23). Their study also demonstrated increased benefits with higher app compliance.

Increased Patient Satisfaction

A systematic review of the ability of smartphone apps to enhance communication with surgical patients was published by De La Cruz Monroy et al. in 2019 (7). They noted an overwhelmingly positive response from patients and care providers who are using mHealth apps in the perioperative setting.

Patients are willing to engage with mHealth apps and use them daily as they feel they are personal to their care. They also provide a sense of security as there is a continuous link to their care providers, and give the patients the opportunity to be involved in research. Some even report using the app simply because they were bored (24). mHealth apps have the potential to provide continuous 24-h monitoring for patients without overburdening the healthcare system. They also have the potential to increase patient compliance by featuring individualized feedback and rewards to patients.

The mHealth app “e-fitback” (Nouveal, e-santé) was used in a study of ERAS for patients undergoing spinal fusion for degenerative conditions (22). It collected post-operative information on pain, temperature, voiding, motor disorders, and blood-stained dressings. The app then triggered an alarm that would instigate a phone call from the ERAS team if needed. Patients responded well to the app, with 82.3% of users reporting feeling satisfied or very satisfied with the mHealth app as a tool to optimize patient care.

Future Directions

One of the fears regarding the utilization of mHealth is that elderly patients would not engage with the technology. A pilot study by von Glinski et al. has demonstrated that as long as patients own and use a smartphone, mHealth apps are well-received by elective spinal surgery patients regardless of age, gender, or procedure invasiveness (5). This is promising and encourages the future development of more apps tailored to surgical patients. Another barrier to the implementation of mHealth apps is privacy concerns. Privacy concerns may relate to the amount of information that the clinician has access to, or the potential for hacking and data leaks which may result in the patient's health data being publicly available. When filling in a questionnaire regarding data privacy using mHealth apps, patients in lower socioeconomic classes had fewer concerns regarding privacy and were more likely to use an mHealth app, meaning greater benefit amongst (25). However, Limited uptake by wealthier individuals diminishes the overall benefit of widespread implementation of mHealth applications

in health. Finally, the 2014 annual study on mHealth application development (26) predicted two further barriers to mHealth application uptake over the 2014–2019 period, practitioner resistance and difficult discoverability of individual applications due to the sheer number of applications available.

mHealth apps may be beneficial for spinal surgery patients with poor access to rehabilitation services (23) or may be useful in complementing traditional services. By reducing the burden of traditional services, it may free up resources so that more patients may benefit without compromising the quality of the service. There is also further potential for mHealth apps to integrate with add-on devices to enhance post-operative monitoring. These could include simple activity monitors or specialized medical devices designed for specific purposes (7). Such communication between a smartphone and external device has already demonstrated clinical utility in spinal surgery (27). Additionally, the processing power of handheld phones could allow mHealth apps to extrapolate the unprocessed data from external devices to generate a much more complex picture than what the device itself could provide. For example, it is possible to use the accelerometry data captured by a smartwatch to calculate gait velocity, smoothness, or asymmetry, rather than just step count.

Integration of data from a mHealth app to a patient's electronic health record (EHR) (28) would allow the data from the mHealth app to be stored on a centralized database for the hospital or local health district (28). This means that while the data would primarily be used by the spinal surgeon and the patient, other clinicians who adopt care of the patient can access the information as well, allowing for better integration between primary, secondary and tertiary care systems.

As it stands, the data captured by mHealth apps is limited to questionnaires and simple measures of health like heart rate and step count by the storage and processing capacity of handheld devices. With advancements in mobile phone technology, it stands to reason that the phone would be able to obtain more complex measures of health. For example, improvements in the sampling rate of the phone's internal accelerometers and gyroscopes, and an increase in phone processing power may allow for constant measurement of gait velocity and smoothness, which could be useful for an mHealth app specific to spinal surgery patients. As the amount of health data captured per minute increases, so does the need for a system capable of sorting through this data, and deciding what is useful or important for the clinician to know, as does the need to quickly upload this data. Thus, some adjuvant technologies such as artificial intelligence (AI) and cellular networks with greater bandwidth (5G+) may play a role in this future when mHealth apps and handheld phone technology are optimized.

CONCLUSION

In conclusion, there have been several mHealth apps specially designed for and tested with spinal surgery patients reported in literature worldwide. Early experiences have shown that mHealth apps are a cost-effective way to provide safe, beneficial,

and satisfactory care to patients. mHealth apps enhance two-way communication between patients and their care providers. They help to deliver patient information in a convenient and individualized fashion. Rehabilitation and follow-up care can be optimized via mobile apps also, allowing patients to take control of their own care and engage with the app as frequently as they like. These optimizations are likely to improve long-term outcomes in terms of better quality of life, less pain, better mobility, and reduced complications. It should be noted that the conclusions drawn from this article are limited by its nature as a narrative review. The present study did not follow PRISMA reporting guidelines, and therefore has a higher risk of bias than a structured narrative review. The quality of studies included in this review was high, with many implementing randomized allocation to intervention groups.

mHealth apps are still in their infancy, and further research into this growing field is necessary. There is no doubt that this technology will integrate further into all fields of medicine, and

it is exciting to witness this significant advancement in patient communication and care.

AUTHOR CONTRIBUTIONS

The first draft of the manuscript was written by MB. All authors listed have made a substantial, direct and intellectual contribution to the work, and approved it for publication.

ACKNOWLEDGMENTS

The NeuroSpine Surgery Research Group (NSURG) aided with manuscript production. The Wearables And Gait Assessment Research (WAGAR) Group provided assistance with wearables literature. The *NeuroSpineClinic*, Sydney Australia, provided clinic assistance for authors.

REFERENCES

- Kay M, Santos J, Takane M. mHealth: new horizons for health through mobile technologies. *World Health Organ.* (2011) 64:66–71.
- Statista. *Percentage of US Adults Who Own a Smartphone.* (2019). Available online at: <https://www.statista.com/statistics/219865/percentage-of-us-adults-who-own-a-smartphone/> (accessed June 3, 2020).
- Georgiou M. Developing A Healthcare App In 2020: What do patients really want? (2020). Available online at: <https://www.imagination.net/blog/developing-a-mobile-health-app-what-patients-really-want/> (accessed June 3, 2020).
- Nilsen W, Kumar S, Shar A, Varoquiers C, Wiley T, Riley WT, et al. Advancing the science of mHealth. *J Health Commun.* (2012) 17(Suppl. 1):5–10. doi: 10.1080/10810730.2012.677394
- von Glinski A, Ishak B, Elia C, Goodmanson R, Pierre C, Norvell DC, et al. Emerging insight in the use of an active post discharge surveillance program in spine surgery: a retrospective pilot study. *World Neurosurg.* (2020) 139:e237–44. doi: 10.1016/j.wneu.2020.03.185
- Nathan JK, Rodoni BM, Joseph JR, Smith BW, Park P. Smartphone use and interest in a spine surgery recovery mobile application among patients in a US academic neurosurgery practice. *Oper Neurosurg.* (2020) 18:98–102. doi: 10.1093/ons/ops061
- De La Cruz Monroy MF, Mosahebi A. The use of smartphone applications (apps) for enhancing communication with surgical patients: a systematic review of the literature. *Surg Innov.* (2019) 26:244–59. doi: 10.1177/1553350618819517
- Stewart JJ, Fayed I, Henault S, Kalantar B, Voyadzis J-M. Use of a smartphone application for spine surgery improves patient adherence with preoperative instructions and decreases Last-minute surgery cancellations. *Cureus.* (2019) 11:e4192. doi: 10.7759/cureus.4192
- Felbaum DR, Stewart JJ, Anaizi AN, Sandhu FA, Nair MN, Voyadzis J-M. Implementation and evaluation of a smartphone application for the perioperative care of neurosurgery patients at an academic medical center: implications for patient satisfaction, surgery cancellations, and readmissions. *Oper Neurosurg.* (2018) 14:303–11. doi: 10.1093/ons/ops112
- Gu Y, Wang L, Zhao L, Liu Z, Luo H, Tao Q, et al. Effect of mobile phone reminder messages on adherence of stent removal or exchange in patients with benign pancreaticobiliary diseases: a prospectively randomized, controlled study. *BMC Gastroenterol.* (2016) 16:105. doi: 10.1186/s12876-016-0522-4
- Lu K, Marino NE, Russell D, Singareddy A, Zhang D, Hardi A, et al. Use of short message service and smartphone applications in the management of surgical patients: a systematic review. *Telemed E Health.* (2018) 24:406–14. doi: 10.1089/tmj.2017.0123
- Martínez-Ramos C, Cerdán MT, Lopez RS. Mobile phone-based telemedicine system for the home follow-up of patients undergoing ambulatory surgery. *Telemed E Health.* (2009) 15:531–7. doi: 10.1089/tmj.2009.0003
- Park LG, Beatty A, Stafford Z, Whooley MA. Mobile phone interventions for the secondary prevention of cardiovascular disease. *Prog Cardiovasc Dis.* (2016) 58:639–50. doi: 10.1016/j.pcad.2016.03.002
- Tofghi B, Abrantes A, Stein MD. The role of technology-based interventions for substance use disorders in primary care: a review of the literature. *Med Clin.* (2018) 102:715–31. doi: 10.1016/j.mcna.2018.02.011
- Morawski K, Ghazinouri R, Krumme A, Lauffenburger JC, Lu Z, Durfee E, et al. Association of a smartphone application with medication adherence and blood pressure control: the MedISAFE-BP randomized clinical trial. *JAMA Intern Med.* (2018) 178:802–9. doi: 10.1001/jamainternmed.2018.0447
- Perring J, Mobbs R, Betteridge C. Analysis of patterns of gait deterioration in patients with lumbar spinal stenosis. *World Neurosurg.* (2020) 141:e55–9. doi: 10.1016/j.wneu.2020.04.146
- Glauser G, Ali ZS, Gardiner D, Ramayya AG, Pessoa R, Grady MS, et al. Assessing the utility of an iOS application in the perioperative care of spine surgery patients: the NeuroPath Pilot study. *mHealth.* (2019) 5:40. doi: 10.21037/mhealth.2019.09.01
- Yoong NKM, Perring J, Mobbs RJ. Commercial postural devices: a review. *Sensors.* (2019) 19:5128. doi: 10.3390/s19235128
- Wang QQ, Zhao J, Huo XR, Wu L, Yang LF, Li JY, et al. Effects of a home care mobile app on the outcomes of discharged patients with a stoma: a randomised controlled trial. *J Clin Nurs.* (2018) 27:3592–602. doi: 10.1111/jocn.14515
- Mobbs RJ, Katsinas CJ, Choy WJ, Rooke K, Maharaj M. Objective monitoring of activity and Gait Velocity using wearable accelerometer following lumbar microdiscectomy to detect recurrent disc herniation. *J Spine Surg.* (2018) 4. doi: 10.21037/jss.2018.12.02
- Debono B, Bousquet P, Sabatier P, Plas J-Y, Lescure J-P, Hamel O. Postoperative monitoring with a mobile application after ambulatory lumbar discectomy: an effective tool for spine surgeons. *Eur Spine J.* (2016) 25:3536–42. doi: 10.1007/s00586-016-4680-4
- Debono B, Corniola MV, Pietton R, Sabatier P, Hamel O, Tessitore E. Benefits of enhanced recovery after surgery for fusion in degenerative spine surgery: impact on outcome, length of stay, and patient satisfaction. *Neurosurg Focus.* (2019) 46:E6. doi: 10.3171/2019.1.FOCUS18669
- Hou J, Yang R, Yang Y, Tang Y, Deng H, Chen Z, et al. The effectiveness and safety of utilizing mobile phone-based programs for rehabilitation after lumbar spinal surgery: multicenter, prospective randomized controlled trial. *JMIR mHealth uHealth.* (2019) 7:e10201. doi: 10.2196/10201

24. Scott AR, Allore EA, Naik AD, Berger DH, Suliburk JW. Mixed-methods analysis of factors impacting use of a postoperative mHealth app. *JMIR mHealth uHealth*. (2017) 5:e11. doi: 10.2196/mhealth.6728
25. Zhou L, Bao J, Watzlaf V, Parmanto B. Barriers to and facilitators of the use of mobile health apps from a security perspective: mixed-methods study. *JMIR mHealth uHealth*. (2019) 7:e11223. doi: 10.2196/11223
26. Research2guidance. *mHealth App Developer Economics 2014*. Berlin: Research2Guidance (2014). Available online at: <https://www.fer.unizg.hr/download/repository/research2guidance-mHealth-App-Developer-Economics-2014.pdf>
27. Ghent F, Mobbs RJ, Mobbs RR, Sy L, Betteridge C, Choy WJ. Assessment and post-intervention recovery after surgery for lumbar disk herniation based on objective gait metrics from wearable devices using the gait posture index. *World Neurosurg*. (2020) 142:e111–e116. doi: 10.1016/j.wneu.2020.06.104
28. Kao CK, Liebovitz DM. Consumer mobile health apps: current state, barriers, and future directions. *PM R*. (2017) 9:S106–15. doi: 10.1016/j.pmrj.2017.02.018

Conflict of Interest: The authors declare that the research was conducted in the absence of any commercial or financial relationships that could be construed as a potential conflict of interest.

Copyright © 2020 Bai, Mobbs, Walsh and Betteridge. This is an open-access article distributed under the terms of the Creative Commons Attribution License (CC BY). The use, distribution or reproduction in other forums is permitted, provided the original author(s) and the copyright owner(s) are credited and that the original publication in this journal is cited, in accordance with accepted academic practice. No use, distribution or reproduction is permitted which does not comply with these terms.



Innovative Technology System to Prevent Wrong Site Surgery and Capture Near Misses: A Multi-Center Review of 487 Cases

David M. Gloystein^{1*}, Bradley A. Heiges², David G. Schwartz³, John G. DeVine⁴ and Deborah Spratt⁵

¹ Dwight David Eisenhower Army Medical Center, Augusta, GA, United States, ² Optim Orthopedics, Savannah, GA, United States, ³ OrthoIndy, Indianapolis, IN, United States, ⁴ Medical College of Georgia, Augusta University, Augusta, GA, United States, ⁵ Surgical Services University of Rochester St. James Hospital, Hornell, NY, United States

OPEN ACCESS

Edited by:

William Robert Walsh,
University of New South
Wales, Australia

Reviewed by:

Paul Simon Unwin,
Independent Researcher, Ludlow,
United Kingdom
Konstantinos Markatos,
Salamina Medical Center, Greece

*Correspondence:

David M. Gloystein
gloystein.research@gmail.com

Specialty section:

This article was submitted to
Orthopedic Surgery,
a section of the journal
Frontiers in Surgery

Received: 18 May 2020

Accepted: 14 September 2020

Published: 23 October 2020

Citation:

Gloystein DM, Heiges BA, Schwartz DG, DeVine JG and Spratt D (2020) Innovative Technology System to Prevent Wrong Site Surgery and Capture Near Misses: A Multi-Center Review of 487 Cases. *Front. Surg.* 7:563337. doi: 10.3389/fsurg.2020.563337

Introduction: Wrong site surgery (WSS) is a preventable error. When these events do occur, they are often devastating to the patient, nursing staff, surgeon, and facility where the surgery was performed. Despite the implementation of protocols and checklists to reduce the occurrence of WSS, the rates are estimated to be unchanged.

Materials and Methods: An innovative technology was designed to prevent WSS through a systems-based approach. The StartBox Patient Safety System was utilized at six sites by 11 surgeons. The incidence of near misses and WSS was reviewed.

Results: The StartBox System was utilized for 487 orthopedic procedures including Spine, Sports Medicine, Hand, and Joint Replacement. There were no occurrences of WSS events. Over the course of these procedures, medical staff recorded 17 near misses utilizing the StartBox System.

Conclusions: StartBox successfully performed all tasks without technical errors and identified 17 near miss events. The use of this system resulted in the occurrence of zero wrong site surgeries.

Keywords: wrong site surgery, wrong patient, wrong side, wrong laterality, wrong procedure, near miss, patient safety, forcing function

INTRODUCTION

Wrong site surgery (WSS) continues to plague medical facilities across the globe despite implementation of initiatives, checklists, and protocols. WSS refers to surgery that is incorrectly performed on the wrong side, wrong spine level, wrong anatomy, wrong patient, or the wrong procedure. Estimates on the incidence of WSS vary widely, ranging from 0.09 to 4.5 per 10,000 procedures (1–6). This potentially translates to between 683 and 34,000 wrong site surgeries per year based upon annual rates of surgical procedures in the United States. Attempting to put these wide ranges in context, Seiden suggests that WSS events occur 50 times a week or more (5); Clarke estimates that a 300-bed hospital can anticipate a report of a WSS event an average of once each (7); and Canale reports that orthopedic surgeons have a 25% chance of performing a WSS at least once in their career (8). The majority of errors are classified as wrong side, ranging from 70 to 81% of overall events (5, 7). Though small in number, the impact of WSS is large and may result

in permanent injury to the patient, damaged reputations for the surgeon and surgical facility, and significantly increased medicolegal costs. When these events occur, they are often devastating to the patient, nursing staff, surgeon, and facility where the surgery was performed.

With the guidance of proper processes, checklists, and safeguards, the Joint Commission has declared that WSS is a preventable event that should never occur. In support of this expectation, the Joint Commission introduced a Universal Protocol in 2004 that provides guidelines for the fundamental elements of a WSS prevention protocol. The Universal Protocol includes requirements for marking of the surgical site, confirmation of patient identity, confirmation of the intended procedure, and review of these details among the surgical team during a time-out immediately prior to the start of surgery (9). While Universal Protocol guidelines are specific in content, implementation of the guidelines can vary widely across hospitals and surgery centers. Even when WSS prevention protocols are implemented, adherence to such protocols among staff members may not be consistent within a given facility or system (2). The Joint Commission provides causes for failures of safety protocols in the OR including distractions and rushing during time-outs (**Table 1**) (10). These factors may help explain the unchanging rates of WSS despite implementation of the Universal Protocol (4).

MATERIALS AND METHODS

The StartBox Patient Safety System (StartBox, Atlanta, GA) is an innovative technology that was evaluated to assess its ability to prevent WSS. This evaluation was performed using cases performed by 11 surgeons at six sites with the StartBox System. The System collects procedure data including a description of the surgery, evaluation of any near misses or other safety benefits added to the case by StartBox, and postoperative evaluation of the occurrence of WSS events defined as any procedure performed at the wrong site including, incorrect procedures, and procedures performed on the wrong patient.

The StartBox System consists of a mobile software application, a safety-engineered blade delivery kit (BDK) and a data reporting tool. The software application of StartBox is an easy-to-implement, standardized platform that improves communication between the surgical team and the patient; between the surgeon's practice and surgical facility; and among care providers along the patient care continuum (**Figure 1**). The application can be loaded on an individual user's personal device, or pre-loaded on a dedicated device provided by the company. The application is compatible with both iOS (Apple) and Android operating systems. The StartBox System is initiated via the mobile application with an audio recording of the surgeon describing the planned procedure to the patient, including site and laterality. The audio file is uploaded to a cloud-based system and becomes accessible to all users of the system, serving as the central source of documentation for the planned surgery. Upon hospital check in, the StartBox patient record is referenced to confirm the correct procedure. Subsequently, the patient's

hospital wristband is scanned and associated with a StartBox BDK labeled with a QR code that references the patient's unique procedure, site, and laterality. The packaging of the BDK is color-coded for ready identification of laterality: *Lavender*, for Left; *Rose*, for Right; *Neutral Gray*, for No Laterality (**Figure 2**). This color-coding is also used in the StartBox software application, which helps prevent the most common type of WSS. The saved audio recording of the decision for surgery is replayed in the preoperative holding area, and in the operating room where surgical personnel listen to the agreed-to procedure discussion just prior to the surgical time-out. At any time between initial consultation in clinic and the start of the procedure in the operation room, StartBox allows for additional voice recordings and playback to remove ambiguity and elaborate on a procedure. Any member of the medical staff can flag errors with the use of a *No Go* function in the StartBox application, which generates a real-time alert in the system, and all *No Gos* must be resolved before the surgery can be initiated. Immediately prior to surgery, the time-out, which includes identification of the patient, site of surgery, and procedure, is conducted as prescribed by the Universal Protocol. This time out is recorded by the application as an additional audio file that is saved to the cloud system to document this confirmation. Upon successful completion of time-out requirements, the BDK is placed on the sterile field. The BDK contains four sterile scalpel blades and delivers each blade in a safe manner, minimizing the potential for sharps injury (**Figure 3**). With the StartBox System, the BDK serves as a key constraint: the blade for first incision is not delivered to the surgeon until the patient's identity, correct procedure, correct site and correct laterality have been confirmed and documented by the surgical team during the time-out.

Upon completion of the procedure, the case data, including near misses, is stored and aggregated to generate predictive analytics related to future WSS prevention protocol improvements and training opportunities. Near misses related to WSS would include incorrectly booked surgery and improperly performed presurgical time-outs (11).

The study was carried out with sequential series at each site using retrospective, deidentified data. The system is designed to protect the confidentiality, availability, and integrity of personal health information as required by HIPAA and satisfy the compliance requirements of institutional ethics committees.

RESULTS

The StartBox System was utilized for 487 orthopedic procedures (**Table 2**). The procedure types include spine, sports medicine, hand, and joint replacement. There were no occurrences of WSS events.

Over the course of these procedures, medical staff recorded 17 *No Gos* (**Table 3**) in the StartBox System. Information for 16 of these cases was either corrected or overridden by the surgeon and successfully completed; one (1) case was postponed to a later date in order to confirm accuracy. The StartBox System was effective in preventing wrong site surgery for each of these near miss events.

TABLE 1 | Causes of wrong site surgery in the OR.**Causes**

When the same provider performs multiple procedures, there is no intraoperative site verification.

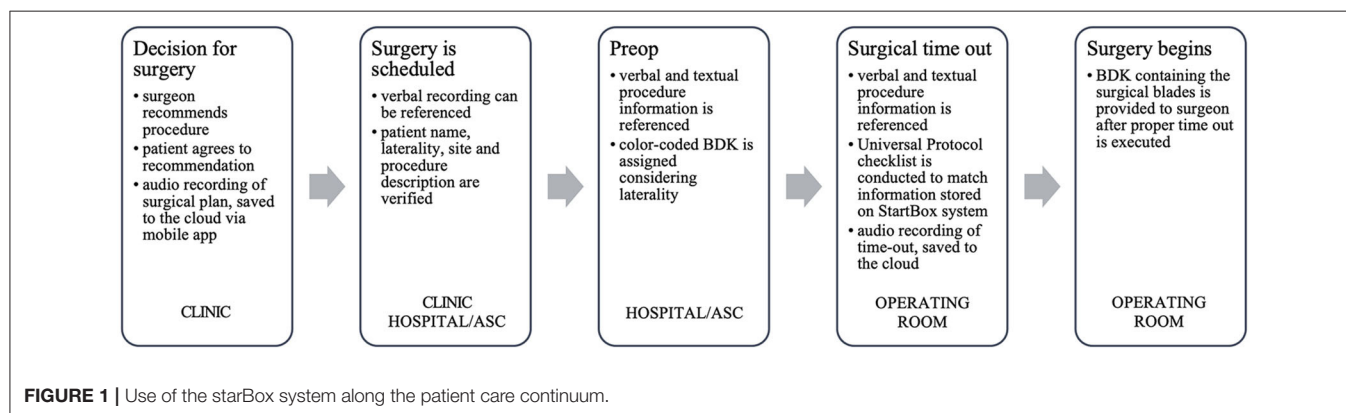
Hand-off communication or briefing process is ineffective.

Primary documentation is not used to verify patient, procedure, site and side immediately prior to incision.

Site marks are removed during prep.

Distractions and rushing occur during time-out, or the time-out occurs before all staff members are ready or before prep and drape.

Time-out is performed without full participation.



Six (6) *No Gos* were due to inconsistent patient information including incorrect date of birth information, naming errors, and an incorrectly recorded sex. Six (6) *No Gos* were due to incorrect procedure information including site or description. Five (5) *No Gos* were due to laterality mismatch.

The majority of *No Gos* were recorded by the preop nurse at check-in on the day of surgery (9), followed by the circulating

nurse in the OR (4) and the clinic scheduler (3). A surgeon recorded one *No Go* (Table 4).

The following examples of *No Gos* are provided for illustration purposes. The First is a revision spine procedure where hardware was to be removed from the left side. The surgeon recorded this in the audio dictation, but the procedure record was saved with no laterality and it was scheduled similarly with no laterality. The



FIGURE 3 | StartBox blade delivery kit ejecting scalpel blades.

preop nurse noted this inconsistency and registered a *No Go* in the StartBox System. Before the patient was prepared for surgery, the surgeon corrected the record to reflect the left-side approach and a matching *Lavender* StartBox BDK was paired. The surgical time-out was then completed correctly, and the procedure was conducted successfully.

A second example is a total knee arthroplasty intended for the right side. The procedure was later scheduled for the left side and was incorrectly approved by the patient via signed informed consent. On the day of surgery, the *No Go* was registered with the StartBox System and the team was notified. Due to the laterality discrepancy, the procedure was canceled. Subsequently, the right side was confirmed as the correct operative site.

Two final examples of *No Gos* were spine cases containing incorrect procedure information. The first had improperly transcribed levels. The inconsistency was flagged at preop (C7 was omitted in a C5, C6, and C7 posterior cervical fusion). The second was a spine case with a mismatched informed consent and dictated preoperative surgical plan (the informed consent described a discectomy and the preoperative surgical dictation described a fusion). The patient identified the error after listening to the dictation at the hospital before being prepped for surgery and inquired with the nurse, who then confirmed with the surgeon. The informed consent was then corrected at preop. Both of these procedures were successfully completed with the StartBox System.

Use of StartBox did not result in any reported impacts or use impedance to patient workflow at the clinic or hospital and there were no delays in surgery due to technical difficulties during the time-out or failure of the system to release a surgical blade after completion of the time-out.

DISCUSSION

Preventing Wrong Site Surgery

British psychologist James Reason suggested in his Swiss Cheese model of accident causation that catastrophic safety failures are almost never caused by isolated errors committed by individuals. Instead, most accidents result from multiple, smaller errors in environments (the holes in the cheese) with serious underlying system flaws. In this model, errors made by individuals result in disastrous consequences. Reason also

emphasized that human error is inevitable, and that a systems approach can catch errors before they occur or block them from causing harm (12).

The Hierarchy of Intervention Effectiveness, first introduced in 1999 by the Institute for Safe Medication Practices, presents a risk management theory that ranks intervention methods from least to most effective. Human-focused interventions such as education, training, rules, policies, and checklists are rated toward the bottom of its scale (13). While not without value, these interventions are less reliable than system-focused interventions such as standardization and computerization. The most highly ranked intervention measures are forcing functions and constraints as they directly prevent the user from making a mistake, thus making them the most powerful and effective error prevention tools (14). Classic examples of forcing functions include a user being prevented from starting a car while it is in gear; or a user being prevented from starting a microwave with the door open (15).

Considering this background, current measures fall short in two categories. First, WSS prevention protocols do not address potential sources of error, according to the Swiss Cheese model. Moreover, relying on a checklist without computerization or constraints is an inferior and generally acknowledged less-effective means of error prevention.

With the end goal of improving WSS prevention protocols and ideally eliminating WSS altogether, the StartBox System was developed to enhance all three intervention methods. System-focused improvements include standardizing and streamlining workflows, as well as complementing existing electronic medical record systems. This system boosts human-oriented methods that contribute to effective communication, such as the huddle described in TeamSTEPPS (Team Strategies and Tools to Enhance Performance and Patient Safety) (16) as well as integrate the checklist recommended by the Universal Protocol (17). Finally, and most importantly, this system adds a physical forcing function as a final constraint prior to the point of no return (the surgical incision).

The goal of this study is to report the early experience using this innovative system comprising the recording of the decision for surgery, verification of the procedure record for all the constituents in the patient care continuum, confirmation of procedure accuracy during the surgery time out, and the use of a physical forcing function before the surgical incision.

In the clinical evaluation that is the focus of this report, StartBox was utilized with 487 procedures to standardize a process that is intended to prevent WSS. Users reported a good experience using the system, including the anecdotal feedback summarized in Table 5. Zero wrong site surgeries occurred.

Capturing Near Misses

Near misses, sometimes referred to as close calls or potential adverse events, are defined as acts of commission or omission that could have harmed the patient but did not cause harm as a result of chance, prevention or mitigation (18). Near miss

TABLE 2 | Count of procedures by type of result.

Type of result	Total	Ankle	Clavicle	Hand	Hip	Knee	Shoulder	Spine
Registered with StartBox	487	2	1	44	8	66	30	336
Near misses aka No Gos (%)	17 (3%)	0	0	0	0	2 (3%)	1 (3%)	14 (4%)
Postponed	1	0	0	0	0	1	0	0
Wrong site surgeries	0	0	0	0	0	0	0	0

analysis is the review of types and causes of error and an investigation of how those errors were mitigated. This type of analysis can contribute toward preventing never events, such as WSS (19).

As a surrogate for WSS, analysis of near miss events may allow organizations to examine the effectiveness of complex systems designed to prevent WSS, without such an event ever occurring (9). A system to capture and analyze near miss data would present a substantial opportunity to reduce or eliminate WSS.

The No Go function of the StartBox System was triggered in 17 of 487 (3%) registered procedures. Quantifying near misses is an important step in understanding the risk of WSS and facilitating a longitudinal review of modified systems and protocols to prevent errors. These errors could have been mitigated by standard prevention protocols, but likely not tracked or reported. Near miss analysis is rare (11). There is limited data on the frequency of near misses, which challenges the ability of institutions to examine existing safety systems. The StartBox System inherently captures this data and allows for near miss analysis. The data generated by the StartBox System may improve the safety of future procedures by identifying opportunities for improvement in communication, workflow, logistics, and training. It also provides a unique complement, rather than competitor, to current safety guidelines and protocols employed at any institution.

For example, in this study there were inconsistencies reported between how the procedure was defined by the surgeon during consultation with the patient preop, and how the hospital described it in its OR schedule. The StartBox System highlighted the differences and ensured a resolution through a change to the procedure description used by the hospital. Of particular concern for spine procedures is wrong-level surgeries. The StartBox System did highlight one near miss of this type, ensuring the correct level was performed. Furthermore, spinal procedures could be considered to have no laterality since they are performed generally on the midline of the body; however, there is frequent laterality to the pathology (e.g., left-sided disc herniation), requiring different room setup or approach to the spine after a midline incision. The StartBox System allowed for further precision to be communicated to the OR team by the surgeon, which was an improvement over previous processes. The system color-coding especially supported the awareness of procedure laterality (including room setup and approach) and contributed to the prevention of this frequent type of WSS.

TABLE 3 | Count of No Go by type.

Type of No Go	Total	Percentage of total (%)
Patient	6	35
Description	4	24
Site	2	12
Laterality	5	29
Total	17	

TABLE 4 | Count of No Gos by reporting individual or area.

Individual or area	Total	Percentage of total (%)
Hospital preop	9	53
OR circulator	4	24
Clinic scheduler	3	18
Surgeon	1	6
Total	17	

Study Limitations

The number of patients in the study is small relative to the volume of surgical procedures at a given institution. The small number of patients limit an effective comparison between sites as well as perform any correlation analyses. Future studies with larger number of patients should provide better opportunity to do so. Additionally, the study at each site was conducted over a relatively short period of time, limiting the ability of the institution to perform in-depth analysis of the near misses and implement considerable systematic change or evaluate effectiveness of changes. Continued evaluation with an increasing number of patients over a longer period of time should help further the appreciation for the incidence of near misses and validate the StartBox System as a robust safety system for WSS prevention.

CONCLUSION

StartBox is designed to prevent wrong site surgery and capture near misses through a real-time, data-driven approach. The system is designed to complement safety checklists, standardize and streamline workflows, integrate computerization, and provide a final constraint to prevent WSS.

TABLE 5 | Summary of feedback from practitioners.

Category	Comment(s)
Patient engagement	Patients love hearing surgeon voice on day of surgery (during playback of recording in preop). Gives confidence to them that best care is being provided, and that safety is paramount.
Learning curve	There is a nominal learning curve to using the technology, like anything new. Once overcome it is easy to use and inobtrusive to staff.
Increased efficiency	Does not add material time to clinic phase or hospital. Ensures proper surgical order is placed early in process, minimizing future corrections. Any clarification needed at hospital can be made in preop, before patient goes to operating room. In the OR, the staff realized it made the timeout(s) more efficient.
Staff engagement	Leveling the hierarchy; everyone is in charge of safety. No secrets in patient care; everyone gets to hear the intended procedure.

This evaluation included 487 surgical procedures during which StartBox successfully performed all tasks without technical errors and identified 17 near miss events that could have led to the occurrence of a wrong site surgery. Zero wrong site surgeries occurred in this study.

DATA AVAILABILITY STATEMENT

The raw data supporting the conclusions of this article will be made available by the authors, without undue reservation.

ETHICS STATEMENT

Ethical review and approval was not required for the study on human participants in accordance with the local legislation and institutional requirements. Written informed consent for participation was not required for this

study in accordance with the national legislation and the institutional requirements.

AUTHOR'S NOTE

The opinions or assertions contained herein are the private views of the authors and are not to be construed as official or reflecting the views of the Department of Defense or the US government. DG is an employee of the US government. This work was prepared as part of their official duties and as such there is no copyright to be transferred.

AUTHOR CONTRIBUTIONS

DG, BH, and DGS performed procedures that are its subject and wrote sections of the manuscript. All authors contributed conception and design of the research, contributed to manuscript revision, read, and approved the submitted version.

REFERENCES

- Devine J, Chutkan N, Norvell DC, Dettori JR. Avoiding wrong site surgery: a systematic review. *Spine*. (2010) 35(Suppl. 9):S28–36. doi: 10.1097/BRS.0b013e3181d833ac
- Devine J, Chutkan N, Norvell DC, Gloystein D. An update on wrong-site spine surgery. *Global Spine J*. (2020) 10(Suppl. 1):41S–4. doi: 10.1177/2192568219846911
- Hall MJ, Schwartzman A, Zhang J, Liu X. Ambulatory surgery data from hospitals and ambulatory surgery centers: United States, 2010. *Natl Health Stat Rep*. (2017) (Suppl. 102) 102:1–5.
- James MA, Seiler JG III, Harrast JJ, Emery SE, Hurwitz S. The occurrence of wrong-site surgery self-reported by candidates for certification by the American Board of Orthopaedic Surgery. *J Bone Joint Surg Am*. (2012) 94(Suppl. 1):e2. doi: 10.2106/JBJS.K.00524
- Seiden SC, Barach P. Wrong-side/wrong-site, wrong-procedure, and wrong-patient adverse events: are they preventable? *Arch Surg*. (2006) 141(Suppl. 9):931–9. doi: 10.1001/archsurg.141.9.931
- Number of All-Listed Procedures for Discharges From Short-Stay Hospitals, by Procedure Category and Age: United States. (2010). Available online at: https://www.cdc.gov/nchs/data/nhds/4procedures/2010pro4_numberprocedureage.pdf (accessed November 28, 2017).
- Clarke JR, Johnston J, Finley ED. Getting surgery right. *Ann Surg*. (2007) 246(Suppl. 3):395–403., discussion 403–5. doi: 10.1097/SLA.0b013e3181469987
- Canale ST. Wrong-site surgery: a preventable complication. *Clin Orthop Relat Res*. (2005) (Suppl. 433) 433:26–9. doi: 10.1097/01.blo.0000159827.93813.53
- Agency for Healthcare Research and Quality, Patient Safety Network. *Universal Protocol for Preventing Wrong Site, Wrong Procedure, Wrong Person Surgery*. (2003). Available online at: https://www.jointcommission.org/standards_information/up.aspx (accessed April 11, 2019).
- Health Research & Educational Trust and Joint Commission Center for Transforming Healthcare. *Reducing the Risks of Wrong-Site Surgery: Safety Practices From The Joint Commission Center for Transforming Healthcare Project*. Chicago, IL: Health Research & Educational Trust (2014). Available online at: www.hpoe.org (accessed December 4, 2017).
- Yoon RS, Alaia MJ. Using “Near misses” analysis to prevent wrong site surgery. *J Healthcare Qual*. (2015) 37(Suppl. 2):126–32. doi: 10.1111/jhq.12037
- Agency for Healthcare Research and Quality. *Systems Approach*. (2017). Available online at: <https://psnet.ahrq.gov/primer/primer/21/systems-approach> (accessed December 6, 2017).
- Medication Error Prevention “Toolbox”. (1999). Available online at: <https://www.ismp.org/newsletters/acutecare/articles/19990602.asp> (accessed December 4, 2017).
- Cafazzo JA, St-Cyr O. From discovery to design: the evolution of human factors in healthcare. *Healthc Q*. (2012) 15:24–9. doi: 10.12927/hcq.2012.22845
- Institute of Medicine (US) Committee on Quality of Health Care in America, Kohn LT, Corrigan JM, Donaldson MS, editors. *To Err is Human: Building*

- a Safer Health System. Creating Safety Systems in Health Care Organizations.* Washington, DC: National Academies Press (2000). p. 8. Available online at: <https://www.ncbi.nlm.nih.gov/books/NBK225188/> (accessed December 4, 2017).
16. *Pocket Guide: TeamSTEPPS – Team Strategies & Tools to Enhance Performance and Patient Safety.* (2013). Available online at: <https://www.ahrq.gov/teamstepps/instructor/essentials/pocketguide.html> (accessed May 23, 2019).
 17. The Joint Commission. *Speak Up.* (2018). Available online at: https://www.jointcommission.org/assets/1/18/UP_Poster1.PDF (accessed May 23, 2019).
 18. Bates DW, Boyle DL, Vander Vliet MB, Schneider J, Leape L. Relationship between medication errors and adverse drug events. *J Gen Intern Med.* (1995) 10:199–205. doi: 10.1007/BF02600255
 19. Aspden P, Corrigan JM, Wolcott J, Erickson SM. *Patient Safety: Achieving a New Standard for Care.* Washington, DC: National Academies Press (2004). p. 11.
- Conflict of Interest:** BH, DGS, and JD have equity investment in StartBox, LLC. DS is a consultant for StartBox, LLC.
- The remaining author declares that the research was conducted in the absence of any commercial or financial relationships that could be construed as a potential conflict of interest.
- At least a portion of this work is authored by David M. Gloystein on behalf of the U.S. Government and, as regards David M. Gloystein and the U.S. Government, is not subject to copyright protection in the United States. Foreign and other copyrights may apply. This is an open-access article distributed under the terms of the Creative Commons Attribution License (CC BY). The use, distribution or reproduction in other forums is permitted, provided the original author(s) and the copyright owner(s) are credited and that the original publication in this journal is cited, in accordance with accepted academic practice. No use, distribution or reproduction is permitted which does not comply with these terms.*



Innovation and New Technologies in Spine Surgery, Circa 2020: A Fifty-Year Review

G. Bryan Cornwall^{1,2*}, Andrea Davis³, William R. Walsh², Ralph J. Mobbs² and Alexander Vaccaro⁴

¹ Shiley-Marcos School of Engineering, University of San Diego, San Diego, CA, United States, ² Surgical Orthopaedic Research Laboratory, Prince of Wales Hospital, University of New South Wales, Sydney, NSW, Australia, ³ Bodkin IP, San Diego, CA, United States, ⁴ Rothman's Orthopaedic Institute, Thomas Jefferson University, Philadelphia, PA, United States

OPEN ACCESS

Edited by:

Vassilios S. Nikolaou,
National and Kapodistrian University
of Athens, Greece

Reviewed by:

Leonidas Roulletiotis,
National and Kapodistrian University
of Athens, Greece
Ashok Navratnamal Johari,
Consultant, Mumbai, India

*Correspondence:

G. Bryan Cornwall
bryancornwall@sandiego.edu

Specialty section:

This article was submitted to
Orthopedic Surgery,
a section of the journal
Frontiers in Surgery

Received: 23 June 2020

Accepted: 27 October 2020

Published: 24 November 2020

Citation:

Cornwall GB, Davis A, Walsh WR,
Mobbs RJ and Vaccaro A (2020)
Innovation and New Technologies in
Spine Surgery, Circa 2020: A
Fifty-Year Review.
Front. Surg. 7:575318.
doi: 10.3389/fsurg.2020.575318

Spine surgery (lumbar, cervical, deformity, and entire spine) has increased in volume and improved in outcomes over the past 50 years because of innovations in surgical techniques and introduction of new technologies to improve patient care. Innovation is described as a process to add value or create change in an enterprise's economic or social potential. This mini review will assess two of three assessments of innovation in spine surgery: scientific publications and patents issued. The review of both scientific publications and issued patents is a unique assessment. The third assessment of innovation: regulatory clearances of medical devices and equipment for spine surgery and their evolution over time, will also be discussed.

Keywords: spine surgery, innovation, new technology, robotics, artificial intelligence, biologics, spine implants, mini review

INTRODUCTION

Improvements and advancements in patient outcomes with spine surgery have been facilitated by many factors including the potential offered by innovations and new technologies. It is necessary to measure outcomes; otherwise, how does one assess whether advancements or benefits are realized? Whether the innovation is in surgical techniques or surgeon training, or efficiencies in surgical care, or the introduction of a new technology, or perhaps new ways to monitor patient outcome, improvements can be derived from process improvements to novel devices.

Innovation is the positive change in process or efficiency that leads to improved value. This may or may not involve an invention or novel new technology. It could be the result of education, introducing a technique or technology from another field, or focusing on other positive metrics and removing inefficiencies or other negative metrics. According to academic business leader and innovation expert, Peter Drucker (1): "At the heart of that activity, entrepreneurship, is innovation: the effort to create purposeful, focused change in an enterprise's economic or social potential." The same description of innovation could be applied to medicine and the advancement of patient care.

The history of spine surgery is replete with innovators and pioneers. Often in the early phase of introducing an innovation or new technology, these innovators may have been reviled or misunderstood and then over time rejoiced. One such example, Dr. Paul Harrington whose story of developing spinal surgery and implants for children afflicted with polio-induced scoliosis was recently published: "Dogged Persistence" (2) by Dr. Mark Asher. An article published a review of the origins of eponymous instruments for spine surgery, all named for surgeon innovators (3). Other articles reported the innovations and inventions of neurosurgeons and spine surgery (4, 5).

Starting in 2001, an annual review of “What’s New in Spine Surgery” was summarized in the *Journal of Bone and Joint Surgery* (6–24). The specific review topics varied each year, but were generally organized into categories of cervical spine, lumbar spine, spinal deformity, biologics in the spine, and occasionally spinal cord injury.

Inventions are the creative process of introducing a new idea which may culminate in a patent. A patent is a contract to protect intellectual property for a period of time in exchange for the public disclosure of said invention (25, 26). Patents however are often only part of the story as other factors influence the translation of an idea into clinical use. These include clinical need, manufacturing cost, reimbursement, and ease of use in solving a problem or improving clinical outcomes.

In 2006 the book: “Emerging Spine Surgery Technologies: Evidence and Framework for Evaluating New Technology” edited by Corbin et al. (27) summarized the emerging technologies in spine surgery of the time (28). Given that innovation is a “focused change,” it is logical that innovation is dynamic and “new” technology is a snapshot of a certain period. For example, Dr. Paul Harrington’s ratcheting spinal hooks with rods were new technology in the early 1960’s but evolved with measured outcomes, continued innovation, and were ultimately replaced by pedicle screw and rod technology. In “Emerging Spine Surgery Technologies” (27), the book is organized into four sections with the majority of the content covering biologic and tissue engineering and surgical techniques including spinal implants and disc replacements.

While this comprehensive textbook provided a nice overview of emerging technologies of the time, there were no chapters covering lateral surgery, resorbable polymers in spine, additive manufacturing or 3D printing, robotics, artificial intelligence (AI), and machine learning applied to spine surgery. The purpose of this mini review is to assess the trends of innovation in spine surgery over time from 1970 through to 2019, a 50-year period. The mini-review is unique in that it combines both a review of the scientific literature and a review of issued patents as a means to evaluate trends in spine surgery over the past 50 years.

MATERIALS AND METHODS

To assess “innovation and new technology” in spine surgery over time, we evaluated two distinct representations of innovation: (1) scientific/clinical interest through peer-reviewed publications, and (2) intellectual property interest through issued United States and European patents. We evaluated the literature in the selected databases over the past 50 years.

Science/Clinical Publications: Pubmed Database

The “Pubmed” database from the US National Institutes of Health was used to assess the number of peer-reviewed scientific publications associated with a given keyword or combination of keywords. As a representation for how relevant each technology is to spine surgery over time, we evaluated the indexed spine

surgery literature using Pubmed as a consistent database. We started with using the keywords: “spine surgery” and assessed the number of publications per year from January 1, 1970 to December 31, 2019. We evaluated the following additional keywords in combination with spine surgery using the logic limiter “AND”: cervical, lumbar, deformity, scoliosis, innovation, new technology, lateral lumbar, resorbable polymer, biologics, disc replacement, image guidance, 3D printing, robotics, and artificial intelligence.

Intellectual Property (Issued Patents): US and EP Patseer Database

The “PatSeer” database was used to assess the number of granted US and EP (European) patents for each category. The Cooperative Patent Classification (29) and the US Patent Classification (30) were used to identify the different technology areas within the spinal innovation field. Where at all possible, the individual patent subclasses were selected that represent each category by their definition. In some cases where there was not a directly corresponding category or art was classified in further classifications of a more comprehensive nature, additional classification and keyword combinations were used to narrow in on the categories selected: biologics, spinal plates, interbody devices, pedicle screws, image guided surgery, and robotic surgery, all related to spine.

RESULTS

Science/Clinical Publications: Pubmed Database

The number of scientific publications with the keyword: “spine surgery,” increased exponentially from 1970 through 2019 as illustrated in **Figure 1A**. With over 100,000 (103,698) peer-reviewed publications starting with 291 publications in 1970 and with over 7,000 publications in 2019, the growth is demonstrated in the plot of number of publications per year. 65.1% of these publications have occurred since 2006, when the *Emerging Technologies in Spine Surgery* (27) book was written.

The spine literature was also characterized using the three main classifications identified in the “What’s New in Spine Surgery” series of articles: cervical, lumbar, and deformity (or scoliosis). For each keyword AND spine surgery, the subset number of publications was determined per year. The results were expressed as a percentage of the number of spine surgery publications per year as demonstrated in **Figure 1A**. The trendline for the keyword deformity AND spine surgery was relatively constant across the 50-year period. On average, 11% of the spine surgery literature had the keyword “deformity” with a standard deviation of 1.4% and the proportion of publications ranging from a high of 14.5% to a low of 7.2% for any given year. The trendline of “lumbar” articles has generally increased over the 50-year period with an average of 38.8% of the articles with a standard deviation of 3.7% ranging from a high of 47.3% to a low of 30.9%. The trendline of “cervical” articles has generally decreased over the 50-year period with an average of 27.9% of the

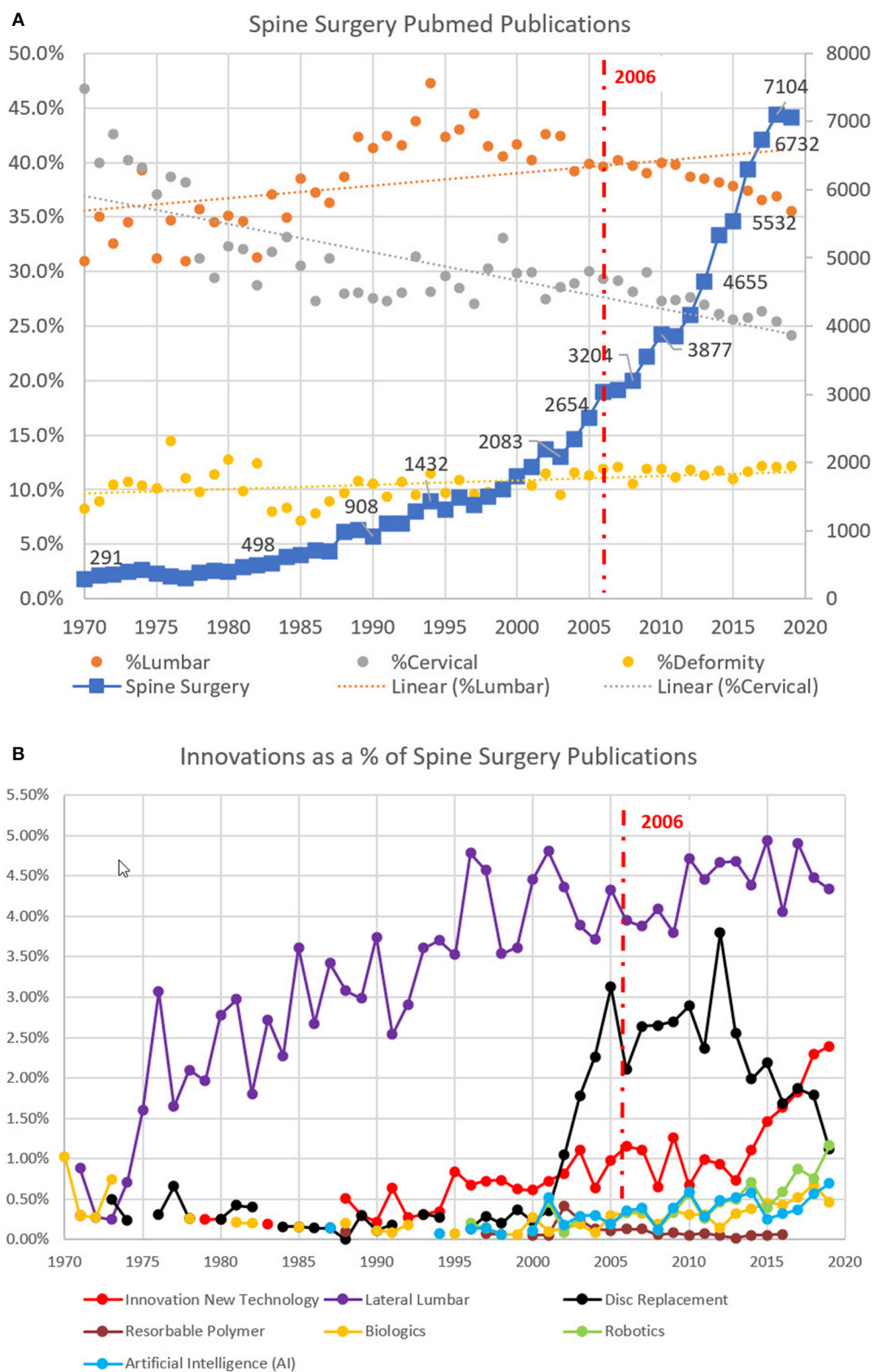


FIGURE 1 | (A) Pubmed keyword search for the time (1970–2019) including keywords: spine surgery AND lumbar, cervical, and deformity. **(B)** Pubmed keyword search for the same period (1970–2019) including keywords: lateral lumbar, disc replacement, and resorbable polymer AND spine surgery.

TABLE 1 | Categories or Technologies and keyword "Spine Surgery."

Keyword	# Publications (1970–2019)	% of Spine Surgery	# Publications (2006–2019)	% of Total Spine Surgery (1970–2019)	# Years with Keyword
Spine Surgery	103,698	100.0%	67,474	65.1%	50
Cervical	28,927	27.9%	17,987	62.2%	50
Deformity	11,568	11.2%	7,861	68.0%	50
Lumbar	40,263	38.8%	25,666	63.7%	50
Innovation or New Technology	1,162	1.1%	970	83.5%	36
Artificial Intelligence (AI)	339	0.3%	298	87.9%	25
Biologics	319	0.3%	272	85.3%	36
Disc Replacement	1,723	1.7%	1,471	85.4%	41
Image Guidance	2,331	2.2%	1,911	82.0%	37
Lateral Lumbar	4,257	4.1%	2,988	70.2%	49
Resorbable Polymer	56	0.05%	31	55.4%	20
Robotics	441	0.4%	403	91.4%	24
3D Printing	190	0.18%	190	100.0%	7

articles with a standard deviation of 4.9% ranging from a high of 46.7% to a low of 24.1%.

The number of publications with the various innovation and new technology keywords AND spine surgery are summarized in **Table 1**. These keywords were also assessed as a percentage of the spine surgery literature over time and plotted in **Figure 1B**. Starting with the keywords: innovation OR new technology AND spine surgery, there were 1,162 publications between 1970 and 2019 with 83% of those articles published after 2006. One technology in the book (27), disc replacements in spine surgery, were featured in seven book chapters. Using the keywords: disc replacement AND spine surgery, there were 1,723 publications between 1970 and 2019 with 85% of those articles published after 2006.

Two examples of new technologies that did not appear in the 2006 Emerging Technologies book (27): resorbable polymers for spine surgery and lateral lumbar spine surgery. Using a similar keyword strategy there were 56 publications with resorbable polymers AND spine surgery with 55.4% of those publications after 2006 and there were 4,257 articles concerning lateral lumbar AND spine surgery with 70% of those published after 2006. Clearly lateral spine surgery has continued to be a relevant innovation while resorbable polymers has not been a new technology that has stood the test of time.

Intellectual Property (Issued Patents): US and EP Patseer Database

The entire dataset of 16,336 records of patent grants from January 1, 1970 to December 31, 2019 was analyzed and plotted in **Figure 2** using the patent analytics software. Publication trends of US and EP granted patents with time are summarized in **Figure 2**. In the first two decades, between 1970 and 1990, there was almost no patenting activity in this domain with the categories having mostly none, but at most 10 granted patents each year. Spinal patenting trends for the mechanical technologies (pedicle screws, spinal plates, and interbodies) and biologics slowly start to grow post 1990. All of them seem to have a decrease in

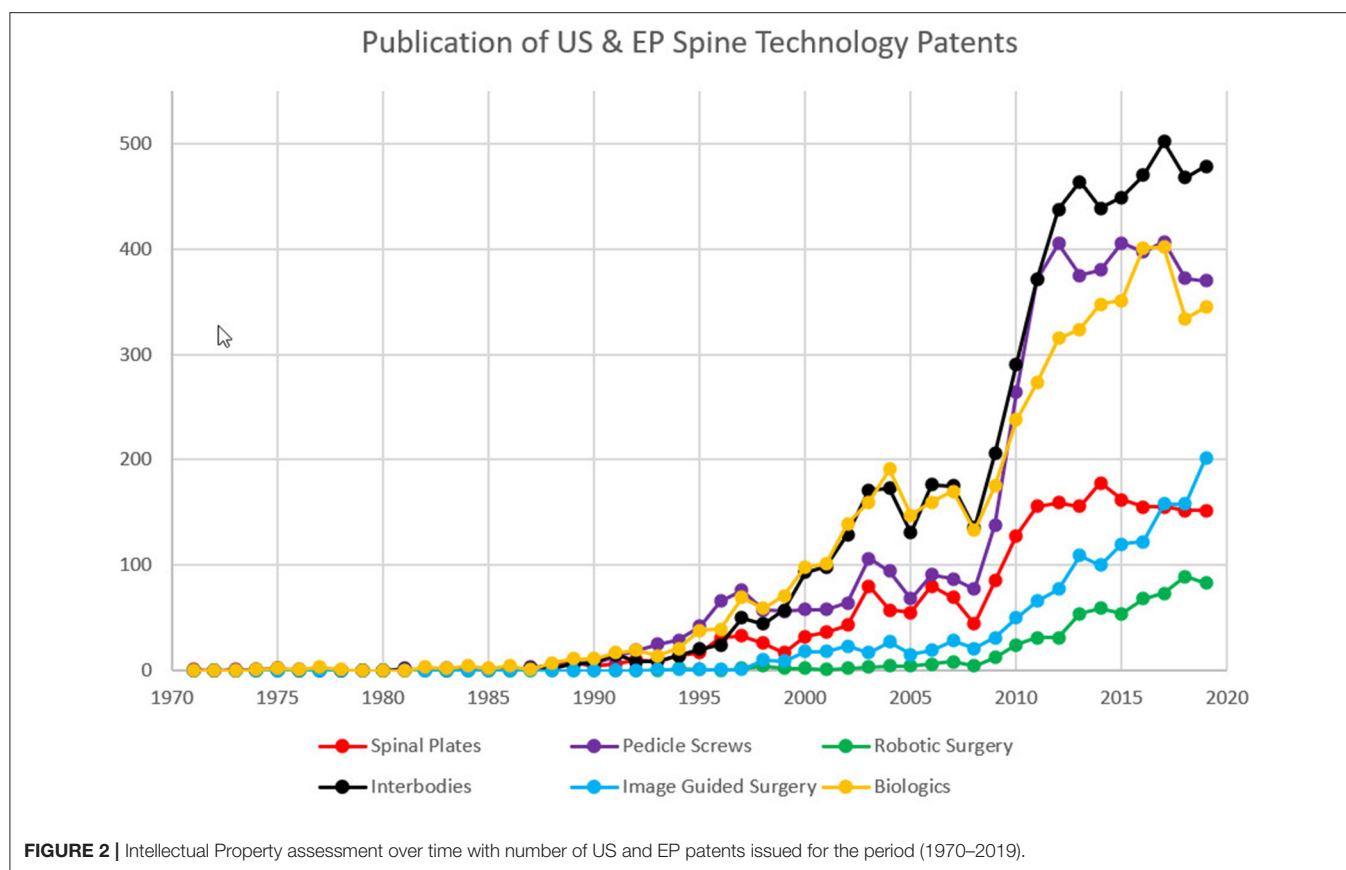
2008, possibly due to the recession of that time, then increase exponentially from that point on for the following 4 years. Starting 2014 the graphical representation shows a plateau with 450–500 patents/year related to interbodies, 150/year related to spinal plates (including cervical, thoracic, and lumbar), 350–400 patents/year related to pedicle screws, and about the same for biologics. The more modern categories of image-guided and robotic surgery have seen a steady increase from about 2008.

The patenting trends have to be seen as a delayed innovation proof in view of the quite lengthy average time to get a patent, which between 2008 and 2015 was about 3.5 years in the US and 5.5 years at the European Patent Office (31).

DISCUSSION

In most of the industrialized world, the metrics associated with spine care are improving (32). More patients are having surgery and those patients are getting better with care. Is this the result of innovation or invention? Companies and even health care systems are perceiving the benefit of innovation largely driven by the greater business community and the focus on innovation across many industries (1).

We were interested in using regulatory clearances as another reflection of interest in innovation and introduction of new technologies over time. However, this investigation proved to be problematic for numerous reasons. First, there is no global database for the regulatory clearance or approval of medical devices. While scientific literature does have global databases such as Pubmed, regulatory approvals tend to be more regional or country specific. Even in a large market covering the European Union, there is currently no medical device database (33, 34). In the largest spine market, the USA, there are three different databases that could be assessed but they cover different time periods and have different relative pros and cons (35). The first is the US Food and Drug Administration (FDA) premarket notification or 510(k) database for devices that are cleared based upon achieving substantial equivalence to another cleared device.



The data goes back to 1976 when medical devices were added to the amended federal food, drug, and cosmetic (FD&C) act. The majority of spine devices introduced to the market fall under the 510(k) pathway (35). The second database is for devices that fall under the premarket announcement (PMA) requiring a clinical study prior to regulatory approval. New technologies such as total disc replacements for both lumbar and cervical fall under this pathway. A third database to investigate is the National Institutes of Health (NIH) US National Library of Medicine ClinicalTrials.gov database of registered clinical trials. There were 784 studies registered with the keywords spine surgery. The assessment of regulatory clearances could provide additional clues about innovation and new technologies introduced into the marketplace. However, the authors considered the disparity of information between these regulatory databases to limit the usefulness of this information in this mini review.

In the 2001 article, “What’s New in Spine Surgery” (6), the authors commented that in the last 20 years from 1981 to 2001, the number of spine fellowship programs had increased from <15 to more than 200. In 2006, the book on Emerging Technologies in Spine (27, 28) described an innovative time and a period of prolific introduction of new technologies hoping to improve patient care. As more and more technologies were introduced, there was more push-back from regulatory bodies in both the United States (US) and in the European Union (EU) to improve the burden of proof and from insurance providers

adding more scrutiny to what technologies would be reimbursed (or paid for).

Patenting trends are strongly influenced by legal and political measures taken in the jurisdiction of filing. Supreme Court decisions, instituting new measures like the PTAB (US Patent and Trials Board) and AIA (Leahy–Smith America Invents Act) all contribute to changes in the big medical device companies’ patent strategies. As seen in **Figure 2**, all the mechanical categories and biologics seem to have a decrease in 2008, possibly due to the recession of that time, then increase exponentially from that point on for the following 4 years. The sharp increase may be in part influenced by the Affordable Care Act signed into law in 2010 and the medical device tax that became effective January 2013 (36).

Another new technology and innovation that was not considered in 2006 was the application of wearable technology sensors (37). Recent work has evaluated the use of “wearables” for objective measurements for outcomes analysis (38). Most clinical studies employ subjective observations to evaluate clinical outcomes. The use of inertial markers or other motion tracking technology to assess objective data could be a potential innovation to improve patient care.

The effect of surgeon training as an innovation in process was not evaluated in detail in this mini-review. Surgeon training can have positive influences on patient outcomes and there has been interesting research performed in this area (39–41). The effect

of training was thought to be difficult to evaluate with both a scientific and intellectual property perspective. There has also been interesting research conducted utilizing new technologies such as 3D printing (42) and virtual reality (43, 44). Hopefully, these new innovations in training with new technologies will translate into improved patient outcomes.

Aging population and technological developments will likely drive innovation in the field of spinal surgery. Growth in patenting is expected in areas that have evolved in the past few years, such as spinal navigation, robotic surgery, minimally invasive surgery, patient-specific implants, and 3D printing.

In 2020, there continues to be an interest in both innovation and in new technologies for spine surgery to improve spine care and clinical outcomes. Innovation has been described as a process to add value or create change in an enterprise's economic or social potential. As the global pandemic associated with Covid-19

continues to unfold, innovation will continue to be necessary for all constituents: patients, surgeons, hospitals, health-care providers, industry, payors, and governments.

AUTHOR CONTRIBUTIONS

Study concept: GC, WW, and AV. Data collection: GC and AD. Data analysis: All authors. First draft: GC. Review and editing: All authors.

ACKNOWLEDGMENTS

The authors would like to thank and acknowledge the University of New South Wales (UNSW) Surgical Orthopedic Research Laboratory (SORL) for the funding to pay the open access publishing fees.

REFERENCES

- Drucker P, Christensen CM. *HBR's 10 Must Reads on Innovation*. In: Harvard BS, editor. (with featured article *The Discipline of Innovation*. Drucker PE, editor). Harvard Business Review (2013). p. 1–172. Available online at: <https://hbr.org/product/hbrs-10-must-reads-on-innovation-with-featured-article-the-discipline-of-innovation-by-peter-f-drucker/11363E-KND-ENG> (cited September 7, 2019).
- Asher MA. *Dogged Persistence: Harrington, Post-Polio Scoliosis, and the Origin of Spine Instrumentation*. Kansas: Chandler Lake Books (2015). p. 1–395.
- Buraimoh M, Basheer A, Taliaferro K, Shaw JH, Haider S, Graziano G, et al. Origins of eponymous instruments in spine surgery. *J Neurosurg Spine*. (2018) 29:696–703. doi: 10.3171/2018.5.SPINE17981
- Babu MA, Heary RF, Nahed BV. Device innovation in neurosurgery: controversy, learning, and future directions. *Neurosurgery*. (2012) 70:789–94. doi: 10.1227/NEU.0b013e318237a68b
- Baron RB, Kessler RA, Bhammar A, Boulis N, Adler JR, Kohli K, et al. Patents and innovation among neurosurgeons from the american association of neurological surgeons. *Cureus*. (2020) 12:e7031. doi: 10.7759/cureus.7031
- Zigler JE, Anderson PA, Bridwell K, Vaccaro A. What's new in spine surgery. *J Bone Joint Surg A*. (2001) 83:1285–92. doi: 10.2106/00004623-200108000-00036
- Zigler JE, Boden S, Anderson PA, Bridwell K, Vaccaro A. What's new in spine surgery. *J Bone Joint Surg A*. (2002) 84:1282–8. doi: 10.2106/00004623-200207000-00035
- Bridwell KH, Anderson PA, Boden SD, Vaccaro AR, Wang JC. What's new in spine surgery. *J Bone Joint Surg A*. (2012) 94:1140–8. doi: 10.2106/JBJS.L.00308
- Hobbs J, Bina R, Dohrmann G, Roitberg B. What's new in spine surgery. *Med Princ Pract*. (2013) 22:101–2. doi: 10.1159/000346294
- Bridwell KH, Anderson PA, Boden SD, Kim HJ, Vaccaro AR, Wang JC. What's new in spine surgery. *J Bone Joint Surg Am*. (2014) 96:1048–54. doi: 10.2106/JBJS.N.00103
- Bridwell KH, Anderson PA, Boden SD, Kim HJ, Vaccaro A, Wang JC. What's new in spine surgery. *J Bone Joint Surg Am*. (2015) 97:1022–30. doi: 10.2106/JBJS.O.00080
- Choma TJ, Brodke DS. What's new in spine surgery. *J Bone Joint Surg*. (2016) 98:1052–8. doi: 10.2106/JBJS.16.00169
- Choma TJ, France JC, Karnes JM. What's new in spine surgery. *J Bone Joint Surg*. (2017) 99:1058–64. doi: 10.2106/JBJS.17.00276
- Choma TJ. What's new in spine surgery. *J Bone Joint Surg*. (2018) 100:1071–4. doi: 10.2106/JBJS.18.00189
- Buchowski JM, Adogwa O. What's new in spine surgery. *J Bone Joint Surg*. (2019). 101:1043–9. doi: 10.2106/JBJS.19.00229
- Buchowski JM, Adogwa O. What's new in spine surgery. *J Bone Joint Surg Am*. (2020). 102:1034–41. doi: 10.2106/JBJS.20.00239
- Zigler JE, Anderson PA, Boden SD, Bridwell KH, Vaccaro AR. What's new in spine surgery. *J Bone Joint Surg A*. (2003) 85:1626–36. doi: 10.2106/00004623-200308000-00051
- Bridwell KH, Anderson PA, Boden SD, Vaccaro AR, Zigler JE. What's new in spine surgery. *J Bone Joint Surg A*. (2004) 86:1587–94. doi: 10.2106/00004623-200407000-00033
- Bridwell KH, Anderson PA, Boden SD, Vaccaro AR, Wang JC. What's new in spine surgery. *J Bone Joint Surg A*. (2005) 87:1892–901. doi: 10.2106/00004623-200508000-00047
- Bridwell KH, Anderson PA, Boden SD, Vaccaro AR, Wang JC. What's new in spine surgery. *J Bone Joint Surg A*. (2006) 88:1897–907. doi: 10.2106/JBJS.F.00346
- Bridwell KH, Anderson PA, Boden SD, Vaccaro AR, Wang JC. What's new in spine surgery. *J Bone Joint Surg A*. (2008) 90:1609–19. doi: 10.2106/JBJS.H.00418
- Bridwell KH, Anderson PA, Boden SD, Vaccaro AR, Wang JC. What's new in spine surgery. *J Bone Joint Surg A*. (2009) 91:1822–34. doi: 10.2106/JBJS.I.00488
- Bridwell KH, Anderson PA, Boden SD, Vaccaro AR, Wang JC. What's new in spine surgery. *J Bone Joint Surg A*. (2010) 92:2017–28. doi: 10.2106/JBJS.J.00434
- Bridwell KH, Anderson PA, Boden SD, Vaccaro AR, Wang JC. What's new in spine surgery. *J Bone Joint Surg A*. (2011) 93:1560–6. doi: 10.2106/JBJS.K.00508
- Ducor P. Intellectual property: coauthorship and coinventorship. *Science*. (2000) 289:873–5. doi: 10.1126/science.289.5481.873
- Konski AF, Wu LX. Inventorship and authorship. *Cold Spring Harb Perspect Med*. (2015) 5:a020859. doi: 10.1101/cshperspect.a020859
- Corbin TP, Connolly PJ, Yuan HA, Bao Q-B, Boden SD (editors). *Emerging Spine Surgery Technologies: Evidence and Framework for Evaluating New Technology*. 1st ed. St. Louis: QMP (Quality Medical Publishing) (2006). p. 1–604.
- Wigfield C. Book Review: “*Emerging Spine Surgery Technologies: Evidence and Framework for Evaluating New Technology*” (2007). Available online at: [https://www.orthopaedicsandtraumajournal.co.uk/article/S0268-0890\(06\)00069-7/pdf](https://www.orthopaedicsandtraumajournal.co.uk/article/S0268-0890(06)00069-7/pdf) (cited September 6, 2019).
- EPO - Cooperative Patent Classification (CPC). Available online at: <https://www.epo.org/searching-for-patents/helpful-resources/first-time-here/classification/cpc.html> (cited May 20, 2020).
- Patent Classification | USPTO. Available online at: <https://www.uspto.gov/patents-application-process/patent-search/classification-standards-and-development> (cited May 20, 2020).
- It's Time to Fix the Global Patent System Before It Breaks Under the Weight of New Applications - IPWatchdog.com | Patents & Patent Law. Available online at: <https://www.ipwatchdog.com/2016/10/24/time-fix-global-patent-system/id=74112/> (cited May 20, 2020).

32. Street J, Lenehan B, Fisher C. The quality of quality of life publications in the spinal literature: Are we getting any better? - Clinical article. *J Neurosurg Spine*. (2009) 11:512–7. doi: 10.3171/2009.4.SPINE08599
33. European Database on Medical Devices (EUDAMED) | Internal Market, Industry, Entrepreneurship and SMEs. Available online at: https://ec.europa.eu/growth/sectors/medical-devices/new-regulations/eudamed_en (cited May 17, 2020).
34. Camus D, Thiveaud D, Jossereau A, Barthélémy CE, Chambrin PY, Hebbrecht G, et al. New European medical device regulation: How the French ecosystem should seize the opportunity of the EUDAMED and the UDI system, while overcoming the constraints thereof. *Therapies*. (2019) 74:73–85. doi: 10.1016/j.therap.2018.12.001
35. Day CS, Park DJ, Rozenshteyn FS, Owusu-Sarpong N, Gonzalez A. Analysis of FDA-approved orthopaedic devices and their recalls. *J Bone Joint Surg Am*. (2016) 98:512–24. doi: 10.2106/JBJS.15.00286
36. Mayfield DL. Medical patents and how new instruments or medications might be patented. *Mo Med*. (2016) 113:456–62.
37. Simpson L, Maharaj MM, Mobbs RJ. The role of wearables in spinal posture analysis: a systematic review. *BMC Musculoskelet Disord*. (2019) 20:55. doi: 10.1186/s12891-019-2430-6
38. Mobbs RJ, Mobbs RR, Choy WJ. Proposed objective scoring algorithm for assessment and intervention recovery following surgery for lumbar spinal stenosis based on relevant gait metrics from wearable devices: the Gait Posture index (GPI). *J Spine Surg*. (2019) 5:300–9. doi: 10.21037/jss.2019.09.06
39. Lopez G, Wright R, Martin D, Jung J, Bracey D, Gupta R. A cost-effective junior resident training and assessment simulator for orthopaedic surgical skills via fundamentals of orthopaedic surgery aaos exhibit selection: AAOS exhibit selection. *J Bone Joint Surg Am*. (2015) 97:659–66. doi: 10.2106/JBJS.N.01269
40. Yaeger KA, Munich SA, Byrne RW, Germano IM. Trends in United States neurosurgery residency education and training over the last decade (2009–2019). *Neurosurg Focus*. (2020) 48:E6. doi: 10.3171/2019.12.FOCUS 19827
41. Tong Y, Fernandez L, Bendo JA, Spivak JM. Enhanced recovery after surgery trends in adult spine surgery: a systematic review. *Int J Spine Surg*. (2020) 14:623–40. doi: 10.14444/7083
42. Clifton W, Nottmeier E, Edwards S, Damon A, Dove C, Refaey K, et al. Development of a novel 3D printed phantom for teaching neurosurgical trainees the freehand technique of C2 laminar screw placement. *World Neurosurg*. (2019) 129:e812–20. doi: 10.1016/j.wneu.2019.06.038
43. Luca A, Giorgino R, Gesualdo L, Peretti GM, Belkhou A, Banfi G, et al. Innovative educational pathways in spine surgery: advanced virtual reality-based training. *World Neurosurg*. (2020) 140:674–80. doi: 10.1016/j.wneu.2020.04.102
44. Ledwos N, Mirchi N, Bissonnette V, Winkler-Schwartz A, Yilmaz R, Del Maestro RF. Virtual reality anterior cervical discectomy and fusion simulation on the novel sim-ortho platform: validation studies. *Oper Neurosurg*. (2020) opaa269. doi: 10.1093/ons/opaa269

Conflict of Interest: GC, WW, RM, and AV are all employed by academic institutions and provide consulting services to spinal device companies. AD was employed by the company Bodkin IP. AD is a patent consultant and her business surrounds Intellectual Property research. There was no compensation for any authors in writing this manuscript.

All authors declare that the research was conducted in the absence of any commercial or financial relationships that could be construed as a potential conflict of interest.

Copyright © 2020 Cornwall, Davis, Walsh, Mobbs and Vaccaro. This is an open-access article distributed under the terms of the Creative Commons Attribution License (CC BY). The use, distribution or reproduction in other forums is permitted, provided the original author(s) and the copyright owner(s) are credited and that the original publication in this journal is cited, in accordance with accepted academic practice. No use, distribution or reproduction is permitted which does not comply with these terms.



Complete Osseointegration of a Retrieved 3-D Printed Porous Titanium Cervical Cage

Wimar van den Brink¹ and Nancy Lamerigts^{2*}

¹ Department Neurosurgery, Isala, Zwolle, Netherlands, ² Emerging Implant Technologies (EIT), Wurmlingen, Germany

OPEN ACCESS

Edited by:

William Robert Walsh,
University of New South
Wales, Australia

Reviewed by:

Paul Simon Unwin,
Independent Researcher, Ludlow,
United Kingdom
Konstantinos Markatos,
Biomedical Research Foundation of
the Academy of Athens
(BRFAA), Greece

*Correspondence:

Nancy Lamerigts
nancy@lamerigts.nl

Specialty section:

This article was submitted to
Orthopedic Surgery,
a section of the journal
Frontiers in Surgery

Received: 11 January 2020

Accepted: 09 September 2020

Published: 26 November 2020

Citation:

van den Brink W and Lamerigts N
(2020) Complete Osseointegration of
a Retrieved 3-D Printed Porous
Titanium Cervical Cage.
Front. Surg. 7:526020.
doi: 10.3389/fsurg.2020.526020

Introduction: Porous 3D-printed titanium has only recently been introduced for spinal applications. Evidence around its use is currently limited to animal studies and only few human case series. This study describes the histological findings of a retrieved EIT cervical cage, explanted 2 years after insertion.

Materials and Methods: The patient underwent a double level C4/C5 & C5/C6 anterior cervical decompression using EIT cervical cages without an anterior plate. Two years later the C6/7 level degenerated and began to cause myelopathic symptoms. In order to address the kyphotic imbalance of the cervical spine and fix the C6/7 level, the surgeon decided to remove the C5/6 cervical cage and bridge the fusion from C4 to C7 inclusive. The retrieved cage was histologically evaluated for bone ingrowth and signs of inflammation.

Results: MRI demonstrated spinal canal stenosis at C6/C7. Plain radiographs confirmed well-integrated cervical cages at 2 years postoperative. The peroperative surgical need to use a chisel to remove the implant at C5/C6 reconfirmed the solid fusion of the segment. Macroscopically white tissue, indicative of bone, was present at both superior and inferior surfaces of the explanted specimen. Histological evaluation revealed complete osseointegration of the 5 mm high EIT Cellular Titanium[®] cervical cage, displaying mature lamellar bone in combination with bone marrow throughout the cage. Furthermore, a pattern of trabecular bone apposition (without fibrous tissue interface) and physiological remodeling activity was observed directly on the cellular titanium scaffold.

Conclusion: This histological retrieval study of a radiologically fused cervical EIT cage clearly demonstrates complete osseointegration within a 2-year time frame. The scaffold exhibits a bone in growth pattern and maturation of bone tissue similar of what has been demonstrated in animal studies evaluating similar porous titanium implants. The complete osseointegration throughout the cage indicates physiological loading conditions even in the central part of the cage. This pattern suggests the absence, or at least the minimization, of stress-shielding in this type of porous titanium cage.

Keywords: osseointegration, 3d printed titanium implant, porous titanium alloy, cervical spine fusion, bone ingrowth spinal cage

INTRODUCTION

Anterior cervical discectomy and fusion (ACDF) is a common procedure in cervical spine surgery. Various types of cage materials and designs, either combined with bone graft material and/or osteoinductive substances, are clinically in use. The size and shape of cages differ, depending on the design philosophy and technical production limitations of the material.

There are five critical areas in the clinical application of cages for spinal fusion that influence clinical results and imaging assessment capabilities. First, the occurrence of pseudoarthrosis (non-union), secondly subsidence and migration, thirdly suboptimal spinal balance, fourthly immunological reactivity due to the cage material and lastly the imaging distortion on MRI and CT scans. With the availability of 3-D printing of titanium in a cellular structure, it became possible to significantly address these clinical issues, being able to manufacture a structure that closely mimics bone, and that provides an optimal rough and porous scaffold for ingrowth of bone. EIT Cellular Titanium[®] has been developed based on the results of various *in-vitro* and *in-vivo* studies, combining the various findings related to adequate pore size, shape, and porosity that would permit maximal bony ingrowth (1–9). The 80% porosity of cellular titanium warrants an elasticity modulus close to the bony environment. Furthermore, distortion on MRI and CT scans is minimized, especially when compared to the distortion observed with massive titanium, or trabecular metal implants. This allows for both a more detailed evaluation of the fusion process, and for evaluation of decompression of the neural structures (data on file VAL 2017-007). Because the 3D printed porous titanium material has only recently been introduced for spinal application, limited clinical studies and proof of fusion are available. In this retrieval study we describe the histological bone in growth pattern in a retrieved EIT Cellular Titanium[®] cervical cage 2 years after implantation.

MATERIALS AND METHODS

The cervical implants applied in the patient were EIT cervical cages (EIT-spine GmbH, Wurmlingen), 3D printed porous titanium cages made from Ti6Al4V ELI powder. Selective Laser Melting (SLM) is used to produce the implants (3D Systems, Denver). The EIT implants consist of a porous titanium scaffold (pore size 700 μm , diamond shaped grid, porosity 80%) and small solid rims. The porous scaffold has a 0.25 mm off-set related to the solid rims, to ensure a direct implant scaffold-endplate contact. The cervical implant is anatomical shaped, with a tapered outline, uncovertebral sparings and a cranial anatomical dome to fit snugly the cervical intervertebral disc space (**Figure 3A**).

The MARS-MRI (Metal Artifact Reduction Sequence) enables a good evaluation of the cervical spine and neural structures with a minimum of artifact, which is also illustrated in the MRI of this patient, having two EIT cages at the levels C4/C5 and C5/C6 (**Figure 2**).



FIGURE 1 | X-ray double level EIT CIF cage C4C5 and C5C6 2 years postop. Arrow indicates symptomatic level.



FIGURE 2 | MRI double level EIT CIF cage 2 years postop Arrow indicates spinal stenosis C6/C7.

The EIT Cellular Titanium[®] cervical cage at the level C5/C6 was extracted during revision surgery and was immediately stored in formaldehyde 4% buffer solution (**Figure 3B**).

The specimen was imbedded in resin (Technovit 9100), trimmed to reach the middle zone of the specimen (red line **Figure 3B**) and 4 sections from one half of the implant were made using a diamond band saw (Exakt). The thin-sections were grounded to a thickness of 25–35 μm stepwise with the Micro grinder machine (Exakt 400 CS, Norderstedt, Germany) and with grinding paper of different grain sizes. As last step the thin sections were polished with polishing paper (4,000 grain size).

The sections were stained with H&E (Gill2) and Masson's Goldner Trichrome. Before staining of the thin-sections the plastic resin was removed via deplast-solution. Therefore, the thin sections were incubated 2x in Xylene and further incubated 2x in Methoxyethyl acetate (MEA), followed by washing in acetone and rinsed with water. The

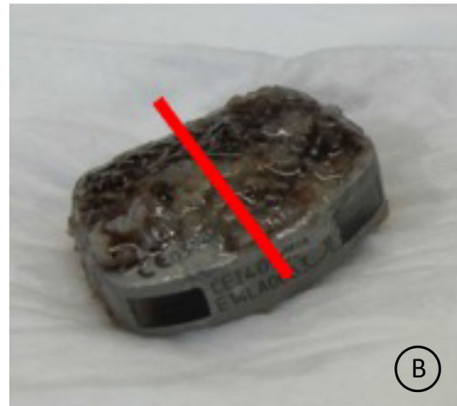


FIGURE 3 | (A) EIT cervical cage. **(B)** Retrieved cervical cage specimen. The red line indicates the intersection line from which the histological sections were cut.

deplasticized sections were stained, dehydrated and cover slipped with mounting medium. The stained thin-sections were scanned with the Zeiss Axio Scan Z.1 System with a 20x magnification.

CASE REPORT AND HISTOLOGICAL RESULTS

The patient (male, 70 yrs old) had a double level (C4/C5, C5/C6) ACDF using EIT Cellular Titanium® cervical cages and no plate for 2 years before renewed symptomatology of the level below occurred (**Figures 1, 2**). Because of the cervical kyphotic malalignment, the surgeon (WBR) elected to sacrifice the C5/6 fused cervical level in order to treat the local symptomatology and restore the cervical lordosis over C5/C6-C6/C7.

The surgeon had to use chisels and force to extract the well-integrated cage.

Macroscopic inspection of the retrieved cage already revealed white tissue, similar to bone, on both caudal and cranial cage-endplate contact areas (**Figure 3B**).

In the HE stained specimen lamellar bone was found in close contact with the titanium surface and the bone extended throughout the cage from endplate to endplate (**Figure 4**). The microscopic analysis confirmed the infiltration of bony tissue in the anterior 2/3th of the cage, bridging the entire height of the 5 mm cage.

No fibrous tissue interface was found between the newly formed bone and the titanium struts (**Figures 5A–C**). The posterior part of the cage was infiltrated with dense fibrous tissue, demonstrating caudal-cranial directed collagen fibers (**Figures 5D–F**). Areas of bone marrow could be seen throughout the section, indicative of mature trabecular bone development.

The Masson's Goldner Trichrome staining showed active bone remodeling in various areas throughout the section with patterns of adaptive reactivity and no appearance of signs of overloading (**Figures 6, 7A–C**). No inflammatory cells or tissue reactions could be observed.

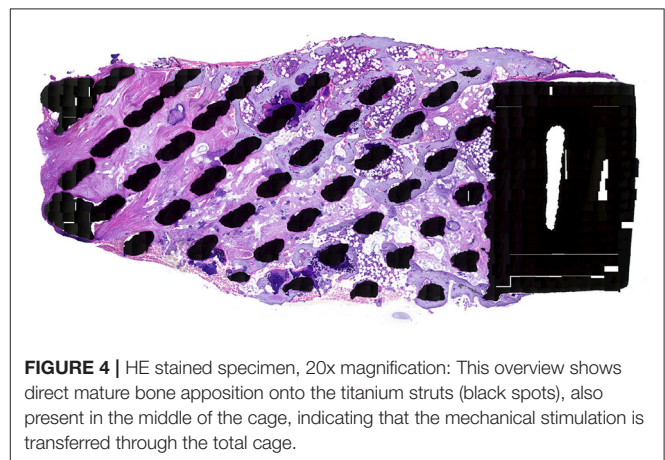


FIGURE 4 | HE stained specimen, 20x magnification: This overview shows direct mature bone apposition onto the titanium struts (black spots), also present in the middle of the cage, indicating that the mechanical stimulation is transferred through the total cage.

DISCUSSION

Titanium alloy has a long track-record in orthopedic surgery for being a great biocompatible material, probably because of the ability of titanium to form a non-reactive TiO_2 surface layer to resist corrosion and create a high surface energy that facilitates bone growth in and around the implant (10, 11). In the early years of spinal fusion surgery the applied solid titanium spinal cages tended to cause stress-shielding, subsidence and imaging issues. The development of PEEK spacers was a logical consequence (12), having more favorable mechanical characteristics with an elasticity modulus close to trabecular bone, avoiding the high rate of subsidence present in the solid titanium cages. Moreover, PEEK did not cause annoying artifacts neither on CT, nor MRI scans, allowing reliable postoperative evaluation of the performed surgery related to the extent of decompression, as well as the bony bridging through and around the cages in due time. Despite these characteristics of PEEK implants, the surface does not allow for bony adherence and thus pseudoarthrosis remains an ongoing issue (4, 8, 13).

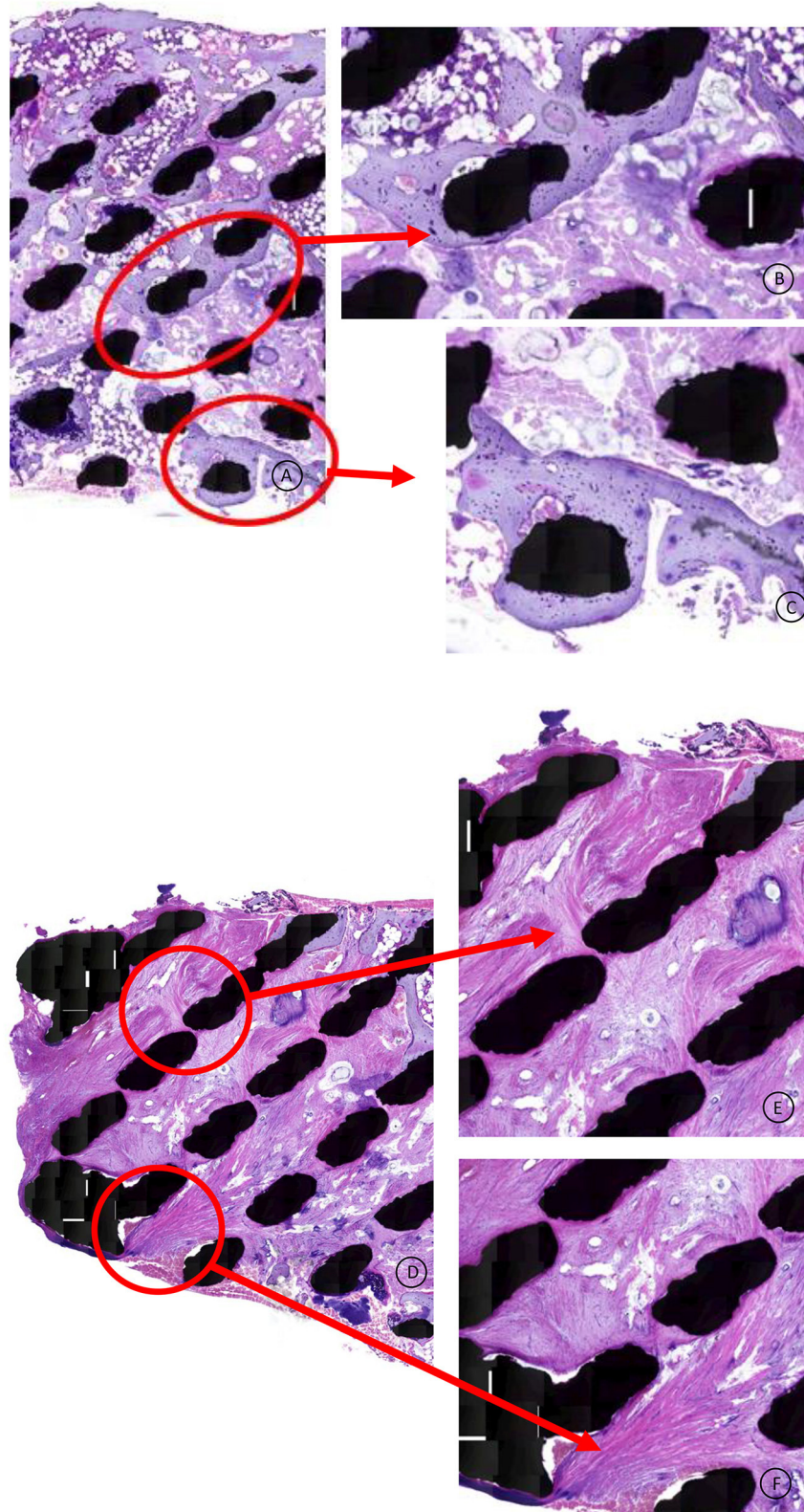


FIGURE 5 | (A–C) HE stained specimen: Higher magnification from the cage middle and surface area. The lamellar bone has a mature, vivid appearance without any fibrous tissue intervening between the titanium and the bone. Healthy bone marrow can be observed throughout the scaffold. **(D–F)** HE stained specimen: Higher magnification from the posterior 1/3th of the cage. Dense collagen fibers are directed in a cranial to caudal trajectory, attaching to the titanium struts.

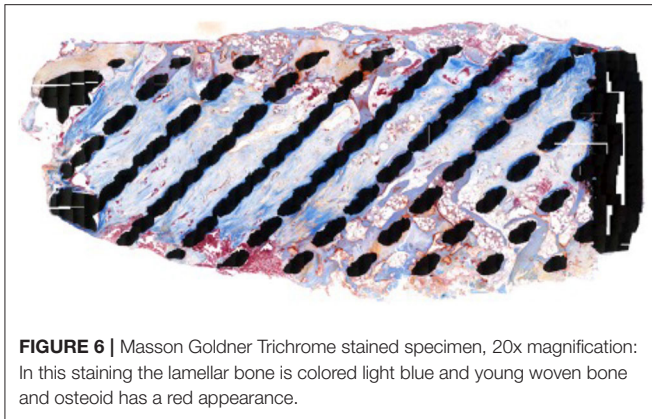


FIGURE 6 | Masson Goldner Trichrome stained specimen, 20x magnification: In this staining the lamellar bone is colored light blue and young woven bone and osteoid has a red appearance.

EIT Cellular Titanium[®], a 3D printed porous titanium scaffold, for application in cervical and lumbar cages, has been designed to tackle the most prominent critical clinical issues related to various cage materials, being the occurrence of pseudoarthrosis (non-union), subsidence, migration and imaging distortion.

The animal study of Wu et al., quantified the difference in direct bone contact between a porous titanium and PEEK cage in the cervical spine in a goat model. Whereas, the porous titanium cages had completely fused between the two vertebrae within 6 months' time, the PEEK cages lacked direct bone contact and exhibited abundant fibrous tissue formation (8). The configuration of the experimental porous titanium cage applied in the Wu study is very similar to the EIT scaffold in relation to pore size, diamond shape lattice and porosity.

Recently the prospective controlled clinical trial on single level ACDF without a plate conducted by Arts et al. (14) was published. This study confirmed the faster consolidation of EIT Cellular Titanium[®] cervical cages in comparison to PEEK cages combined with autograft. Perhaps the difference of bony ingrowth throughout the porous cage instead of just surrounding the cage (such as PEEK and solid titanium implants) accounts for this difference according to the authors. Interestingly to note is despite the lack of bone graft or biomaterial in the porous titanium cages, the fusion process was accelerated in the early postoperative phase.

Titanium appears to have better bone integrative qualities in a specific porous configuration in comparison to a solid design. An ideal pore-shape in a "diamond-configuration," a pore-size around 700 μm and a porosity of about 80% demonstrated the highest amount of osteogenic activity and osseointegration *in-vitro* and *in-vivo* (1, 2, 6, 7, 15). The porosity appears to have a positive effect on the differentiation markers, the number of osteocytes and the amount of matured bone tissue in direct contact with the titanium surface (9, 16). The histology of this cervical retrieval cage is in line with the histological findings of the animal studies described above, being abundant bone apposition of lamellar, mature bone in direct contact with the trabecular struts of the porous scaffold.

Wolff's law states that bone will adapt to the loads under which it is placed (17) and cancellous bone aligns itself with internal stress lines. Mechanical loading is of key importance for osteocyte survival (18). The animal study of Lamerigts et al., assessed *in-vivo* the effect of various loading conditions on bone graft incorporation. The histology of the incorporation and remodeling process of morselized bone graft was quantified for various loading regimes. Non-loaded conditions resulted in disappearance of the graft material, leaving the critical size defect in the femoral condyle empty (19). The finding of healthy lamellar bone, in direct contact with the titanium struts throughout the retrieved cage strongly suggests that mechanical loading is also taking place in the center of the 5-mm high porous titanium cage.

Observing bone ingrowth more prominently in the anterior 2/3th of the cage, is in line with computed tomographic osteoabsorptiometry observations, indicating the largest force transmission in the peripheral marginal zones, with higher bone density in the anterior part of the vertebrae in the lower cervical levels (20).

The elastic behavior of a material is related to its elasticity modulus as well as its structural composition. A solid titanium cube will exhibit a different elastic behavior compared to a titanium lattice with 80% porosity. The "bulk elasticity modulus" of EIT Cellular Titanium[®] is rather similar to PEEK (21). There was no sign of stress-shielding in the retrieval cage; stress-shielding is a significant negative side effect that can impair graft incorporation and fusion in cages with a box shaped design made of stiff material (22).

Magnetic Resonance Imaging is the diagnostic tool of choice when short or long-term postoperative complications occur after spinal surgery. Paramagnetic metal implants like titanium can provoke artifacts that impair the evaluation of MRI images and subsequent diagnostic and surgical work-up. Attributing significant porosity to a metal implant can reduce the MRI artifacts (23), which was also demonstrated in this case report with double level porous titanium cages.

CONCLUSION

This histological retrieval study of a radiologically fused cervical EIT cage clearly demonstrates the complete osseointegration of the EIT Cellular Titanium[®] scaffold 2 years postoperative. The scaffold exhibits a bone in growth pattern and maturation of bone tissue similar of what has been demonstrated in animal studies with comparable porous titanium implants. The complete osseointegration throughout the cage indicates physiological loading conditions even in the central part of the cage, suggestive of avoiding the occurrence of stress-shielding.

Results of ongoing clinical and pre-clinical research on the EIT Cellular Titanium[®] Cages will further substantiate in the very near future the value of this new material in obtaining spinal fusion.

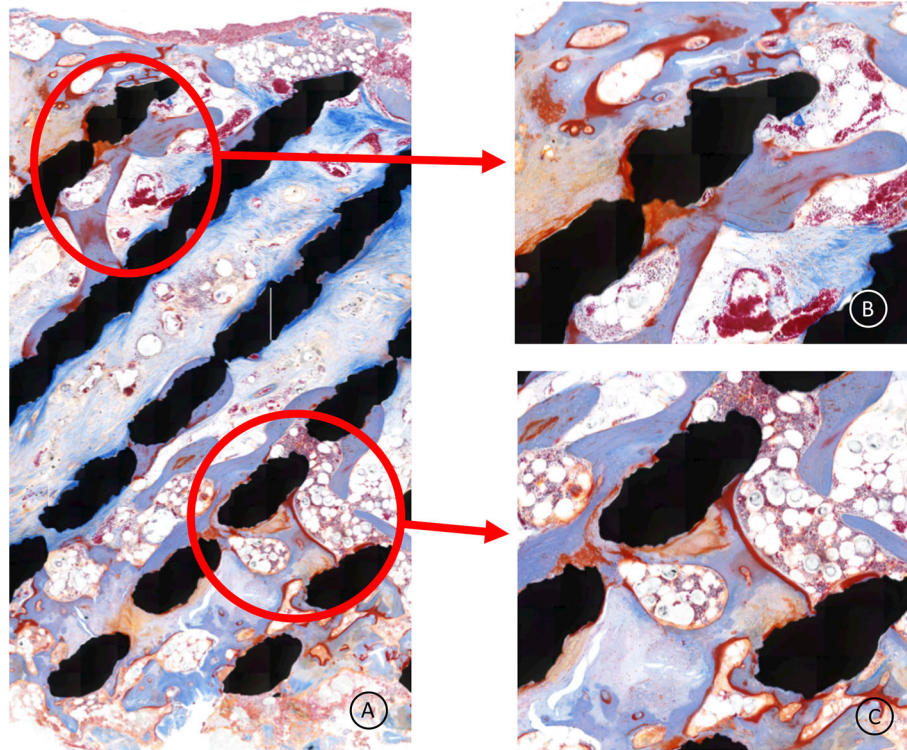


FIGURE 7 | (A–C) Higher magnification of the cage central part; the bone (light blue) is remodeling, demonstrating adaptive reactivity. The red lining is osteoid, indicating active bone apposition by osteoblasts. No signs of inflammation are present. The whitish bullous tissue is healthy bone marrow.

DATA AVAILABILITY STATEMENT

The datasets generated for this study are available on request to the corresponding author.

ETHICS STATEMENT

Ethical review and approval was not required for the study on human participants in accordance with the local legislation and institutional requirements. Written informed consent for participation was not required for this study in accordance with the national legislation and

the institutional requirements. Written informed consent was not obtained from the individual(s) for the publication of any potentially identifiable images or data included in this article.

AUTHOR CONTRIBUTIONS

WB delivered clinical material, including imaging and reviewed, and corrected the draft manuscript. NL organized histological preparation and evaluation of the specimen and prepared draft manuscript. All authors contributed to the article and approved the submitted version.

REFERENCES

- Devine D, Arens D, Burelli S, Bloch HR, Boure L. *In-vivo* evaluation of the osseointegration of new highly porous Trabecular Titanium™. *Orthop Proc.* (2012) 94-B:201.
- Fukuda A, Takemoto M, Saito T, Fujibayashi S, Neo M, Pattanayak DK, et al. Osteoinduction of porous Ti implants with a channel structure fabricated by selective laser melting. *Acta Biomater.* (2011) 7:2327–36. doi: 10.1016/j.actbio.2011.1.037
- Gittens R, Olivares-Navarrete R, Schwartz Z, Boyan B. Implant osseointegration and the role of microroughness and nanostructures: lessons for spine implants. *Acta Biomater.* (2014) 10:3363–71. doi: 10.1016/j.actbio.2014.03.037
- Olivares-Navarrete R, Gittens RA, Schneider JM, Hyzy SL, Haithcock DA, Ullrich PF, et al. Osteoblasts exhibit a more differentiated phenotype and increased bone morphogenetic protein production on titanium alloy substrates than on poly-ether-ether-ketone. *Spine J.* (2012) 12:265–72. doi: 10.1016/j.spinee.2012.02.002
- Olivares-Navarrete R, Hyzy S, Slosar P, Schneider J, Schwartz Z, Boyan B. Implant materials generate different peri-implant inflammatory factors: poly-ether-ether-ketone promotes fibrosis and microtextured titanium promotes osteogenic factors. *Spine.* (2015) 40:399–404. doi: 10.1097/BRS.0000000000000778
- Taniguchi N, Fujibayashi S, Takemoto M, Sasaki K, Otsuki B, Nakamura T, et al. Effect of pore size on bone ingrowth into porous titanium implants fabricated by additive manufacturing: an *in vivo* experiment. *Mater Sci Eng C.* (2016) 59:690–701. doi: 10.1016/j.msec.2015.10.069

7. Van Bael S, Chai YC, Truscetto S, Moesen M, Kerckhofs G, Van Oosterwyck H, et al. The effect of pore geometry on the *in vitro* biological behavior of human periosteum-derived cells seeded on selective laser-melted Ti6Al4V bone scaffolds. *Acta Biomater.* (2012) 8:2824–34. doi: 10.1016/j.actbio.2012.04.001
8. Wu SH, Li Y, Zhang YQ, Li XK, Yuan CF, Hao YL, et al. Porous Titanium-6 Aluminum-4 vanadium cage has better osseointegration and less micromotion than a poly-ether-ether-ketone cage in sheep vertebral fusion. *Artif Organs.* (2013) 37:E191–E201. doi: 10.1111/aor.12153
9. Shah F, Snis A, Matic A, Thomsen P, Palmquist A. 3D printed Ti6Al4V implant surface promotes bone maturation and retains a higher density of less aged osteocytes at the bone-implant interface. *Acta Biomaterialia.* (2016) 30:357–67. doi: 10.1016/j.actbio.2015.11.013
10. Enders J, Coughlin D, Mroz T, Vira S. Surface technologies in spinal fusion. *Neurosurg Clin N Am.* (2020) 31:57–64. doi: 10.1016/j.nec.2019.08.007
11. Shah F, Trobos M, Thomsen P, Palmquist A. Commercially pure titanium (cp-Ti) versus titanium alloy (Ti6Al4V) materials as bone anchored implants-Is one truly better than the other. *Mat Science and Engineering: C.* (2016) 62:960–6. doi: 10.1016/j.msec.2016.01.032
12. Kunder S, Rijkers K, Caelers I, de Bie R, Koehler P, van Santbrink H. Lumbar interbody fusion. A historical overview and a future perspective. *Spine.* (2018) 43:1161–8. doi: 10.1097/BRS.0000000000002534
13. Rao P, Pelletier M, Walsh W, Mobbs R. Spine interbody implants: material selection and modification, functionalization and bioactivation of surfaces to improve osseointegration. *Orth Surg.* (2014) 6:81–9. doi: 10.1111/os.12098
14. Arts M, Torensma B, Wolfs J. Porous titanium cervical interbody fusion device in the treatment of degenerative cervical radiculopathy; 1 year results of a prospective controlled trial. *Spine J.* (2020) 20:1065–72. doi: 10.1016/j.spinee.2020.03.008
15. Van der Stok J, Van der Jagt OP, Amin Yavari S, De Haas ME, Waarsing JH, Jahr H, et al. Selective laser melting-produced porous titanium scaffolds regenerate bone in critical size cortical bone defects. *J Orthop Res.* (2013) 12:792–9. doi: 10.1002/jor.22293
16. Cheng A, Cohen DJ, Boyan BD, Schwartz Z. Laser-sintered constructs with bio-inspired porosity and surface micro/nano-roughness enhance mesenchymal stem cell differentiation and matrix mineralization *in vitro*. *Calcif Tissue Int.* (2016) 99:625–37. doi: 10.1007/s00223-016-0184-9
17. Wolff J. *The Law of Bone Remodeling*. Berlin; New York, NY: Springer (1986).
18. Bakker A, Klein-Nulend J, Burger E. Shear stress inhibits while disuse promotes osteocyte apoptosis. *Biochem Biophys Res Commun.* (2004) 320:1163–8. doi: 10.1016/j.bbrc.2004.06.056
19. Lamerigts N, Buma P, Huiskes R, Slooff T. Incorporation of morsellized bone graft under controlled loading conditions. A new animal model in the goat. *Biomaterials.* (2000) 21:741–7. doi: 10.1016/S0142-9612(99)00247-1
20. Mueler-Gerbl M, Weißer S, Linsenmeier U. The distribution of mineral density in the cervical vertebral endplates. *Eur Spine J.* (2008) 17:432–8. doi: 10.1007/s00586-008-0601-5
21. Youngs Modulus comparison of various materials GUM00001 rev A/ VAL 2017-007 Depuysynthes.com
22. Epari D, Kandziora F, Duda G. Stress shielding in box and cylinder cervical interbody fusion cage designs. *Spine.* (2005) 8:908–14. doi: 10.1097/01.brs.0000158971.74152.b6
23. Carter LN, Addison O, Naji N, Seres P, Wilman AH, Shepherd DET, et al. Reducing MRI susceptibility artifacts in implants using additively manufactured porous Ti-6Al-4V structures. *Acta Biomater.* (2020) 107:338–48. doi: 10.1016/j.actbio.2020.02.038

Conflict of Interest: The authors declare that the research was conducted in the absence of any commercial or financial relationships that could be construed as a potential conflict of interest.

Copyright © 2020 van den Brink and Lamerigts. This is an open-access article distributed under the terms of the Creative Commons Attribution License (CC BY). The use, distribution or reproduction in other forums is permitted, provided the original author(s) and the copyright owner(s) are credited and that the original publication in this journal is cited, in accordance with accepted academic practice. No use, distribution or reproduction is permitted which does not comply with these terms.



Perspectives on the Treatment of Lumbar Disc Degeneration: The Value Proposition for a Cell-Based Therapy, Immunomodulatory Properties of Discogenic Cells and the Associated Clinical Evaluation Strategy

Lara Ionescu Silverman^{1,2*}, Will Heaton¹, Niloofar Farhang¹, Lindsey Hart Saxon¹, Galina Dulatova¹, Daniel Rodriguez-Granrose¹, Flagg Flanagan¹ and Kevin T. Foley^{1,2,3}

¹ DiscGenics Inc., Salt Lake City, UT, United States, ² Department of Neurosurgery, University of Tennessee Health Science Center, Memphis, TN, United States, ³ Semmes-Murphey Clinic, Memphis, TN, United States

OPEN ACCESS

Edited by:

William Robert Walsh,
University of New South
Wales, Australia

Reviewed by:

Rema A. Oliver,
University of New South
Wales, Australia
Claudia Di Bella,
The University of Melbourne, Australia

*Correspondence:

Lara Ionescu Silverman
lara@discgenics.com

Specialty section:

This article was submitted to
Orthopedic Surgery,
a section of the journal
Frontiers in Surgery

Received: 27 April 2020

Accepted: 25 November 2020

Published: 16 December 2020

Citation:

Silverman LI, Heaton W, Farhang N, Saxon LH, Dulatova G, Rodriguez-Granrose D, Flanagan F and Foley KT (2020) Perspectives on the Treatment of Lumbar Disc Degeneration: The Value Proposition for a Cell-Based Therapy, Immunomodulatory Properties of Discogenic Cells and the Associated Clinical Evaluation Strategy. *Front. Surg.* 7:554382. doi: 10.3389/fsurg.2020.554382

Low back pain (LBP) is a serious medical condition that affects a large percentage of the population worldwide. One cause of LBP is disc degeneration (DD), which is characterized by progressive breakdown of the disc and an inflamed disc environment. Current treatment options for patients with symptomatic DD are limited and are often unsuccessful, so many patients turn to prescription opioids for pain management in a time when opioid usage, addiction, and drug-related deaths are at an all-time high. In this paper, we discuss the etiology of lumbar DD and currently available treatments, as well as the potential for cell therapy to offer a biologic, non-opioid alternative to patients suffering from the condition. Finally, we present an overview of an investigational cell therapy called IDCT (Injectable Discogenic Cell Therapy), which is currently under evaluation in multiple double-blind clinical trials overseen by major regulatory agencies. The active ingredient in IDCT is a novel allogeneic cell population known as Discogenic Cells. These cells, which are derived from intervertebral disc tissue, have been shown to possess both regenerative and immunomodulatory properties. Cell therapies have unique properties that may ultimately lead to decreased pain and improved function, as well as curb the numbers of patients pursuing opioids. Their efficacy is best assessed in rigorous double-blinded and placebo-controlled clinical studies.

Keywords: opioids, disc degeneration, regenerative medicine, cell therapy, low back pain, IDCT

LOW BACK PAIN AND DISC DEGENERATION

Low back pain (LBP) is a leading cause of disability worldwide (1), and the leading cause of years lived with disability in developed countries (2). The 2010 Global Burden of Disease Study estimated that LBP is among the top 10 diseases and injuries that account for the highest number of DALYs (disability-adjusted life years) worldwide (3). In the US, low back pain (LBP)

affects 12–30% of US adults at a given time (4) and the annual expenditure to treat LBP is estimated to be over \$100 billion (1), creating a significant burden on the economy as well as individual patients. Not only is there direct expense from treating LBP, but also one third of all occupational musculoskeletal injuries and illnesses resulting in work disability are attributed to LBP (5). This means that there is a significant loss of productivity and indirect costs from missing work. Current treatment options for patients with LBP may prove unsuccessful in alleviating pain or improving disability, forcing patients to look for other ways to seek relief. Often, this means turning to prescription opioids for pain management in a time when opioid usage, addiction and drug-related deaths are at an all-time high (<https://www.cdc.gov/drugoverdose/epidemic/index.html>). In fact, LBP is the most common, non-cancer reason for opioid prescription in the United States (6, 7). According to the CDC, there were 168 million prescriptions of opioids in 2018 (8), and nearly 68,000 opioid overdose deaths in the U.S. that year (9). Driving down the use (and abuse) of opioids by developing safer, more effective treatments for LBP is a critical task for the healthcare community.

A major cause (up to 39%) of LBP is disc degeneration (DD) (10–12), a condition in which the intervertebral disc breaks down and causes pain. The intervertebral disc, which is comprised of a gelatinous central nucleus pulposus and an outer annulus fibrosus, is avascular, hypoxic, and hypocellular (13), making it perhaps more prone to degenerative conditions. The condition features an imbalance in cytokines that leads to tissue breakdown and direct pain sensation (14). This breakdown is exacerbated by the depleted capacity of local cells to produce new extracellular matrix molecules as well as an imbalance in anabolic/catabolic signals such as matrix metalloproteinases in the tissue (13). These changes result in global tissue structure damage that may be manifested by acute and chronic pain, and may eventually result in structural failure, requiring surgical intervention. Also, degenerated discs are characterized by an upregulation of inflammatory cytokines such as interleukins and tumor necrosis factor- α (14). Other properties of DD include pathologic innervation, vascularization, and changes to the endplate.

Many risk factors are associated with developing lumbar DD, including genetic predisposition, acute injury, and modifications to adjacent levels (such as fusion surgeries) that result in abnormal biomechanics (15). Clinically, patients who experience chronic LBP seek medical attention to reduce their pain and disability as well as to increase their quality of life. Treating low back pain is a complex medical task, further challenged by the interplay of psychosocial factors, chronicity, and comorbidities (16). MRI is often used to evaluate the lumbar spine for Modic changes and Pfirrmann scores of lumbar discs (17), which indicate DD; however such imaging does not always correlate with patient symptomatology and therefore is not the sole driver of therapy selection (18). Clinical presentation must correlate with the radiographic findings. Discography may also help diagnose symptomatic lumbar disc degeneration, but has been used less in recent years due to concerns around worsening the disease from the procedure itself (19).

Currently, treatment of LBP that reduces the need for surgical intervention and opioid prescription is an unmet medical need that is recognized by the medical community (20, 21). Historically, epidural steroid injections were utilized as a non-surgical method to treat DD; however, lack of definitive efficacy in controlled studies has decreased the use of this treatment when patients lack radiculopathy (22). Approaches such as nerve stimulation and nerve ablation have been considered but are not yet well-proven for the treatment of DD. In 2018, a Global Spine Care Initiative outlined that treatments for LBP should be limited to non-interventional treatments (yoga, massage, and pain medications) (23), as other approaches do not have sufficient evidence of efficacy. Currently, there are no non-invasive treatments available that have shown robust clinical evidence in reducing pain and disability and increasing quality of life. Further, no treatments exist that have proven the ability to eliminate the need for surgical interventions. One common surgical intervention is fusion surgery, which has mixed outcomes and can lead to long-term opioid abuse and addiction, especially in patients who sought pain relief from opioids prior to surgery (24, 25). Patients suffering from DD need a proven, non-invasive alternative for treating LBP.

CELL THERAPY TO TREAT LBP

LBP induced by DD has been historically challenging to treat. Small molecules and biomaterials have been clinically evaluated but have shown mixed success. For example, growth factor GDF-5 did not show success in double-blinded clinical trials (26), and various anti-inflammatory proteins including tumor necrosis factor and IL-6 inhibitors have shown mixed success even when patients and providers were blinded in clinical trials (27). The anti-inflammatory proteins have limited evidence of having long-term effects, possibly due to their short half-lives ranging from ~3 to 20 days dependent on the molecule (28–31), which is much less than what is considered chronic LBP (>12 weeks) (32). Similarly, biomaterials have not shown robust success. While some pain reduction has been seen, the outcomes are mechanical in nature and lack any biologically active component that could cause regeneration (33, 34). Additionally, complications are prevalent with biomaterials, including biomaterial leaking out of the disc and causing additional pain, and excess stiffness causing endplate fracture (35, 36). As a result, neither anti-inflammatory proteins nor biomaterials present an ideal approach to treating DD.

More recently, delivery of a live cell population into the disc is under consideration as an option that can fill this treatment need (37). There are several reasons a cell therapy may be more successful at treating LBP than the other approaches. First, cells may have a longer residence time than small molecules, some of which have half-lives of <24 h (38–40). Also, cells can have multiple mechanisms of action that can more appropriately tackle a complex disease such as DD. Finally, cells can respond to the local micro-environment, suitably replacing the local cell population and potentially promoting a more normal local milieu through their paracrine signaling. However, cell therapies also

face some specific challenges in the disc, particularly due to the harsh environment (low pH and oxygen) that may inhibit proper cellular functionality (41).

Cell therapy-based treatments also face notable challenges associated with commercializing such medicines. Attaining manufacturing consistency and suitable scale is a challenge with live cells, and depending on the FDA pathway being utilized, regulators may expect drug-style compliance to the Code of Federal Regulations (CFR). The FDA regulates cell therapies under one of two pathways, which delineates their level of involvement. Therapies that are minimally manipulated, homologous or meet other narrow criteria have limited regulatory oversight and fall within Section 361 of FDA's 21 CFR Part 1271 regulation. Therapies that contain cells that have been substantially changed, or manipulated through the manufacturing process, are regulated under Section 351 of 21 CFR 1271, and require more regulatory involvement (42). The section 351 regulatory path closely follows that of traditional pharmaceutical products, including preclinical studies, manufacturing/quality oversight, and clinical trial execution (42). The section 351 route also involves designating a specific mechanism of action, which is often difficult to achieve as large rates of non-responding patients in cell therapy clinical trials make the mechanism of action difficult to define (43).

Nonetheless, despite these potential environmental, manufacturing and regulatory hurdles, multiple cell therapies (43), including an allogeneic cell therapy treatment our group is developing called IDCT, are in clinical evaluation. Such treatments hold promise as a potential therapeutic approach to curb opioid abuse among patients suffering from the condition.

OVERVIEW OF INJECTABLE DISC CELL THERAPY (IDCT) AND IMMUNOMODULATORY EVALUATION

IDCT is novel cell therapy under clinical evaluation for the treatment of LBP caused by DD. The active ingredient is a live population of Discogenic Cells, which originate from donated adult intervertebral disc tissue. After undergoing a proprietary growth process, the cells are frozen for storage and thawed immediately prior to use. The cells are delivered directly into the painful, degenerated disc through a needle placed via fluoroscopic guidance. Discogenic Cells are allogeneic in nature as the starting material is from a donor and the cells are expanded, modified, and subsequently frozen, and then delivered to different people (in contrast to autologous therapies, which begin and end with the same patient). Also, because the donor cells in IDCT originate from the disc and are then reintroduced into the recipient's disc, the product is homologous. Due to the fact that the cells are more-than-minimally manipulated, the manufacture of these cells requires a high level of regulatory oversight to ensure proper standards are being met (21 CFR 210/211). During this process, large quantities of Discogenic Cells can be produced in a single lot, making the treatment scalable to the DD patient population.

During the growth process, cells exhibit phenotypic changes from that of cells found in the native disc tissue. Specifically, the cells lose expression of CD24 (44), which is a marker for nucleus pulposus cells (45). Also, Discogenic Cells have a unique surface marker expression profile that includes high expression of CD73, CD90, and HLA-ABC and a low expression of CD34 and HLA-DR/DQ/DP (44). The cells generate the extracellular matrix found within native intervertebral disc tissue, including proteoglycan and collagen. The matrix production has been measured *in vitro* using techniques such as histology (44), PCR and biochemical assays. Further, evaluation of the cells in animal models of disc degeneration demonstrated normalization of disc height and tissue architecture in both rabbits (44) and dogs (46).

We hypothesize that improvement in disc height *in vivo* may alleviate compression on nerves which cause pain and may modify the local microenvironment in a way that may reduce overall catabolic changes, and therefore inflammation and pain. Improved disc height observed in animal models when using other cell therapies has shown correlation to a reduction in pain when tested in human clinical trials, although the results lack robustness (47–49).

Another important aspect of treating disc degeneration is to address the inflammation within the disc that may contribute directly to pain sensation and tissue breakdown. Because the treatment is allogeneic, understanding the potential immunogenicity of the treatment is critical prior to clinical evaluation. Confirming the absence of surface markers CD40, CD80, and CD86, which are required for effector T cell induction (50), is important in a potential allogeneic cell therapy. Also, activated T-cell assays can evaluate the potential for immune rejection and also assess whether the therapy has immunomodulatory effects. In these studies, we evaluated these key properties prior to clinical evaluation.

Methods

Intervertebral disc tissue was obtained from consented male and female donors through DonorConnect (Murray, Utah) and cells were harvested and processed into Discogenic Cells as described in (44). In order to mitigate the risks of adventitious agents being present in the tissue, a Medical Director reviewed donor medical records to determine donor eligibility according to government guidelines, which includes a review of serology and risk factors. Ten lots of Discogenic Cells were analyzed for cell surface antigen expression by flow cytometry using the following fluorescence-conjugated mouse antihuman monoclonal antibodies: CD40, CD80, CD86 (BD Biosciences, San Jose, CA). Appropriate isotype controls were run in parallel. Also, cell lines known to be positive for each antigen were procured from ATCC (Manassas, Virginia) and evaluated to ensure that a positive signal was attainable. The cells were blocked in PBS containing 0.5% human serum albumin (Baxter, Deerfield, IL) and 25 µg/mL Fc-block (BD Biosciences) for 10–20 min. Cells were subsequently stained with antibodies for 30–60 min at 4°C protected from light and subsequently washed and resuspended in PBS containing 0.5% human serum albumin. 7-AAD (BD Biosciences) was used as a dead cell exclusion marker. A minimum of 10,000 events were collected on a Cytotflex Flow Cytometer (Beckman Coulter, Indianapolis, IN,

USA) using CytExpert Software for data acquisition and FlowJo Software for analysis.

Immunomodulatory properties of IDCT were analyzed by testing the ability of IDCT to inhibit proliferation of T-cells from two different donors. Healthy peripheral blood mononuclear cells were obtained from two vendors (Precision for Medicine and STEMCELL Technologies) and T-cells were isolated from them using the EasySepTM Human CD4⁺ T Cell Isolation Kit (STEMCELL Technologies, Vancouver, BC) according to manufacturer's instructions. Subsequently, T-Cells were activated using CD3/CD28 T-cell activator (STEMCELL Technologies) and cultured in T-cell expansion media (Immunocult XF T Cell Expansion Medium, STEMCELL Technologies) for 6 days according to manufacturer's instructions. During this culture time, Discogenic Cells were plated at a density of 100,000 cells/well in recovery media (DMEM/F-12 with 15% FBS, 50 µg/mL gentamicin, and 2.5 µg/mL Amphotericin B) in a 96-well plate and allowed to attach and equilibrate for 3 days. Discogenic Cells were then mitomycin treated (40 µg/mL) for 2 h at 37°C and 5% CO₂. T-cells which had been cultured and expanded for 6-days were added to mitomycin treated Discogenic Cells at 100,000 cells/well and co-cultured for 3 days. On the third day of co-culture, BrdU was added to a concentration of 10 µM, and cells were incubated at 37°C, 5% CO₂ for 3 h prior to analysis of proliferation of T-cells using a colorimetric BrdU assay (MilliporeSigma, Burlington, MA), according to manufacturer's instructions. A student's *T*-test was used to determine differences between groups with significance set to $p < 0.05$.

Results and Discussion

Discogenic Cells were generated and achieve normal morphology (**Figure 1A**). Flow cytometry revealed lack of expression of co-stimulatory markers CD40, CD80, and CD86 (50) (**Figure 1B**). This absence of T cell induction is hypothesized to lead to minimal immunogenicity of Discogenic Cells. Next, when combined with activated human T-cells, Discogenic Cells did not increase T-cell expansion, but in fact suppressed T-cell expansion (**Figure 1C**), demonstrating a lack of immunogenicity in this assay as well as an immunomodulatory effect on T-cells. Such findings may indicate that Discogenic Cells could directly modulate pain sensation in a degenerated disc environment.

IDCT cells are derived from the tissue type they are intended to treat, which may result in better outcomes than using cells not accustomed to the disc environment. These Discogenic Cells, which differ from the cells originally obtained from the disc tissue, are both immunomodulatory and regenerative and thus have the potential to impact the pathophysiology of disc degeneration.

NEXT STEPS: ONGOING CLINICAL EVALUATION OF IDCT

Treatment of patients with lumbar disc degeneration utilizing cell therapy has been explored in prior clinical studies, showing the feasibility of this approach. In early-stage human clinical trials, multiple types of mesenchymal stem cells (51–53) and

chondrocytes (48, 54, 55) have been used. These studies have shown the injection delivery method to be feasible and the treatments to be safe. In small, open-label studies without controls, the treatments reduced pain and, in some instances, reduced Pfirrmann scores (52, 53). Given the strong placebo effect that can be encountered when evaluating treatments for pain, blinded studies that utilize control arms are needed to evaluate the true effects of cell therapy. For example, in a study utilizing a subpopulation of mesenchymal stromal cell (MSCs), pain was modestly reduced compared to control, but none of the regenerative parameters [such as Pfirrmann score, disc height or magnetic resonance imaging (MRI)] improved over time (56). Thus, while the approach seems promising, the ideal cell type remains elusive.

Preliminary safety and efficacy of IDCT is under evaluation in 60 patients with single-level, symptomatic DD across 14 sites (clinicaltrials.gov identifier NCT03347708). Institutional review board approval has been obtained. The subjects who meet all eligibility criteria are being randomized to one of four treatment cohorts: low dose IDCT ($n = 20$), high dose IDCT ($n = 20$), vehicle ($n = 10$), and placebo ($n = 10$). Each subject receives a single intradiscal injection of his or her assigned treatment into the target symptomatic lumbar intervertebral disc. The delivery is through a needle placed percutaneously into the disc using fluoroscopic guidance, so no surgical procedure is needed.

Following treatment, there is a 1-year period of subject observation and evaluation before evaluating the data, with a 1-year extension period to gather additional data. We are exploring a number of endpoints that would allow for a determination of whether a single injection of IDCT can safely and effectively treat symptomatic lumbar DD patients. For all assessments, patients are instructed to maintain their long-term chronic pain medication usage, and refrain from taking acute pain medications for 24 h before each assessment.

In this study, we evaluate patient-reported outcomes to assess whether a single injection of IDCT can reduce pain and disability, and improve quality of life. Pain is evaluated using the Visual Analog Score (VAS), which evaluates pain from “no pain at all” (score of 0) to “worst imaginable pain” (score of 100). This tool, used since 1923, is sensitive to treatment effects and correlates positively to other self-reporting measures of pain intensity (57). Disability is measured via the Oswestry Disability Index, which is a 10-section questionnaire that takes 3–5 min to complete, and is a commonly used outcome-measure for low back pain patients (58). Finally, the EQ-5D questionnaire is being used to measure quality of life; it has been widely used to assess low back pain patients in prior studies (59).

Because the placebo effect can affect patient-reported outcomes, we are also exploring some less subjective, behavior-based measures. First, we are assessing patients for the “Timed up and Go” (TUG) test, which measures how long it takes for a patient to stand up from a chair, walk three meters, and return (60). A faster TUG time is thought to indicate that the patient has less pain and disability (61, 62). We are also evaluating whether there is a decrease in pain medication usage after a single injection of IDCT. A reduction in pain

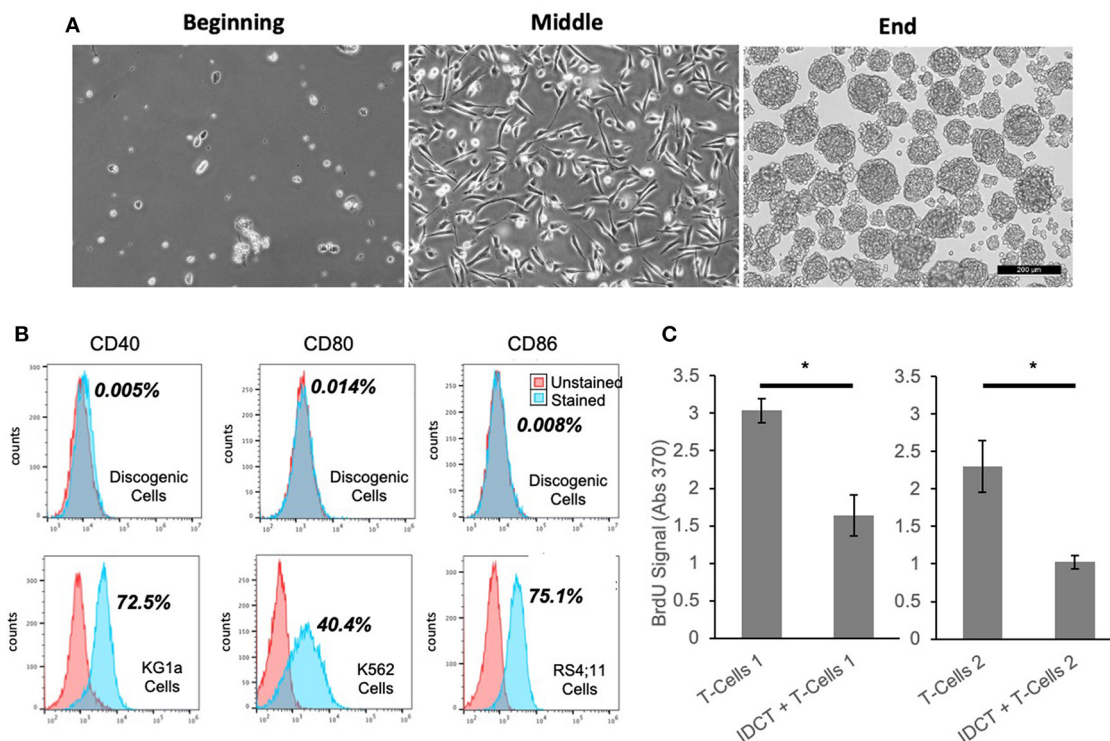


FIGURE 1 | Unique properties of discogenic cells. **(A)** The morphology of the cells change from the beginning to the end of the process, where the Discogenic Cell phenotype is attained (Scale bar is 200 μ M; one representative set of images shown from $n = 10$). **(B)** Flow cytometry of Discogenic Cells shows a lack of co-stimulatory markers CD40, CD80, and CD86, which if expressed could induce T-cell activation and rejection. Ten Discogenic Cell samples tested; one representative dataset shown. Control cells show positive expression of the markers, validating the method. The quantitative result for the percentage of stained cells positive for each marker is shown in bold next to the histograms. **(C)** Measurement of proliferation of CD3/CD28 stimulated T-Cells from two different donors, with or without Discogenic Cell co-culture. Proliferation was measured by BrdU assay. Overall this indicates the ability of IDCT to inhibit T-cell proliferation thus indicating it has potential immunomodulatory capabilities ($n = 5$ technical replicates, $*p < 0.05$ by Student's *T*-Test).

medication might indicate that IDCT has the potential to drive down opioid use and abuse, which is a major public health problem in the US (63). Changes in pain medication usage have been noted in other studies, such as the Phase II study for lumbar DD by Mesoblast (*data not published, based on press release*). The final behavior-based assessment is to evaluate time to subsequent spine intervention (discectomy, fusion, etc.) to see if a single injection of IDCT can delay the need for additional procedures.

Additionally, we are assessing structural changes to the spine that may serve as surrogates to patient reported or behavior-based outcomes. Sequential X-ray images of the spine taken prior to treatment and over the course of 2 years will be evaluated for changes in angular and translational motion, as well as in disc height. Also, sequential MRI images (T1, T2) will be evaluated for changes to Pfirrmann score (17) and Modic score, as well as disc height and disc volume. Where possible, the exploratory MRI sequences T1-rho and T2 relaxometry will be evaluated. Upon unblinding, radiographic changes will be associated with patient-reported outcomes to better understand the mechanism for pain/disability improvement, should it be

identified. Imaging may also be proposed as a surrogate endpoint for future trials.

Concurrent with the US Phase I/II study, the Pharmaceuticals and Medical Devices Agency (PMDA) has allowed DiscGenics a Clinical Trial Notification (CTN) to execute a double-blind, sham-controlled study in Japan at 6 sites (clinicaltrials.gov identifier NCT03955315). The study will enroll 38 subjects with single-level, symptomatic lumbar DD. Each subject will be randomized to receive a single injection of either low dose IDCT, high dose IDCT, or sham procedure. They will be followed for 6 months with a 6-month extension to gather additional data. The same clinical outcomes measures described above will be utilized, along with a Japan-specific pain score (JOABPEQ).

CONCLUSION

Disc degeneration is a major cause of LBP and is associated with disability worldwide. Current treatment options have limited efficacy. Unfortunately, this means that patients suffering from this condition often turn to opioids to manage their pain. No

treatment has been found for DD that addresses the underlying problems of tissue architecture breakdown and an imbalance of cytokines. Cell therapies, which offer the potential to help regenerate disc tissue and moderate intradiscal inflammation, present a potentially viable option for treating DD. Several cell therapy clinical studies have been completed and more are ongoing, including the evaluation of IDCT. Rigorous clinical evaluation of candidate treatments must be performed, given the bias that may occur when evaluating subjective outcomes such as self-reported pain levels. Also, improved imaging techniques and new diagnostic tools will facilitate the development of better means for assessing this disorder. Given their potential to modify the biologic processes underlying disc degeneration, cell therapies hold the promise of being an effective treatment option for DD that mitigates pain and disability. Following the approval of such treatments, patients may no longer need to use opioids to manage their LBP.

DATA AVAILABILITY STATEMENT

The datasets generated for this article are not readily available because the datasets are confidential. Requests to

access the datasets should be directed to Lara Silverman, lara@discgenics.com.

AUTHOR CONTRIBUTIONS

LS, NF, LH, and KF contributed writing to the manuscript. WH, NF, GD, and DR-G performed laboratory studies and contributed to figures. FF and KF provided guidance and reviewed the manuscript. All authors agreed to be accountable for the content of this work and reviewed the final content prior to publication.

FUNDING

This work was funded privately by DiscGenics, Inc.

ACKNOWLEDGMENTS

We would like to acknowledge Amanda Jones for contributing images to this manuscript. Also, we want to acknowledge Alex Smirnov for contributing references about opioid trends.

REFERENCES

- Hoy D, March L, Brooks P, Blyth F, Woolf A, Bain C, et al. The global burden of low back pain: estimates from the Global Burden of Disease 2010 study. *Annals Rheum Dis.* (2014) 73:968–74. doi: 10.1136/annrheumdis-2013-204428
- Driscoll T, Jacklyn G, Orchard J, Passmore E, Vos T, Freedman G, et al. The global burden of occupationally related low back pain: estimates from the Global Burden of Disease 2010 study. *Annals Rheum Dis.* (2014) 73:975–81. doi: 10.1136/annrheumdis-2013-204631
- Vos T, Memish ZA. Years lived with disability (YLDs) for 1160 sequelae of 289 diseases and injuries 1990–2010: a systematic analysis for the Global Burden of Disease Study 2010. *Lancet.* (2012) 380:2163–96. doi: 10.1016/S0140-6736(12)61729-2
- Davis MA, Onega T, Weeks WB, Lurie JD. Where the United States spends its spine dollars: expenditures on different ambulatory services for the management of back and neck conditions. *Spine.* (2012) 37:1693–701. doi: 10.1097/BRS.0b013e3182541f45
- Statistics BoL. *Nonfatal Occupational Injuries and Illnesses Requiring Days Away From Work.* (2013). Available online at: <https://www.bls.gov/news.release/pdf/osh2.pdf> (accessed March 30, 2015).
- Ringwalt C, Gugelmann H, Garrettson M, Dasgupta N, Chung AE, Proescholdbell SK, et al. Differential prescribing of opioid analgesics according to physician specialty for Medicaid patients with chronic noncancer pain diagnoses. *Pain Res Manag.* (2014) 19:179–85. doi: 10.1155/2014/857952
- Tisamarie B. Sherry M, PhD, Adrienne Sabety B, Nicole Maestas M. Documented pain diagnoses in adults prescribed opioids: results from the national ambulatory medical care survey, 2006–2015. *Annals Intern Med.* (2020) 169:892–4. doi: 10.7326/M18-0644
- U.S. Opioid Prescribing Rate Maps. Available online at: <https://www.cdc.gov/drugoverdose/maps/rxrate-maps.html> (accessed March 12, 2020).
- Opioid Summaries by State: NIH National Institute on Drug Abuse. Available online at: <https://www.drugabuse.gov/drugs-abuse/opioids/opioid-summaries-by-state> (accessed May 22, 2019).
- Freemont AJ. The cellular pathobiology of the degenerate intervertebral disc and discogenic back pain. *Rheumatology.* (2009) 48:5–10. doi: 10.1093/rheumatology/ken396
- Anderson DG, Tannoury C. Molecular pathogenic factors in symptomatic disc degeneration. *Spine J.* (2005). 5(6 Suppl):260S–6S. doi: 10.1016/j.spinee.2005.02.010
- Zhang YG, Guo TM, Guo X, Wu SX. Clinical diagnosis for discogenic low back pain. *Int J Biol Sci.* (2009) 5:647–58. doi: 10.7150/ijbs.5.647
- Pattappa G, Li Z, Peroglio M, Wismer N, Alini M, Grad S. Diversity of intervertebral disc cells: phenotype and function. *J Anatomy.* (2012) 221:480–96. doi: 10.1111/j.1469-7580.2012.01521.x
- Wuertz K, Haglund L. Inflammatory mediators in intervertebral disk degeneration and discogenic pain. *Global Spine J.* (2013) 3:175–84. doi: 10.1055/s-0033-1347299
- Sakai D, Andersson GB. Stem cell therapy for intervertebral disc regeneration: obstacles and solutions. *Nat Rev Rheumatol.* (2015) 11:243–56. doi: 10.1038/nrrheum.2015.13
- Koes BW, van Tulder MW, Thomas S. Diagnosis and treatment of low back pain. *BMJ.* (2006) 332:1430–4. doi: 10.1136/bmj.332.7555.1430
- Pfirrmann CW, Metzdorf A, Zanetti M, Hodler J, Boos N. Magnetic resonance classification of lumbar intervertebral disc degeneration. *Spine.* (2001) 26:1873–8. doi: 10.1097/00007632-200109010-00011
- Taher F, Essig D, Lebl DR, Hughes AP, Sama AA, Cammisa FP, et al. Lumbar degenerative disc disease: current and future concepts of diagnosis and management. *Adv Orthop.* (2012) 2012:970752. doi: 10.1155/2012/970752
- Cuellar JM, Stauff MP, Herzog RJ, Carrino JA, Baker GA, Carragee EJ. Does provocative discography cause clinically important injury to the lumbar intervertebral disc? A 10-year matched cohort study. *Spine J.* (2016) 16:273–80. doi: 10.1016/j.spinee.2015.06.051
- Chou L, Ranger TA, Peiris W, Cicuttini FM, Urquhart DM, Sullivan K, et al. Patients' perceived needs for medical services for non-specific low back pain: a systematic scoping review. *PLoS ONE.* (2018) 13:e0204885. doi: 10.1371/journal.pone.0204885
- Friedly J, Standaert C, Chan L. Epidemiology of spine care: the back pain dilemma. *Phys Med Rehabil Clin N Am.* (2010) 21:659–77. doi: 10.1016/j.pmr.2010.08.002
- Acaroglu E, Nordin M, Randhawa K, Chou R, Cote P, Mmopelwa T, et al. The Global Spine Care Initiative: a summary of guidelines on invasive interventions for the management of persistent and disabling spinal pain in low- and middle-income communities. *Euro Spine J.* (2018) 27(Suppl 6):870–8. doi: 10.1007/s00586-017-5392-0

23. Chou R, Cote P, Randhawa K, Torres P, Yu H, Nordin M, et al. The Global Spine Care Initiative: applying evidence-based guidelines on the non-invasive management of back and neck pain to low- and middle-income communities. *Euro Spine J.* (2018) 27(Suppl 6):851–60. doi: 10.1007/s00586-017-5433-8
24. Connolly J, Javed Z, Raji MA, Chan W, Kuo YF, Baillargeon J. Predictors of long term opioid use following lumbar fusion surgery. *Spine.* (2017) 42:1405–11. doi: 10.1097/BRS.0000000000002133
25. Kalakoti P, Hendrickson NR, Bedard NA, Pugely AJ. Opioid utilization following lumbar arthrodesis: trends and factors associated with long-term use. *Spine.* (2018) 43:1208–16. doi: 10.1097/BRS.0000000000002734
26. *clinicaltrials.gov. A Multicenter, Randomized, Double-blind, Placebo Controlled, Clinical Trial to Evaluate the Safety, Tolerability and Preliminary Effectiveness of 2 Doses of Intradiscal rhGDF-5 (Single Administration) for the Treatment of Early Stage Lumbar Disc Degeneration - Study Results.* ClinicalTrials.gov (2016). Available online at: <https://clinicaltrials.gov/ct2/show/results/NCT01124006> (accessed December 1, 2019).
27. Risbud MV, Shapiro IM. Role of cytokines in intervertebral disc degeneration: pain and disc content. *Nat Rev Rheumatol.* (2014) 10:44–56. doi: 10.1038/nrrheum.2013.160
28. Okuda Y. Review of tocilizumab in the treatment of rheumatoid arthritis. *Biologics.* (2008) 2:75–82. doi: 10.2147/BTT.S1828
29. Weisman MH, Moreland LW, Furst DE, Weinblatt ME, Keystone EC, Paulus HE, et al. Efficacy, pharmacokinetic, and safety assessment of adalimumab, a fully human anti-tumor necrosis factor- α monoclonal antibody, in adults with rheumatoid arthritis receiving concomitant methotrexate: a pilot study. *Clin Ther.* (2003) 25:1700–21. doi: 10.1016/S0149-2918(03)80164-9
30. Klotz U, Teml A, Schwab M. Clinical pharmacokinetics and use of infliximab. *Clin Pharmacokinet.* (2007) 46:645–60. doi: 10.2165/00003088-200746080-00002
31. Combe B. Update on the use of etanercept across a spectrum of rheumatoid disorders. *Biologics.* (2008) 2:165–73. doi: 10.2147/BTT.S1379
32. Koes BW, van Tulder M, Lin CWC, Macedo LG, McAuley J, Maher C. An updated overview of clinical guidelines for the management of non-specific low back pain in primary care. *Eur Spine J.* (2010) 19:2075–94. doi: 10.1007/s00586-010-1502-y
33. Bowles RD, Setton LA. Biomaterials for intervertebral disc regeneration and repair. *Biomaterials.* (2017) 129:54–67. doi: 10.1016/j.biomaterials.2017.03.013
34. Chamoli U, Lam M, Diwan AD. *Replacing the Nucleus Pulposus for Degenerative Disc Disease and Disc Herniation: Disc Preservation Following Discectomy.* Cham: SpringerLink (2019). doi: 10.1007/978-3-319-33037-2_94-1
35. Durdag E, Ayden O, Albayrak S, Atci IB, Armagan E. Fragmentation to epidural space: first documented complication of Gelstix(TM.). *Turk Neurosurg.* (2014) 24:602–5. doi: 10.5137/1019-5149.JTN.9328-13.1
36. Berlemann U, Schwarzenbach O. An injectable nucleus replacement as an adjunct to microdiscectomy: 2 year follow-up in a pilot clinical study. *Eur Spine J.* (2009) 18:1706–12. doi: 10.1007/s00586-009-1136-0
37. Smith LJ, Silverman L, Sakai D, Le Maitre CL, Mauck RL, Malhotra NR, et al. Advancing cell therapies for intervertebral disc regeneration from the lab to the clinic: Recommendations of the ORS spine section. *JOR Spine.* (2018) 1:e1036. doi: 10.1002/jsp2.1036
38. El Bialy I, Jiskoot W, Reza Nejadnik M. Formulation, delivery and stability of bone morphogenetic proteins for effective bone regeneration. *Pharm Res.* (2017) 34:1152–70. doi: 10.1007/s11095-017-2147-x
39. Vukicevic S, Basic V, Rogic D, Basic N, Shih MS, Shepard A, et al. Osteogenic protein-1 (bone morphogenetic protein-7) reduces severity of injury after ischemic acute renal failure in rat. *J Clin Invest.* (1998) 102:202–14. doi: 10.1172/JCI2237
40. Wakefield LM, Winokur TS, Hollands RS, Christopherson K, Levinson AD, Sporn MB. Recombinant latent transforming growth factor beta 1 has a longer plasma half-life in rats than active transforming growth factor beta 1, and a different tissue distribution. *J Clin Invest.* (1990) 86:1976–84. doi: 10.1172/JCI114932
41. Farhang N SL, Bowles RD. Improving cell therapy survival and anabolism in harsh musculoskeletal disease environments. *Tissue Eng Part B Rev.* (2020) 26. doi: 10.1089/ten.teb.2019.0324
42. Silverman LI, Flanagan F, Rodriguez-Granrose D, Simpson K, Saxon LH, Foley KT. Identifying and managing sources of variability in cell therapy manufacturing and clinical trials. *Regen Eng Transl Med.* (2019) 5:354–61. doi: 10.1007/s40883-019-00129-y
43. Schol J, Sakai D. Cell therapy for intervertebral disc herniation and degenerative disc disease: clinical trials. *Int Orthop.* (2019) 43:1011–25. doi: 10.1007/s00264-018-4223-1
44. Silverman LI, Dulatova G, Tandeski T, Erickson IE, Lundell B, Toplon D, et al. In vitro and in vivo evaluation of discogenic cells, an investigational cell therapy for disc degeneration. *Spine J.* (2020) 20:138–49. doi: 10.1016/j.spinee.2019.08.006
45. Fujita N, Miyamoto T, Imai J, Hosogane N, Suzuki T, Yagi M, et al. CD24 is expressed specifically in the nucleus pulposus of intervertebral discs. *Biochem Biophys Res Commun.* (2005) 338:1890–6. doi: 10.1016/j.bbrc.2005.10.166
46. Hiraishi S SJ, Sakai D, Nukaga T, Erickson I, Silverman L, Foley K, et al. Discogenic cell transplantation directly from a cryopreserved state in an induced intervertebral disc degeneration canine model. *JOR Spine.* (2018) 1:1013. doi: 10.1002/jsp2.1013
47. Kumar H, Ha DH, Lee EJ, Park JH, Shim JH, Ahn TK, et al. Safety and tolerability of intradiscal implantation of combined autologous adipose-derived mesenchymal stem cells and hyaluronic acid in patients with chronic discogenic low back pain: 1-year follow-up of a phase I study. *Stem Cell Res Ther.* (2017) 8:262. doi: 10.1186/s13287-017-0710-3
48. Mochida J, Sakai D, Nakamura Y, Watanabe T, Yamamoto Y, Kato S. Intervertebral disc repair with activated nucleus pulposus cell transplantation: a three-year, prospective clinical study of its safety. *Eur Cell Mater.* (2015) 29:202–12; discussion 12. doi: 10.22203/eCM.v029a15
49. Meisel HJ, Ganey T, Hutton WC, Libera J, Minkus Y, Alasevic O. Clinical experience in cell-based therapeutics: intervention and outcome. *Eur Spine J.* 15(Suppl 3):397–405. doi: 10.1007/s00586-006-0169-x
50. Van Gool SW, Vandenbergh P, de Boer M, Ceuppens JL. CD80, CD86 and CD40 provide accessory signals in a multiple-step T-cell activation model. *Immunol Rev.* (1996) 153:47–83. doi: 10.1111/j.1600-065X.1996.tb00920.x
51. Noriega DC, Ardura F, Hernandez-Ramajo R, Martin-Ferrero MA, Sanchez-Lite I, Toribio B, et al. Intervertebral disc repair by allogeneic mesenchymal bone marrow cells: a randomized controlled trial. *Transplantation.* (2016) 101:1945–51. doi: 10.1097/TP.0000000000001484
52. Yoshikawa T, Ueda Y, Miyazaki K, Koizumi M, Takakura Y. Disc regeneration therapy using marrow mesenchymal cell transplantation: a report of two case studies. *Spine.* (2010) 35:E475–80. doi: 10.1097/BRS.0b013e3181cd2cf4
53. Orozco L, Soler R, Morera C, Alberca M, Sánchez A, García-Sancho J. Intervertebral disc repair by autologous mesenchymal bone marrow cells: a pilot study. *Transplantation.* (2011) 92:822–8. doi: 10.1097/TP.0b013e3182298a15
54. Hohaus C, Ganey TM, Minkus Y, Meisel HJ. Cell transplantation in lumbar spine disc degeneration disease. *Euro Spine J.* (2008) 17(Suppl 4):492–503. doi: 10.1007/s00586-008-0750-6
55. Coric D, Pettine K, Sumich A, Boltes MO. Prospective study of disc repair with allogeneic chondrocytes presented at the 2012. Joint spine section meeting. *J Neurosurg.* (2012) 18:85–95. doi: 10.3171/2012.10.SPINE12512
56. Intervertebral disc repair Phase 2 trial update from Mesoblast. *News-Medicalnet.* (2012). Available online at: <http://www.news-medical.net/news/20120417/Intervertebral-disc-repair-phase-2-trial-update-from-Mesoblast.aspx?page=2> (accessed December 1, 2019).
57. Haefeli M, Elfering A. Pain assessment. *Euro Spine J.* (2006) 15(Suppl 1):S17–24. doi: 10.1007/s00586-005-1044-x
58. A Mehra DB, S Disney, PB Pynsent. Oswestry disability index scoring made easy. *Ann R Coll Surg Engl.* (2008) 90:497–9. doi: 10.1308/003588408X300984
59. Finch AP, Dritsaki M, Jommi C. Generic preference-based measures for low back pain: which of them should be used? *Spine.* (2016) 41:E364–74. doi: 10.1097/BRS.0000000000001247
60. Hirano K, Imagama S, Hasegawa Y, Ito Z, Muramoto A, Ishiguro N. Impact of low back pain, knee pain, and timed up-and-go test on quality of life in community-living people. *J Orthop Sci.* (2014) 19:164–71. doi: 10.1007/s00776-013-0476-0

61. Gautschi OP, Corniola MV, Smoll NR, Joswig H, Schaller K, Hildebrandt G, et al. Sex differences in subjective and objective measures of pain, functional impairment, and health-related quality of life in patients with lumbar degenerative disc disease. *Pain*. (2016) 157:1065–71. doi: 10.1097/j.pain.0000000000000480
62. Gautschi OP, Corniola MV, Joswig H, Smoll NR, Chau I, Jucker D, et al. The timed up and go test for lumbar degenerative disc disease. *J Clin Neurosci*. (2015) 22:1943–8. doi: 10.1016/j.jocn.2015.04.018
63. Meyer R, Patel AM, Rattana SK, Quock TP, Mody SH. Prescription opioid abuse: a literature review of the clinical and economic burden in the United States. *Popul Health Manag*. (2014) 17:372–87. doi: 10.1089/pop.2013.0098

Conflict of Interest: The authors declare that this study received funding from DiscGenics Inc. The funder had the following involvement with the study: study design, collection, analysis, interpretation of data, the writing of this article and the decision to submit it for publication.

Copyright © 2020 Silverman, Heaton, Farhang, Saxon, Dulatova, Rodriguez-Granrose, Flanagan and Foley. This is an open-access article distributed under the terms of the Creative Commons Attribution License (CC BY). The use, distribution or reproduction in other forums is permitted, provided the original author(s) and the copyright owner(s) are credited and that the original publication in this journal is cited, in accordance with accepted academic practice. No use, distribution or reproduction is permitted which does not comply with these terms.



Development of a Computer-Aided Design and Finite Element Analysis Combined Method for Affordable Spine Surgical Navigation With 3D-Printed Customized Template

Peter Endre Eltes^{1,2,3*}, Marton Bartos⁴, Benjamin Hajnal², Agoston Jakab Pokorni², Laszlo Kiss^{1,2,3}, Damien Lacroix⁵, Peter Pal Varga¹ and Aron Lazary^{1,6}

¹ National Center for Spinal Disorders, Buda Health Center, Budapest, Hungary, ² In Silico Biomechanics Laboratory, National Center for Spinal Disorders, Buda Health Center, Budapest, Hungary, ³ School of Ph.D. Studies, Semmelweis University, Budapest, Hungary, ⁴ Do3D Innovations Ltd., Budapest, Hungary, ⁵ Department of Mechanical Engineering, INSIGNEO Institute for In Silico Medicine, The University of Sheffield, Sheffield, United Kingdom, ⁶ Department of Spinal Surgery, Semmelweis University, Budapest, Hungary

OPEN ACCESS

Edited by:

Ralph Jasper Mobbs,
University of
New South Wales, Australia

Reviewed by:

Alexandre Terrier,
École Polytechnique Fédérale de
Lausanne, Switzerland
Konstantinos Markatos,
Salamina Medical Center, Greece

*Correspondence:

Peter Endre Eltes
peter.eltes@bhc.hu;
eltespeter@yahoo.com

Specialty section:

This article was submitted to
Orthopedic Surgery,
a section of the journal
Frontiers in Surgery

Received: 14 July 2020

Accepted: 18 December 2020

Published: 25 January 2021

Citation:

Eltes PE, Bartos M, Hajnal B,
Pokorni AJ, Kiss L, Lacroix D,
Varga PP and Lazary A (2021)
Development of a Computer-Aided
Design and Finite Element Analysis
Combined Method for Affordable
Spine Surgical Navigation With
3D-Printed Customized Template.
Front. Surg. 7:583386.
doi: 10.3389/fsurg.2020.583386

Introduction: Revision surgery of a previous lumbosacral non-union is highly challenging, especially in case of complications, such as a broken screw at the first sacral level (S1). Here, we propose the implementation of a new method based on the CT scan of a clinical case using 3D reconstruction, combined with finite element analysis (FEA), computer-assisted design (CAD), and 3D-printing technology to provide accurate surgical navigation to aid the surgeon in performing the optimal surgical technique by inserting a pedicle screw at the S1 level.

Materials and Methods: A step-by-step approach was developed and performed as follows: (1) Quantitative CT based patient-specific FE model of the sacrum was created. (2) The CAD model of the pedicle screw was inserted into the sacrum model in a bicortical convergent and a monocortical divergent position, by overcoming the geometrical difficulty caused by the broken screw. (3) Static FEAs (Abaqus, Dassault Systemes) were performed using 500 N tensile load applied to the screw head. (4) A template with two screw guiding structures for the sacrum was designed and manufactured using CAD design and 3D-printing technologies, and investment casting. (5) The proposed surgical technique was performed on the patient-specific physical model created with the FDM printing technology. The patient-specific model was CT scanned and a comparison with the virtual plan was performed to evaluate the template accuracy

Results: FEA results proved that the modified bicortical convergent insertion is stiffer (6,617.23 N/mm) compared to monocortical divergent placement (2,989.07 N/mm). The final template was created via investment casting from cobalt-chrome. The template design concept was shown to be accurate (grade A, Gertzbein-Robbins scale) based on the comparison of the simulated surgery using the patient-specific physical model and the 3D virtual surgical plan.

Conclusion: Compared to the conventional surgical navigation techniques, the presented method allows the consideration of the patient-specific biomechanical parameters; is more affordable, and the intraoperative X-ray exposure can be reduced. This new patient- and condition-specific approach may be widely used in revision spine surgeries or in challenging primary cases after its further clinical validation.

Keywords: 3D printing, computed tomography, navigation, finite element simulation, spine surgery, surgical guidance/navigation

INTRODUCTION

Spinal fixation is a routine procedure for the treatment of unstable spine due to trauma, congenital malformations, degenerative diseases, and tumors (1). The accurate placement of screws in the spine is challenging, given the risk of damage to neighboring anatomical structures (spinal cord, nerve roots, arteries, and veins) (2, 3). Computer-assisted surgery (CAS) has been adopted as a safe and accurate guiding system for the placement of pedicle and lateral mass screws in the spine (4). CAS navigation systems use optical tracking via infrared cameras incorporating 3D geometries from pre-operative CT scans or in combination with fluoroscopy-based imaging (5, 6) or intraoperative CT scans (7). Optimal registration of the spine geometry to the navigational instruments is crucial for precise screw insertion. During surgery, it is often required to perform intraoperative CT scans or use fluoroscopy to re-register the system (5–7). Surgical manipulation after obtaining the intraoperative CT or fluoroscopy images may cause CAS registration errors, which can result in screw malposition. This phenomenon cannot be completely excluded even with a state of the art intraoperative CT technology (7). First concept of individual templates was first introduced by Radermacher et al. (8) in the early 90's by using computer controlled milling device for the manufacturing process. Currently, the 3D-printed patient-specific surgical navigation templates are accurate (9, 10), decrease surgical time, reduce intraoperative X-ray exposure (11), and can be more accessible compared to traditional CT or fluoroscopy-based systems (12, 13). The decline in the costs of 3D-printing technology is expected to continue due to its continuous and fast development (14–16). The MySpine (Medacta International SA, Castel San Pietro, CH) patient-matched pedicle targeting guide for pedicle screw placement (17) is an already clinically available device for the large international spine surgical community. However, in less developed areas of the world, where complex spinal deformity is relatively common and advanced CAS technology is not available (11, 18) 3D-printed templates are still not as widely implemented in the clinical practice, as it would be desirable.

The revision surgery of a lumbosacral non-union can be complicated by an implant related failure, with a broken pedicle screw. In the S1 segment, the convergent bicortical screw trajectory provides superior anchoring compared to any other directions, but the proper insertion of the new screws in a revision surgery due to the broken screw is extremely difficult without surgical navigation. Here, we

present a complex clinical case in which the accurate surgical technique required the development of a computer-aided design (CAD) and finite-element analysis (FEA) combined method for affordable spine surgical navigation with a 3D-printed customized navigation template.

METHODS

Clinical Case

The study was approved by the National Ethics Committee of Hungary and the National Institute of Pharmacy and Nutrition (reference number: OGYÉI/163-4/2019). Informed consent was obtained from the patient. A 38-years-old patient underwent multiple spine surgeries at the L5–S1 level over a 5-years period with transforaminal interbody fusion (TLIF). During the latest surgery, implant removal and S1 left side nerve root decompression were performed. Six months later, the patient was referred to our institution due to manifestation of mechanical low back pain, with no sign of sensorimotor deficit. Medical imaging at admission (**Figure 1**) demonstrated a broken S1 left side pedicle screw deep in the sacral bone, and a non-union in the L5–S1 intervertebral space. A revision surgery aiming at the re-fusion of the LV/SI segment was decided.

Patient-Specific 3D Geometry Definition

For the study Quantitative Computed Tomography (QCT) scans were used, performed with a Hitachi Presto CT machine (Hitachi Presto, Hitachi Medical Corporation, Tokyo, Japan) using an in-line calibration phantom with five cylindrical insertions of known mean equivalent bone mineral density (BMD) values (0, 0.5, 0.1, 0.15, and 0.2 g/cm³) with an intensity of 225 mA and voltage of 120 kV. The imaging protocol was previously defined in the MySpine project (ICT-2009.5.3 VPH, Project ID: 269909) (19, 20), and the images were reconstructed with a voxel size of 0.6 × 0.6 × 0.6 mm³. The data were extracted from the hospital PACS in DICOM file format. To comply with the ethical approval of the patient data protection, deidentification of the DICOM data was performed using the freely available Clinical Trial Processor software (Radiological Society of North America, <https://www.rsna.org/ctp.aspx>) (21). The thresholding algorithm and manual segmentation tools (erase, paint, fill, etc.) in Mimics image analysis software (Mimics Research, Mimics Innovation Suite v21.0, Materialize, Leuven, Belgium) were used (**Figure 2**) to define the geometry of the sacrum and the broken screw.

The resulting masks (group of voxels) were homogeneously filled by preserving the outer contour of the geometrical

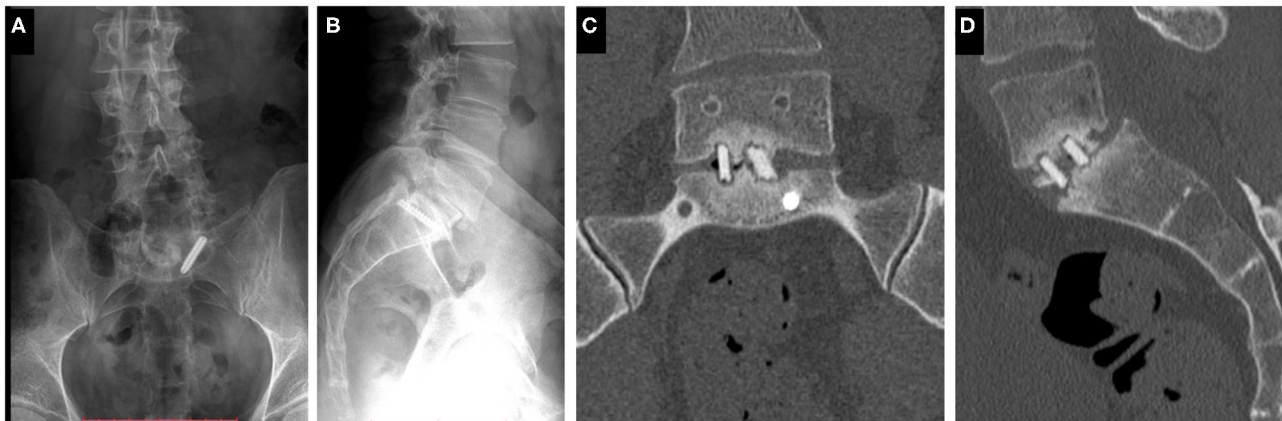


FIGURE 1 | Clinical case of a 38-years-old male patient suffering from low back pain. The patient previously underwent multiple surgeries at the L5–S1 level. A broken left sacral screw can be identified on the standing X-ray images of the patient (**A**, Coronal, **B**, Sagittal plane). Signs of non-union are identifiable in the intervertebral space on the CT scan images of the L5 vertebra and the sacrum (**C**, Coronal, **D**, Sagittal plane).

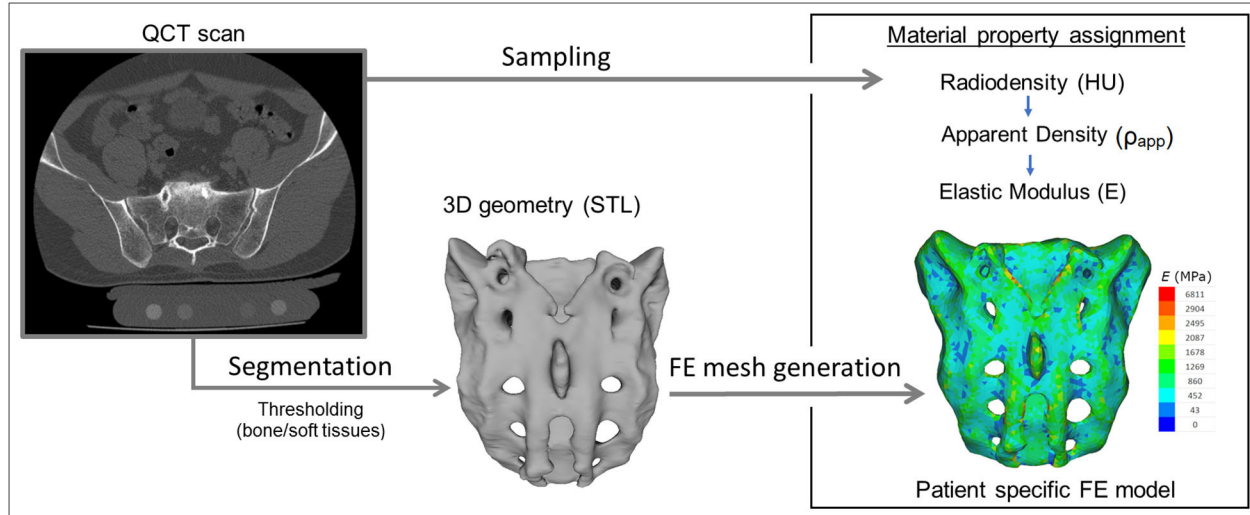


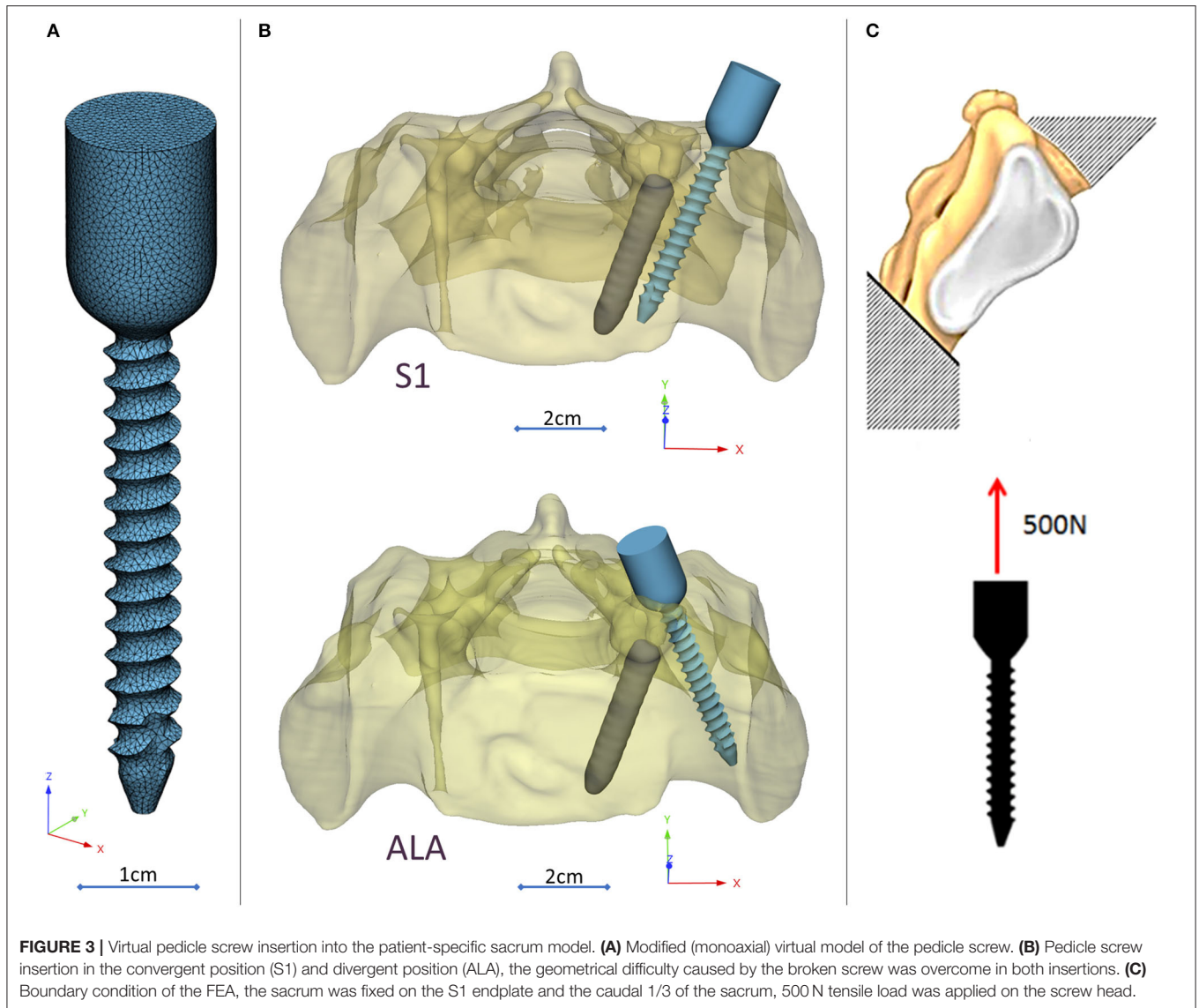
FIGURE 2 | Patient-specific geometry and FE model definition. QCT based segmentation was used to define the sacrum geometry. Hounsfield Unit (HU) values of the QCT images were converted into bone mineral density (BMD) equivalent values. Elastic properties of the sacral bone were estimated using a set of density to elasticity relationships from the literature to convert the BMD equivalent value at each element of the FE mesh to Apparent Density (ρ_{app}) (22, 23) and then to the Elastic Modulus (E).

border in 2D. From the mask, a triangulated surface mesh was automatically generated. On the 3D geometries surface smoothing (iteration: 6, smooth factor: 0.7, with shrinkage compensation) and uniform remeshing was applied (target triangle edge length 0.6 mm, sharp edge preservation, sharp edge angle 60°).

Surgical Planning and FE Model Generation

A CD Horizon Legacy (Medtronic) polyaxial pedicle screw, 45 mm long and 6.5 mm in diameter, was scanned with the

ScanBox 3D scanner (Smart Optics Sensortechnik GmbH, Bochum, Germany). The model of the screw was reconstructed and modified (from polyaxial to monoaxial head) in 3-matic (Mimics Research, Mimics Innovation Suite v21.0, Materialize, Leuven, Belgium) software. The triangulated surface mesh of the screw model was uniformly re-meshed (target triangle edge length: 0.6 mm, sharp edge preservation, sharp edge angle: 60°) (Figure 3A). The screw model was virtually inserted into the 3D model of the patient's sacrum in two positions (convergent: S1, divergent: ALA), using the Mimics software's STL import tool (Figure 3B) with the consideration of the broken screw. Two



non-manifold assemblies were created in the Mimics software containing the broken screw, implanted screw, and sacrum for the convergent (S1) and divergent (ALA) positions.

The assembly was exported to the 3-matic software where nine FE meshes were generated for each of the implantation scenarios (S1, ALA). The broken screw, inserted implant, and sacrum-implant interface had a triangle set with an edge length of 0.6 mm. The outer surface of the sacrum mesh was changed in the nine models by defining the uniform triangle mesh edge length as 2.0, 2.5, 3.0, 3.5, 4.0, 4.5, 5.0, 5.5, and 6.0 mm. Adaptive meshing protocol was used for the volume mesh creation with 10-node tetrahedral elements. The maximum edge length of the meshing process corresponded with the initial edge length of the sacrum surface mesh (**Supplementary Figure 1**), for the screw and the broken screw the same FE mesh parameters was used in all models.

The material property assignment for the volumetric elements representing the sacral bone tissue was performed in two steps (**Figure 2**): first, conversion of the HU (*Hounsfield Unit*) values to BMD values based on the in-line phantom was performed, the conversion curve was assumed to be linear according to studies (22, 24). The obtained relationship between the HU and the apparent bone density for each element was $\rho_{app} = -0.0829 + 0.0026 HU$ (ρ_{app} [g/cm³]). Then, the bone tissue was assumed to be isotropic and linearly elastic with a Poisson's ratio of 0.3 (25). Conversion curves between the density and the elastic modulus of the bone were based on the correlation established by Kopperdahl et al. (23), $E = -34.7 + 3,230 \cdot \rho_{app}$, (bone elastic modulus = E [MPa]). The FE models were exported to the Abaqus/CAEv11 (Dassault Systemes, Simulia Corp, Providence, RI, USA). For the broken and the inserted pedicle screws the material properties were defined as follows: Poisson's ratio of 0.3 (26), elastic modulus of 114,000 MPa (26). Between the screws

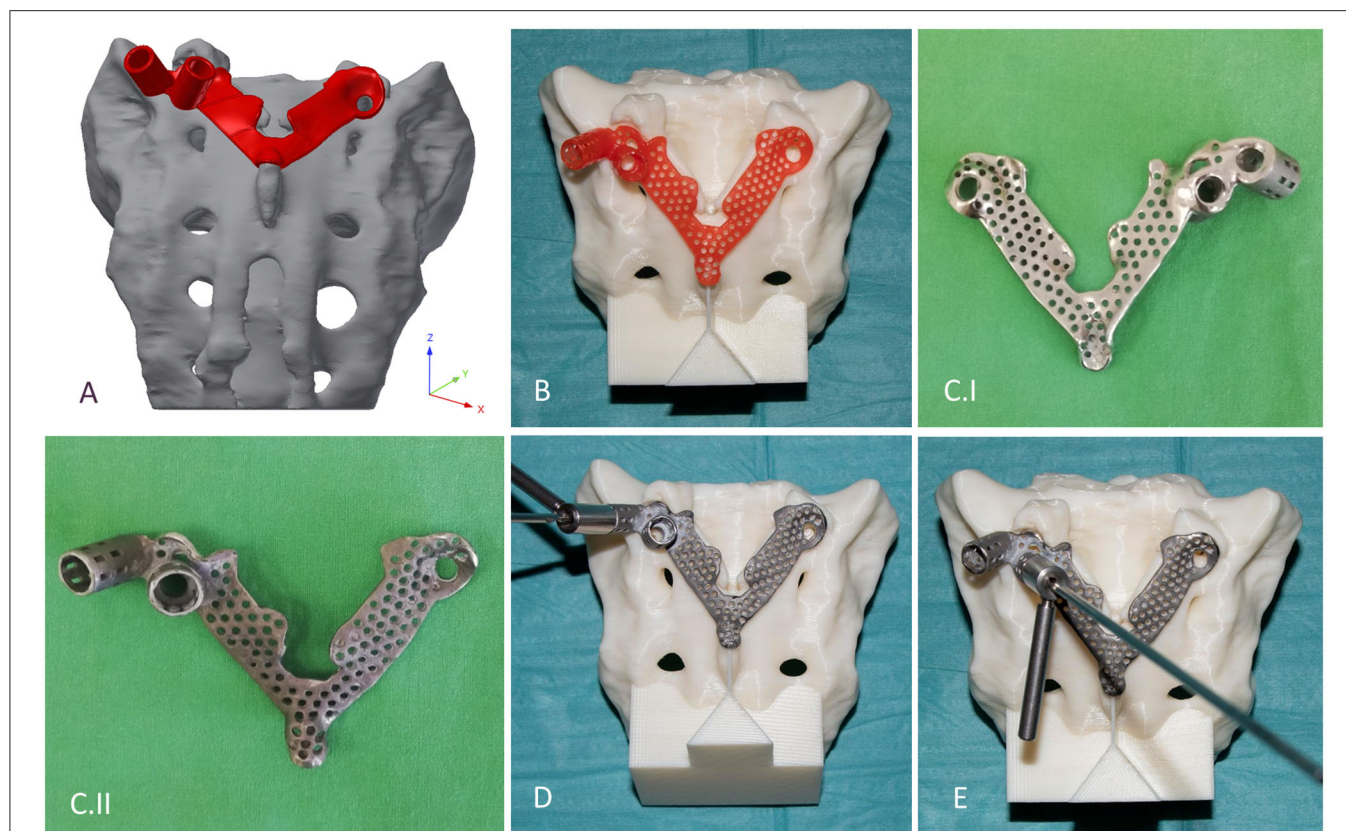


FIGURE 4 | Design, manufacturing, and accuracy evaluation of the navigation template. **(A)** Template's virtual model created via CAD software. **(B)** 3D-printed (MSLA technology) template (red) fits exactly on the 3D-printed (FDM technology) patient-specific physical model. **(C.I,II)** Final navigation template created via investment casting from cobalt-chrome **(C.I)** ventral surface polished, **(C.II)** dorsal surface). Evaluation of the drilling accuracy was performed on the physical model in the **(D)** convergent position (S1) and **(E)** divergent position (ALA).

and the sacrum tie connections were used. The finite element model was subjected to a static of 500 N tensile load applied to the screw head and it was fixed at the S1 endplate and lower third of the sacrum (Figure 3C).

Navigation Template Design, Manufacturing, and Accuracy Evaluation

The template design was based on the axis of the virtually inserted screw, individual geometry, and surface of the cranial/dorsal part of the sacrum. In the 3-matic software the two axes and surface for the template/sacrum contact were defined based on the STL assembly (broken screw, inserted implant, sacrum). The contact surface and the axes were exported to the Autodesk Fusion 360 (Autodesk Inc., California, U.S.A.) CAD software which was used for the finalization of the design (Figure 4A). The virtual model of the template was printed with masked stereolithography (MSLA) technology based 3D-printing machine (VOXEL L 3D-Printer; Parameters: building size: 125 × 65 × 65 mm, layer thickness: 0.05 mm; Material: Voxeltek Cast Resin; Do3D, Hungary) (Figure 4B). The used photopolymer resin can be used as a pattern for investment casting. Finally, the model was produced in a dental laboratory via investment casting (Hexacast induction centrifugal casting machine; Parameters:

start torque: 0–21 Nm, maximum melting mass: 100 g, max heating: 1,750°C, dimensions (width × height × depth): 660 × 390 × 645 mm; Material: CoCr; PiDental, Hungary) from cobalt-chrome (Figures 4C.I,II). The accuracy of the casted part was tested via 3D scanning ScanBox 3D scanner (Smart Optics Sensortechnik GmbH, Bochum, Germany) and compared to the 3D-printed model. The point clouds resulting from the scanning were aligned and compared in the 3-matic software with the part comparison module (Figure 5).

The accuracy of the template was tested on a patient-specific sacrum physical model, 3D-printed with a Fused Deposition Modeling (FDM) printer (Dimension 1200es 3D-Printer; Parameters: building size: 254 × 254 × 305 mm, layer thickness: 0.330–0.254 mm; Material: ABSplus/ivory; Stratasys, Israel). The drill template was placed on the FDM sacrum model; then, a cylinder inlet was connected to the template to support the drill bit, and the drilling of the model was performed according to the S1 and ALA positions (Figures 4D,E).

The template was removed and two CT scans were performed of the sacrum model with drill bits inserted in the S1 and ALA positions. The CT scan images were imported into the Mimics software where the segmentation (thresholding) and 3D reconstruction of the patient-specific

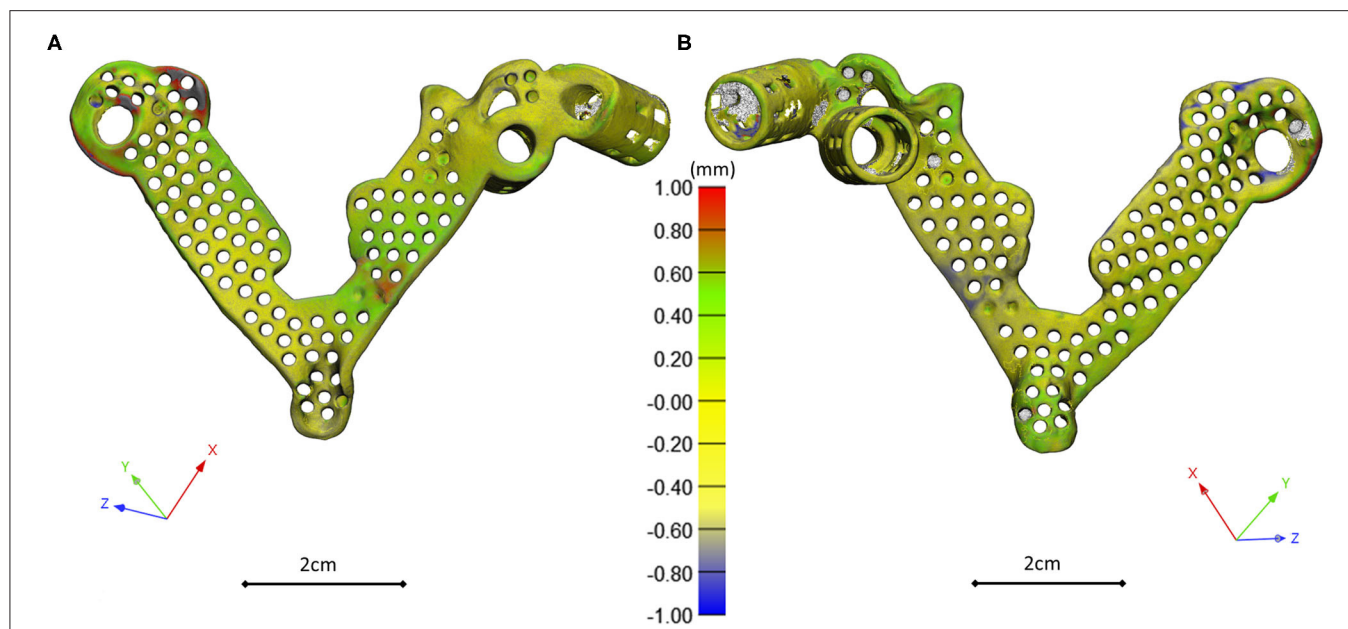


FIGURE 5 | 3D scanning based geometrical accuracy measurement. Cobalt-chrome investment casted navigation template's geometrical accuracy compared to the 3D-printed navigation template model created with MSLA technology. The color map (Scale; min = -1 mm, max = 1 mm) shows the geometrical difference, projected on the 3D-printed navigation template triangle based mesh model vertices (**A** ventral view, **B** dorsal view).

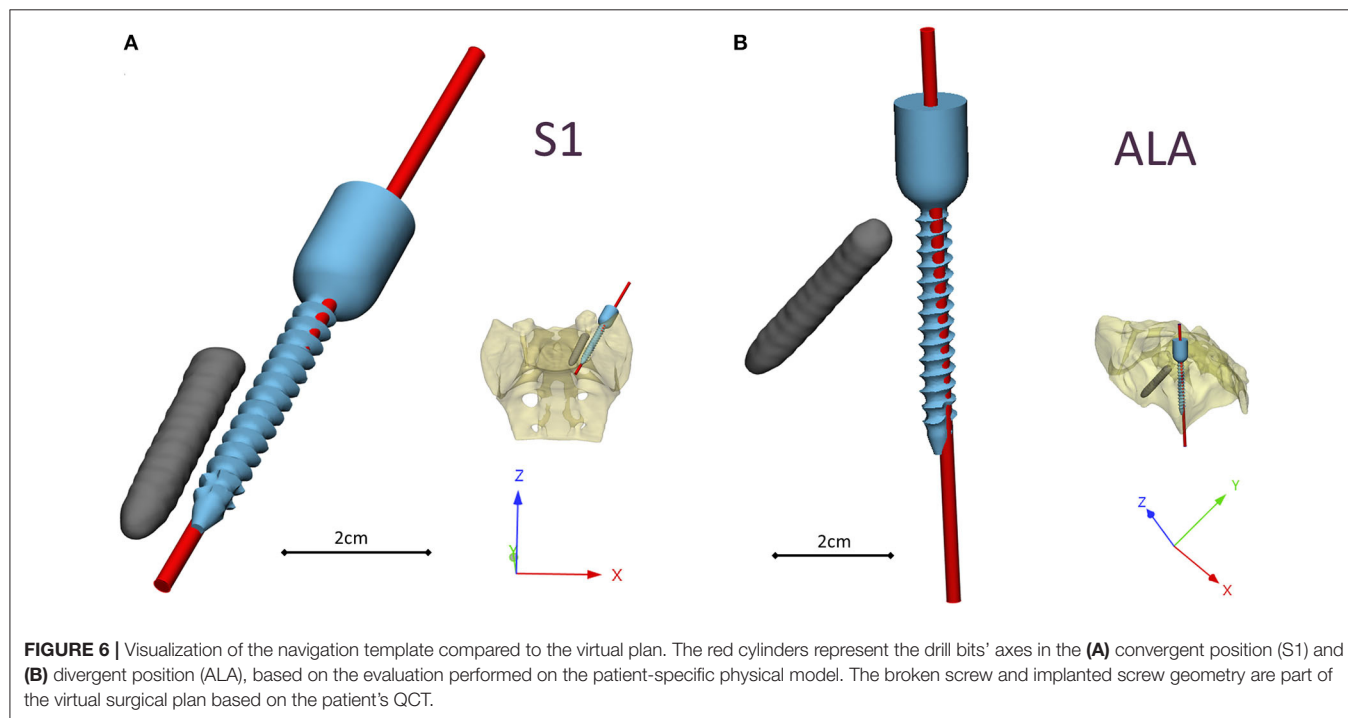
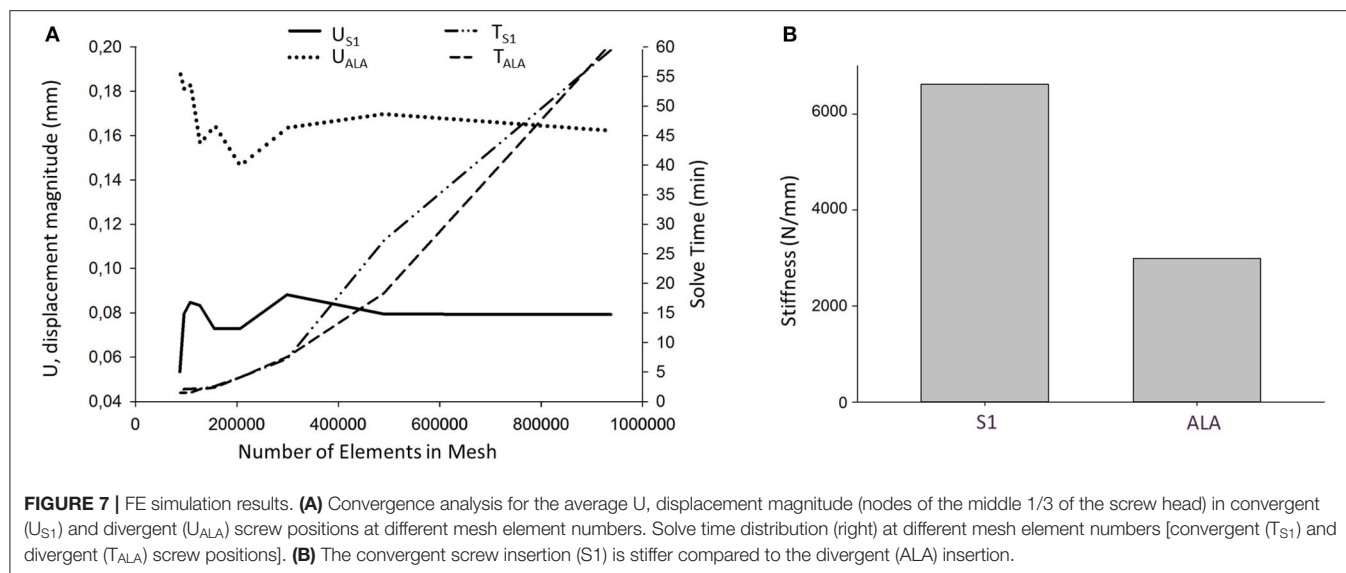


FIGURE 6 | Visualization of the navigation template compared to the virtual plan. The red cylinders represent the drill bits' axes in the (**A**) convergent position (S1) and (**B**) divergent position (ALA), based on the evaluation performed on the patient-specific physical model. The broken screw and implanted screw geometry are part of the virtual surgical plan based on the patient's QCT.

FDM sacrum model geometry and drill bits were performed. The models were registered to the initial sacrum geometry derived from the QCT via point based rigid registration by selecting anatomical landmarks in the caudal part of the sacrum (**Supplementary Figure 2**). This step was followed by an

automatic global registration inside the 3-matic software. The registration accuracy was measured with the part comparison module of the 3-matic software (**Supplementary Figure 3**). The centerline for the drill bit 3D geometry was defined and an analytical primitive (cylinder, 2.5 mm in diameter) was fitted



to define the drilling axis. In 3-matic software 3D angle measurement tool, line to line module (World Coordinate System, XYZ coordinates) was used to quantify the accuracy of the screw insertion by defining the angles in the 3D space between the virtual screw centerline and the drill bit centerline.

RESULTS

Navigation Template Geometrical Accuracy and Performance

The investment casted cobalt-chrome drill template retains the geometrical properties of the pattern (3D-printed drill template model created with MSLA technology) based on the 3D scanning evaluation **Figure 6**. To evaluate the drill template's performance, we used a 3D-printed patient-specific physical model. The physical model with the two drilling positions was scanned with CT, segmented and aligned to the virtual surgical plan (**Supplementary Figures 2, 3**). The drill template allowed a highly accurate screw insertion in both investigated positions (**Figure 6**). The cylinders representing the drilling axes were not perfectly colinear and coincident with the screws in the virtual surgical plan, the 3D angle between the screw centerline and the drill bit centerline for the S1 was $\alpha = 4.42^\circ$ and for the ALA was $\alpha = 2.4^\circ$.

FEA Results

Nine models were created for each screw insertion scenario ($N = 9$, S1 and $N = 9$, ALA) with increasing element numbers based on the virtual surgical plan. The FE simulation results converged above 2×10^5 elements for both screw insertion scenarios at ~ 5 min solve times on two cores. The solve time at two cores for the S1 orientation was higher compared to the ALA (**Figure 7A**). The convergent bicortical screw insertion (S1) provided a stiffer ($6,617.23 \pm 1,106.24$ N/mm) situation based on the nine FE model compared to the monocortical divergent screw position FE model values ($2,989.07 \pm 240.24$ N/mm) (**Figure 7B**).

DISCUSSION

Comparative studies have been published in recent years (27–29), demonstrating the reliability, efficacy, and advantages of 3D printed navigational templates compared to other navigational methods or free-hand technique. In this study, we present a technology development process in order to create a patient-specific drill template in a complex clinical case, in which a broken screw causes geometrical difficulty for new screw insertion. In order to safely insert the new screw, without compromising the local bone structure we developed a virtual surgical plan based on the QCT of the patient. This allowed us to test two different screw positions in the model and to design a drill template for safe screw insertion at the level of the first sacral vertebra with a geometrical difficulty caused by a broken screw from a previous surgery. The present study demonstrates the accuracy and applicability of a developed workflow which allows the creation of an affordable, metal, individualized navigational template by integration of FEA in the design and surgical planning process.

The integration of FEA in the pedicle screw intraoperative navigation was investigated by Van den Abbeele et al. (30), however, the application of FEA in the design process of a navigational template in spine surgery by integrating the patient bone mineral density related material properties is new. The results of the simulations showed that the convergent S1 insertion is significantly stiffer than the divergent ALA insertion. This finding is supported by cadaveric experimental studies (31, 32) and clinical experience as well (33). The biomechanical difference of the convergent and divergent insertions rely on the differences in the local bone mineral densities (34).

The combination of the 3D-printing technology and cobalt-chrome casting makes the manufacturing process more affordable. Investment casting of cobalt-chrome is a widely used technology in dental laboratories (35). 3D-printed patterns for casting is an accepted method in dentistry (35, 36); however, its application in spine surgery navigational templates is novel.

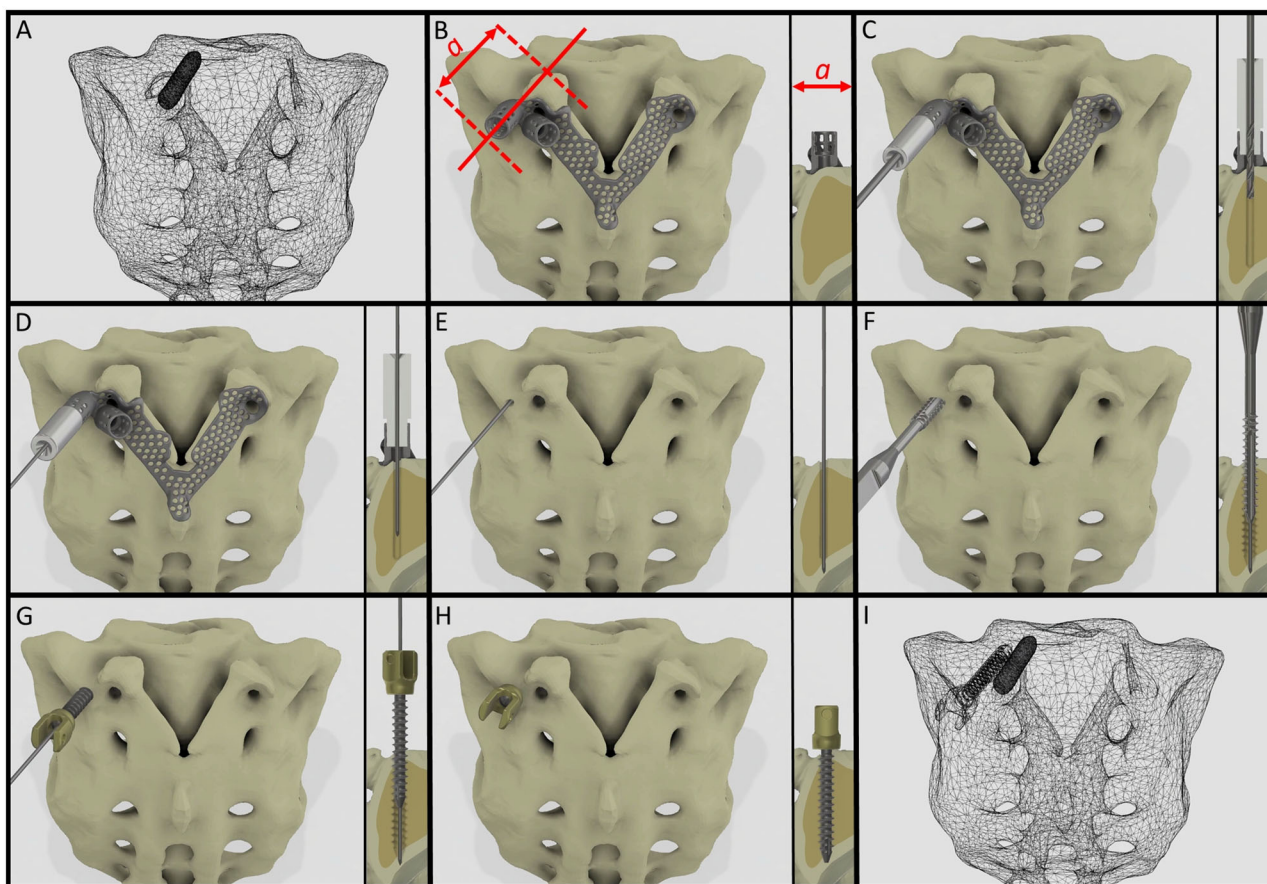


FIGURE 8 | Proposed surgical technique for safe and accurate screw insertion in convergent position. **(A)** Transparent surface mesh of the patient's sacrum with the broken screw. **(B)** Section plane dimension and orientation, and drill template position on the sacrum. **(C)** Stainless steel cylinder inlet connected to the navigation template for the drill bit. **(D)** Stainless steel cylinder inlet connected to the template for the Kirschner wire. **(E)** The inlet cylinder and template are removed, the Kirschner wire's position is unchanged. **(F)** Cannulated tap is introduced along the Kirschner wire. **(G)** Cannulated pedicle screw is introduced in the sacrum along the Kirschner wire. **(H)** Final position of the screw. **(I)** Transparent surface mesh of the sacrum with the broken and convergently inserted pedicle screw geometry.

The production of individualized metal navigational templates for screw insertion can be achieved via selective laser sintering 3D-printing technology of titanium-based alloys (37), but at a higher cost and lower accessibility compared to dental casting. Metal templates are robust, resistant to damage, and can also be easily autoclaved (37).

It is widely accepted in the literature to use cadavers for testing, evaluating the fitting accuracy of a navigational template (38). FDM technology can produce geometrically accurate spine physical models (39) and the different designs can be tested as well as the drilling accuracy can be evaluated. The use of FDM models for design process evaluation and development is advantageous due to the possibility to include retrospective patient imaging data with complex anatomical/geometrical variation (deformities, tumors, etc.) which is extremely difficult to control and integrate in the case of cadaveric specimen studies. Based on our FEA results, the S1 screw insertion's surgical plan and drill template position is recommended for surgical implementation. Despite the fact that the virtual screw axis

and the drill bit centerline are not colinear and coincident (3D angle $\alpha > 0$) according to the Gertzbein-Robbins scale (40) the template theoretically allows an accurate (grade A) screw insertion (Figure 6). We present the surgical technique for the screw insertion with the developed drill template (Figure 8 and Supplementary Video 1). The suggested screw insertion surgical technique uses the philosophy of the minimally invasive pedicle screw insertion techniques (MIS) by using a Kirschner wire, cannulated tap, and pedicle screw. This technique can easily be performed by any spine surgeon familiar with MIS pedicle screw insertion.

Limitations of this study include the fact that the developed template is presented using a single case, however the workflow can be applied for different parts of the spine with different geometrical difficulties/pathologies. The presented FEA models' loading conditions are simplified as well as the material property assignments; more complex FEA investigations would be desirable. In the future, a randomized study of specific subtypes of spinal pathologies (tumors, deformities, etc.) with a

larger sample size would be preferred to demonstrate the clinical efficacy and cost-effectiveness of the developed methodology.

CONCLUSION

A patient-specific template for pedicle screw insertion allows the surgeon to insert the screw into its optimal position. The advantages of our technique compared to the conventional surgical navigation tools are the affordability, the potential to reduce intraoperative X-ray exposure, and the possibility for the consideration of patient-specific bone geometry and biomechanics. This new patient- and condition-specific approach can be widely used in revision spine surgeries or in challenging primary cases after its further clinical validations.

DATA AVAILABILITY STATEMENT

The datasets generated for this study are available on request to the corresponding author.

ETHICS STATEMENT

The studies involving human participants were reviewed and approved by National Ethics Committee of Hungary and the National Institute of Pharmacy and Nutrition (reference number: OGYÉI/163-4/2019). The patients/participants provided their written informed consent to participate in this study. Written informed consent was obtained from the individual(s) for the

publication of any potentially identifiable images or data included in this article.

AUTHOR CONTRIBUTIONS

PEE, AL, PPV, MB, and DL: research design. PEE, AL, MB, BH, AJP, and LK: acquisition of data. PEE, AL, MB, BH, AJP, and DL: analysis and/or interpretation of data. All authors: drafting the paper or revising it critically and approval of the submitted and final versions.

FUNDING

The financial support from the Hungarian Scientific Research Fund (award number: OTKA FK123884) was gratefully acknowledged.

ACKNOWLEDGMENTS

The author would like to thank to Julia Szita, Ph.D. student, National Center for Spinal Disorders, Budapest for constructive criticism and the proofreading of the manuscript.

SUPPLEMENTARY MATERIAL

The Supplementary Material for this article can be found online at: <https://www.frontiersin.org/articles/10.3389/fsurg.2020.583386/full#supplementary-material>

REFERENCES

- Gaines RW Jr. The use of pedicle-screw internal fixation for the operative treatment of spinal disorders. *J Bone Joint Surg Am.* (2000) 82:1458. doi: 10.2106/00004623-200010000-00013
- Kast E, Mohr K, Richter H-P, Börm W. Complications of transpedicular screw fixation in the cervical spine. *Eur Spine J.* (2006) 15:327–34. doi: 10.1007/s00586-004-0861-7
- Faraj AA, Webb JK. Early complications of spinal pedicle screw. *Eur Spine J.* (1997) 6:324–6. doi: 10.1007/BF01142678
- Merloz P, Tonetti J, Pittet L, Coulomb M, Lavalley S, Troccaz J, et al. Computer-assisted spine surgery. *Comput Aided Surg Off J Int Soc Comput Aided Surg.* (1998) 3:297–305. doi: 10.3109/10929089809148150
- Foley KT, Simon DA, Rampersaud YR. Virtual fluoroscopy: computer-assisted fluoroscopic navigation. *Spine (Phila Pa 1976).* (2001) 26:347–351. doi: 10.1097/00007632-200102150-00009
- Nolte L-P, Slomczykowski MA, Berlemann U, Strauss MJ, Hofstetter R, Schlénzka D, et al. A new approach to computer-aided spine surgery: fluoroscopy-based surgical navigation. *Eur Spine J.* (2000) 9:S078–88. doi: 10.1007/PL00010026
- Ishikawa Y, Kanemura T, Yoshida G, Matsumoto A, Ito Z, Tauchi R, et al. Intraoperative, full-rotation, three-dimensional image (O-arm)-based navigation system for cervical pedicle screw insertion. *J Neurosurg Spine.* (2011) 15:472–8. doi: 10.3171/2011.6.SPINE10809
- Radermacher K, Portheine F, Anton M, Zimolong A, Kaspers G, Rau G, et al. Computer assisted orthopaedic surgery with image based individual templates. *Clin Orthop Relat Res.* (1998) 354:28–38. doi: 10.1097/00003086-199809000-00005
- Putzier M, Strube P, Cecchinato R, Lamartina C, Hoff EK. A new navigational tool for pedicle screw placement in patients with severe scoliosis: a pilot study to prove feasibility, accuracy, and identify operative challenges. *Clin Spine Surg.* (2017) 30:E430–9. doi: 10.1097/BSD.0000000000000220
- Jiang L, Dong L, Tan M, Qi Y, Yang F, Yi P, et al. A modified personalized image-based drill guide template for atlantoaxial pedicle screw placement: a clinical study. *Med Sci Monit.* (2017) 23:1325–33. doi: 10.12659/MSM.900066
- Garg B, Gupta M, Singh M, Kalyanasundaram D. Outcome and safety analysis of 3D-printed patient-specific pedicle screw jigs for complex spinal deformities: a comparative study. *Spine J.* (2019) 19:56–64. doi: 10.1016/j.spinee.2018.05.001
- Cristina Mancarella AL, Roberto Delfini FG, i, Mancarella C, Gregori F, Delfini R. Spinal neuronavigation and 3D-printed tubular guide for pedicle screw placement: a really new tool to improve safety and accuracy of the surgical technique? *J Spine.* (2015) 4:1–3. doi: 10.4172/2165-7939.1000e118
- Guo F, Dai J, Zhang J, Ma Y, Zhu G, Shen J, et al. Individualized 3D printing navigation template for pedicle screw fixation in upper cervical spine. *PLoS ONE.* (2017) 12:e0171509. doi: 10.1371/journal.pone.0171509
- Choonara YE, du Toit LC, Kumar P, Kondiah PPD, Pillay V. 3D-printing and the effect on medical costs: a new era? *Expert Rev Pharmacoecon Outcomes Res.* (2016) 16:23–32. doi: 10.1586/14737167.2016.1138860
- Marro A, Bandukwala T, Mak W. Three-dimensional printing and medical imaging: a review of the methods and applications. *Curr Probl Diagn Radiol.* (2016) 45:2–9. doi: 10.1067/j.cpradiol.2015.07.009
- Weller C, Kleer R, Piller FT. Economic implications of 3D printing: market structure models in light of additive manufacturing revisited. *Int J Prod Econ.* (2015) 164:43–56. doi: 10.1016/j.ijpe.2015.02.020
- Lamartina C, Cecchinato R, Fekete Z, Lipari A, Fiechter M, Berjano P. Pedicle screw placement accuracy in thoracic and lumbar spinal surgery with a patient-matched targeting guide: a cadaveric study. *Eur Spine J.* (2015) 24:937–41. doi: 10.1007/s00586-015-4261-y
- Sheha ED, Gandhi SD, Colman MW. 3D printing in spine surgery. *Ann Transl Med.* (2019) 7:S164. doi: 10.21037/atm.2019.08.88

19. Castro-Mateos I, Pozo JM, Lazary A, Frangi A. 3D Vertebra segmentation by feature selection active shape model. In: *Recent Advances in Computational Methods and Clinical Applications for Spine Imaging*. Cham: Springer (2015). p. 241–5. doi: 10.1007/978-3-319-14148-0_22
20. van Rijsbergen M, van Rietbergen B, Barthelemy V, Eltes P, Lazary Á, Lacroix D, et al. Comparison of patient-specific computational models vs. clinical follow-up, for adjacent segment disc degeneration and bone remodelling after spinal fusion. *PLoS ONE*. (2018) 13:e0200899. doi: 10.1371/journal.pone.0200899
21. Aryanto KYE, Oudkerk M, van Ooijen PMA. Free DICOM de-identification tools in clinical research: functioning and safety of patient privacy. *Eur Radiol*. (2015) 25:3685–95. doi: 10.1007/s00330-015-3794-0
22. Rho JY, Hobatho MC, Ashman RB. Relations of mechanical properties to density and CT numbers in human bone. *Med Eng Phys*. (1995) 17:347–55. doi: 10.1016/1350-4533(95)97314-F
23. Kopperdahl DL, Morgan EF, Keaveny TM. Quantitative computed tomography estimates of the mechanical properties of human vertebral trabecular bone. *J Orthop Res*. (2002) 20:801–5. doi: 10.1016/S0736-0266(01)00185-1
24. Couteau B, Hobatho M-C, Darmana R, Brignola J-C, Arlaud J-Y. Finite element modelling of the vibrational behaviour of the human femur using CT-based individualized geometrical and material properties. *J Biomech*. (1998) 31:383–6. doi: 10.1016/S0021-9290(98)00018-9
25. Charriere E, Sirey F, Zysset PK. A finite element model of the L5-S1 functional spinal unit: development and comparison with biomechanical tests *in vitro*. *Comput Methods Biomech Biomed Eng*. (2003) 6:249–61. doi: 10.1080/10255840310001606099
26. Welsch G, Boyer R, Collings EW. *Materials Properties Handbook: Titanium Alloys*. Russell Township, OH: ASM International (1993).
27. Fan Y, Du J, Zhang J, Liu S, Xue X, Huang Y, et al. Comparison of accuracy of pedicle screw insertion among 4 guided technologies in spine surgery. *Med Sci Monit Int Med J Exp Clin Res*. (2017) 23:5960. doi: 10.12659/MSM.905713
28. Li Y, Lin J, Wang Y, Luo H, Wang J, Lu S, et al. Comparative study of 3D printed navigation template-assisted atlantoaxial pedicle screws versus free-hand screws for type II odontoid fractures. *Eur Spine J*. (2020). doi: 10.1007/s00586-020-06644-9. [Epub ahead of print].
29. Wen ZJ, Gao ZC, Lu T, Wang YB, Liang H, He XJ. Comparison of the effect of navigation template assisted spinal pedicle fixation and traditional pedicle screw fixation: a meta-analysis. *Zhongguo Gu Shang China J Orthop Traumatol*. (2018) 31:1069–76. doi: 10.3969/j.issn.1003-0034.2018.11.017
30. Van den Abbeele M, Valiadis JM, Lima LVPC, Khalifé P, Rouch P, Skalli W. Contribution to FE modeling for intraoperative pedicle screw strength prediction. *Comput Methods Biomech Biomed Engin*. (2018) 21:13–21. doi: 10.1080/10255842.2017.1414200
31. Von Strempele A, Trenkmann S, Krönauer I, Kirsch L, Sukopp C. The stability of bone screws in the os sacrum. *Eur Spine J*. (1998) 7:313–20. doi: 10.1007/s005860050081
32. Zhu Q, Lu WW, Holmes AD, Zheng Y, Zhong S, Leong JCY. The effects of cyclic loading on pull-out strength of sacral screw fixation: an *in vitro* biomechanical study. *Spine (Phila Pa 1976)*. (2000) 25:1065–. doi: 10.1097/00007632-200005010-00005
33. Kato M, Taneichi H, Suda K. Advantage of pedicle screw placement into the sacral promontory (tricortical purchase) on lumbosacral fixation. *J Spinal Disord Tech*. (2015) 28:E336–42. doi: 10.1097/BSD.0b013e31828ffc70
34. Sabry FF, Xu R, Nadim Y, Ebraheim NA. Bone density of the first sacral vertebra in relation to sacral screw placement: a computed tomography study. *Orthopedics*. (2001) 24:475–7.
35. Misch CE. *Dental Implant Prosthetics-E-Book*. St. Louis, MO: Elsevier Health Sciences (2004).
36. Bhaskaran E, Azhagarasan NS, Miglani S, Ilango T, Krishna GP, Gajapathi B. Comparative evaluation of marginal and internal gap of Co–Cr copings fabricated from conventional wax pattern, 3D printed resin pattern and DMLS tech: an *in vitro* study. *J Indian Prosthodont Soc*. (2013) 13:189–95. doi: 10.1007/s13191-013-0283-5
37. Wang D, Wang Y, Wang J, Song C, Yang Y, Zhang Z, et al. Design and fabrication of a precision template for spine surgery using selective laser melting (SLM). *Materials (Basel)*. (2016) 9:608. doi: 10.3390/ma9070608
38. Sallent A, Ramírez M, Catalá J, Rodríguez-Baeza A, Bagó J, de Albert M, et al. Precision and safety of multilevel cervical transpedicular screw fixation with 3D patient-specific guides; a cadaveric study. *Sci Rep*. (2019) 9:15686. doi: 10.1038/s41598-019-51936-w
39. Eltes PE, Kiss L, Bartos M, Gyorgy ZM, Csakany T, Bereczki F, et al. Geometrical accuracy evaluation of an affordable 3D printing technology for spine physical models. *J Clin Neurosci*. (2020) 72:438–46. doi: 10.1016/j.jocn.2019.12.027
40. Gertzbein SD, Robbins SE. Accuracy of pedicular screw placement *in vivo*. *Spine (Phila Pa 1976)*. (1990) 15:11–4. doi: 10.1097/00007632-199001000-00004

Conflict of Interest: MB was employed by the company DO3D Innovations Ltd.

The remaining authors declare that the research was conducted in the absence of any commercial or financial relationships that could be construed as a potential conflict of interest.

Copyright © 2021 Eltes, Bartos, Hajnal, Pokorni, Kiss, Lacroix, Varga and Lazary. This is an open-access article distributed under the terms of the Creative Commons Attribution License (CC BY). The use, distribution or reproduction in other forums is permitted, provided the original author(s) and the copyright owner(s) are credited and that the original publication in this journal is cited, in accordance with accepted academic practice. No use, distribution or reproduction is permitted which does not comply with these terms.



Robotics in Spine Surgery: A Technical Overview and Review of Key Concepts

S. Harrison Farber, Mark A. Pacult, Jakub Godzik, Corey T. Walker, Jay D. Turner, Randall W. Porter and Juan S. Uribe*

Department of Neurosurgery, Barrow Neurological Institute, St. Joseph's Hospital and Medical Center, Phoenix, AZ, United States

OPEN ACCESS

Edited by:

Ralph Jasper Mobbs,
University of New South
Wales, Australia

Reviewed by:

Tim Sebastian Peltz,
University of New South
Wales, Australia
Ziya Levent Gokaslan,
Brown University, United States
Bawarjan Schatlo,
University of Göttingen, Germany

*Correspondence:

Juan S. Uribe
neuropub@barrowneuro.org

Specialty section:

This article was submitted to
Orthopedic Surgery,
a section of the journal
Frontiers in Surgery

Received: 30 June 2020

Accepted: 26 January 2021

Published: 23 February 2021

Citation:

Farber SH, Pacult MA, Godzik J,
Walker CT, Turner JD, Porter RW and
Uribe JS (2021) Robotics in Spine
Surgery: A Technical Overview and
Review of Key Concepts.
Front. Surg. 8:578674.
doi: 10.3389/fsurg.2021.578674

The use of robotic systems to aid in surgical procedures has greatly increased over the past decade. Fields such as general surgery, urology, and gynecology have widely adopted robotic surgery as part of everyday practice. The use of robotic systems in the field of spine surgery has recently begun to be explored. Surgical procedures involving the spine often require fixation via pedicle screw placement, which is a task that may be augmented by the use of robotic technology. There is little margin for error with pedicle screw placement, because screw malposition may lead to serious complications, such as neurologic or vascular injury. Robotic systems must provide a degree of accuracy comparable to that of already-established methods of screw placement, including free-hand, fluoroscopically assisted, and computed tomography-assisted screw placement. In the past several years, reports have cataloged early results that show the robotic systems are associated with equivalent accuracy and decreased radiation exposure compared with other methods of screw placement. However, the literature is still lacking with regard to long-term outcomes with these systems. This report provides a technical overview of robotics in spine surgery based on experience at a single institution using the ExcelsiusGPS (Globus Medical; Audobon, PA, USA) robotic system for pedicle screw fixation. The current state of the field with regard to salient issues in robotics and future directions for robotics in spinal surgery are also discussed.

Keywords: minimally invasive spine surgery, neuronavigation, pedicle screw fixation, robotics, robotic spine surgery

INTRODUCTION

In the past decade, the role of robotic systems in surgical fields has expanded, and innovations have flourished (1). Early adopters of this technology have included specialties such as general surgery, urology, and gynecology, where robotics have augmented the ability to manipulate tissue in body cavities (2–4). Early incorporation of robotic systems in these fields has spurred innovation and led to their use in other surgical subspecialties; more recently, robotic systems have been introduced to the field of spine surgery (5).

Treatment of spinal pathologies often requires fixation via the placement of pedicle screws. Techniques for pedicle screw placement were first described in the late 1950s, and since that time, they have undergone a wealth of adaptation and methodological advances. These advances include the description of open and percutaneous approaches using a variety of navigated

techniques (6–11). Pedicle screw placement has emerged a prime area of opportunity for the inclusion of robotics in spine surgery. Pedicle screw malposition can lead to serious adverse neurovascular complications, which can contribute to poor outcomes and require reoperation. Accurate screw placement is therefore fundamental to reducing possible iatrogenic complications and improving surgical outcomes.

A key determinant of the widespread adoption of robotics in spine surgery is efficient and accurate screw placement. The accuracy of robotic systems must be similar to or better than that of well-established methods of pedicle screw placement, including free-hand, fluoroscopically assisted, or computer tomography (CT)-assisted screw placement. These systems offer the theoretical advantage of automating inherently repetitive tasks that are subject to human error. Early reports of the use of robotic technologies in spine surgery have shown equivalent accuracy compared with other methods of screw placement (11). Multiple robotic systems have been approved by the U.S. Food and Drug Administration for use. The most current technologies include the ExcelsiusGPS (Globus Medical, Audubon, PA, USA), Mazor X Stealth Edition (Medtronic, Dublin, Ireland), and the ROSA ONE Spine (Zimmer Biomet, Warsaw, IN, USA). These three systems are all now commercially available (12). Unfortunately, direct comparisons of screw placement accuracy between these systems are difficult because of the significant cost and time associated with their adoption.

Herein, we provide a technical overview of the incorporation of robotics in spine surgery based on our institutional experience using the ExcelsiusGPS robotic system for pedicle screw fixation. We also discuss salient issues regarding this technology based on our experience and consider future directions for robotics in spinal surgery.

OPERATIVE TECHNIQUE

Exact operative technique and surgical workflow will vary on the basis of the specific robotic system that is used. This section will discuss the use of the ExcelsiusGPS system (Globus Medical; Audubon, PA, USA). Robotic systems may be considered for any spinal fusion procedure with planned placement of pedicle screw fixation. At our institution (Barrow Neurological Institute, Phoenix, AZ, USA), robotics have most commonly been incorporated into lumbar fusion procedures, including anterior lumbar interbody fusion, lateral lumbar interbody fusion (13), and transforaminal lumbar interbody fusion (14). Percutaneous pedicle screw fixation has been the most common technique, although open screw placement has been performed as well. Additionally, patients may be placed in the prone or lateral position, depending on the procedure being performed.

Patient positioning and operating room set up are shown in **Figure 1**. The patient is prepped and draped in the usual sterile fashion. First, two small incisions are made over the posterior superior iliac spine bilaterally. The dynamic reference base array and the surveillance marker are then affixed to the posterior superior iliac spine bilaterally. These markers are positioned

with a superolateral trajectory. The intraoperative CT registration fixture is then attached to the dynamic reference base array. An intraoperative CT scan using O-arm (Medtronic; Dublin, Ireland) is then performed and is coregistered to the patient's preoperative imaging. A trajectory plan may then be created for each pedicle screw. Alternatively, screw trajectories may be preplanned before the procedure using a preoperative CT scan to decrease intraoperative time. Screw plans may be adjusted and confirmed at this point (**Figure 2**). The robotic end effector arm then moves into position to guide all movements along this planned trajectory. All subsequent steps can be performed through the end effector arm.

First, a stab skin incision is made. The bovie electrocautery is used to dissect through the subcutaneous tissue and the fascia. Importantly, the fascia should be excised medial to the skin incision to allow for the appropriate trajectory toward the screw entry point. The bur is then placed on bone at the screw entry point to create a pilot hole for screw placement. This step is important to prevent skiving of the drill off of the cortical bone and facilitate smooth entry into the cancellous channel. Tapping is then performed under navigation for comparison with the planned trajectory. Finally, the pedicle screw is placed under navigation and is also compared with the planned trajectory (**Figure 3A**). Once the pedicle screw is in place, the software notifies the surgeon of correct positioning. For each step, a force meter confirms that an appropriate amount of force is being placed on the instruments. The accuracy of screw placement is usually confirmed with a postplacement intraoperative CT scan and may be compared with the planned trajectory.

OTHER SURGICAL CONSIDERATIONS

In our experience, screws have been most commonly placed in a percutaneous fashion. However, open screw placement is also done in appropriate scenarios, such as when accompanied by a spinal decompression for degenerative pathologies. In an open procedure, the dynamic reference base array and the intraoperative CT registration fixture are placed on a spinous process above and below the operative segments rather than on the posterior superior iliac spine. All subsequent steps may be performed in the fashion described above, with care taken not to disrupt the dynamic reference base array within the operative field. In the open exposure, the screw entry site may be directly visualized, and cortical bone may be drilled away to facilitate screw placement.

The above-described technique is for patients who are placed in the traditional prone position. More recently, there has been increasing interest in performing single-position surgery in the lateral position for lumbar fusion, including both anterior lumbar interbody fusion and lateral lumbar interbody fusion, accompanied by pedicle screw fixation. We have used the robotic system for screw placement in this position as well (**Figure 3B**). In these procedures, the interbody is placed initially through either an anterior or a lateral incision. Pedicle screw fixation is then performed. In the lateral position, the down-side screw trajectory should be modified to decrease medialization

Abbreviations: CT, computed tomography.

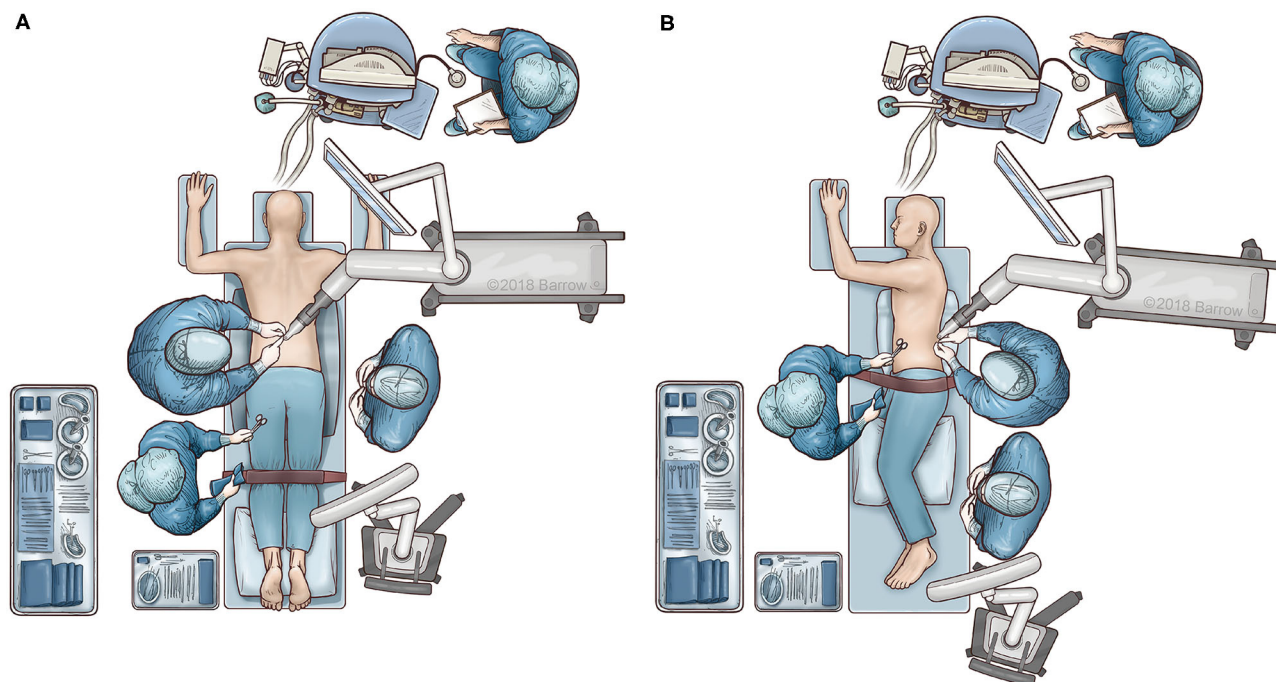


FIGURE 1 | Illustration of surgical workflow. The patient is placed in either a prone or lateral decubitus position. In both positions, the robotic system is placed opposite to the scrub table to simplify draping and ease of access. **(A)** In the prone position, the surgeon stands opposite to the robot. **(B)** In the lateral position, the surgeon stands on the same side as the robotic arm. Used with permission from Barrow Neurological Institute, Phoenix, Arizona.

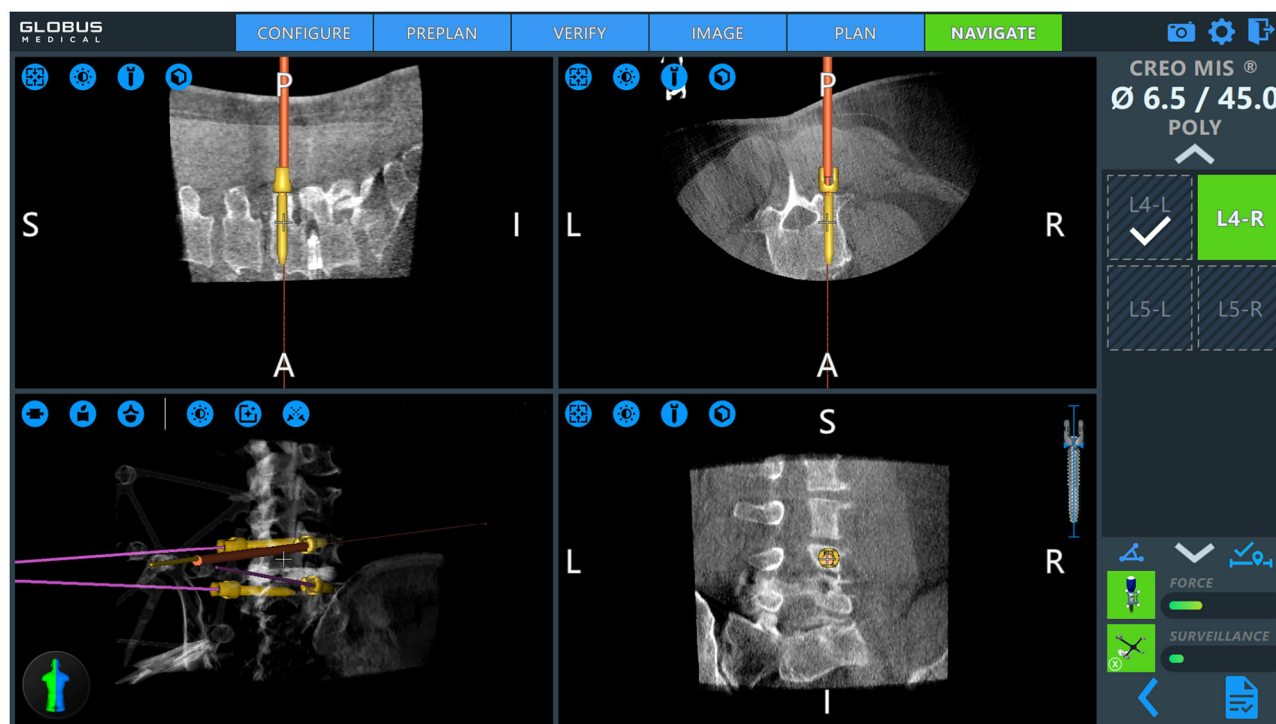


FIGURE 2 | Intraoperative pedicle screw placement using the ExcelsiusGPS robotics system (Globus Medical; Audobon, PA, USA). Screw placement is demonstrated for a right-sided L4 pedicle screw. Used with permission from Barrow Neurological Institute, Phoenix, Arizona.

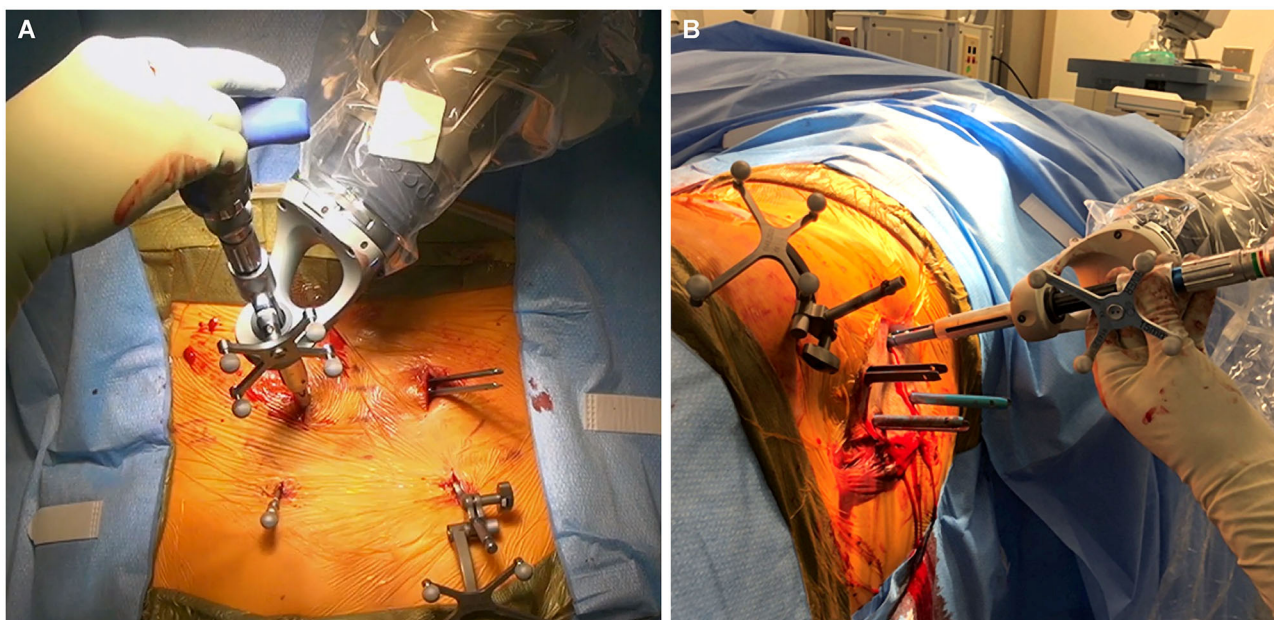


FIGURE 3 | Intraoperative images obtained during robotically assisted pedicle screw placement. **(A)** Pedicle screw placement in the prone position. The dynamic reference base array and surveillance marker are attached to the posterior superior iliac spine bilaterally. **(B)** Pedicle screw placement in the lateral position. Used with permission from Barrow Neurological Institute, Phoenix, Arizona.

of the screw. This modification helps to maintain sterility during placement of down-side screws. Sequential steps are otherwise unchanged.

PEDICLE SCREW PLACEMENT ACCURACY

Widespread adoption of robotic systems for pedicle screw placement must entail safe and reliable accuracy. The most common classification system used in the literature is the Gertzbein-Robbins classification (15). The reported accuracy of pedicle screw placement using robotic systems has generally been high, with rates as high as 94%–98% (16–21). Current literature is mixed regarding the accuracy of robotically placed pedicle screws compared with traditional open freehand techniques. Some studies have reported inferior accuracy with robotically assisted pedicle screw placement. One randomized controlled trial found that 93% of pedicle screws placed with the freehand technique were Gertzbein-Robbins A or B compared with 85% for those placed with the ROSA SpineAssist robot (22).

However, several studies have since reported non-inferiority or superiority of robotically assisted pedicle screw placement. A meta-analysis that included 10 studies found robotically assisted pedicle screw placement performed better than freehand screw placement in terms of “perfect accuracy” (odds ratio 95% confidence interval: 1.38–2.07; $P < 0.01$) as well as “clinically acceptable” (odds ratio 95% confidence interval: 1.17–2.08; $P < 0.01$) (23). Two other meta-analyses reported similar results, showing increased accuracy of robotically assisted pedicle screw

placement compared with freehand screw placement (11, 24). A more recent meta-analysis that included nine randomized controlled trials with a total of 696 patients also found the accuracy of pedicle screw placement to be higher with use of robotic systems than with freehand techniques, although results varied on the basis of the different robotic systems that were used (25).

Another technique for pedicle screw fixation that has been widely adopted includes use of navigation with intraoperative CT scan. Some surgeons argue that accuracy of screw placement with use of navigation is high enough that they would not need the use of a robotic arm. Based on our experience, we support the use of a robotic arm for multiple reasons. First, with current technology a CT scan may now be performed pre-operatively. Screw planning is done prior to surgery and this can significantly decrease surgical time compared to the use of intraoperative CT scanning. The ability to plan the screw trajectory ahead of surgery maximizes the fidelity of screw placement. Important considerations such as screw size, length, trajectory, and avoidance of the superior facet are all addressed prior to skin incision. Second, the use of the robotic arm mitigates the human error that is ever present in repetitive manual tasks. Lastly, the authors’ experience has been that pedicle screw placement using the robotic arm is less taxing physically for the surgeon.

OPERATIVE TIME

Another important factor to consider with regard to the incorporation of robotics into spine surgery is the additional

operative time required to use this technology. Multiple studies have found that increased operative times were associated with robotic systems. A commonly considered factor that may contribute to this phenomenon is the steep learning curve for use of this technology. The learning curve associated with robotics has been documented previously by multiple authors who have shown improved accuracy after an initial learning period (26, 27). More persistent exposure to these systems and continued improvements in technology will likely continue to decrease the operative time for these procedures.

RADIATION EXPOSURE

A purported advantage of robotic systems is decreased radiation exposure. The surgeon is not exposed to the initial (preoperative or intraoperative) CT. Minimal intraoperative radiation is then required to register the robotic system to this scan using fluoroscopy. When intraoperative CT is used, no additional fluoroscopy is required for registration. Decreased radiation exposure to the surgeon during robotic procedures has been validated (28). Other studies have shown that decreased overall and per-screw radiation exposure times are associated with robotic systems (29, 30). One randomized controlled trial found that radiation exposure to the surgeon was 10 times lower during robotic procedures compared with fluoroscopy-guided screw placement (31).

FUTURE DIRECTIONS

The use of robotic systems in spine surgery is rapidly evolving. Continued adaptation will be important for future expansion in this field. These adaptations should include improvements in efficiency and surgical workflow to facilitate widespread adoption of these systems. Such improvements would involve enhanced imaging software to aid with patient registration, to minimize error, and to assist with trajectory planning both preoperatively and intraoperatively. The aim of robotic systems is to automate repetitive tasks that are subject to alteration and human error. As automation becomes more standardized, this may lead to more

uniform patient outcomes. The indications for use of robotic systems will likely continue to expand. Currently, most literature involves fixation of the thoracolumbar spine. Both cervical and pelvic fixation may incorporate robotic systems in the future. In addition, applications for robotics may expand to include more complex spinal procedures, such as decompression, resection of neoplastic lesions, and complex deformity procedures. With more widespread use, head-to-head investigations that compare various robotic systems may help delineate the relative strengths and weaknesses of each system. Finally, the economic viability of these systems should continue to be addressed. Their use will remain limited to resource-rich settings if costs remain very high.

CONCLUSIONS

Robotic systems have been widely adopted throughout the United States and in various surgical subspecialties. This innovative technology continues to permeate the field of spine surgery. These systems offer the potential advantages of increased accuracy of screw placement, decreased operative time, and decreased radiation exposure. However, there is a challenging learning curve, and various technical factors of these systems are continuously being reassessed to improve operative efficiency and to meet these goals. Maintaining clinical equipoise with established methods of screw placement, including freehand screw placement and various forms of navigation, will be important for further adoption of these systems in our field.

AUTHOR CONTRIBUTIONS

All authors listed have made a substantial, direct and intellectual contribution to the work, and approved it for publication.

ACKNOWLEDGMENTS

The authors thank the staff of Neuroscience Publications at Barrow Neurological Institute for assistance with manuscript preparation.

REFERENCES

- Childers CP, Maggard-Gibbons M. Estimation of the acquisition and operating costs for robotic surgery. *JAMA*. (2018) 320:835–6. doi: 10.1001/jama.2018.9219
- Trastulli S, Farinella E, Cirocchi R, Cavaliere D, Avenia N, Sciannameo F, et al. Robotic resection compared with laparoscopic rectal resection for cancer: systematic review and meta-analysis of short-term outcome. *Colorectal Dis*. (2012) 14:e134–56. doi: 10.1111/j.1463-1318.2011.02907.x
- Sammon J, Trinh QD, Menon M. Robotic radical prostatectomy: a critical analysis of surgical quality. *Curr Opin Urol*. (2011) 21:195–9. doi: 10.1097/MOU.0b013e328344e570
- Lowery WJ, Leath CA III, Robinson RD. Robotic surgery applications in the management of gynecologic malignancies. *J Surg Oncol*. (2012) 105:481–7. doi: 10.1002/jso.22080
- Roser F, Tatagiba M, Maier G. Spinal robotics: current applications and future perspectives. *Neurosurgery*. (2013) 72(Suppl. 1):12–8. doi: 10.1227/NEU.0b013e318270d02c
- Boucher HH. A method of spinal fusion. *J Bone Joint Surg Br*. (1959) 41-B:248–59. doi: 10.1302/0301-620X.41B2.248
- Roy-Camille R, Roy-Camille M, Demeulenaere C. Osteosynthesis of dorsal, lumbar, and lumbosacral spine with metallic plates screwed into vertebral pedicles and articular apophyses. *Presse Med*. (1970) 78:1447–8.
- Magerl FP. Stabilization of the lower thoracic and lumbar spine with external skeletal fixation. *Clin Orthop Relat Res*. (1984) 189:125–41. doi: 10.1097/00003086-198410000-00014
- Foley KT, Gupta SK. Percutaneous pedicle screw fixation of the lumbar spine: preliminary clinical results. *J Neurosurg*. (2002) 97(Suppl. 1):7–12. doi: 10.3171/spi.2002.97.1.0007
- Schwarzenbach O, Berlemann U, Jost B, Visarius H, Arm E, Langlotz F, et al. Accuracy of computer-assisted pedicle screw placement. An *in vivo* computed tomography analysis. *Spine (Phila Pa 1976)*. (1997) 22:452–8. doi: 10.1097/00007632-199702150-00020
- Verma R, Krishan S, Haendlmayer K, Mohsen A. Functional outcome of computer-assisted spinal pedicle screw placement: a systematic review and

- meta-analysis of 23 studies including 5,992 pedicle screws. *Eur Spine J.* (2010) 19:370–5. doi: 10.1007/s00586-009-1258-4
12. Jiang B, Azad TD, Cottrill E, Zygorakis CC, Zhu AM, Crawford N, et al. New spinal robotic technologies. *Front Med.* (2019) 13:723–9. doi: 10.1007/s11684-019-0716-6
 13. Walker CT, Godzik J, Xu DS, Theodore N, Uribe JS, Chang SW. Minimally invasive single-position lateral interbody fusion with robotic bilateral percutaneous pedicle screw fixation: 2-dimensional operative video. *Oper Neurosurg (Hagerstown).* (2019) 16:E121. doi: 10.1093/ons/opy240
 14. Godzik J, Walker CT, Theodore N, Uribe JS, Chang SW, Snyder LA. Minimally invasive transforaminal interbody fusion with robotically assisted bilateral pedicle screw fixation: 2-dimensional operative video. *Oper Neurosurg (Hagerstown).* (2019) 16:E86–7. doi: 10.1093/ons/opy288
 15. Gertzbein SD, Robbins SE. Accuracy of pedicular screw placement *in vivo*. *Spine (Phila Pa 1976).* (1990) 15:11–4. doi: 10.1097/00007632-199001000-00004
 16. Tsai TH, Wu DS, Su YF, Wu CH, Lin CL. A retrospective study to validate an intraoperative robotic classification system for assessing the accuracy of kirschner wire (K-wire) placements with postoperative computed tomography classification system for assessing the accuracy of pedicle screw placements. *Medicine (Baltimore).* (2016) 95:e4834. doi: 10.1097/MD.00000000000004834
 17. Kuo KL, Su YF, Wu CH, Tsai CY, Chang CH, Lin CL, et al. Assessing the intraoperative accuracy of pedicle screw placement by using a bone-mounted miniature robot system through secondary registration. *PLoS ONE.* (2016) 11:e0153235. doi: 10.1371/journal.pone.0153235
 18. Keric N, Doenitz C, Haj A, Rachwal-Czyzewicz I, Renovanz M, Wesp DMA, et al. Evaluation of robot-guided minimally invasive implantation of 2067 pedicle screws. *Neurosurg Focus.* (2017) 42:E11. doi: 10.3171/2017.2.FOCUS16552
 19. van Dijk JD, van den Ende RP, Stramigioli S, Kochling M, Hoss N. Clinical pedicle screw accuracy and deviation from planning in robot-guided spine surgery: robot-guided pedicle screw accuracy. *Spine (Phila Pa 1976).* (2015) 40:E986–91. doi: 10.1097/BRS.0000000000000960
 20. Devito DP, Kaplan L, Dietl R, Pfeiffer M, Horne D, Silberstein B, et al. Clinical acceptance and accuracy assessment of spinal implants guided with Spine Assist surgical robot: retrospective study. *Spine (Phila Pa 1976).* (2010) 35:2109–15. doi: 10.1097/BRS.0b013e3181d323ab
 21. Kantelhardt SR, Martinez R, Baerwinkel S, Burger R, Giese A, Rohde V. Perioperative course and accuracy of screw positioning in conventional, open robotic-guided and percutaneous robotic-guided, pedicle screw placement. *Eur Spine J.* (2011) 20:860–8. doi: 10.1007/s00586-011-1729-2
 22. Ringel F, Stuer C, Reinke A, Preuss A, Behr M, Auer F, et al. Accuracy of robot-assisted placement of lumbar and sacral pedicle screws: a prospective randomized comparison to conventional freehand screw implantation. *Spine (Phila Pa 1976).* (2012) 37:E496–501. doi: 10.1097/BRS.0b013e31824b7767
 23. Fan Y, Du JP, Liu JJ, Zhang JN, Qiao HH, Liu SC, et al. Accuracy of pedicle screw placement comparing robot-assisted technology and the free-hand with fluoroscopy-guided method in spine surgery: an updated meta-analysis. *Medicine (Baltimore).* (2018) 97:e10970. doi: 10.1097/MD.00000000000010970
 24. Shin BJ, James AR, Njoku IU, Hartl R. Pedicle screw navigation: a systematic review and meta-analysis of perforation risk for computer-navigated versus freehand insertion. *J Neurosurg Spine.* (2012) 17:113–22. doi: 10.3171/2012.5.SPINE11399
 25. Li HM, Zhang RJ, Shen CL. Accuracy of pedicle screw placement and clinical outcomes of robot-assisted technique versus conventional freehand technique in spine surgery from nine randomized controlled trials: a meta-analysis. *Spine (Phila Pa 1976).* (2020) 45:E111–9. doi: 10.1097/BRS.00000000000003193
 26. Hu X, Lieberman IH. What is the learning curve for robotic-assisted pedicle screw placement in spine surgery? *Clin Orthop Relat Res.* (2014) 472:1839–44. doi: 10.1007/s11999-013-3291-1
 27. Schatlo B, Martinez R, Alaid A, von Eckardstein K, Akhavan-Sigari R, Hahn A, et al. Unskilled unawareness and the learning curve in robotic spine surgery. *Acta Neurochir (Wien).* (2015) 157:1819–23; discussion 23. doi: 10.1007/s00701-015-2535-0
 28. Han X, Tian W, Liu Y, Liu B, He D, Sun Y, et al. Safety and accuracy of robot-assisted versus fluoroscopy-assisted pedicle screw insertion in thoracolumbar spinal surgery: a prospective randomized controlled trial. *J Neurosurg Spine.* (2019). doi: 10.3171/2018.10.SPINE18487. [Epub ahead of print].
 29. Fan Y, Du J, Zhang J, Liu S, Xue X, Huang Y, et al. Comparison of accuracy of pedicle screw insertion among 4 guided technologies in spine surgery. *Med Sci Monit.* (2017) 23:5960–8. doi: 10.12659/MSM.905713
 30. Hyun SJ, Kim KJ, Jahng TA, Kim HJ. Minimally invasive robotic versus open fluoroscopic-guided spinal instrumented fusions: a randomized controlled trial. *Spine (Phila Pa 1976).* (2017) 42:353–8. doi: 10.1097/BRS.0000000000001778
 31. Villard J, Ryang YM, Demetriades AK, Reinke A, Behr M, Preuss A, et al. Radiation exposure to the surgeon and the patient during posterior lumbar spinal instrumentation: a prospective randomized comparison of navigated versus non-navigated freehand techniques. *Spine (Phila Pa 1976).* (2014) 39:1004–9. doi: 10.1097/BRS.0000000000000351

Conflict of Interest: JU receives consulting fees and royalties from NuVasive Medical, Inc., and is a consultant for Masonix, Inc., and SI Bone, Inc. JT receives consulting fees and royalties from NuVasive Medical, Inc. RP is the owner and founder of The Medical Memory, Inc.

The remaining authors declare that the research was conducted in the absence of any commercial or financial relationships that could be construed as a potential conflict of interest.

Copyright © 2021 Farber, Pacult, Godzik, Walker, Turner, Porter and Uribe. This is an open-access article distributed under the terms of the Creative Commons Attribution License (CC BY). The use, distribution or reproduction in other forums is permitted, provided the original author(s) and the copyright owner(s) are credited and that the original publication in this journal is cited, in accordance with accepted academic practice. No use, distribution or reproduction is permitted which does not comply with these terms.



Therapeutic Effect of Large Channel Endoscopic Decompression in Lumbar Spinal Stenosis

Fei-Long Wei^{1†}, Ming-Rui Du^{1†}, Tian Li^{2†}, Kai-Long Zhu^{1†}, Yi-Li Zhu², Xiao-Dong Yan¹, Yi-Fang Yuan¹, Sheng-Da Wu¹, Bo An¹, Hao-Ran Gao^{1*}, Ji-Xian Qian^{1*} and Cheng-Pei Zhou^{1*}

OPEN ACCESS

Edited by:

Vassilios S. Nikolaou,
National and Kapodistrian University
of Athens, Greece

Reviewed by:

Konstantinos Markatos,
Salamina Medical Center, Greece
Bo Li,
Sun Yat-sen University, China

*Correspondence:

Cheng-Pei Zhou
zhoucpei@126.com
Ji-Xian Qian
pasmiss2012@163.com
Hao-Ran Gao
xh_ghr@qq.com

[†]These authors have contributed
equally to this work

Specialty section:

This article was submitted to
Orthopedic Surgery,
a section of the journal
Frontiers in Surgery

Received: 07 September 2020

Accepted: 26 May 2021

Published: 18 June 2021

Citation:

Wei F-L, Du M-R, Li T, Zhu K-L,
Zhu Y-L, Yan X-D, Yuan Y-F, Wu S-D,
An B, Gao H-R, Qian J-X and
Zhou C-P (2021) Therapeutic Effect of
Large Channel Endoscopic
Decompression in Lumbar Spinal
Stenosis. *Front. Surg.* 8:603589.
doi: 10.3389/fsurg.2021.603589

¹ Department of Orthopedics, Tangdu Hospital, Fourth Military Medical University, Xi'an, China, ² School of Basic Medicine, Fourth Military Medical University, Xi'an, China

Background: Percutaneous endoscopic decompression (PED) is a minimally invasive surgical technique that is now used for not only disc herniation but also lumbar spinal stenosis (LSS). However, few studies have reported endoscopic surgery for LSS. Therefore, we conducted this study to evaluate the outcomes and safety of large channel endoscopic decompression.

Methods: Forty-one patients diagnosed with LSS who underwent PED surgery were included in the study. The estimated blood loss, operative time, length of hospital stay, hospital costs, reoperations, complications, visual analogue scale (VAS) score, Oswestry Disability Index (ODI) score, Japanese Orthopaedic Association (JOA) score and SF-36 physical-component summary scores were assessed. Preoperative and postoperative continuous data were compared through paired-samples *t*-tests. The significance level for all analyses was defined as $p < 0.05$.

Results: A total of 41 consecutive patients underwent PED, including 21 (51.2%) males and 20 (48.8%) females. The VAS and ODI scores decreased from preoperatively to postoperatively, but the JOA and SF-36 physical component summary scores significantly increased. The VAS (lumbar) score decreased from 5.05 ± 2.33 to 0.45 ± 0.71 ($P = 0.000$); the VAS (leg) score decreased from 5.51 ± 2.82 to 0.53 ± 0.72 ($P = 0.000$); the ODI score decreased from 52.80 ± 20.41 to 4.84 ± 3.98 ($P = 0.000$), and the JOA score increased from 11.73 ± 4.99 to 25.32 ± 2.12 ($P = 0.000$). Only 1 patient experienced an intraoperative complication (2.4%; dural tear), and 1 patient required reoperation (2.4%).

Conclusions: Surgical treatment for LSS is to sufficiently decompress and minimize the trauma and complications caused by surgery. This study did not reveal any obvious shortcomings of PED and suggested PED is a safe and effective treatment for LSS.

Keywords: lumbar spinal stenosis, outcomes, safety, large channel, endoscopic decompression

INTRODUCTION

Degenerative lumbar spinal stenosis (LSS) is characterized by changes in the spinal structure (such as facet joints and ligaments) due to aging, resulting in a reduction in the diameter of the spinal canal (1). LSS is the most common spinal pathology in the elderly population, and the number of patients who need to undergo surgery for the disease has increased (2–4). In the United States, the prevalence of relatively narrow LSS (i.e., 12 mm tube diameter) is as high as 22.5% in the general population, and that of absolute stenosis (i.e., 10 mm tube diameter) is as high as 7.3% (5). These figures increase sharply with age, reaching 47.2 and 19.4%, respectively, among people aged 60 years or older (6). LSS greatly reduces patient quality of life (7).

Minimally invasive surgery techniques are becoming increasingly important in spinal surgery to protect the multifidus muscle, a stabilizer for the spine and locomotor actions (2, 8, 9). At present, endoscopic surgery, a minimally invasive surgery technique, is considered to be an extension of alternative to spinal surgery (10). The surgical indications for endoscopic spine surgery are still increasing due to the release of practical and reliable clinical results (11, 12). Spinal endoscopy is now used to treat not only disc herniation but also LSS (13). Previously, a key obstacle was the need to remove enough bone and the ligamentum flavum under continuous visualization to achieve decompression (14). Advances in technology have made it possible to treat LSS with percutaneous endoscopic decompression (PED) (14, 15).

Although many surgical techniques are available for the treatment of lumbar spinal stenosis, there is little evidence to support this rapidly developing surgical technique, and clinicians often rely on their own opinions and experience (16–18). Few studies have investigated endoscopic surgery for LSS, and their evaluation indicators were relatively simple (19–21). Therefore, we conducted this study to evaluate the efficacy and safety of endoscopic surgery for LSS. In addition, this is the first study to systematically evaluate the application of large channel endoscopy in LSS.

METHODS

Patient Selection

This was a retrospective study. The study protocol was approved by the hospital ethics committee and performed according to the Declaration of Helsinki. Between January 2012 and December 2018, 41 patients diagnosed with LSS who underwent PED were included in the study. The inclusion criteria were as follows: (1) patients with LSS due to neurogenic claudication; (2) Central stenosis or lateral stenosis who need surgery; (3) Low-grade (Meyerding grade 1 or 2) isthmic spondylolisthesis or degenerative spondylolisthesis; (4) patients with imaging findings consistent with the symptoms. The exclusion criteria included trauma, active infection, malignant tumors, spinal deformity, previous lumbar fusion, multi-segment fusion, multi-level, high-grade (Meyerding grade 3 or 4) isthmic spondylolisthesis or degenerative spondylolisthesis; obvious lumbar instability in the

surgical segment (the change of Cobb angle in hyperextension and flexion is $>11^\circ$ or displacement is >3 mm). A representative case is shown in **Figure 1**.

Surgical Procedure

The patients were treated with large-channel endoscopic decompression. The PED operation was performed with bilateral decompression through a unilateral approach. After general anesthesia, each patient was placed in the prone position, and then, the operating table was adjusted to expand the lumbar lamina space. The positioning point was located at the midpoint of the interlaminar space of the facet joint under X-ray. Then, a 15 mm incision was made at the positioning point; the skin and fascia were cut, and they were expanded step by step with a 3rd grade cannula. The depth of the expansion cannula was confirmed under fluoroscopy without breaking the ligament flavum. After the position of the cannula was confirmed to be satisfactory, the working cannula was inserted, and the expansion cannula was removed; the spinal endoscope was connected and inserted. First, the soft tissues on the lamina and ligamentum flavum were cleaned endoscopically. Bony decompression was performed using a high-speed drill under direct endoscopic vision, and then, the ligamentum flavum was removed, completing ipsilateral decompression. Then, the cannula was tilted to remove the contralateral ligamentum flavum and part of the medial bone of the upper articular process to complete contralateral decompression. After the exploration step showed that the extent of decompression was sufficient, the working sleeve was pulled out, and finally, the wound was sutured.

Outcome Measures

The blood loss, operative time, length of hospital stay, costs, reoperation rate and complications were assessed. We recorded the visual analogue scale (VAS), Oswestry Disability Index (ODI), Japanese Orthopaedic Association (JOA) and SF-36 physical component summary scores of the patients before surgery and at 2 and 3 years after surgery.

Statistical Analysis

The statistical analyses were performed by SPSS (version 23.0; IBM, Chicago, IL). Preoperative and postoperative continuous data were compared through paired-samples *t*-tests. The significance level for all analyses was defined as $p < 0.05$.

RESULTS

Forty-one patients were included in this study, including 21 (51.2%) males and 20 (48.8%) females. The mean age was 56.76 ± 13.35 years. The patients had a mean body mass index of 25.34 ± 3.10 kg/m². The most common surgical segment in both groups was L4/5. The mean operative time was 113.41 ± 28.69 min (60–150 min); the volume of intraoperative blood loss was 121.78 ± 82.03 mL (10–300 mL); the length of hospital stay was 10.34 ± 2.84 days (6–23 days); and the total cost was 3.57 ± 0.45 ten thousand yuan (2.89–4.62 ten thousand yuan) (**Table 1**).

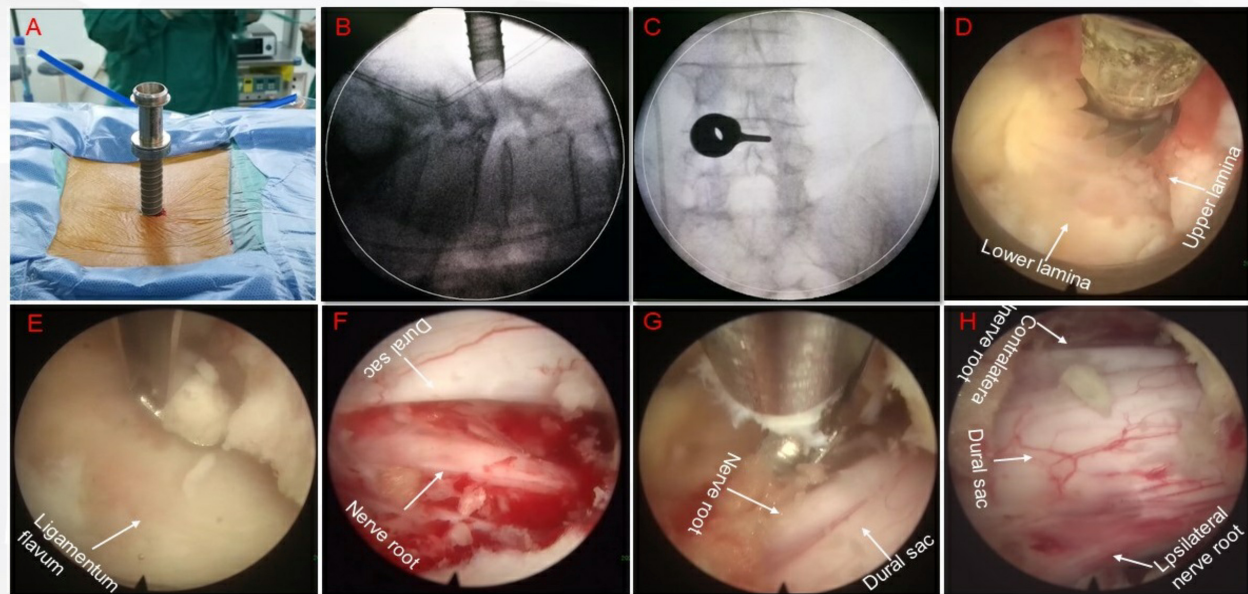


FIGURE 1 | A representative case. **(A)** Place the working channel; **(B)** Lateral X-ray fluoroscopy confirms that the channel is facing the intervertebral space; **(C)** Positive X-ray fluoroscopy confirms that the channel is located inside the facet joint; **(D)** Clean up the soft tissue on the surface of the lamina, confirm the lamina space and upper and lower lamina; **(E)** Remove the lamina and expose the ligamentum flavum; **(F)** Decompression of the nerve root on the same side, ranging from the initial segment of the nerve root, down to the inner edge of the pedicle, explore the ipsilateral nerve root canal to achieve at least 270° decompression of the nerve root canal; **(G)** Decompression of the contralateral nerve root; **(H)** After the decompression, the dural sac and bilateral nerve roots are visible.

TABLE 1 | Clinical characteristics of included patients.

Variables	PED (N = 41)
Age	56.76 ± 13.35
Gender	
Male	21 (51.2%)
Female	20 (48.8%)
BMI	25.34 ± 3.10
Smoker	
Yes	7 (17.1%)
No	34 (82.9%)
Hypertension	
Yes	5 (12.2%)
No	36 (87.8%)
Diabetes	
Yes	3 (7.3%)
No	38 (92.7%)
Operative segments	
1	37 (90.2%)
2	4 (9.8%)
3	0 (0.0%)
Operative time(min)	113.41 ± 28.69
Blood loss (mL)	121.78 ± 82.03
Hospital stay	10.34 ± 2.84
Cost	35735.68 ± 4493.08

Plus-minus values are means ± SD.

As shown in **Figures 2, 3**, the VAS and ODI scores significantly decreased from pre- to postoperatively, and the JOA and SF-36 physical component summary scores increased significantly ($P < 0.05$). Comparing the 2-year data, the VAS (lumbar), VAS (leg) and ODI scores increased slightly with significant differences ($P < 0.05$).

Only 1 patient experienced intra-complications (2.4%; dural tear). After 1 week of conservative treatment, the patient exhibited satisfactory recovery. No patients experienced postoperative complications, and 1 patient required reoperation (2.4%) (**Table 2**).

DISCUSSION

LSS is a common disease that is increasing in frequency in the elderly population worldwide, but it is also common in adults (older than 35–40 years) who commonly perform manual labor and excessively load their spine with heavy loads (22). Conventional laminectomy decompression is a surgical method commonly used for the treatment of LSS (2, 23, 24). The posterior column structure is severely damaged during laminectomy and related facet joint resection, and postoperative complications such as lumbar instability can occur (25, 26). Lumbar interbody fusion is a common treatment for LSS and can prevent lumbar spine instability (27). The resection of joint and soft-tissue structures is also required for the decompression of LSS. With the development of endoscopic technology, it is possible to achieve decompression without

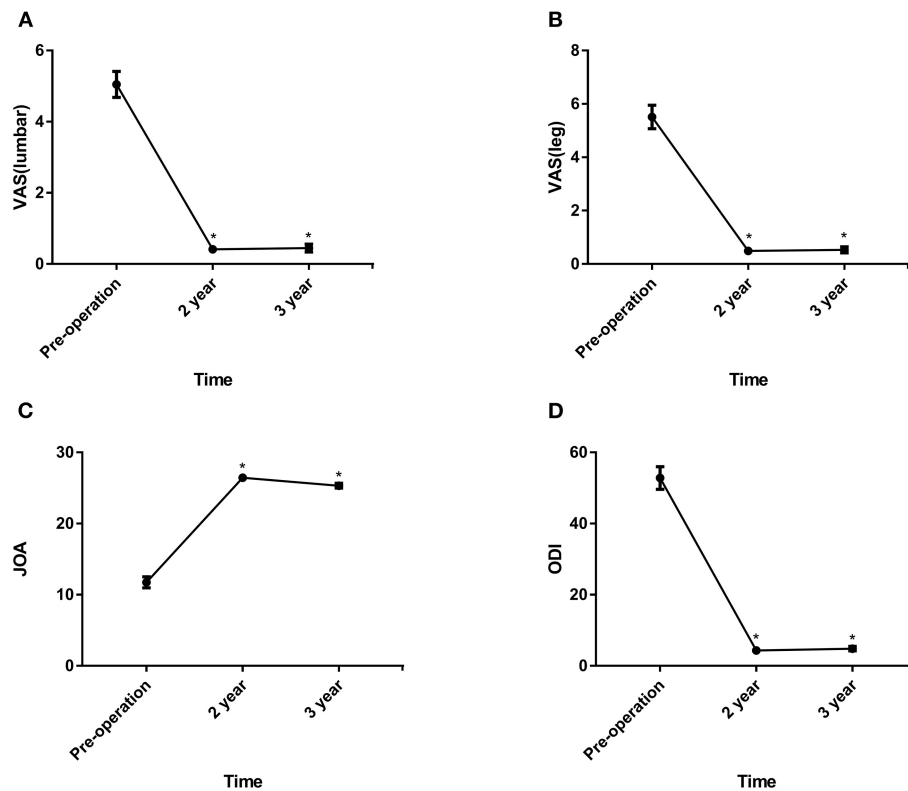


FIGURE 2 | (A–D) The VAS (lumbar), VAS (leg), JOA and ODI scores before surgery and at 24 and 36 months postoperatively. VAS, visual analogue scale; JOA, Japanese Orthopaedic Association; ODI, Oswestry Disability Index. * $P < 0.01$, within-group comparisons between at baseline, 24 and 36 months.

destroying these structures (8, 28). However, there is little evidence to support this rapidly developing surgical technique. Therefore, we conducted this study to evaluate the outcomes of PED surgery for LSS. This retrospective trial included 41 patients with LSS, including patients with or without degenerative spondylolisthesis.

The presence of degenerative spondylolisthesis is generally considered a sign of instability, although there is no consensus on the definition of the term (29). Some studies have shown that patients with degenerative spondylolisthesis may be at risk of iatrogenic spondylolisthesis or an increased degree of spondylolisthesis after decompression surgery (30). However, the clinical consequences of spondylolisthesis have been controversial for decades (31). In addition, few studies support the widespread use of fusion surgery in patients with lumbar spinal stenosis, regardless of whether there is spondylolisthesis (32). Despite the lack of a consensus on the definition of instability, surgeons often use decompression and fusion surgery as a means to prevent postoperative instability (29). Two studies have provided the main basis for this fusion surgery (33, 34), but its validity has been questioned (32). The results of a previous study revealed that the clinical efficacy of PED was reliable during a follow-up. A recent study showed that there were no substantial benefits of additionally

performing fusion surgery for LSS, even in the presence of spondylolisthesis (29).

Although some studies have reported good clinical outcomes and a low complication rate for endoscopic lumbar decompression, its effect on LSS has not yet been proven. Our study showed that PED also has a satisfactory effect on LSS. In addition, advantages have been reported for PED over traditional surgery, for example, better clinical outcomes, a lower complication rate, a shorter hospital stay, and faster rehabilitation (35, 36). The slow deterioration of surgical results over time has been described, and a similar situation was found in our study at the third-year follow-up (37, 38). Overall, the patients achieved satisfactory results over an average of 3 years of follow-up. Since minimally invasive surgery eliminates the need for the removal of spinal canal structures or reduces the extent of resection, this method seems to reduce the consequences of surgery (39, 40). Postoperative ODI and VAS were significantly improved compared with preoperative values which was similar with previous study (19, 20). Our study showed that 1 patient had dural tear (complication rate of 2.4%). Dural injuries have been reported in the literature to occur at a rate ranging from 0% to ~5% (41–44). In addition, 1 patient required reoperation (2.4%) for incomplete decompression. The reoperation rate is much lower than previous study (16.7%) (20).

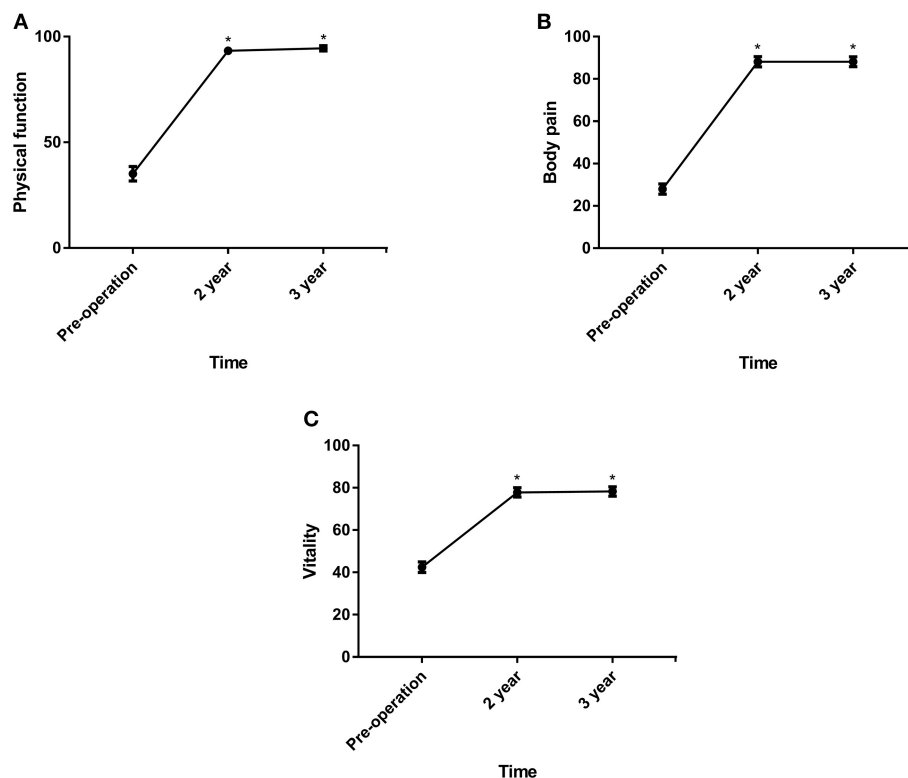


FIGURE 3 | (A–C) The SF-36 physical component summary scores (physical function, body pain and vitality) before surgery and at 24 and 36 months postoperatively. * $P < 0.01$, within-group comparisons between at baseline, 24 and 36 months.

TABLE 2 | Complication and reoperation of included patients.

Outcome	PED
All complications	1 (2.4%)
Intra-complication	1 (2.4%)
Post-complication	0 (0.0%)
Reoperation	1 (2.4%)

To date, it is still difficult to determine well-defined parameters based on evidence-based medicine standards that require fusion in addition to decompression. Some experts have pointed out that patients with predominantly leg symptoms and no signs of segmental instability or deformities should use stability-preserving decompression techniques to avoid fusion (38). Our study revealed that all patients, with or without mild degenerative spondylolisthesis, exhibited satisfactory results. The results were consistent with those of previous studies (23, 29).

This study had some limitations. In this study, the follow-up time was short, and the long-term efficacy of the PED treatment could not be evaluated. Endoscopic techniques have not been used for the treatment of LSS for very long, so the technique is not well-established. Endoscopic decompression still needs to be improved further, and the operation time can be shortened.

In conclusion, the purpose of surgical treatment for LSS is to sufficiently decompress and minimize the trauma and

complications caused by surgery. In general, this study did not reveal any obvious shortcomings of PED. Therefore, we recommend PED for LSS. However, prospective randomized controlled trials are needed to verify these results. The cases that require fusion as well as decompression need to be urgently identified.

DATA AVAILABILITY STATEMENT

The raw data supporting the conclusions of this article will be made available by the authors, without undue reservation.

ETHICS STATEMENT

The studies involving human participants were reviewed and approved by the Clinical Research Ethics Committee of the Tangdu Hospital. The patients/participants provided their written informed consent to participate in this study.

AUTHOR CONTRIBUTIONS

F-LW, J-XQ, H-RG, TL, K-LZ, and C-PZ contributed to the revised the work critically. All authors have approved the final version to be published and have agreed to be accountable for all aspects of the work. All authors contributed substantially to the

conception and design of the work, acquisition and interpretation of data, and the drafted work.

FUNDING

This work was supported by grants from the National Natural Science Foundation of China (No. 81871818).

REFERENCES

- Wei F-L, Liu Y, Zhou C-P, Sun S-G, Zhu K-L, Du M-R, et al. Management for lumbar spinal stenosis: protocol for a network meta-analysis and systematic review. *J Ortho Surg.* (2020) 28:1–6. doi: 10.1177/2309499020975212
- Haddadi K, Ganjeh Qazvini HR. Outcome after surgery of lumbar spinal stenosis: a randomized comparison of bilateral laminotomy, trumpet laminectomy, and conventional laminectomy. *Front Surg.* (2016) 3:19. doi: 10.3389/fsurg.2016.00019
- Ma X-L, Zhao X-W, Ma J-X, Li F, Wang Y, Lu B. Effectiveness of surgery versus conservative treatment for lumbar spinal stenosis: a system review and meta-analysis of randomized controlled trials. *Int J Surg.* (2017) 44:329–38. doi: 10.1016/j.ijisu.2017.07.032
- Wei FL, Zhou CP, Liu R, Zhu KL, Du MR, Gao HR, et al. Management for lumbar spinal stenosis: a network meta-analysis and systematic review. *Int J Surg.* (2020) 85:19–28. doi: 10.1016/j.ijisu.2020.11.014
- Kreiner DS, Shaffer WO, Baisden JL, Gilbert TJ, Summers JT, Toton JE, et al. An evidence-based clinical guideline for the diagnosis and treatment of degenerative lumbar spinal stenosis (update). *Spine J.* (2013) 13:734–43. doi: 10.1016/j.spinee.2012.11.059
- Kalichman L, Cole R, Kim DH, Li L, Suri P, Guermazi A, et al. Spinal stenosis prevalence and association with symptoms: the framingham study. *Spine J.* (2009) 9:545–50. doi: 10.1016/j.spinee.2009.03.005
- Katz JN, Harris MB. Clinical practice. *Lumb Spinal Steno N Eng J Med.* (2008) 358:818–25. doi: 10.1056/NEJMcp0708097
- Guiot BH, Khoo LT, Fessler RG. A minimally invasive technique for decompression of the lumbar spine. *Spine.* (2002) 27:432–8. doi: 10.1097/00007632-200202150-00021
- Choi CM, Chung JT, Lee SJ, Choi DJ. How I do it? Biportal endoscopic spinal surgery (BESS) for treatment of lumbar spinal stenosis. *Acta Neurochir.* (2016) 158:459–63. doi: 10.1007/s00701-015-2670-7
- Lee C-H, Choi M, Ryu DS, Choi I, Kim CH, Kim HS, et al. Efficacy and safety of full-endoscopic decompression via interlaminar approach for central or lateral recess spinal stenosis of the lumbar spine: a meta-analysis. *Spine.* (2018) 43:1756–64. doi: 10.1097/BRS.00000000000002708
- Ahn Y. Endoscopic spine discectomy: indications and outcomes. *Int Ortho.* (2019) 43:909–16. doi: 10.1007/s00264-018-04283-w
- Wei FL, Gao H, Yan X, Yuan Y, Qian S, Gao Q, et al. Comparison of postoperative outcomes between patients with positive and negative straight leg raising tests who underwent full-endoscopic transforaminal lumbar discectomy. *Sci Rep.* (2020) 10:16516. doi: 10.1038/s41598-020-73357-w
- Ahn Y. Percutaneous endoscopic decompression for lumbar spinal stenosis. *Exp Rev Med Dev.* (2014) 11:605–16. doi: 10.1586/17434440.2014.940314
- Torudom Y, Dilokhuttakarn T. Two portal percutaneous endoscopic decompression for lumbar spinal stenosis: preliminary study. *Asian Spine J.* (2016) 10:335–42. doi: 10.4184/asj.2016.10.2.335
- Ruetten S, Komp M, Merk H, Godolias G. Surgical treatment for lumbar lateral recess stenosis with the full-endoscopic interlaminar approach versus conventional microsurgical technique: a prospective, randomized, controlled study. *J Neuro Spine.* (2009) 10:476–85. doi: 10.3171/2008.7.17634
- Zaina F, Tomkins-Lane C, Carragee E, Negrini S. Surgical versus non-surgical treatment for lumbar spinal stenosis. *Cochr Datab Syst Rev.* (2016) CD 2016:010264. doi: 10.1002/14651858.CD010264.pub2
- Chang W, Yuwen P, Zhu Y, Wei N, Feng C, Zhang Y, et al. Effectiveness of decompression alone versus decompression plus fusion for lumbar spinal stenosis: a systematic review and meta-analysis. *Arch Orthop Trauma Surg.* (2017) 137:637–50. doi: 10.1007/s00402-017-2685-z
- Yavin D, Casha S, Wiebe S, Feasby TE, Clark C, Isaacs A, et al. Lumbar fusion for degenerative disease: a systematic review and meta-analysis. *Neurosurgery.* (2017) 80:701–15. doi: 10.1093/neuros/nyw162
- Hwa Eum J, Hwa Heo D, Son SK, Park CK. Percutaneous biportal endoscopic decompression for lumbar spinal stenosis: a technical note and preliminary clinical results. *J Neuro Spine.* (2016) 24:602–7. doi: 10.3171/2015.7.SPINE15304
- Eun SS, Eum JH, Lee SH, Sabal LA. Biportal endoscopic lumbar decompression for lumbar disk herniation and spinal canal stenosis: a technical note. *J Neuro Surg Cent Eur Neuro.* (2017) 78:390–6. doi: 10.1055/s-0036-1592157
- Kim HS, Paudel B, Jang JS, Oh SH, Lee S, Park JE, et al. Percutaneous full endoscopic bilateral lumbar decompression of spinal stenosis through uniportal-contralateral approach: techniques and preliminary results. *World Neuro.* (2017) 103:201–9. doi: 10.1016/j.wneu.2017.03.130
- Usman M, Ali M, Khanzada K, Ishaq M, Naeemul H, Aman R, et al. Unilateral approach for bilateral decompression of lumbar spinal stenosis: a minimal invasive surgery. *J Coll Phys Surg Pakistan.* (2013) 23:852–6.
- Ghogawala Z, Dziura J, Butler WE, Dai F, Terrin N, Magge SN, et al. Laminectomy plus fusion vs. laminectomy alone for lumbar spondylolisthesis. *N Eng J Med.* (2016) 374:1424–34. doi: 10.1056/NEJMoa1508788
- Zhao X-W, Ma J-X, Ma X-L, Li F, He W-W, Jiang X, et al. Interspinous process devices (IPD) alone versus decompression surgery for lumbar spinal stenosis (LSS): a systematic review and meta-analysis of randomized controlled trials. *Int J Surg.* (2017) 39:57–64. doi: 10.1016/j.ijisu.2017.01.074
- Haheer TR, O'Brien M, Dryer JW, Nucci R, Zipnick R, Leone DJ. The role of the lumbar facet joints in spinal stability. Identification of alternative paths of loading. *Spine.* (1994) 19:2667–70. doi: 10.1097/00007632-199412000-00012
- Jasper GP, Francisco GM, Telfeian AE. A retrospective evaluation of the clinical success of transforaminal endoscopic discectomy with foraminotomy in geriatric patients. *Pain Phys.* (2013) 16:225–9. doi: 10.36076/ppj.2013/16/225
- Kaiser MG, Eck JC, Groff MW, Watters WC, Dailey AT, Resnick DK, et al. Guideline update for the performance of fusion procedures for degenerative disease of the lumbar spine. Part 1: introduction and methodology. *J Neuro Spine.* (2014) 21:2–6. doi: 10.3171/2014.4.SPINE14257
- Khoo LT, Fessler RG. Microendoscopic decompressive laminotomy for the treatment of lumbar stenosis. *Neurosurgery.* (2002) 51:S146–54. doi: 10.1097/00006123-200211002-00020
- Försth P, Olafsson G, Carlsson T, Frost A, Borgström F, Fritzell P, et al. A randomized, controlled trial of fusion surgery for lumbar spinal stenosis. *N Eng J Med.* (2016) 374:1413–23. doi: 10.1056/NEJMoa1513721
- Johnsson K, Redlund-Johnell I, Udén A, Willner S. Preoperative and postoperative instability in lumbar spinal stenosis. *Spine.* (1989) 14:591–3. doi: 10.1097/00007632-198906000-00008
- Hasegawa K, Kitahara K, Shimoda H, Ishii K, Ono M, Homma T, et al. Lumbar degenerative spondylolisthesis is not always unstable: clinicobiomechanical evidence. *Spine.* (2014) 39:2127–35. doi: 10.1097/BRS.00000000000000621
- Martin C, Gruszczynski A, Braunsfurth H, Fallatah S, O'Neil J, Wai E. The surgical management of degenerative lumbar spondylolisthesis: a systematic review. *Spine.* (2007) 32:1791–8. doi: 10.1097/BRS.0b013e3180bc219e
- Herkowitz H, Kurz L. Degenerative lumbar spondylolisthesis with spinal stenosis. A prospective study comparing decompression with decompression

Sponsors were not involved in study design or implementation plans.

ACKNOWLEDGMENTS

We would like to thank the National Natural Science Foundation of China for making this research possible.

- and intertransverse process arthrodesis. *The Journal of bone and joint surgery. Am Vol.* (1991) 73:802–8. doi: 10.2106/00004623-199173060-00002
34. Bridwell K, Sedgewick T, O'Brien M, Lenke L, Baldus C. The role of fusion and instrumentation in the treatment of degenerative spondylolisthesis with spinal stenosis. *J Spinal Dis.* (1993) 6:461–72. doi: 10.1097/00002517-199306060-00001
 35. Feng F, Xu Q, Yan F, Xie Y, Cai L. Comparison of 7 surgical interventions for lumbar disc herniation: a network meta-analysis. *Pain Phys.* (2017) 20:E863–71. doi: 10.36076/ppj.20.5.E863
 36. Tu Z, Li YW, Wang B, Lu G, Li L, Kuang L, et al. Clinical outcome of full-endoscopic interlaminar discectomy for single-level lumbar disc herniation: a minimum of 5-year follow-up. *Pain Phys.* (2017) 20:E425–30. doi: 10.36076/ppj.2017.E430
 37. Atlas SJ, Keller RB, Wu YA, Deyo RA, Singer DE, et al. Long-term outcomes of surgical and nonsurgical management of lumbar spinal stenosis: 8 to 10 year results from the maine lumbar spine study. *Spine.* (2005) 30:936–43. doi: 10.1097/01.brs.0000158953.57966.c0
 38. Komp M, Hahn P, Oezdemir S, Giannakopoulos A, Heikenfeld R, Kasch R, et al. Bilateral spinal decompression of lumbar central stenosis with the full-endoscopic interlaminar versus microsurgical laminotomy technique: a prospective, randomized, controlled study. *Pain Phys.* (2015) 18:61–70. doi: 10.36076/ppj/2015.18.61
 39. Iida YA, Kataoka OS, Sho TO, Sumi MA, Hirose TE, Bessho YA, et al. Postoperative lumbar spinal instability occurring or progressing secondary to laminectomy. *Spine.* (1990) 15:1186–9. doi: 10.1097/00007632-199011010-00018
 40. Zander T, Rohlmann A, Klöckner C, Bergmann G. Influence of graded facetectomy and laminectomy on spinal biomechanics. *Eur Spine J.* (2003) 12:427–34. doi: 10.1007/s00586-003-0540-0
 41. Ruetten S, Komp M, Merk H, Godolias G. Use of newly developed instruments and endoscopes: full-endoscopic resection of lumbar disc herniations via the interlaminar and lateral transforaminal approach. *J Neuro Spine.* (2007) 6:521–30. doi: 10.3171/spi.2007.6.6.2
 42. Nie H, Zeng J, Song Y, Chen G, Wang X, Li Z, et al. Percutaneous endoscopic lumbar discectomy for L5-S1 disc herniation via an interlaminar approach vs. a transforaminal approach: a prospective randomized controlled study with 2-year follow up. *Spine.* (2016) 41(Suppl. 19):B30–37. doi: 10.1097/BRS.0000000000001810
 43. Song H, Hu W, Liu Z, Hao Y, Zhang X. Percutaneous endoscopic interlaminar discectomy of L5-S1 disc herniation: a comparison between intermittent endoscopy technique and full endoscopy technique. *J Orthop Surg Res.* (2017) 12:162. doi: 10.1186/s13018-017-0662-4
 44. Liu X, Yuan S, Tian Y, Wang L, Gong L, Zheng Y, et al. Comparison of percutaneous endoscopic transforaminal discectomy, microendoscopic discectomy, and microdiscectomy for symptomatic lumbar disc herniation: minimum 2-year follow-up results. *J Neuro Spine.* (2018) 28:317–25. doi: 10.3171/2017.6.S.P.I.N.E.172

Conflict of Interest: The authors declare that the research was conducted in the absence of any commercial or financial relationships that could be construed as a potential conflict of interest.

Copyright © 2021 Wei, Du, Li, Zhu, Zhu, Yan, Yuan, Wu, An, Gao, Qian and Zhou. This is an open-access article distributed under the terms of the Creative Commons Attribution License (CC BY). The use, distribution or reproduction in other forums is permitted, provided the original author(s) and the copyright owner(s) are credited and that the original publication in this journal is cited, in accordance with accepted academic practice. No use, distribution or reproduction is permitted which does not comply with these terms.



Establishment and Verification of a Perioperative Blood Transfusion Model After Posterior Lumbar Interbody Fusion: A Retrospective Study Based on Data From a Local Hospital

Bo Liu¹, Junpeng Pan¹, Hui Zong² and Zhijie Wang^{1*}

¹ Department of Spinal Surgery, The Affiliated Hospital of Qingdao University, Qingdao, China, ² Department of Neurology, The People's Hospital of Qingyun, Dezhou, China

OPEN ACCESS

Edited by:

William Robert Walsh,
University of New South
Wales, Australia

Reviewed by:

Takahiro Makino,
Hayaishi Hospital, Japan
Yuxin Tong,
Jilin University, China

*Correspondence:

Zhijie Wang
simonwang1969@163.com

Specialty section:

This article was submitted to
Orthopedic Surgery,
a section of the journal
Frontiers in Surgery

Received: 14 April 2021

Accepted: 27 July 2021

Published: 30 August 2021

Citation:

Liu B, Pan J, Zong H and Wang Z
(2021) Establishment and Verification
of a Perioperative Blood Transfusion
Model After Posterior Lumbar
Interbody Fusion: A Retrospective
Study Based on Data From a Local
Hospital. *Front. Surg.* 8:695274.
doi: 10.3389/fsurg.2021.695274

Objective: We aimed to analyze the related risk factors for blood transfusion and establish a blood transfusion risk model during the per-operative period of posterior lumbar interbody fusion (PLIF). It could provide a reference for clinical prevention and reduction of the risk of blood transfusion during the peri-operative period.

Methods: We retrospectively analyzed 4,378 patients who underwent PLIF in our hospital. According to whether they were transfused blood or not, patients were divided into the non-blood transfusion group and the blood transfusion group. We collected variables of each patient, including age, sex, BMI, current medical history, past medical history, surgical indications, surgical information, and preoperative routine blood testing. We randomly divide the whole population into training group and test group according to the ratio of 4:1. We used the multivariate regression analyses get the independent predictors in the training set. The nomogram was established based on these independent predictors. Then, we used the AUC, calibration curve and DCA to evaluate the nomogram. Finally, we verified the performance of the nomogram in the validation set.

Results: Three or more lumbar fusion segments, preoperative low hemoglobin, with hypertension, lower BMI, and elder people were risk factors for blood transfusion. For the training and validation sets, the AUCs of the nomogram were 0.881 (95% CI: 0.865–0.903) and 0.890 (95% CI: 0.773–0.905), respectively. The calibration curve shows that the nomogram is highly consistent with the actual observed results. The DCA shows that the nomogram has good clinical application value. The AUC of the nomogram is significantly larger than the AUCs of independent risk factors in the training and validation set.

Conclusion: Three or more lumbar fusion segments, preoperative low hemoglobin, with hypertension, lower BMI, and elder people are associated with blood transfusion during

the peri-operative period. Based on these factors, we established a blood transfusion nomogram and verified that it can be used to assess the risk of blood transfusion after PLIF. It could help clinicians to make clinical decisions and reduce the incidence of peri-operative blood transfusion.

Keywords: posterior lumbar interbody fusion, blood transfusion, risk factors, nomogram, a retrospective study

INTRODUCTION

Posterior lumbar interbody fusion (PLIF) is a classic surgical method currently used by clinicians to treat lumbar degenerative diseases such as lumbar disc herniation, lumbar spinal stenosis, and lumbar spondylolisthesis (1). PLIF was reported to have a significant effect on relieving lumbar pain and improving radicular symptoms of the lower extremities. It can achieve good segmental fusion and fixation. In addition, it can completely restore the height of the intervertebral space to maintain the physiological curvature of the spine (2–4). However, PLIF is an open operation, during which the muscles on both sides of the spinous process need to be completely stripped. There are many blood vessels running in this area, and some areas of the blood vessels will inevitably be damaged during the operation (5).

The total blood loss during the peri-operative period is approximately 800–1,000 ml, and with the increase in the surgical segment, the blood loss during the peri-operative period also increases (6, 7). In clinical practice, the traditional method to solve severe per-ioperative anemia is allogeneic blood transfusion, which can quickly alleviate the condition and correct anemia (8, 9). However, it may bring about a series of problems, such as increased economic burden, iatrogenic infection, and postoperative complication rate (10). Especially for middle-aged and elderly patients during the peri-operative period, massive bleeding affects the heart, kidney, lung and other functions, leading to abnormal blood coagulation, incision infection, organ insufficiency and a series of complications (11, 12).

At present, nomograms are widely used in the prognosis and diagnosis of clinical medicine. In a nomogram, multiple risk factors can be combined to predict the probability of an outcome, and the results can be visualized. Nomogram is widely used in the diagnosis and prognosis of diseases. It can integrate multiple risk factors to make a comprehensive assessment of the risk of diseases, and visualize the results to make them easy to understand (13). After consulting the literature, we found that there are relatively few studies on the risk factors for blood transfusion during the peri-operative period of PLIF, and no researchers have established and verified the clinical prediction model of blood transfusion after PLIF. Therefore, this study aims to investigate the risk factors for postoperative blood transfusion and the incidence of blood transfusion in patients with PLIF for the treatment of lumbar degenerative diseases and to establish and verify a predictive nomogram of postoperative blood transfusion on this basis.

Abbreviations: PLIF, Posterior Lumbar Interbody Fusion; DCA, decision curve analysis; ROC, receiver operating characteristic; OR, odds ratio; AUC, area under the curve; CI, confidence interval; BMI, body mass index.

METHODS

Collection of Patients' Clinical Data

We retrospectively analyzed the clinical diagnosis and treatment data of patients who underwent PLIF. All of the patients underwent a standard posterior spinal fusion. This study was approved by the Ethics Committee of the Affiliated Hospital of Qingdao University. From January 2015 to December 2020, 5069 patients were in compliance with the requirements. Of these, 691 were excluded: 319 patients with incomplete clinical data such as blood routine training results; 247 were second revision surgery and were diagnosed of lumbar infectious diseases; 68 patients with severe complications within 3 days after the operation, such as spinal cord injury, renal or liver dysfunction; 57 used anti-coagulant and anti-platelet drugs within 15 days. Ultimately, 4,378 patients were included in this study. Although clinical blood transfusion events are still controversial, the criteria of the blood transfusion group in our hospital is that hemoglobin was <70 g/L or hemoglobin was <80 g/L, but patients had symptoms of anemia within 14 days.

We collected variables of each patient, included demographic data, past medical history, concomitant diseases, surgical indications, preoperative routine blood examination, intraoperative fusion segments. The fusion segments were defined as the segments number of lumbar interbody fusion, it was only PLIF without decompression at other levels. All data were collected independently from the hospital's medical record system by two surgeons, and any disputed data were modified with the consent of the two physicians who extracted the data. The surgical method was standard PLIF, and the surgeons were all senior chief physicians in charge. Each patient entered the clinical path for unified process management. We randomly divide the whole population into training group and test group according to the ratio of 4:1.

Statistical Analysis

All statistical analyses were performed in the R software (version 4.0.3, R Foundation for Statistical Computing, Austria). The normality of continuous variables was determined by Shapiro-Wilk training. Normally distributed data are represented by the Mean \pm SD, non-normally distributed data are represented by the Quartiles and categorical data are represented by numbers or percentages. Univariate analysis was performed on the training set, the continuous variables were evaluated using Student's *t*-test or the Mann-Whitney *U*-test, while categorical variables were subjected to the chi-square test. Then, multivariate regression analysis was used on the training set to determine the independent predictors of blood transfusion after lumbar fusion. *P* < 0.05 (two-sided) was considered significant.

TABLE 1 | Comparison of demographic and preoperative data of the two groups of patients.

	Non-transfusion (n = 4,122)	Transfusion (n = 256)	$t/z/\chi^2$	<i>p</i>
Sex			−0.986	0.324
Female	2,136 (51.8)	124 (48.4)		
Male	1,986 (48.2)	132 (51.6)		
Age (years)			135.697	<0.001
<55	1,658 (40.2)	24 (9.4)		
55–65	1,183 (28.7)	70 (27.3)		
>65	1,281 (31.1)	162 (63.3)		
BMI (kg/m ²)	25.50 (23.30, 27.90)	24.20 (21.80, 26.72)	−5.995	<0.001
Comorbidities (%)				
Hypertension	1,392 (33.8)	110 (43.0)	−2.968	0.003
Diabetes mellitus	801 (19.4)	50 (19.5)	0.000	1.000
Coronary heart disease	571 (13.9)	43 (16.8)	−1.224	0.221
Cerebral thrombosis	33 (0.8)	2 (0.8)	0.000	1.000
Respiratory diseases	228 (5.5)	21 (8.2)	−1.650	0.099
Digestive system diseases	371 (9.0)	21 (8.2)	−0.321	0.748
Other	545 (13.2)	38 (14.8)	−0.646	0.518
Indications for surgery (%)			2.051	0.562
Lumbar disc herniation	1,776 (43.1)	115 (45.5)		
Spinal stenosis	1,170 (28.4)	71 (28.1)		
Lumbar spondylolisthesis	869 (21.1)	45 (17.8)		
Other	307 (7.4)	22 (8.6)		
Previous history (%)				
Surgical history	1,476 (35.8)	113 (44.1)	−2.612	0.009
Blood transfusion	106 (2.6)	4 (1.6)	−0.796	0.426
Allergies	80 (1.9)	3 (1.2)	−0.639	0.523
Smoking	681 (16.5)	37 (14.5)	−0.781	0.435
Alcohol	541 (13.1)	31 (12.1)	−0.372	0.710
ABO (%)			−1.296	0.195
A	1,206 (29.3)	62 (24.2)		
AB	446 (10.8)	32 (12.5)		
B	1,355 (32.9)	81 (31.6)		
O	1,115 (27.0)	81 (31.6)		
RH (%)			−0.451	0.652
Negative (−)	16 (0.4)	2 (0.8)		
Positive (+)	4,106 (99.6)	254 (99.2)		
Laboratory tests				
Hb	139.00 (129.00, 150.00)	128.00 (116.00, 138.00)	−11.166	<0.001
NRBC	5.02 (4.30, 5.65)	4.80 (4.17, 5.50)	−2.132	0.033
MCH	30.50 (29.50, 31.50)	30.60 (29.60, 31.83)	−2.108	0.035
MCHC	339.00 (332.00, 346.00)	339.00 (331.00, 346.25)	−0.020	0.984
MCV	89.80 (87.10, 92.40)	90.10 (87.60, 93.62)	−2.366	0.018

(Continued)

TABLE 1 | Continued

	Non-transfusion (n = 4,122)	Transfusion (n = 256)	$t/z/\chi^2$	<i>p</i>
WBC	6.16 (5.16, 7.51)	5.94 (5.08, 6.98)	−2.308	0.021
PLT	131.00 (96.00, 171.00)	133.50 (97.75, 165.00)	−0.429	0.668
Decompression Fusion Segment			407.256	<0.001
1	1,695 (41.1)	36 (14.1)		
2	1,815 (44.0)	55 (21.5)		
≥3	612 (14.8)	165 (64.5)		

Meaningful variables of logistics multifactor regression analysis were included in R software, and a nomogram was constructed. The AUC of the ROC curve was used to illustrate the predictive ability of the model. The calibration curve is an image comparison between the predicted risk and the patient's true risk. The closer the predicted risk is to the standard curve, the better the compliance of the model. The decision curve analysis method was used to evaluate the net benefit and the effectiveness of the nomogram. Finally, in the training and validation sets, the independent nomogram and each meaningful variable subgroup were analyzed and compared, and the nomogram and the ROC curve of each independent predictor were generated to compare the predictive ability.

RESULTS

Demographic Characteristics of the Patients

From January 2015 to December 2020, a total of 4,378 patients underwent lumbar fusion in the Affiliated Hospital of Qingdao University, of whom 256 patients had blood transfusions during the peri-operative period, and the blood transfusion rate during the perioperative period was 5.8%. **Table 1** demonstrates the baseline characteristics. There was no significant difference between the two groups ($P > 0.05$). This shows that there is comparability between the two. Among them, there were 2,118 males and 2,260 females. The average age of the patients was 56.73 ± 14.11 years, and the average body mass index (BMI) was 25.64 ± 3.63 kg/m². Among these patients, there were 1,731 patients with 1 fusion segment, 1,870 patients with two fusion segments, and 777 patients with three or more fusion segments.

Independent Risk Factors for Blood Transfusion in Training Set

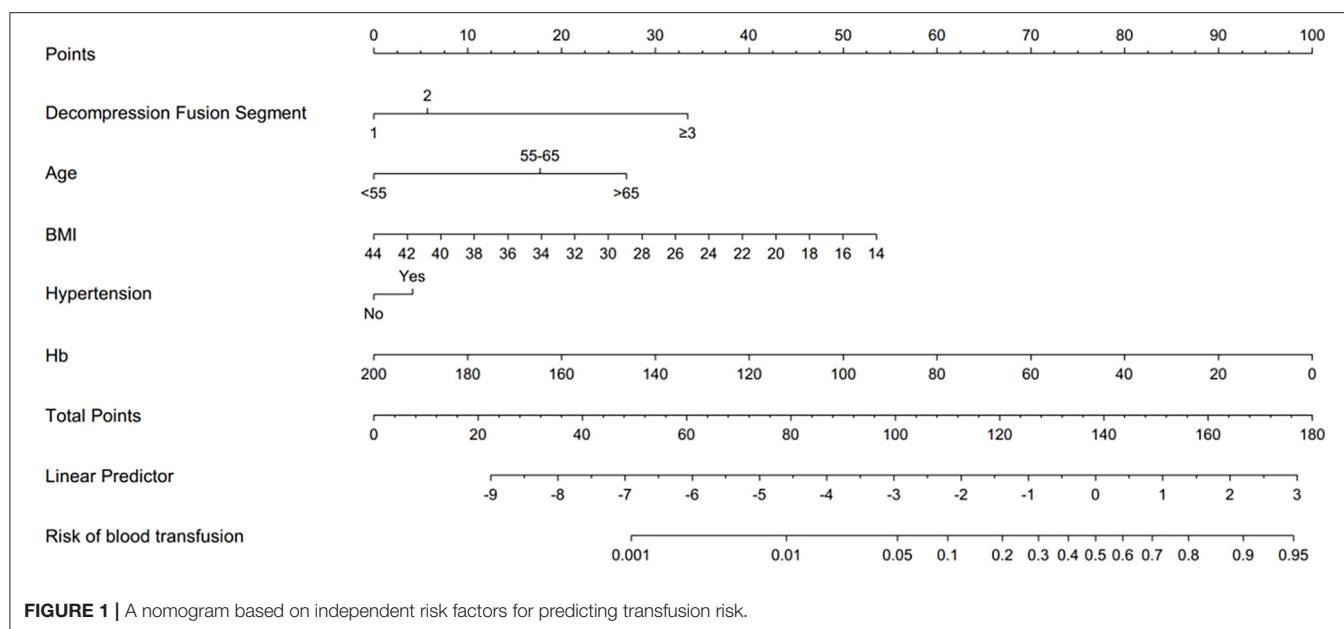
In the training set, 205 patients received blood transfusion within 14 days after lumbar fusion, and the incidence of postoperative blood transfusion was 5.85%. The multivariate regression analysis showed that three or more lumbar fusion segments, preoperative low hemoglobin, with hypertension,

TABLE 2 | Univariate and multivariate logistic analyses for risk factors of blood transfusion.

	Univariable			Multivariable		
	OR	95%CI	P	OR	95%CI	p
Sex						
Female	–	–	–			
Male	1.179	0.889–1.564	0.252			
Age	1.094	1.078–1.111	<0.001	1.082	1.065–1.099	<0.001
BMI	0.862	0.825–0.900	<0.001	0.855	0.813–0.899	<0.001
Comorbidities						
Hypertension	1.366	1.025–1.820	0.033	1.427	1.028–1.982	0.034
Diabetes mellitus	0.975	0.681–1.397	0.892			
Coronary heart disease	1.410	0.978–2.034	0.065			
Cerebral thrombosis	0.534	0.073–3.927	0.538			
Digestive system diseases	1.449	0.851–2.466	0.172			
Respiratory diseases	0.890	0.534–1.483	0.655			
Other	1.073	0.715–1.609	0.734			
Indications for surgery						
Lumbar disc herniation	0.918	0.421–2.004	0.830			
Lumbar spinal stenosis	0.975	0.56–1.699	0.930			
Lumbar spondylolisthesis	1.184	0.665–2.111	0.566			
Previous history						
Surgical history	1.628	1.227–2.162	0.001			
Blood transfusion	0.548	0.172–1.746	0.309			
Allergies	0.240	0.033–1.736	0.158			
Smoking	0.960	0.654–1.409	0.836			
Alcohol	0.875	0.565–1.355	0.549			
ABO						
A	–	–	–			
AB	1.400	0.858–2.283	0.178			
B	1.148	0.785–1.679	0.475			
O	1.419	0.970–2.074	0.071			
RH						
Negative	–	–	–			
Positive	0.340	0.075–1.543	0.162			
Laboratory tests						
Hb	0.960	0.953–0.967	<0.001	0.981	0.972–0.989	<0.001
NRBC	0.809	0.703–0.931	0.003			
MCH	1.064	0.991–1.143	0.088			
MCHC	1.001	0.989–1.012	0.902			
MCV	1.037	1.008–1.067	0.012			
WBC	0.919	0.853–0.990	0.027			
PLT	1.000	0.998–1.002	0.910			
Decompression Fusion Segment						
1	–	–	–	–	–	–
2	1.565	0.971–2.523	0.066	1.473	0.892–2.433	0.130
≥3	12.889	8.466–19.624	<0.001	12.438	7.893–19.600	<0.001

lower BMI, and elder people were independent predictors of blood transfusion after PLIF (Table 2). Among them, the AUC of the three or more fusion segments ROC in the training set was 0.745, and the corresponding AUC of the validation set was 0.758. In addition, the AUC of age in

the training set was 0.773, while the corresponding AUC in the validation set was 0.778. Age and three or more fusion segments were the main influencing factors of the model, indicating that these two parameters have the greatest impact on the model.



Development and Validation of the Nomogram

We used five independent predictors to build a nomogram (Figure 1). For example, one patient in the clinic, with three or more fusion segments on PLIF, aged over 65 years, BMI is 18 kg/m², hypertension history, and the preoperative hemoglobin was 100 g/L. We calculated the score of each single index, and then, the single item scores could be added together. Total score is 35 + 27.5 + 45 + 5 + 50 = 162.5 points. The probability of perioperative blood transfusion is as high as 85%. In the training set, the AUC of our nomogram was 0.881 (95% CI = 0.853–0.910, $p < 0.001$) (Figure 2A), showing good accuracy in predicting the risk of blood transfusion in patients after lumbar fusion. The calibration curve shows that there is good agreement between the predicted and observed results in terms of the probability of blood transfusion (Figure 2B). Furthermore, DCA shows that there is a net benefit to using this nomogram to predict postoperative blood transfusion if the patient and physician threshold probability is <72% (Figure 2C).

A total of 876 patients were included in the training set, and 51 patients received blood transfusion within 14 days after lumbar fusion. In the training set, the AUC of the nomogram blood transfusion probability prediction model was 0.890 (95% CI = 0.848–0.932, $p < 0.001$) (Figure 2D), and the calibration curve showed that the prediction of blood transfusion probability was in good agreement with the observation (Figure 2E). In addition, the DCA proved that if the threshold probability of patients and doctors is <62%, using a nomogram to predict postoperative blood transfusion has a net benefit (Figure 2F).

Evaluation the Predictability of Nomogram

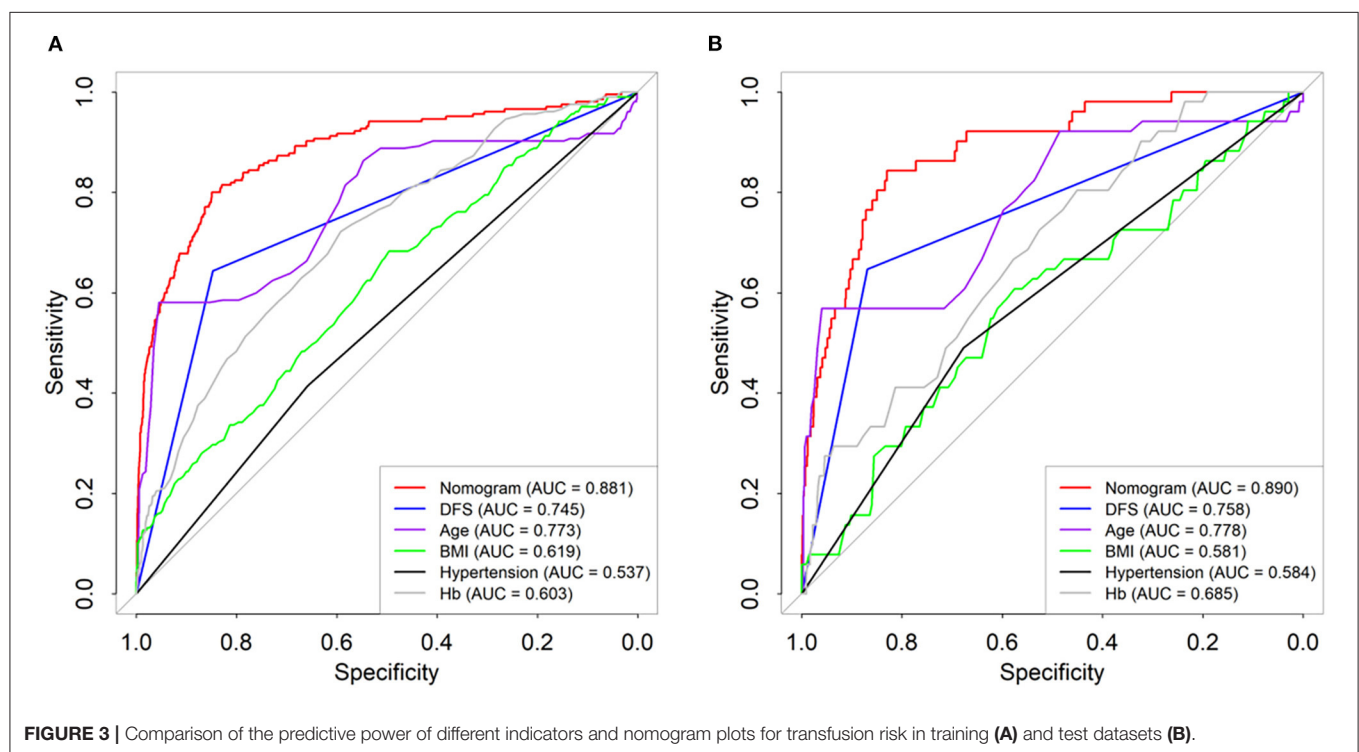
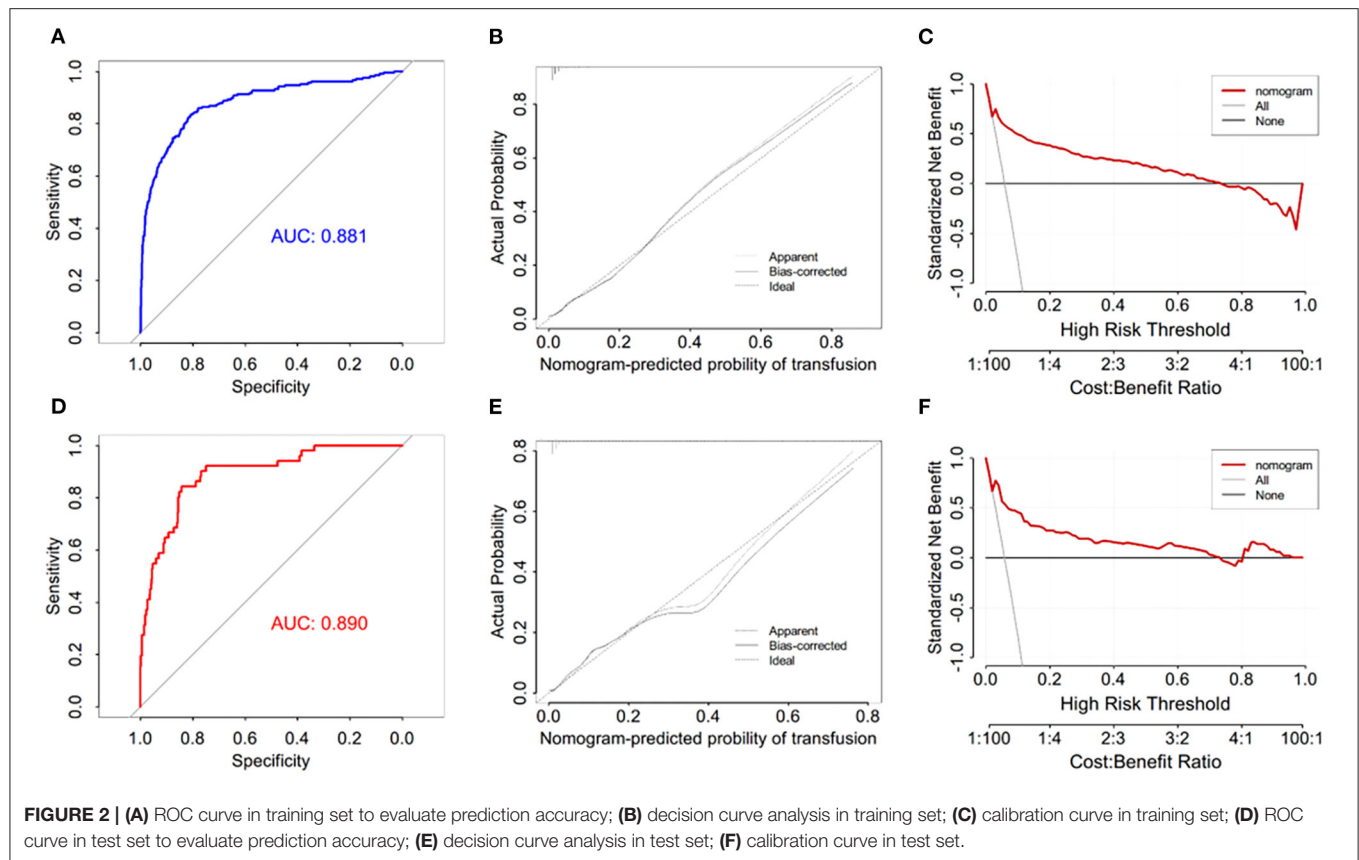
By comparing the ROC curve of the nomogram with the ROCs of other independent risk factors, the results showed that the AUC of the nomogram blood transfusion risk predictor was

significantly higher than that of the blood transfusion risk predictor of patients after PLIF ($P < 0.001$) (Figure 3A). Similar to the training set, the AUC was also significantly higher than the AUC of each independent predictor in the validation set ($P < 0.001$) (Figure 3B).

DISCUSSION

Spine surgery has a long operation time and large associated wounds, especially when dealing with cancellous bone with abundant blood supply, and it is often accompanied by obvious peri-operative bleeding, usually requiring multiple blood transfusions (14). As an important strategy for the treatment of anemia, allogeneic blood transfusion is extremely important to ensure the safety of patients after surgery. The reported incidence of peri-operative blood transfusion is quite different. The incidence in our study was ~3%, which is lower than the 11–18% reported abroad (15, 16) and far lower than the 32.6% reported in China (17). Wong et al. (18) found that the injection of tran-examic acid can effectively reduce the blood loss and blood transfusion rate after PLIF without causing pulmonary embolism and venous thrombosis of the lower extremities.

After reviewing previous relevant literature, we found that Wang et al. (17) concluded that preoperative low hemoglobin, fusion stage, long operation time, and high total intraoperative blood loss are risk factors for blood transfusion. However, the sample size in this model was relatively small, the blood transfusion rate was ~30% higher, and there was no distinction between the training group and the validation group to verify the effectiveness and accuracy of the model. White et al. (19) also found that female sex, age ≥ 65 years, long-segment fixation and fusion, surgical fixation to the pelvis, and other factors can increase the risk of massive blood loss during surgery. Butler et al. (20) showed that increasing age, ASA grading of multilevel



surgery, and prolonged operation time were risk factors affecting lumbar fusion, but neither of them established a predictive model for postoperative blood transfusion. The results of our study show that ≥ 3 lumbar fusion segments, preoperative low hemoglobin, a history of hypertension, low BMI, and advanced age are risk factors for blood transfusion. This is consistent with domestic and foreign studies on some independent risk factors and establishes and verifies the risk model of blood transfusion after PLIF.

This study found that three or more fusion segments was a risk factor affecting peri-operative blood transfusion. The increase in inter-vertebral fusion segments means an increase in the number of inter-vertebral disc removals. It is often necessary to scrape the endplate cartilage of the upper and lower vertebral bodies of the inserted segments before inserting the inter-vertebral fusion cage. At the same time, it is necessary to extensively strip the paravertebral muscles and soft tissues during the operation to insert the pedicle screws and decompress the spinal canal, which will increase intraoperative bleeding. Morcos et al. (15) also found that multi-segment fusion was an independent risk factor for perioperative blood transfusion, and the blood transfusion rate was 6 times higher. More decompressed and fused segments mean a longer operation time. Many studies have found that the operation time and the number of fusion segments were important predictors of blood transfusion. The probability of blood transfusion increases by 4.2% for every additional hour of operation time. The probability of peri-operative blood transfusion for each additional fusion segment increases by 6 times (16, 21, 22). Aoude et al. (23) showed that the operation time and blood loss were related to an increase in the fusion segments. Therefore, the operation time can be reduced by reducing intra-operative fusion, thereby reducing the risk of peri-operative blood transfusion.

It is worth noting that lower hemoglobin before surgery can also increase the blood transfusion rate of patients during the perioperative period. The lower the red blood cell count, hemoglobin, and hematocrit of the patient before surgery, the poorer their ability to compensate for bleeding during surgery, and the higher the probability that blood transfusions will be required during the peri-operative period. Research by Myers et al. (24) showed that patients with lumbar fusion with preoperative anemia have a higher postoperative infection rate and blood transfusion rate and a longer postoperative hospital stay. In a large-sample retrospective study, Wu et al. (25) showed that preoperative HCT $\leq 39\%$ was associated with an increase in the 30-day postoperative mortality rate. In addition, Carson et al. (26) showed that when Hb ≤ 80 g/L, with every 10 g/L decrease, the risk of death increased by 2.5-fold. Rasouli et al. (27) believed that when preoperative Hb ≤ 100 g/L, the perioperative infection rate increased significantly ($\sim 4.23\%$), the preoperative hemoglobin content was 110–130 g/L, and the postoperative infection rate was significantly reduced ($\sim 0.84\%$). Early identification and correction of preoperative anemia patients is of great significance. We can infuse concentrated red blood cells in advance to supplement hemoglobin to normal levels. Otherwise, patients in the perioperative period are prone to anemia, leading to related complications in multiple organs of

the human body, increasing the risk of surgical incision infection, prolonging the hospital stay, and increasing the risk of death.

Older age is one of the risk factors that affect peri-operative blood transfusion. Rasouli et al. (27) showed that age ≥ 50 years was an independent risk factor for increased blood transfusion risk in the 13,170 patients undergoing lumbar fusion surgery. Yoshihara and Yoneoka (28) showed that middle-aged and elderly patients were more likely to receive allogeneic blood transfusions than middle-aged and young patients. Similarly, Hu et al. (29) collected clinical data from more than 4,000 patients who underwent total knee arthroplasty in the Affiliated Hospital of Qingdao University and found that advanced age was an independent predictor of peri-operative blood transfusion. The older the patient's age is, the worse the hematopoietic function, and the greater the decreases in the lifespan and function of red blood cells. Coupled with the decline of the digestive function of elderly patients, these changes will lead to deficiencies in hematopoietic materials such as iron and vitamins. These findings suggest that once elderly patients undergo lumbar spine surgery, the hematopoietic system cannot replenish blood cells in a short period of time, leading to varying degrees of anemia during the perioperative period. This requires rapid allogeneic blood transfusion treatment.

Patients with lower BMI have relatively low body weight and a relatively low blood volume. The same absolute amount of bleeding leads to an increase in the bleeding score of the patient, and anemia is more likely to occur during the perioperative period. In patients with a low BMI, the proportion of the spine relative to the whole body is relatively large, which may lead to an increase in bleeding scores during spinal surgery (30). The risk of peri-operative blood transfusion in patients with hypertension accompanied by disease is higher than that in patients without hypertension. The author believes that this may be related to changes in the patients' cardiovascular systems caused by hypertension. These patients also have the habit of taking oral anti-hypertensive drugs and anticoagulants such as aspirin. Moreover, these patients are older and have vascular sclerosis, hyalinosis, decreases in capillary contraction and blood clotting abilities, and more intra-operative bleeding (31). Perioperative blood pressure control is not ideal, and the amounts of bleeding and drainage are higher than those in healthy patients.

Our research has some limitations. First, as this is a retrospective study, some data are missing or incomplete, and the conclusions of this study need to be further demonstrated in prospective randomized controlled studies. Second, the sample size of this study was not large enough, and the patient variables were not all included. Furthermore, patients diagnosed with spinal tumors, infection, tuberculosis, trauma fractures, and spinal deformities were excluded from this study. Considering that these groups are more prone to anemia during the perioperative period, it will be necessary to further collect data on patients with these diseases. In addition, postoperative complications such as pneumonia, urinary tract infection, and deep vein thrombosis of the lower extremities were not included. The analysis of the correlations between these complications and blood transfusion is difficult. Our study only included patients

from a single medical center; a multicenter study with a large sample size will be required to confirm the results.

CONCLUSION

Three or more lumbar fusion segments, preoperative low hemoglobin, with hypertension, lower BMI, and elder people are associated with blood transfusion during the perioperative period. Based on these factors, we established a blood transfusion nomogram and verified that it can be used to assess the risk of blood transfusion after PLIF. It could help clinicians to make clinical decisions and reduce the incidence of perioperative blood transfusion.

REFERENCES

- Mobbs RJ, Phan K, Malham G, Seex K, Rao PJ. Lumbar interbody fusion: techniques, indications and comparison of interbody fusion options including PLIF, TLIF, MI-TLIF, OLIF/ATP, LLIF and ALIF. *J Spine Surg.* (2015) 1:2–18. doi: 10.3978/j.issn.2414-469X.2015.10.05
- Ekman P, Moller H, Tullberg T, Neumann P, Hedlund R. Posterior lumbar interbody fusion versus posterolateral fusion in adult isthmic spondylolisthesis. *Spine.* (2007) 32:2178–83. doi: 10.1097/BRS.0b013e31814b1bd8
- Luo J, Cao K, Yu T, Li L, Huang S, Gong M, et al. Comparison of posterior lumbar interbody fusion versus posterolateral fusion for the treatment of isthmic spondylolisthesis. *Clin Spine Surg.* (2017) 30:E915–22. doi: 10.1097/BSD.0000000000000297
- de Kunder SL, van Kuijk S, Rijkers K, Caelers I, van Hemert W, de Bie RA, et al. Transforaminal lumbar interbody fusion (TLIF) versus posterior lumbar interbody fusion (PLIF) in lumbar spondylolisthesis: a systematic review and meta-analysis. *Spine J.* (2017) 17:1712–21. doi: 10.1016/j.spinee.2017.06.018
- Elgafy H, Bransford RJ, McGuire RA, Dettori JR, Fischer D. Blood loss in major spine surgery: are there effective measures to decrease massive hemorrhage in major spine fusion surgery? *Spine.* (2010) 35(9 Suppl.):S47–56. doi: 10.1097/BRS.0b013e3181d833f6
- Xu D, Ren Z, Chen X, Zhuang Q, Hui S, Sheng L, et al. The further exploration of hidden blood loss in posterior lumbar fusion surgery. *Orthop Traumatol Surg Res.* (2017) 103:527–30. doi: 10.1016/j.otsr.2017.01.011
- Ren Z, Li S, Sheng L, Zhuang Q, Li Z, Xu D, et al. Topical use of tranexamic acid can effectively decrease hidden blood loss during posterior lumbar spinal fusion surgery: a retrospective study. *Medicine.* (2017) 96:e8233. doi: 10.1097/MD.00000000000008233
- Carson JL, Stanworth SJ, Roubinian N, Fergusson DA, Triulzi D, Doree C, et al. Transfusion thresholds and other strategies for guiding allogeneic red blood cell transfusion. *Cochrane Database Syst Rev.* (2016) 10:D2042. doi: 10.1002/14651858.CD002042.pub4
- Mueller MM, Van Remoortel H, Meybohm P, Aranko K, Aubron C, Burger R, et al. Patient blood management: recommendations from the 2018 Frankfurt Consensus Conference. *JAMA.* (2019) 321:983–97. doi: 10.1001/jama.2019.0554
- Carson JL, Carless PA, Hebert PC. Transfusion thresholds and other strategies for guiding allogeneic red blood cell transfusion. *Cochrane Database Syst Rev.* (2012) 10:CD002042. doi: 10.1002/14651858.CD002042.pub3
- Jang SY, Cha YH, Yoo JI, Oh T, Kim JT, Park CH, et al. Blood transfusion for elderly patients with hip fracture: a nationwide cohort study. *J Korean Med Sci.* (2020) 35:e313. doi: 10.3346/jkms.2020.35.e313
- Loftus TJ, Brakenridge SC, Murphy TW, Nguyen LL, Moore FA, Efron PA, et al. Anemia and blood transfusion in elderly trauma patients. *J Surg Res.* (2018) 229:288–93. doi: 10.1016/j.jss.2018.04.021
- Lubelski D, Feghali J, Nowacki AS, Alentado VJ, Planchard R, Abdullah KG, et al. Patient-specific prediction model for clinical and quality-of-life outcomes after lumbar spine surgery. *J Surg Res.* (2021) 1–9. doi: 10.3171/2020.8.SPINE20577

DATA AVAILABILITY STATEMENT

The original contributions presented in the study are included in the article/supplementary material, further inquiries can be directed to the corresponding author/s.

AUTHOR CONTRIBUTIONS

BL performed the data analysis. BL and JP wrote the manuscript. BL, HZ, and ZW contributed to the manuscript revise. JP and HZ contributed to literature search and data extraction. BL and ZW conceived and designed the study. All authors contributed to the article and approved the submitted version.

- Kushioka J, Yamashita T, Okuda S, Maeno T, Matsumoto T, Yamasaki R, et al. High-dose tranexamic acid reduces intraoperative and postoperative blood loss in posterior lumbar interbody fusion. *J Neurosurg Spine.* (2017) 26:363–7. doi: 10.3171/2016.8.SPINE16528
- Morcos MW, Jiang F, McIntosh G, Johnson M, Christie S, Wai E, et al. Predictors of blood transfusion in posterior lumbar spinal fusion: a Canadian spine outcome and research network study. *Spine.* (2018) 43:E35–9. doi: 10.1097/BRS.0000000000002115
- Basques BA, Anandasivam NS, Webb ML, Samuel AM, Lukasiewicz AM, Bohl DD, et al. Risk factors for blood transfusion with primary posterior lumbar fusion. *Spine.* (2015) 40:1792–7. doi: 10.1097/BRS.00000000000001047
- Wang H, Wang K, Lv B, Xu H, Jiang W, Zhao J, et al. Establishment and assessment of a nomogram for predicting blood transfusion risk in posterior lumbar spinal fusion. *J Orthop Surg Res.* (2021) 16:39. doi: 10.1186/s13018-020-02053-2
- Wong J, El BH, Rampersaud YR, Lewis S, Ahn H, De Silva Y, et al. Tranexamic acid reduces perioperative blood loss in adult patients having spinal fusion surgery. *Anesth Analg.* (2008) 107:1479–86. doi: 10.1213/ane.0b013e3181831e44
- White S, Cheung ZB, Ye I, Phan K, Xu J, Dowdell J, et al. Risk factors for perioperative blood transfusions in adult spinal deformity surgery. *World Neurosurg.* (2018) 115:e731–7. doi: 10.1016/j.wneu.2018.04.152
- Butler JS, Burke JP, Dolan RT, Fitzpatrick P, O'Byrne JM, McCormack D, et al. Risk analysis of blood transfusion requirements in emergency and elective spinal surgery. *Eur Spine J.* (2011) 20:753–8. doi: 10.1007/s00586-010-1500-0
- Zheng F, Cammisa FJ, Sandhu HS, Girardi FP, Khan SN. Factors predicting hospital stay, operative time, blood loss, and transfusion in patients undergoing revision posterior lumbar spine decompression, fusion, and segmental instrumentation. *Spine.* (2002) 27:818–24. doi: 10.1097/00007632-200204150-00008
- Nuttall GA, Horlocker TT, Santrach PJ, Oliver WJ, Dekutoski MB, Bryant S. Predictors of blood transfusions in spinal instrumentation and fusion surgery. *Spine.* (2000) 25:596–601. doi: 10.1097/00007632-200003010-00010
- Aoude A, Nooh A, Fortin M, Aldebeyan S, Jarzem P, Ouellet J, et al. Incidence, predictors, and postoperative complications of blood transfusion in thoracic and lumbar fusion surgery: an analysis of 13,695 patients from the American College of Surgeons National Surgical Quality Improvement Program Database. *Global Spine J.* (2016) 6:756–64. doi: 10.1055/s-0036-1580736
- Myers E, O'Grady P, Dolan AM. The influence of preclinical anaemia on outcome following total hip replacement. *Arch Orthop Trauma Surg.* (2004) 124:699–701. doi: 10.1007/s00402-004-0754-6
- Wu WC, Schiffner TL, Henderson WG, Eaton CB, Poses RM, Uttley G, et al. Preoperative hematocrit levels and postoperative outcomes in older patients undergoing noncardiac surgery. *JAMA.* (2007) 297:2481–8. doi: 10.1001/jama.297.22.2481

26. Carson JL, Noveck H, Berlin JA, Gould SA. Mortality and morbidity in patients with very low postoperative Hb levels who decline blood transfusion. *Transfusion*. (2002) 42:812–8. doi: 10.1046/j.1537-2995.2002.00123.x
27. Rasouli MR, Restrepo C, Maltenfort MG, Purtill JJ, Parvizi J. Risk factors for surgical site infection following total joint arthroplasty. *J Bone Joint Surg Am*. (2014) 96:e158. doi: 10.2106/JBJS.M.01363
28. Yoshihara H, Yoneoka D. Predictors of allogeneic blood transfusion in spinal fusion in the United States, 2004–2009. *Spine*. (2014) 39:304–10. doi: 10.1097/BRS.0000000000000123
29. Hu C, Wang YH, Shen R, Liu C, Sun K, Ye L, et al. Development and validation of a nomogram to predict perioperative blood transfusion in patients undergoing total knee arthroplasty. *BMC Musculoskelet Disord*. (2020) 21:315. doi: 10.1186/s12891-020-03328-9
30. Jain A, Sponseller PD, Newton PO, Shah SA, Cahill PJ, Njoku DB, et al. Smaller body size increases the percentage of blood volume lost during posterior spinal arthrodesis. *J Bone Joint Surg Am*. (2015) 97:507–11. doi: 10.2106/JBJS.N.01104
31. Lei F, Li Z, He W, Tian X, Zheng L, Kang J, et al. Hidden blood loss and the risk factors after posterior lumbar fusion surgery: a retrospective

study. *Medicine*. (2020) 99:e20103. doi: 10.1097/MD.00000000000020103

Conflict of Interest: The authors declare that the research was conducted in the absence of any commercial or financial relationships that could be construed as a potential conflict of interest.

Publisher's Note: All claims expressed in this article are solely those of the authors and do not necessarily represent those of their affiliated organizations, or those of the publisher, the editors and the reviewers. Any product that may be evaluated in this article, or claim that may be made by its manufacturer, is not guaranteed or endorsed by the publisher.

Copyright © 2021 Liu, Pan, Zong and Wang. This is an open-access article distributed under the terms of the Creative Commons Attribution License (CC BY). The use, distribution or reproduction in other forums is permitted, provided the original author(s) and the copyright owner(s) are credited and that the original publication in this journal is cited, in accordance with accepted academic practice. No use, distribution or reproduction is permitted which does not comply with these terms.



Clinical Features and Efficacy Analysis of Redundant Nerve Roots

Jianzhong Xu and Yong Hu*

Department of Spinal Surgery, Ningbo No.6 Hospital, Ningbo, China

Introduction: Redundant nerve roots (RNRs) are common finding in lumbar spinal stenosis patients. Up to now, many relevant studies were carried out on the mechanism, pathogenic factors, and clinical features of redundant nerve roots. However, there are few studies on the surgical methods. In this study, posterior lumbar interbody fusion and internal fixations were used in 30 patients with RNRs in our hospital. Moreover, we also proposed new ideas about different types and subtypes of RNRs using patterns and their corresponding MRI images.

Methods: Thirty patients with lumbar spinal stenosis and RNRs were enrolled in this study and underwent surgery between January 2009 and December 2014. Redundant nerve roots are identified as elongated, tortuous, or serpiginous nerve roots present in the subarachnoid space on sagittal T2-weighted magnetic resonance imaging (MRI) studies. Patients were treated with posterior decompression, intervertebral disc resection, and instrumented interbody fusion. The age, sex, disease course, operative time, intraoperative blood loss, operative segments were recorded. Outcome measures recorded to identify symptom improvement included pre-operative and post-operative visual analog scale (VAS), pre-operative and post-operative Oswestry Disability Index (ODI) and pre-operative and post-operative Japanese Orthopedic Association (JOA) scores.

Results: VAS back pain, VAS leg pain VAS, ODI, and JOA with standard deviations were 6.4 ± 0.9 , 7.1 ± 0.8 , 43.0 ± 2.2 , and 10.3 ± 2.6 , respectively. At 3 months post-operatively, VAS back pain, VAS leg pain VAS, ODI, and JOA with standard deviations were 1.4 ± 0.5 , 1.6 ± 0.6 , 13.0 ± 1.6 , and 25.0 ± 1.8 , respectively. Nerve redundancy resolved in all cases on post-operative MRI.

Conclusion: Posterior lumbar laminectomy and instrumented interbody fusion relieves low back and leg pain in patients with lumbar spinal stenosis and RNRs and can alleviate the tortuous appearance of the cauda equina in the decompressed segment.

Keywords: redundant nerve roots, lumbar vertebrae, instrumented fusion, posterior lumbar interbody fusion, magnetic resonance imaging

INTRODUCTION

Redundant nerve roots (RNRs) were first described by Verbiest (1), and subsequently named by Cressman and Pawl (2). RNRs are characterized by a tortuosity of elongated and enlarged nerve roots in the subarachnoid space of the lumbar spine. The reported prevalence of RNRs varies, with some researchers determining prevalence values of 33.8–42% in patients with lumbar spinal

OPEN ACCESS

Edited by:

Ralph Jasper Mobbs,
University of New South
Wales, Australia

Reviewed by:

Konstantinos Markatos,
Salamina Medical Center, Greece
Ziya Levent Gokaslan,
Brown University, United States

*Correspondence:

Yong Hu
huyong610@163.com

Specialty section:

This article was submitted to
Orthopedic Surgery,
a section of the journal
Frontiers in Surgery

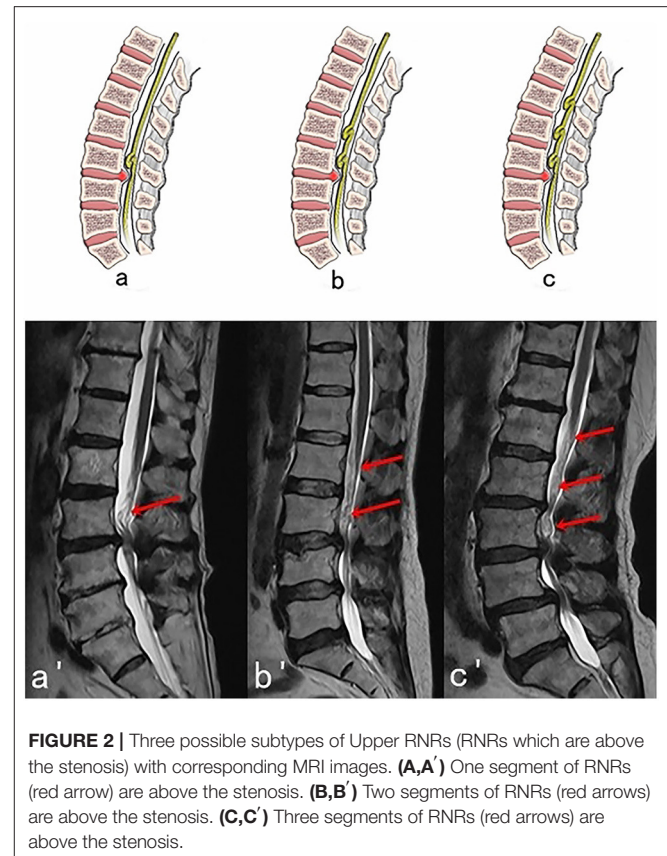
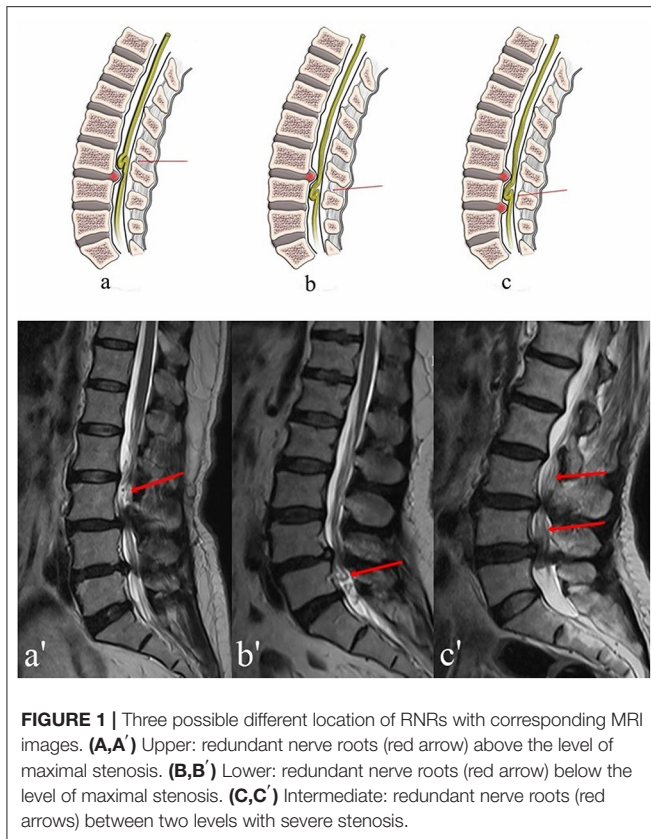
Received: 13 November 2020

Accepted: 29 September 2021

Published: 01 November 2021

Citation:

Xu J and Hu Y (2021) Clinical Features
and Efficacy Analysis of Redundant
Nerve Roots. *Front. Surg.* 8:628928.
doi: 10.3389/fsurg.2021.628928



stenosis (3). It has been recognized that RNRs develop as a response to lumbar spinal stenosis (4). The purpose of the study was to investigate clinical efficacy of posterior lumbar interbody fusion and internal fixation of patients with lumbar spinal stenosis and RNRs. Also, at the first time, we use pattern diagrams and their corresponding MRI images to discuss a possible classification of RNRs which includes Upper, Lower, and Intermediate RNRs (Figures 1–3).

METHODS

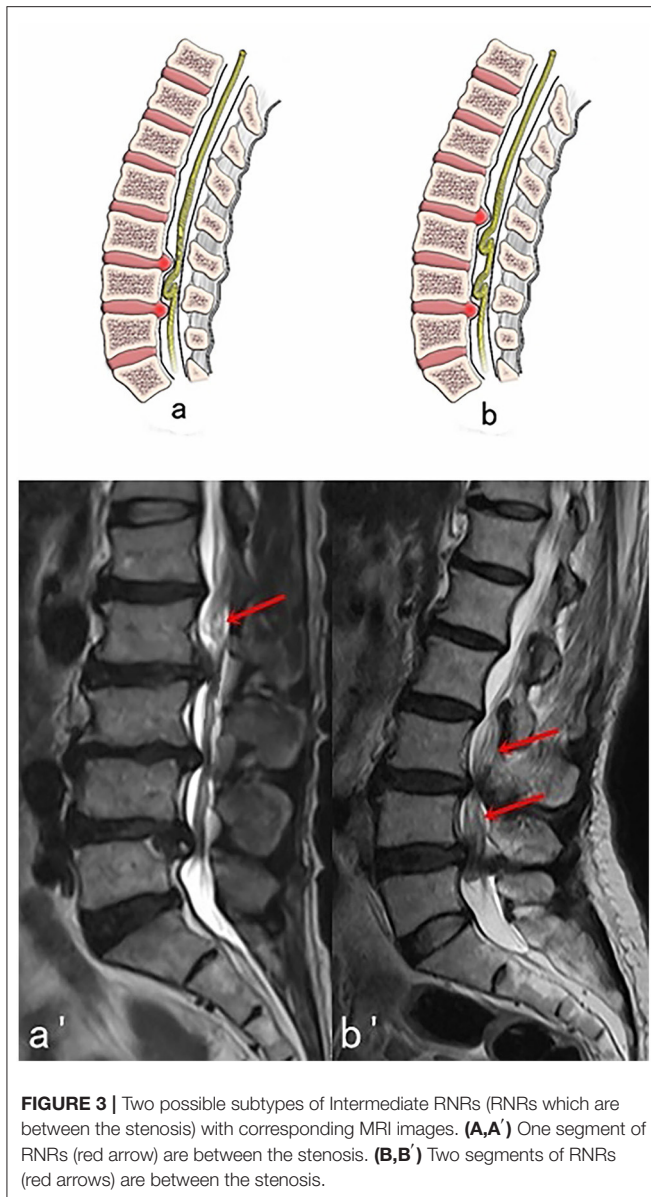
General Information

Between January 2009 to December 2014, 30 patients with lumbar spinal stenosis with evidence of RNRs on MRI were treated in our hospital with posterior lumbar decompression and instrumented interbody fusion. Eleven men and 19 women (mean age, 57.6 years) with lumbar spinal stenosis and RNRs were included in this study. The ethics committee of Ningbo No.6 Hospital approved this study. The inclusion criteria included: (1) cauda equina redundancy; (2) intermittent neurological symptoms (3) history of neurogenic claudication; (4) MRI or CT confirmed central spinal canal stenosis (central sagittal diameter <10 mm, or dural sac area <100 mm²) (5, 6) (5) non-surgical treatment was ineffective. Exclusion criteria included: (1) spinal arteriovenous malformation, arteriovenous malformation; (2) intraspinal tumor; (3) death or loss of follow-up due to non-spinal diseases. There were 11 males and 19 females with an

average age of 57.6 years (range, 49–70 years). The presurgical course of disease ranged from 2 months to 5 years, with an average of 15.1 months. There were 8 patients with lumbar spondylolisthesis, 6 with single level stenosis, 14 with two level stenosis, 8 with three level stenosis, and 2 with four level stenosis. The cauda equina was located above the stenosis in 22 cases, below it in 5 cases, and within it in 3 cases.

Surgical Methods

After general anesthesia was induced, patients were placed into the prone position. The skin was cut longitudinally centering over the spinous processes of the lumbar spine. The fascia was divided on either side of the spinous processes, exposing the lamina, facet joints, and transverse processes. Pedicle screws were placed using anatomic landmarks and screw tracts were tapped prior to placement of appropriate length pedicle screws (Kangsheng, China). Complete laminectomy with lateral recess and foraminal decompression was performed to expand the volume of the spinal canal and neural foramen as much as possible. Thickened and calcified ligamentum flavum and facet joints hypertrophy was addressed during the decompression and compressive portions of the intervertebral disc were removed to completely decompress redundant nerve roots and cauda equina. The upper and lower endplates at each fusion level were cleaned of residual nucleus pulposus with a curette and cartilaginous endplate removed with a shaver. The intervertebral space was



washed with isotonic saline before it was packed with autologous local bone graft and an interbody fusion cage filled with bone graft (Grafton, Medtronic, United States). Precut, pre-contoured rods were placed (Kangsheng, China). A drain was placed before the wound was closed in layers using absorbable suture.

Post-operative Treatment

Perioperative treatment included protocols to prevent infection with routine antibiotics, low-dose steroid administration, and prophylactic protection of gastric mucosa. After patients had recovered from anesthesia, the patients were encouraged to actively move their lower extremity with ankle joint flexion and extension exercises and straight leg raises. The drainage tube was removed according to the drainage volume (24 h flow rate <50 ml). After 3–5 days, patients wore a lumbar brace to ambulate. Lumbar MRI was obtained 1 week after surgery. Patients began

TABLE 1 | Comparison of pre-operative and 3 month post-operative back pain VAS, leg pain VAS, ODI, and JOA scores (average \pm standard deviation).

Time	Back pain VAS	Leg pain VAS	ODI score	JOA score
Pre-operative	6.4 \pm 0.9	7.1 \pm 0.8	43.0 \pm 2.2	10.3 \pm 2.6
Post-operative	1.4 \pm 0.5	1.6 \pm 0.6	13.0 \pm 1.6	25.0 \pm 1.8
t-value	27.22	30.07	70.26	27.97
P-value	<0.05	<0.05	<0.05	<0.05

VAS, visual analog scale; ODI, Oswestry Disability Index; JOA, Japanese Orthopedic Association Scores.

TABLE 2 | Patient characteristics.

Variable	n = 30
Sex (n, %)	
Male	18 (60%)
Female	12 (40%)
Age (x \pm s)	61.47 \pm 8.00
Stenosis level (n, %)	
L1/2	2 (6.7%)
L2/3	3 (10%)
L3/4	12 (40%)
L3–L5	2 (6.7%)
L4/5	10 (33.3%)
L4–S1	1 (3.3%)
Location of RNRs (n, %)	
Lower	6 (20%)
Intermediate	3 (10%)
Upper	21 (70%)
Blood loss (ml) (median, interquartile range)	500 (400–625)
Outcome (n, %)	
Unchanged	2 (6.7%)
Fair	8 (26.7%)
Good	13 (43.3%)
Excellent	7 (23.3%)

exercises to strengthen paraspinal and abdominal muscles 6 weeks after the operation.

Evaluation Standard

The operative time, intraoperative blood loss, post-operative complications, visual analog scale (VAS), Oswestry Disability Index (ODI), and Japanese Orthopedic Association (JOA) score were compared before and after surgery. The first two post-operative improvement rates were calculated for most measures as: [(pre-treatment score – post-treatment score) / pre-treatment score] \times 100%. JOA score post-operative improvement rate was calculated as: (post-treatment score – pre-treatment score) / (29 – before treatment) \times 100%. Overall efficacy evaluation criteria: Fischgrund criteria was used to determine the surgical efficacy: excellent: waist or leg pain symptoms completely or almost completely disappeared, daily activities no longer affected; good:

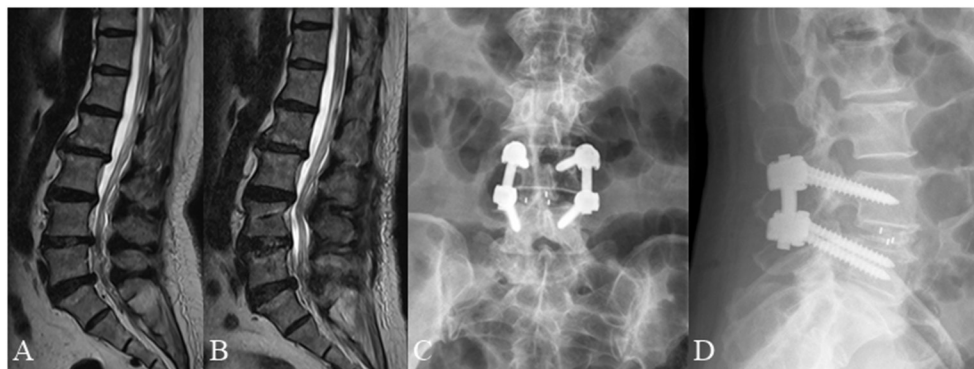


FIGURE 4 | A 66 year old female complained of low back pain for 3 months underwent posterior lumbar decompression and instrumented interbody fusion at L4/5. **(A)** Pre-operative lumbar MRI showed that the nerve roots were redundant above the L4/5 intervertebral disc. **(B)** Post-operative lumbar MRI obtained 3 days after surgery demonstrated significant relief of RNRs. **(C,D)** Lumbar radiographs obtained 3 months after surgery demonstrate internal fixation in good position without cage subsidence or migration.



FIGURE 5 | A 70 year old female complained of low back pain and right lower extremity pain for 2 months before she underwent posterior lumbar interbody fusion at L3/4 and L4/L5. **(A)** Pre-operative lumbar MRI showed that the nerve roots were redundant between the L3/4 and L4/L5 intervertebral disc. **(B)** Post-operative MRI obtained 3 days after surgery showed significant improvement with resolution of RNRs. **(C,D)** Lumbar radiographs obtained 3 months after surgery demonstrate internal fixation in good position without cage subsidence or migration.

post-operative symptoms improved significantly, occasional low back pain and leg numbness, daily activities were not affected; fine: post-operative symptoms improved, intermittent episodes of low back pain or numbness of lower limbs, daily activities affected; poor: post-operative symptoms did not improve or improved and then returned to pre-operative level, daily activities were significantly affected.

Statistical Analysis

The SPSS software version 20.0 (IBM Corporation, NY, USA) was used in the statistical analysis, and the paired sample *t*-test was used. A significance level of $P < 0.05$ was used.

RESULTS

Clinical Efficacy

All 30 patients were followed for between 12 and 30 months with an average follow up of 23.3 months (Tables 1, 2). The operative time was between 85 and 220 min with an average time of 130 min. Intraoperative estimated blood loss (EBL) ranged from 300 to 1,000 ml with an average EBL

of 545 ml. Radiologists confirmed RNRs of the cauda equina were present in all 30 patients. Redundant nerve roots were located above the level of the stenosis (Upper RNRs) in 21 cases (70%), below it (Lower RNRs) in 6 cases (20%), and between the stenosis levels (Intermediate RNRs) in 3 cases (10%). Redundant nerve roots disappeared in all cases on post-surgical MRI (Figures 4–6). Pre-operative low back pain VAS, leg pain VAS, ODI, and JOA score were 6.4 ± 0.9 , 7.1 ± 0.8 , 43.0 ± 2.2 , and 10.3 ± 2.6 , respectively. Low back pain VAS, leg pain VAS, ODI, and JOA score at 3 months after surgery were (1.4 ± 0.5) , (1.6 ± 0.6) , (13.0 ± 1.6) , and (25.0 ± 1.8) , respectively. These differences for all three variables were statistically significant ($P < 0.05$). The improvement rate of VAS for low back pain was $77.1 \pm 9.0\%$; the improvement rate of VAS for leg pain was $77.6 \pm 9.1\%$; the improvement rate for ODI score was $69.8 \pm 3.6\%$; the improvement rate for JOA score was $78.3 \pm 9.1\%$. At 12 months after surgery, the interbody fusion rate was 83.3%. Efficacy evaluation demonstrated excellent outcome in 7 cases, good outcome in 13 cases, fair outcome in 8 cases, and symptoms were unchanged in 2 cases. The good or excellent rate was



FIGURE 6 | A 59 year old female complained of low back pain and left and right lower extremity pain for 3 months underwent posterior lumbar interbody fusion at L4/5. **(A)** Pre-operative lumbar MRI showed that the nerve roots were redundant below the L4/5 intervertebral disc. **(B)** Post-operative MRI obtained 3 days after surgery showed significant improvement with resolution of RNRs. **(C,D)** Lumbar radiographs obtained 3 months after surgery demonstrate internal fixation in good position without cage subsidence or migration.

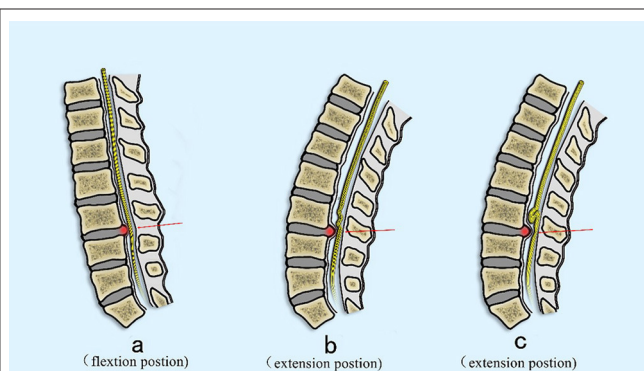


FIGURE 7 | Proposed mechanism of the development of RNRs. **(A)** The nerve is pulled proximally by the flexed position commonly seen in patients with symptomatic spinal stenosis (arrow). **(B)** The nerve becomes relaxed in the extended position, but still is deformed at the site of maximal stenosis secondary to a disc extrusion (red arrow). **(C)** In an extension position, the nerve is redundant cranial to the compressed section but cannot redistribute past the compressed section due to stenosis (red arrow).

66.7%. After 3 months, the patients were allowed an unrestricted activity level.

Post-operative Complications

The surgical incisions of all patients healed uneventfully. No nerve root injury, cauda equina injury, infection, cerebrospinal fluid leakage, lower extremity venous thrombosis, subsidence, or displacement of intervertebral cage were documented.

DISCUSSION

Redundant nerve roots are a common finding in which elongated, tortuous, or serpiginous nerve roots are present in the subarachnoid space (7). This condition has a clear causal relationship with central spinal stenosis, which is of great importance for the diagnosis of lumbar spinal stenosis (8).

Studies (4) have shown that the occurrence rate of RNRs in patients with lumbar spinal stenosis is between 33.8 and 42.3%, with risk factors including advanced age, female gender, and patients with severe neurological symptoms (9–11). Clinical manifestations are mostly similar to those seen with spinal stenosis such as leg pain with intermittent claudication and low back pain. Besides, the pathogenesis of RNRs is still unclear. Suzuki et al. (3) proposed a possible mechanism for the formation of RNRs in the 1980s: RNRs are most likely the pathological result of a chronic compression force at the level of spinal canal stenosis (12). Their study with histopathologic evaluation identified nerve fiber degeneration and neuronal loss due to continuous mechanical compression of the nerve roots, which were confined to the nerves in the narrowed section of the spinal canal [(13, 14); Figure 7]. In the present study, 30 patients underwent routine imaging with lumbar MRI after lumbar interbody fusion surgery. The lumbar spine MRI was obtained and reviewed 1 week after surgery with disappearance of RNRs noted in all cases. The rate of excellent and good outcomes was 66.7% based on evaluation using Fischgrund criteria.

Kirkaldy-Willis and Hill (15) noted that all treatments for spinal degenerative diseases (including surgical treatment) can alleviate the clinical symptoms but fail to deal with underlying fundamental degenerative processes to cure the disease. In this light, Spengler (16) stated that indications for surgery depend on the patient's need for improved quality of life in the future. Therefore, patients with RNRs on MRI are indicated for surgery, which doesn't rely on the presence of RNRs but is based on the presence of: severe pain in the lower extremities causing difficulty with activities of daily living, signs of objective nerve damage such as weakness, muscle atrophy, and neurogenic claudication symptoms which limit walking or standing of patients for longer than 3 months and can't be alleviated via non-surgical treatment.

The purpose of surgical treatment for patients with lumbar spinal stenosis is to enlarge the volume of the spinal canal, relieve nerve compression, and reconstruct the stability of the spine (17). For the group of patients who predominantly suffer from claudicatory leg pain, the key element of the surgery is

to successfully decompress the spinal nerves, thus encouraging us to treat these patients with posterior lumbar instrumented interbody fusion with total laminectomy. The advantage of this surgery is that extensive spinal canal decompression can be achieved by removing the lamina, facet joints, spinous processes, and associated ligaments.

Patients with RNRs often have adhesions around the cauda equina, thus requiring careful and meticulous technique when performing decompression of redundant nerve roots. Besides, it should be mentioned that thorough decompression is required to remove all elements of the spinal canal which can cause compression of nerve roots (bone spurs, hypertrophic ligamentum flavum, displaced intervertebral disc material, and hypertrophic facet joints) to restore nerve root freedom. For patients with lumbar spine MRI showing foraminal stenosis, decompression of the nerve root canal is also needed.

Due to the presence of RNRs, attention has been paid not only to abnormalities of the bone and soft tissues that make up the spinal canal, but also to the condition of the nerve roots within the dural sac. In patients with RNRs, the nerve root may be more tightly compressed. In the flexion position, the nerve root is elongated, and it is easy to produce distortion, entanglement, and adhesions over time. Furthermore, with the demyelination and fibrosis which may be associated with severe stenosis, the symptoms of low back and leg pain may be more severe and the prognosis after surgery will be worse. Ono et al. (9) pointed out that patients with RNRs are also featured with worse clinical manifestations and symptoms compared with other lumbar spinal stenosis patients. Chen et al. (18) showed that in 93 patients with lumbar spinal stenosis who underwent surgery, RNR patients had a poorer prognosis in post-operative pain, limb numbness, and walking ability than those without RNRs.

The present study showed that RNRs of the cauda equina are not uncommon in patients with lumbar spinal canal stenosis. RNRs of the cauda equine are frequently observed in the superior of the stenosis level (Upper) but can also be observed in both inferior and superior (Intermediate), and less frequently in inferior localizations (Lower) only (19). So, it is of great importance to classify different types of RNRs. To make a clear and vivid presentation, we use pattern diagrams and their corresponding MRI images to discuss a possible classification of RNRs which includes Upper, Lower and Intermediate RNRs (Figures 1–3).

REFERENCES

- Verbiest H. A radicular syndrome from developmental narrowing of the lumbar vertebral canal. *J Bone Joint Surg.* (1954) 36-B:230–7. doi: 10.1302/0301-620X.36B2.230
- Cressman MR, Pawl RP. Serpentine myelographic defect caused by a redundant nerve root. *J Neurosurg.* (1968) 28:391–3.
- Suzuki K, Ishida Y, Ohmori K, Sakai H, Hashizume Y. Redundant nerve roots of the cauda equina: clinical aspects and consideration of pathogenesis. *Neurosurgery.* (1989) 24:521–8. doi: 10.1097/00006123-198904000-00006

This study has several limitations. Due to the small sample size of this case group, it is difficult to comment on its generalizability. In addition, because of the lack of a control group, there may be bias in the evaluation of our surgical treatment, and our results can't be compared against other surgical or non-surgical options. In the future, the studies on the relationship of nerve root redundancy and the lumbar spinal stenosis degree with outcome after different surgical procedures should be conducted.

CONCLUSION

Posterior lumbar decompression and instrumented interbody fusion and internal fixation can effectively decompress stenotic segments and free nerve roots, alleviate the redundancy of the nerve roots and improve low back and leg pain. Moreover, while RNRs are relatively common in patients with lumbar spinal stenosis, patients with RNRs often present with worse clinical symptoms and prognosis (20, 21). Therefore, when evaluating patients with lumbar spinal stenosis, the lumbar spine MRI should be used routinely to not only assess the degree and location of canal stenosis but also to evaluate the position and state of the nerve roots in order to provide a clearer understanding and better prognostic guidance when considering surgical options.

DATA AVAILABILITY STATEMENT

The original contributions presented in the study are included in the article/supplementary material, further inquiries can be directed to the corresponding author/s.

ETHICS STATEMENT

The studies involving human participants were reviewed and approved by Ningbo No.6 Hospital. Written informed consent for participation was not required for this study in accordance with the national legislation and the institutional requirements. Written informed consent was obtained from the individual(s) for the publication of any potentially identifiable images or data included in this article.

AUTHOR CONTRIBUTIONS

All authors listed have made a substantial, direct and intellectual contribution to the work, and approved it for publication.

- Tsuji H, Tamaki T, Itoh T, Yamada H, Motoe T, Tatezaki S, et al. Redundant nerve roots in patients with degenerative lumbar spinal stenosis. *Spine.* (1985) 10:72–82.
- Genevay S, Atlas SJ. Lumbar spinal stenosis. *Best Pract Res Clin Rheumatol.* (2010) 24:253–65. doi: 10.1016/j.berh.2009.11.001
- Ganz JC. Lumbar spinal stenosis: postoperative results in terms of preoperative posture-related pain. *J Neurosurg.* (1990) 72:71–4. doi: 10.3171/jns.1990.72.1.0071
- Hakan T, Celikoglu E, Aydoseli A, Demir K. The redundant nerve root syndrome of the cauda equina. *Turk Neurosurg.* (2008) 18:204–6. doi: 10.1016/j.surneu.2007.11.008

8. Nogueira-Barbosa MH, Savarese LG, Herrero CFPDS, Defino HLA. Redundant nerve roots of the cauda equina: review of the literature. *Radiol Brasil.* (2012) 45:155–9. doi: 10.1590/S0100-39842012000300007
9. Ono A, Suetsuna F, Irie T. Clinical significance of the redundant nerve roots of the cauda equina documented on magnetic resonance imaging. *J Neurosurg Spine.* (2007) 7:27–32. doi: 10.3171/SPI-07/07/027
10. Gulati DR, Rout D. Myelographic block caused by redundant lumbar nerve root. Case report. *J Neurosurg.* (1973) 38:504–5. doi: 10.3171/jns.1973.38.4.0504
11. Pau A, Turtas S. Redundant nerve roots of the cauda equina. A case report. *Acta Neurochirur.* (1976) 33:311–7. doi: 10.1007/BF01886678
12. George E, Moiel RH, Bragg TG. The “redundant” or “knotted” nerve root: a clue to spondylotic cauda equina radiculopathy. Case report. *J Neurosurg.* (1970) 32:252–4. doi: 10.3171/jns.1970.32.2.0252
13. Suzuki K, Takatsu T, Inoue H, Teramoto T, Ishida Y, Ohmori K. Redundant nerve roots of the cauda equina caused by lumbar spinal canal stenosis. *Spine.* (1992) 17:1337–42.
14. Zheng F, Farmer JC, Sandhu HS, O’Leary PF. A novel method for the quantitative evaluation of lumbar spinal stenosis. *HSS J.* (2006) 2:136–40. doi: 10.1007/s11420-006-9006-3
15. Kirkaldy-Willis WH, Hill RJ. A more precise diagnosis for low-back pain. *Spine.* (1979) 4:102–9.
16. Spengler DM. Degenerative stenosis of the lumbar spine. *J Bone Joint Surg Am.* (1987) 69:305–8.
17. Fritsch CG, Ferreira ML, Maher CG, Herbert RD, Pinto RZ, Koes B, et al. The clinical course of pain and disability following surgery for spinal stenosis: a systematic review and meta-analysis of cohort studies. *Eur Spine J.* (2017) 26:324–35. doi: 10.1007/s00586-016-4668-0
18. Chen J, Wang J, Wang B, Xu H, Lin S, Zhang H. Post-surgical functional recovery, lumbar lordosis, and range of motion associated with MR-detectable redundant nerve roots in lumbar spinal stenosis. *Clin Neurol Neurosurg.* (2016) 140:79–84. doi: 10.1016/j.clineuro.2015.11.016
19. Gke E, Beyhan M. Magnetic resonance imaging findings of redundant nerve roots of the cauda equina. *World J Radiol.* (2021) 13:29–39. doi: 10.4329/wjr.v13.i1.29
20. Cong L, Zhu Y, Yan Q, Tu G. A meta-analysis on the clinical significance of redundant nerve roots in symptomatic lumbar spinal stenosis. *World Neurosurg.* (2017) 105:95–101. doi: 10.1016/j.wneu.2017.05.103
21. Villafañe FE, Harvey A, Kettner N. Redundant nerve root in a patient with chronic lumbar degenerative canal stenosis. *J Chiropractic Med.* (2017) 16:236–41. doi: 10.1016/j.jcm.2017.02.001

Conflict of Interest: The authors declare that the research was conducted in the absence of any commercial or financial relationships that could be construed as a potential conflict of interest.

Publisher’s Note: All claims expressed in this article are solely those of the authors and do not necessarily represent those of their affiliated organizations, or those of the publisher, the editors and the reviewers. Any product that may be evaluated in this article, or claim that may be made by its manufacturer, is not guaranteed or endorsed by the publisher.

Copyright © 2021 Xu and Hu. This is an open-access article distributed under the terms of the Creative Commons Attribution License (CC BY). The use, distribution or reproduction in other forums is permitted, provided the original author(s) and the copyright owner(s) are credited and that the original publication in this journal is cited, in accordance with accepted academic practice. No use, distribution or reproduction is permitted which does not comply with these terms.



Comparison of C2-3 Pedicle Screw Fixation With C2 Spinous Muscle Complex and Iliac Bone Graft for Instable Hangman Fracture

Dingli Xu¹, Kaifeng Gan², Yang Wang³, Yulong Wang¹ and Weihu Ma^{3*}

¹ The Affiliated Hospital of Medical School, Ningbo University, Ningbo, China, ² Ningbo City Medical Treatment Center Lihuli Hospital, Ningbo, China, ³ Ningbo No.6 Hospital, Ningbo, China

OPEN ACCESS

Edited by:

Gun Woo Lee,
Yeungnam University, South Korea

Reviewed by:

Wen-Fei Ni,
The Second Affiliated Hospital and
Yuying Children's Hospital of Wenzhou
Medical University, China
Baorong He,
Xi'an Honghui Hospital, China

*Correspondence:

Weihu Ma
944973037@qq.com

Specialty section:

This article was submitted to
Orthopedic Surgery,
a section of the journal
Frontiers in Surgery

Received: 10 June 2021

Accepted: 18 October 2021

Published: 26 November 2021

Citation:

Xu D, Gan K, Wang Y, Wang Y and
Ma W (2021) Comparison of C2-3
Pedicle Screw Fixation With C2
Spinous Muscle Complex and Iliac
Bone Graft for Instable Hangman
Fracture. *Front. Surg.* 8:723078.
doi: 10.3389/fsurg.2021.723078

Purpose: To compare the effect between C2 spinous muscle complex graft and iliac bone graft in C2-3 pedicle screw fixation for instable Hangman fracture. Using axial spinous muscle complex instead of iliac bone for instable Hangman fracture can decrease neck pain, bone donor site complication, and operation time.

Method: The outcomes of C2-3 pedicle screw fixation with C2 spinous muscle complex were compared with iliac bone graft in 18 and 21 patients with instable Hangman fracture. The mean age was 49.1 ± 15.8 years in the complex group and 55.3 ± 12.2 years in the Iliac group, and the mean time to surgery of the patients was 3.3 ± 0.6 days in the complex group and 3.6 ± 0.9 days in the iliac group. Outcome measures including operation time, blood loss, visual analog scale (VAS) for pain, Japanese orthopedic association score (JOA), American spine injury association classification (ASIA), and bone fusion time were collected from medical records. In addition, the postoperative complications were also recorded.

Results: There were significant differences in operation time and intraoperative blood loss between the two groups ($P < 0.01$). Also a significant difference was found in VAS score and JOA score between the two groups ($P = 0.0012$ and $P < 0.001$, respectively) at 1-month follow-up, whereas, no significant difference was found at other visit time. In the final visit, all patients showed good bone fusion, and two patients shows incision edema and exudation in the iliac group.

Conclusion: C2-3 pedicle screw fixation with C2 spinous muscle complex graft maybe a feasible and safe procedure for instable Hangman fracture.

Keywords: instable Hangman fracture, C2 spinous muscle complex, donor-site complications, surgical procedures, bone graft

INTRODUCTION

Hangman fracture, known as traumatic spondylolisthesis of the axis, was first discovered in 1866 in dead criminals from judicial hanging and was named by Schneider et al. in 1965 (1). According the Levine and Edwards classification (2), fractures with severe circumferential disco-ligamentous injuries and a variable degree of translation or angulation of the C2 on the C3

vertebra are thought to be unstable and require rigid immobilization. The commonly used surgical methods are posterior C2-3 pedicle screw fixation and iliac bone graft, which have shown good clinical outcomes (3). Biomechanical studies in cadavers have suggested that posterior C2-3 fusion is possibly better than other techniques such as anterior graft and plating and C2 par fixation (4). However, some researchers have reported neck pain and donor-site complications such as pain, hematoma, oedema, infection, and pseudoarthrosis (5).

Therefore, researchers have increased interest in the axial spinous process. Sinha and Goyal used the C2 spinous process as a bone graft and waded it using titanium cables for C1-2 posterior fusion in five patients with atlantoaxial dislocation to minimize the donor-site complications and posterior neck pain (6). Similarly, our group reported that 27 patients with atlantoaxial fracture who were treated with C1-2 pedicle screw fixation combined with axial spinous muscle complex had satisfactory recovery (7). Moreover, we used the axial spinous process in atlantoaxial surgery (8). Besides, many studies reported that the preservation of muscle attachments of cervical spine is beneficial in cervical ROM and axial symptom. Riew et al. reviewed 11 articles on preserving the C2 muscle attachments and/or C7-preserving cervical laminoplasty and reported a similar result that preservation of the posterior cervical muscle has better clinical outcomes (9). Preservation of the cervical muscles such as the semispinalis cervicis muscle prevents postoperative neck pain and maintains cervical alignment.

In this study, we performed posterior C2-3 pedicle screw fixation using the axial spinous muscle complex to minimize the posterior complications of unstable Hangman fractures, and the schematic of the C2 spinous muscle complex graft is shown in **Figure 1**. We compared the outcomes between pedicle screw fixation with axial spinous muscle complex and with iliac bone grafts for unstable Hangman fractures.

MATERIALS AND METHODS

In this study, we retrospectively reviewed patients with unstable Hangman fractures who were treated with C2-3 pedicle screw fixation with axial spinous muscle complex or iliac bone graft between September 2014 and April 2017 at Ningbo Number 6 Hospital. All procedures involving human participants were performed in accordance with the ethical standards of the institution and the 1964 Helsinki Declaration, and its later amendments or comparable ethical standards. The study was approved by the Bioethics Committee of the Ningbo No.6 Hospital of Ningbo University. All patients provided informed consent.

Inclusion criteria were as follows: (1) age >18 years; (2) presence of unstable Hangman fracture; and (3) absence of abnormal cervical vertebral abnormalities. Exclusion criteria were as follows: (1) presence of severe diseases such as cardiopathy; (2) presence of diseases that may influence bone structure, such as rheumatoid arthritis; and (3) absence of intact follow-up medical records. A total of 39 patients (complex group: 18 patients and iliac group: 21 patients) were enrolled

in this retrospective comparative study (**Figure 2**). The clinical and demographic characteristics of the patients are presented in **Table 1**.

Three patients in the complex group had associated injury, which included distal radial fracture (one patient) and proximal ulnar fracture (two patients). Similarly, patients in the iliac group also had associated injury, which included proximal humeral fractures (two patients). The associated injuries were treated conservatively.

Outcome Evaluation

Clinical outcomes were measured using the visual analog scale (VAS) for pain (from 0 to 10, no pain to most severe pain) (10) and Japanese orthopedic association score (JOA) for cervical function, which consisted of four parts (from 0 to 17, higher score means better cervical function) (11). Radiological outcomes such as bone fusion and correct positioning were evaluated by cervical X-ray and CT-scan. Radiological assessments were performed by an experienced radiologist and a spine surgeon who worked together to establish consensus, but were not involved in the treatment or reporting of results.

Surgical Technique

All patients were first treated with skull traction for 1–2 days with forces ranging from 3 to 5 kg for some degree of reduction.

C2-3 Pedicle Screw Fixation With the C2 Spinous Muscle Complex

The patients were positioned prone on the surgical table under general anesthesia, and their heads were fixed with a Mayfield frame (Integra LifeScience. Inc., American). Thereafter, a midline incision was made and the C2-3 posterior structures were exposed; however, the muscles were not detached from the C2 spinous process. The C2 pedicle screw (Shanghaisanyou, China) was inserted in the lateral mass of the C2, with a gantry angle of 15°–25° and an inward camber angle of 20°–25°. Subsequently, a C3 pedicle screw was inserted in the lateral mass of the C3 with a gantry angle of ~10° and an inward camber angle of 35°–45°. Thereafter, the posterior three-fourth of the C2 spinous was cut by a bone saw and displaced into the preprocessed C2-3 posterior arch. A rod was placed combined with pedicle screws to ensure tight contact between the C2 spinous muscle complex and the bone graft bed of the C2-3 posterior arch (**Figure 3**).

C2-3 Pedicle Screw Fixation With the Iliac Bone Graft

The patients were positioned prone on the surgical table under general anesthesia, and their heads were fixed with a Mayfield frame (Integra LifeScience. Inc., Plainsboro, NJ, USA). Firstly, the iliac bones were obtained. Thereafter, a midline incision was made and the C2-3 posterior structures were exposed. The C2 pedicle screw (Shanghaisanyou, China) was inserted in the lateral mass of the C2, with a gantry angle of 15°–25° and an inward camber angle of 20°–25°. Subsequently, a C3 pedicle screw was inserted in the lateral mass of the C3, with a gantry angle of ~10° and an inward camber angle of 35°–45°. The bone graft bed was prepared in the C2-3 posterior arch and placed on the iliac bone.

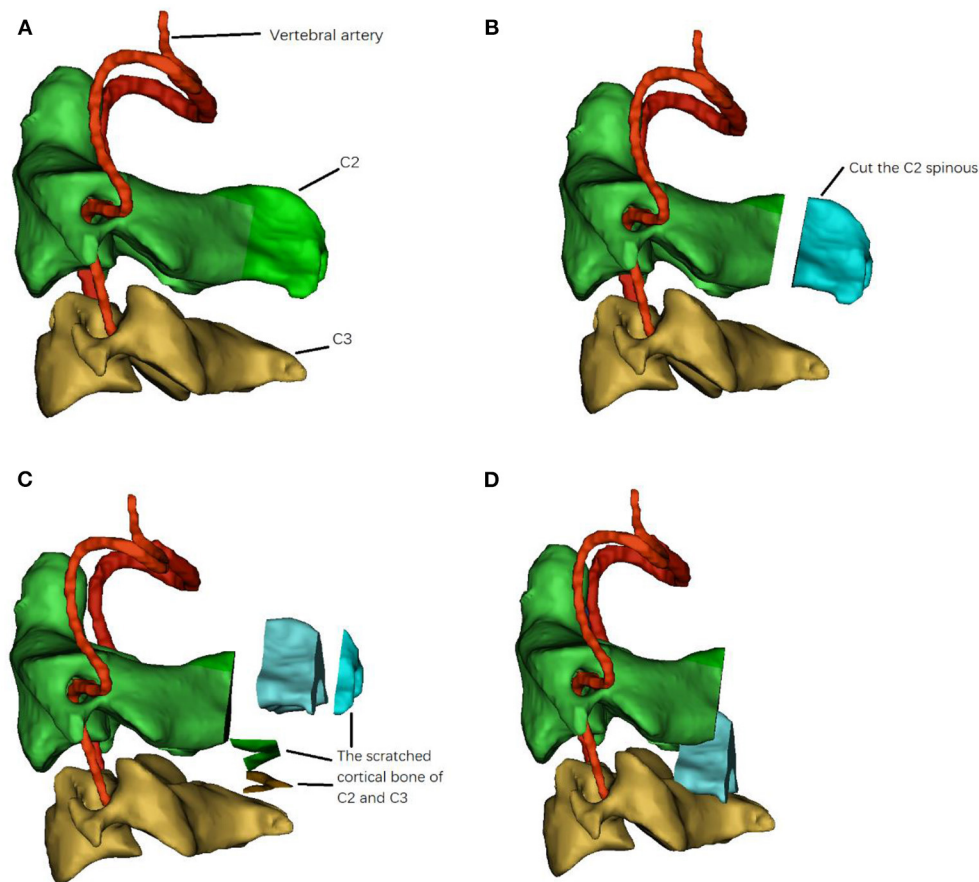


FIGURE 1 | The diagram of C2 spinous muscle complex graft. **(A)** the anatomy of C2, C3 and vertebral artery, **(B)** Cut down the posterior 3/4 of C2 spinous, **(C)** scratch the cortical of C2 and C3 for bone graft, **(D)** displace the C2 spinous muscle complex graft into C2-3 posterior arch.

The rod was placed in combination with pedicle screws to ensure tight contact between the iliac bone and the bone graft bed.

The entire procedure was monitored under C-arm fluoroscopy. At the end of the surgery, CT scan was performed to confirm the fractural realignment and screw placement.

Postoperative Protocol

The same postoperative protocol was applied in both the groups in this study. Patients were allowed out of bed on the second postoperative day with neck collar support, immobilized for at least 3 months, and kept away from smoking. After 2 weeks, the sutures were removed. The radiological outcomes and clinical outcomes were evaluated at each follow-up visit.

Statistical Analysis

SPSS for Windows, Version 19.0, (SPSS Inc., Chicago, IL, USA) was used for all statistical analyses. Descriptive statistics are presented as mean \pm standard deviation (SD). The means of parametric and non-parametric variables were compared between the two groups using the independent-samples *t*-test and the Mann-Whitney *U* test, respectively. The Chi-square

test was used to compare categorical variables between the two groups. Statistical significance was set at $P < 0.05$.

RESULTS

In this study, all patients were followed up for >24 months, and no statistical difference was found in the clinical and demographic characteristics of the two groups (**Table 1**). Differences between preoperative and postoperative VAS and JOA scores were detected, without statistical significance (independent-samples *t*-test; $P > 0.05$). At 1-month follow-up visit, significant improvement in the VAS and JOA scores was found (independent-samples *t*-test; $P < 0.05$). Significant differences in the operative time, blood loss, and outcome measures were found between the two groups (**Table 2**). All patients had bone fusion at the final follow-up visit, and none of the patients had internal fixation failure.

Postoperative Complications

Complication data were obtained from the medical records. In the iliac group, four (19.0%) patients had superficial wound oedema in the donor site and one (4.8%) patient had exudation

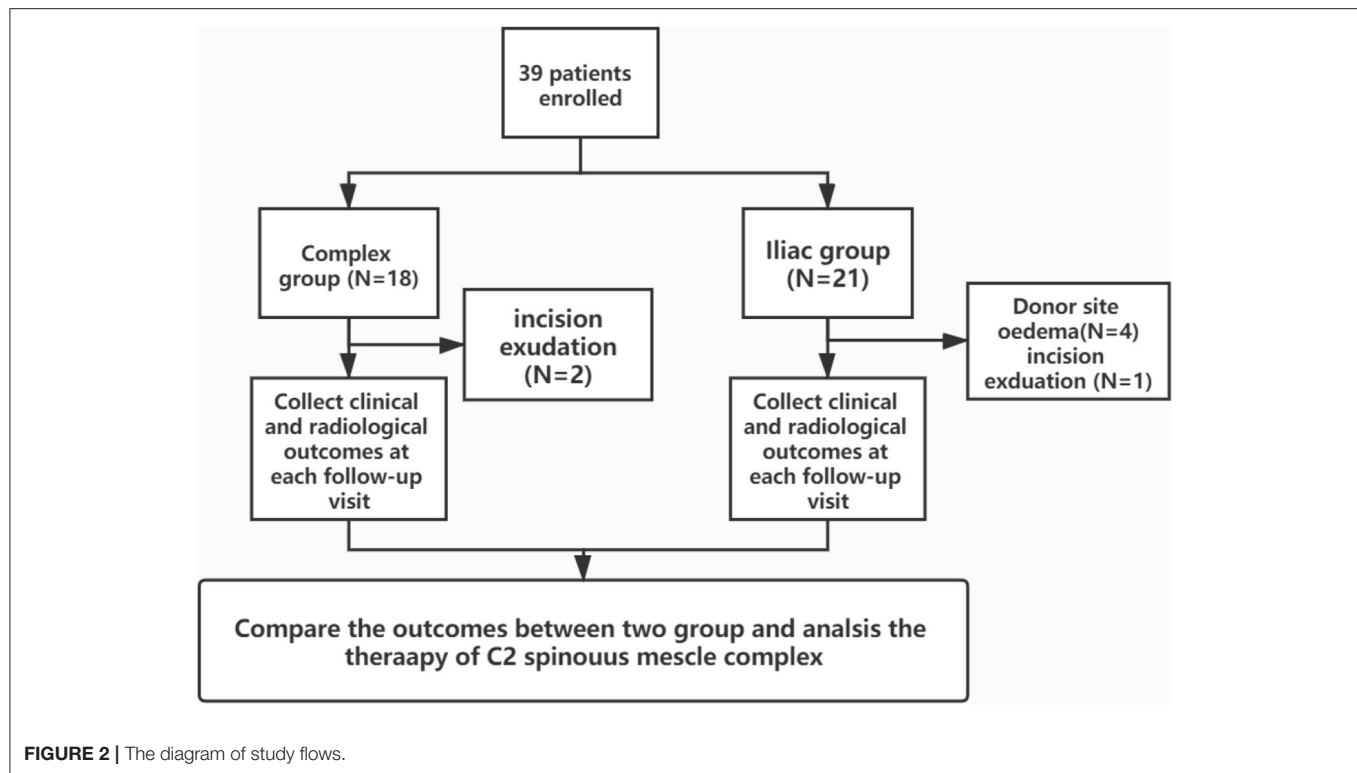


TABLE 1 | The clinical and demographic characteristics of the two groups.

Variable	Complex group (n = 18)	Iliac group (n = 21)	p-value*
Mean age, years	49.1 ± 15.8	55.3 ± 12.2	0.16
Gender, n (%)			
Male	12 (66.7%)	13 (61.9%)	0.51
Female	6 (33.3%)	8 (38.1%)	
Fracture cause, n (%)			
Fall	5 (27.8%)	6 (28.6)	0.80
Vehicle injure	10 (55.5%)	13 (61.9%)	
Other	3 (16.7%)	2 (9.5%)	
Fracture type, n (%)**			
II	11 (61.1%)	12 (57.1%)	0.85
IIA	4 (22.2%)	4 (19.1%)	
III	3 (16.7%)	5 (23.8%)	
Mean time to surgery, days	3.3 ± 0.6	3.6 ± 0.7	0.29

*Independent-samples t-test or Mann-Whitney U test for continuous variables; chi-squared test for categorical variables.

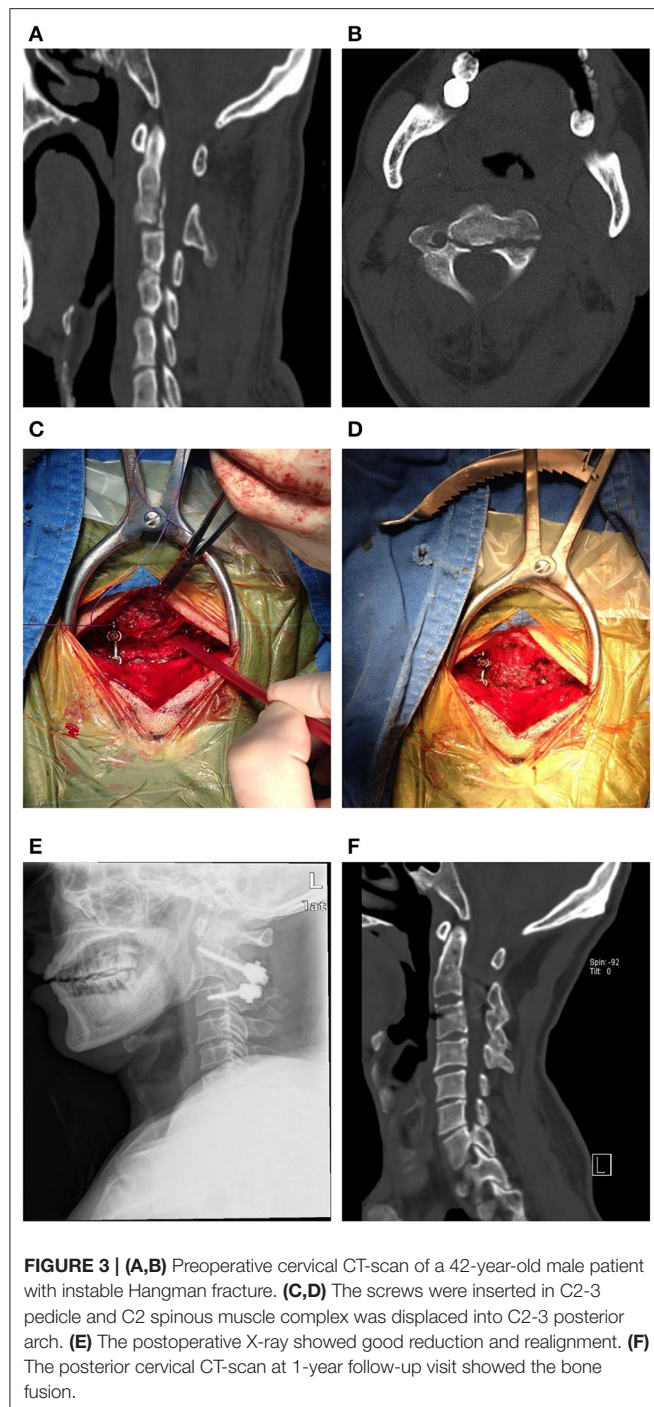
**Levine and Edwards classification.

in the cervical midline incision, which was successfully managed by dressing exchange. Three (14.3%) patients who complained of donor-site pain and five (23.8%) patients who complained of neck pain were treated conservatively. In the complex group, two (11.1%) patients had exudation in the cervical midline incision, which was successfully managed by conservation treatment. A significant difference in postoperative complications was found between the two groups (Chi-square test, $P < 0.05$).

DISCUSSION

Instable Hangman fracture or traumatic spondylolisthesis of the axis is defined as the bilateral fracture of the axial pars interarticularis combined with severe circumferential disc and ligamentous injuries or a variable degree of translation or angulation of the C2 on the C3 vertebra (12). Most of the unstable hangman fractures are preferentially treated with surgery, including anterior graft and plating, C2 par fixation, C2-3 posterior pedicle screw fixation, and C2 lag screw-rod fixation (13–17). Recently, the most common surgical procedure that provides better biomechanical strength and has a short learning curve is C2-3 posterior pedicle screw fixation (18). Jeong et al. reported that the VAS and NDI scores of 13 patients with unstable Hangman fracture who underwent posterior C2-3 fixation had significantly improved after operation and were maintained up to the 12-month follow-up visit (final visit) (19). Similarly, Our group reported that 35 patients with unstable Hangman fracture who were treated with C2–C3 posterior short-segment fixation and fusion had satisfactory reduction and realignment without complications or reoperation (20).

However, some patients treated with C2-3 pedicle screw fixation and fusion may complain of neck pain and donor-site complications. Lang et al. reported that six patients with instable Hangman fracture who underwent minimally invasive C2-3 pedicle screw fixation showed better recovery in neck pain than those patients who were treated with conventional open surgery (21). Skeppholm et al. reported that 45 patients who underwent cervical decompression with bone graft showed donor-site complications at 1-year follow-up visit (22). Hence,



we used C2-3 pedicle screw fixation with the C2 spinous muscle complex for instable Hangman fracture to minimize neck pain and donor-site complications.

In this study, the mean operative time was 2.2 h in the complex group and 2.8 h in the iliac group, and the mean blood loss was 224.4 mL in the complex group and 293.6 mL in the iliac group. The operative time and blood loss were significantly less in the complex group than in the iliac group ($P < 0.01$). Harvesting

TABLE 2 | Comparison of surgical characteristics and outcome measures between two groups.

Variable	Complex group (n = 18)	Iliac group (n = 21)	p-value*
Blood loss, ml	224.4 ± 35.8	293.6 ± 45.6	<0.01 [‡]
Operation time, h	2.2 ± 0.24	2.8 ± 0.32	<0.01 [‡]
Mean VAS			
Preoperative	5.5 ± 1.2	5.1 ± 0.8	0.48
1 month postoperative	2.5 ± 0.5	3.0 ± 0.7	0.012 [‡]
6 months postoperative	1.1 ± 0.7	1.2 ± 0.6	0.21
12 months postoperative	0.8 ± 0.3	1.0 ± 0.4	0.12
24 months postoperative	0.5 ± 0.2	0.6 ± 0.3	0.52
Mean JOA			
Preoperative	10.8 ± 1.0	10.5 ± 1.1	0.46
1 month postoperative	14.0 ± 0.7	13.1 ± 1.0	<0.01 [‡]
6 months postoperative	15.2 ± 0.6	14.7 ± 0.8	0.34
12 months postoperative	16.1 ± 0.4	15.9 ± 0.6	0.62
24 months postoperative	16.4 ± 0.6	16.3 ± 0.3	0.35

*Independent-samples t-test for parametric variables; Mann-Whitney U test for non-parametric variables.

[‡]P-Value < 0.05.

VAS, visual analog scale score; JOA, Japanese orthopedic association score.

the autogenous iliac bone during surgery may result in longer operative time and greater blood loss.

The mean preoperative and 1-, 6-, 12-, and 24-months follow-up VAS scores were 5.5, 2.5, 1.1, 0.8, and 0.5, respectively, in the complex group and 5.1, 3.0, 1.2, 1.0, and 0.6, respectively, in the iliac group. A significant difference was found in the 1-month follow-up VAS scores of the two groups ($P < 0.05$). Similarly, a significant difference was found in the 1-month follow-up JOA scores of the two groups ($P < 0.05$). In addition, although differences in the JOA and VAS scores were detected at other visit times, they were non-significant ($P > 0.05$). Our group has reported that treatment with the C2 spinous muscle complex yields significantly superior outcomes with respect to operative time, blood loss, neck pain, and bone fusion time in patients with atlantoaxial instability (8). Lin et al. reported that 53 patients who were treated with open-door laminoplasty and unilateral preservation of the muscular-ligament complex had better cervical range of motion, C0-2 Cobb angle, and C2–C7 sagittal vertical axis than the 37 patients who underwent traditional open-door laminoplasty at the 16.7-month follow-up. Surgical damage to the posterior muscular-ligament complex may induce loss of cervical sagittal balance (23). Secer et al. reported that 27 patients with cervical spondylotic myelopathy underwent open-door laminoplasty with protection of muscles, and they yielded significant better results in neck ROM and cervical axial pain (24). Although, the axial spinous muscle complex preservation benefit in neck mobility postoperatively, Cheng et al. reported that 60 patients treated with cervical operation and reconstruction of C2 spinous process and muscle. Although the ROM in cervical spine has a decrease from $43.35^\circ \pm 7.55^\circ$ to $34.83^\circ \pm 7.41^\circ$, but it has been significantly improved compared with the traditional method (25).

Armaghani et al. reported that of the 50 patients treated with anterior cervical discectomy and iliac bone graft fusion, two patients had superficial wound infection and a postoperative hematoma and five patients complained of donor-site pain (26). In addition, Silber et al. reported that of the 134 patients who underwent cervical surgery with iliac crest bone graft, 35 patients had donor-site pain and 21 patients had abnormal sensation at donor site (27). In our study, three (14.3%) patients had donor-site pain, four (19.0%) patients had incision oedema, and two patients had neck pain in the iliac group. In the complex group, no patient had neck pain; however, two (11.1%) patients had exudation in the cervical midline incision. A significant difference was found in neck pain and donor-site complications between the two groups (chi-square test, $P < 0.05$).

Therefore, it is not uncommon for patients complaining of donor-site complications. Consequently, the use of the C2 spinous muscle complex to displace the iliac bone not only prevents donor-site complications, but also improves cervical function and neck pain.

This study has some limitations. First, the sample size was small and the follow-up period was short, and we can enroll more patients for our further study. Second, we did not obtain patients who had undergone rehabilitation treatment or other life habits, such as smoking and physical work, which may have affected the clinical outcomes to some degree.

In conclusion, although C2-3 pedicle screw fixation with iliac bone graft is a widely used treatment for unstable Hangman fractures, patients may experience donor-site complications and neck pain. The use of the C2 spinous muscle complex, instead of the iliac bone, may yield better outcomes such as preventing donor-site complications, better recovery of neck pain and cervical function, reducing the operative time, and decreasing blood loss. However, more research is required to

determine whether C2-3 pedicle screw fixation combined with C2 spinous muscle complex for unstable Hangman fractures can be performed prior to conventional C2-3 pedicle screw fixation with an iliac bone graft.

DATA AVAILABILITY STATEMENT

The raw data supporting the conclusions of this article will be made available by the authors, without undue reservation.

ETHICS STATEMENT

The studies involving human participants were reviewed and approved by the Bioethics Committee of the Ningbo No.6 Hospital of Ningbo University. The patients/participants provided written informed consent to participate in this study.

AUTHOR CONTRIBUTIONS

DX, KG, YaW, YuW, and WM contributed to the study conception, design, and commented on previous versions of the manuscript. Material preparation, data collection, and analysis were performed by DX, KG, YaW, and WM. The first draft of the manuscript was written by DX. All authors read and approved the final manuscript.

FUNDING

This study was conducted in accordance with the ethical principles of the Helsinki Declaration and was approved by the Ethics Committee of Ningbo Number 6 Hospital (approval number: 2019003), and the Nature Science Foundation of Zhejiang (LY19H060002).

REFERENCES

- Schneider RC, Livingston KE, Cave AJ, Hamilton G. "Hangman's fracture" of the cervical spine. *J Neurosurg.* (1965) 22:141–54. doi: 10.3171/jns.1965.22.2.0141
- Levine AM, Edwards CC. The management of traumatic spondylolisthesis of the axis. *J Bone Joint Surg Am Vol.* (1985) 67:217–26. doi: 10.2106/00004623-198567020-00007
- Salunke P, Karthigeyan M, Sahoo SK, Prasad PK. Multiplanar realignment for unstable Hangman's fracture with Posterior C2-3 fusion: a prospective series. *Clin Neurol Neurosurg.* (2018) 169:133–8. doi: 10.1016/j.clineuro.2018.03.024
- Duggal N, Chamberlain RH, Perez-Garza LE, Espinoza-Larios A, Sonntag VK, Crawford NR. Hangman's fracture: a biomechanical comparison of stabilization techniques. *Spine.* (2007) 32:182–7. doi: 10.1097/01.brs.0000251917.83529.0b
- Scheerlinck LM, Muradin MS, van der Bilt A, Meijer GJ, Koole R, Van Cann EM. Donor site complications in bone grafting: comparison of iliac crest, calvarial, and mandibular ramus bone. *Int J Oral Maxillofac Implants.* (2013) 28:222–7. doi: 10.11607/jomi.2603
- Sinha AK, Goyal S. Myoarchitectonic advancement of the C2 spinous process for C1-C2 posterior fusion: a novel technique. *J Neurosci Rural Pract.* (2015) 6:267–71. doi: 10.4103/0976-3147.153237
- Ma W, Zhao H, Jiang W, Xu N, Hu X, Li G, et al. The effects of axial spinous process-muscle-vasculum complex transplantation for posterior atlantoaxial fusion. *Chin J Orthop.* (2018) 15:927–34. doi: 10.3760/cma.j.issn.0253-2352.2018.15.005
- Xu D, Jiang W, Ruan C, Wang Y, Hu X, Chen Y, et al. Efficacy comparison of posterior atlantoaxial screw-rod fixation combined with spinous process muscle-vessel complex bone graft or iliac bone graft for atlantoaxial instability. *Chin J Trauma.* (2019) 10:871–9.
- Riew KD, Raich AL, Dettori JR, Heller JG. Neck pain following cervical laminoplasty: does preservation of the C2 muscle attachments and/or C7 matter? *Evid Based Spine Care J.* (2013) 4:42–53. doi: 10.1055/s-0033-1341606
- Dixon JS, Bird HA. Reproducibility along a 10 cm vertical visual analogue scale. *Ann Rheum Dis.* (1981) 40:87–9. doi: 10.1136/ard.40.1.87
- Tetreault L, Kopjar B, Nouri A, Arnold P, Barbagallo G, Bartels R, et al. The modified Japanese orthopaedic association scale: establishing criteria for mild, moderate and severe impairment in patients with degenerative cervical myelopathy. *Eur Spine J.* (2017) 26:78–84. doi: 10.1007/s00586-016-4660-8
- Effendi B, Roy D, Cornish B, Dussault RG, Laurin CA. Fractures of the ring of the axis. A classification based on the analysis of 131 cases. *J Bone Joint Surg Br Vol.* (1981) 63-b:319–27. doi: 10.1302/0301-620X.63B3.7263741
- Wang S, Wang Q, Yang H, Kang J, Wang G, Song Y, et al. Novel technique for unstable Hangman's fracture: lag screw-rod (LSR) technique. *Eur Spine J.* (2017) 26:1284–90. doi: 10.1007/s00586-016-4630-1
- Wang L, Liu C, Zhao Q, Tian J. Posterior pedicle screw fixation for complex atlantoaxial fractures with atlanto-dental interval of ≥ 5 mm

- or C2-C3 angulation of ≥ 11 degrees. *J Orthop Surg Res.* (2014) 9:104. doi: 10.1186/s13018-014-0104-5
15. Ge C, Hao D, He B, Mi B. Anterior cervical discectomy and fusion versus posterior fixation and fusion of C2-3 for unstable hangman's fracture. *J Spinal Disord Techn.* (2015) 28:E61–66. doi: 10.1097/BSD.0000000000000150
 16. Xu H, Zhao J, Yuan J, Wang C. Anterior discectomy and fusion with internal fixation for unstable hangman's fracture. *Int Orthop.* (2010) 34:85–8. doi: 10.1007/s00264-008-0658-0
 17. Salunke P, Sahoo SK, Krishnan P, Chatterjee D, Sodhi HB. Are C2 pars-pedicle screws alone for type II Hangman's fracture overrated? *Clin Neurol Neurosurg.* (2016) 141:7–12. doi: 10.1016/j.clineuro.2015.11.019
 18. Chittiboina P, Wylen E, Ogden A, Mukherjee DP, Vannemreddy P, Nanda A. Traumatic spondylolisthesis of the axis: a biomechanical comparison of clinically relevant anterior and posterior fusion techniques. *J Neurosurg Spine.* (2009) 11:379–87. doi: 10.3171/2009.4.SPINE08516
 19. Jeong DH, You NK, Lee CK. Posterior C2-C3 fixation for unstable Hangman's fracture. *Korean J Spine.* (2013) 10:165–9. doi: 10.14245/kjs.2013.10.3.165
 20. Ma W, Xu R, Liu J, Cho KH, Kim SH. Posterior short-segment fixation and fusion in unstable Hangman's fractures. *Spine.* (2011) 36:529–33. doi: 10.1097/BRS.0b013e3181d60067
 21. Lang Z, Tian W, Liu Y, Liu B, Yuan Q, Sun Y. Minimally invasive pedicle screw fixation using intraoperative 3-dimensional fluoroscopy-based navigation (CAMISS Technique) for hangman fracture. *Spine.* (2016) 41:39–45. doi: 10.1097/BRS.0000000000001111
 22. Skeppholm M, Olerud C. Pain from donor site after anterior cervical fusion with bone graft: a prospective randomized study with 12 months of follow-up. *Eur Spine J.* (2013) 22:142–7. doi: 10.1007/s00586-012-2456-z
 23. Lin S, Zhou F, Sun Y, Chen Z, Zhang F, Pan S. The severity of operative invasion to the posterior muscular-ligament complex influences cervical sagittal balance after open-door laminoplasty. *Eur Spine J.* (2015) 24:127–35. doi: 10.1007/s00586-014-3605-3
 24. Secer HI, Harman F, Aydar MH, Kahraman S. Open-door laminoplasty with preservation of muscle attachments of C2 and C7 for cervical spondylotic myelopathy: retrospective study. *Turk Neurosurg.* (2018) 28:257–62. doi: 10.5137/1019-5149.JTN.20007-17.1
 25. Cheng Z, Chen W, Yan S, Li W, Qian S. Expansive open-door cervical laminoplasty: *in situ* reconstruction of extensor muscle insertion on the c2 spinous process combined with titanium miniplates internal fixation. *Medicine (Baltimore).* (2015) 94:e1171. doi: 10.1097/MD.0000000000001171
 26. Armaghani SJ, Even JL, Zern EK, Braly BA, Kang JD, Devin CJ. The evaluation of donor site pain after harvest of tricortical anterior iliac crest bone graft for spinal surgery: a prospective study. *Spine.* (2016) 41:E191–196. doi: 10.1097/BRS.0000000000001201
 27. Silber JS, Anderson DG, Daffner SD, Brislin BT, Leland JM, Hilibrand AS, et al. Donor site morbidity after anterior iliac crest bone harvest for single-level anterior cervical discectomy and fusion. *Spine.* (2003) 28:134–9. doi: 10.1097/00007632-200301150-00008

Conflict of Interest: The authors declare that the research was conducted in the absence of any commercial or financial relationships that could be construed as a potential conflict of interest.

Publisher's Note: All claims expressed in this article are solely those of the authors and do not necessarily represent those of their affiliated organizations, or those of the publisher, the editors and the reviewers. Any product that may be evaluated in this article, or claim that may be made by its manufacturer, is not guaranteed or endorsed by the publisher.

Copyright © 2021 Xu, Gan, Wang, Wang and Ma. This is an open-access article distributed under the terms of the Creative Commons Attribution License (CC BY). The use, distribution or reproduction in other forums is permitted, provided the original author(s) and the copyright owner(s) are credited and that the original publication in this journal is cited, in accordance with accepted academic practice. No use, distribution or reproduction is permitted which does not comply with these terms.



A Novel Three-Dimensional Computational Method to Assess Rod Contour Deformation and to Map Bony Fusion in a Lumbopelvic Reconstruction After En-Bloc Sacrectomy

Peter Endre Eltes^{1,2*†}, Mate Turbucz^{1,3†}, Jennifer Fayad^{1,4}, Ferenc Bereczki^{1,3}, György Szóke⁵, Tamás Terebessy⁵, Damien Lacroix⁶, Peter Pal Varga⁷ and Aron Lazary^{2,7}

OPEN ACCESS

Edited by:

Ralph Jasper Mobbs,
University of New South
Wales, Australia

Reviewed by:

Alexandre Terrier,
Swiss Federal Institute of Technology
Lausanne, Switzerland
Liang Jiang,
Peking University Third
Hospital, China

*Correspondence:

Peter Endre Eltes
eltespeter@yahoo.com

[†]These authors have contributed
equally to this work

Specialty section:

This article was submitted to
Orthopedic Surgery,
a section of the journal
Frontiers in Surgery

Received: 20 April 2021

Accepted: 24 November 2021

Published: 05 January 2022

Citation:

Eltes PE, Turbucz M, Fayad J,
Bereczki F, Szóke G, Terebessy T,
Lacroix D, Varga PP and Lazary A
(2022) A Novel Three-Dimensional
Computational Method to Assess Rod
Contour Deformation and to Map
Bony Fusion in a Lumbopelvic
Reconstruction After En-Bloc
Sacrectomy. *Front. Surg.* 8:698179.
doi: 10.3389/fsurg.2021.698179

¹ In Silico Biomechanics Laboratory, National Center for Spinal Disorders, Buda Health Center, Budapest, Hungary,

² Department of Spine Surgery, Semmelweis University, Budapest, Hungary, ³ School of PhD Studies, Semmelweis University, Budapest, Hungary, ⁴ Department of Industrial Engineering, Alma Mater Studiorum, Università di Bologna, Bologna, Italy, ⁵ Department of Orthopaedics, Semmelweis University, Budapest, Hungary, ⁶ INSIGNEO Institute for In Silico Medicine, Department of Mechanical Engineering, The University of Sheffield, Sheffield, United Kingdom, ⁷ National Center for Spinal Disorders, Buda Health Center, Budapest, Hungary

Introduction: En-bloc resection of a primary malignant sacral tumor with wide oncological margins impacts the biomechanics of the spinopelvic complex, deteriorating postoperative function. The closed-loop technique (CLT) for spinopelvic fixation (SPF) uses a single U-shaped rod to restore the spinopelvic biomechanical integrity. The CLT method was designed to provide a non-rigid fixation, however this hypothesis has not been previously tested. Here, we establish a computational method to measure the deformation of the implant and characterize the bony fusion process based on the 6-year follow-up (FU) data.

Materials and Methods: Post-operative CT scans were collected of a male patient who underwent total sacrectomy at the age of 42 due to a chordoma. CLT was used to reconstruct the spinopelvic junction. We defined the 3D geometry of the implant construct. Using rigid registration algorithms, a common coordinate system was created for the CLT to measure and visualize the deformation of the construct during the FU. In order to demonstrate the cyclical loading of the construct, the patient underwent gait analysis at the 6th year FU. First, a region of interest (ROI) was selected at the proximal level of the construct, then the deformation was determined during the follow-up period. In order to investigate the fusion process, a single axial slice-based voxel finite element (FE) mesh was created. The Hounsfield values (HU) were determined, then using an empirical linear equation, bone mineral density (BMD) values were assigned for every mesh element, out of 10 color-coded categories (1st category = 0 g/cm³, 10th category 1.12 g/cm³).

Results: Significant correlation was found between the number of days postoperatively and deformation in the sagittal plane, resulting in a forward bending tendency

of the construct. Volume distributions were determined and visualized over time for the different BMD categories and it was found that the total volume of the elements in the highest BMD category in the first postoperative CT was 0.04 cm^3 , at the 2nd year, FU was 0.98 cm^3 , and after 6 years, it was 2.30 cm^3 .

Conclusion: The CLT provides a non-rigid fixation. The quantification of implant deformation and bony fusion may help understate the complex lumbopelvic biomechanics after sacrectomy.

Keywords: computational method, sacrectomy, bony fusion, bone mineral density, lumbopelvic reconstruction, implant deformation, biomechanics, computed tomography

INTRODUCTION

Sacral tumors are rare pathologies, and their management typically generates a complex medical problem (1). The most common primary sacral tumors are chordomas, representing 40% of all primary sacral neoplasms (2). Chordoma is a malignant mesenchymal tumor with notochordal origin (3) characterized by a high recurrence rate and a very limited response to non-surgical treatments. The surgical treatment is one of the most challenging fields in spine surgery because of the complicated anatomy of the sacral site. In most cases, only en-bloc surgical procedures, such as partial or total sacrectomy can guarantee optimal local control; but several problems such as bowel, bladder and sexual dysfunction; infection; massive blood loss; and spinopelvic instability can be associated with these surgeries (4, 5).

Beyond the primary goal of the surgery (e.g., wide, en-bloc resection of the tumor mass), the optimal spinopelvic reconstruction, focusing on biomechanical stability and soft tissue restoration, is also indispensable (6). Several different techniques were developed for lumbopelvic stabilization after sacropelvic tumor resection (7). However, long-term follow-up data and comparative studies of the different techniques are rare or still missing. There is no gold standard, and relatively high complication rates (i.e., non-union, screw loosening, rod breakage) are reported with all reconstruction strategies (7, 8). The “en-bloc” resection of a sacral chordoma by performing a total sacrectomy with soft tissue and bony reconstruction, and lumbopelvic stabilization can be achieved with the closed-loop technique (1, 7). The technique uses a “U” shaped rod which is attached to the iliac and transpedicular screws to rebuild the spinopelvic connection (Figure 1). The closed-loop technique (CLT) was first introduced by Varga et al. (1), and it was adopted by others (9) and further developed (10).

The CLT method was designed to provide a non-rigid fixation, however this hypothesis has not been tested previously. Based on the hypothesis, implant deformation and continuous bone remodeling at the fusion site is expected. Here, we aimed to develop a generalizable method, based on patient-specific 3D geometries derived from a representative patient's computed tomography (CT) scans in order to investigate the permanent implant construct's contour deformation, and map the bony fusion process over a 6-year follow-up (FU). Long FU (more than 2 years) can provide evidence about the success of the

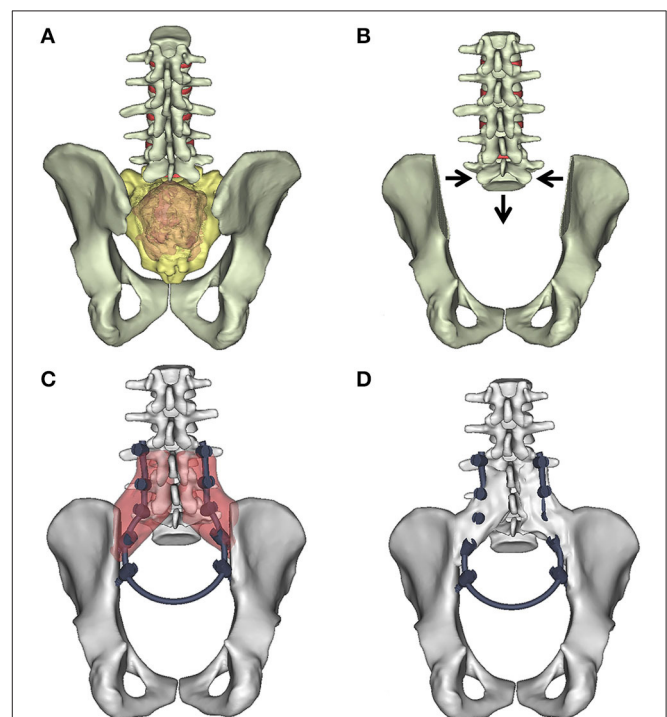


FIGURE 1 | “Closed-Loop” lumbosacral reconstruction technique after total en-bloc sacrectomy. **(A)** Extended tumor mass affects the whole sacrum. **(B)** Geometrical change in the 3D geometry of the spino-pelvic junction after en-bloc total sacrectomy. The iliac bone is cut by an oscillating saw bilaterally; the medial cortical surface of the iliac bone is left on the specimen. The lumbosacral facet joints with the intervertebral discs are removed. The dural sac (together with the cauda equina) is cut through immediately below L5. The distance between the L5 vertebra and the iliac bone is reduced (direction of the arrows). **(C)** In the L3–5 vertebral body and bilaterally into the iliac bones, screws are inserted and connected with a single 5.5 mm diameter “U” shaped rod according to the patient's reduced **(C)** local dimensions and attached to the screws. The red areas mark the place for the artificial bone substitute, mixed with autologous bone graft. **(D)** The re-established connection between the lumbar spine and the pelvis. At the side of the graft **(D)** after 2 years bony fusion is expected.

reconstruction, if no implant-related failure occurred. In the case of deformity correction, the deformation of the implant construct (rod) has been investigated *via* contour deformation measurements (11–14). However, in the case of lumbopelvic



FIGURE 2 | Pre- and postop imaging of a 42 years old male patient who underwent total en-block sacrectomy and received a Closed-Loop spino-pelvic reconstruction. **(A,B)** Preop T2, MRI images of a large sacral chordoma [**(A)** sagittal, **(B)** axial plane]. The extended tumor mass affected the whole sacrum with significant soft tissue extension to the retroperitoneum and cranially involving the paravertebral muscles. **(C,D)** Standing X-ray images of the patient at 6-month FU [**(C)** sagittal, **(D)** coronal plane]. **(E,F)** CT scan at 24-month FU period. Signs of bony fusion are visible between the L4 and L5 vertebrae and the iliac bone [**(E)** posterior view of the 3D rendered CT images; **(F)** coronal view at the fusion site].

reconstructions, the permanent contour deformation over the FU period has not been investigated so far.

METHODS

In this study, a clinical case is used to present a method for the evaluation of the implant construct's contour deformation in a lumbopelvic reconstruction, based on the postoperative (postop) CT scans *via* image processing methods (exp segmentation, rigid registration). The bony fusion was mapped in the CT scans by quantifying the Hounsfield unit (HU) values of the voxels in the region of interest and converted into bone mineral density (BMD) equivalent values.

Clinical Case

The criteria for case selection were: the previous publication of the surgery, with video documentation and long

(more than 2 years) FU, and the patient's ability to walk after surgery.

The patient's (**Figure 2**) case and surgery were presented at the European Spine Journal, *Open Operating Theatre* (OOT) platform (15, 16). The 42-year-old male patient had mild and non-specific low back pain for 4–5 years. He had experienced minor problems with defecation and urination for 1 year, and a palpable lump had been observed for some months in the sacral region. Neurological examination showed normal motor and sphincter function but mild hypesthesia in the perianal region. Radiological examinations revealed an extended tumor mass affecting the whole sacrum with significant soft tissue extension to the retroperitoneum and cranial involvement of the paravertebral muscles as far as the L3 spinal level on the right side (**Figure 2**). Open biopsy-based histological examination confirmed the diagnosis of chordoma. Total “en-bloc” sacrectomy, combined with soft tissue and

TABLE 1 | Retrospectively collected CT scans.

Postop years		1		2		3	4	5	6			
Number of CT scan	1	2	3	4	5	6	7	8	9	10	11	12
Days after surgery	7	34	83	138	250	446	656	1027	1384	1734	1937	2112

CT, computed tomography.

bony reconstruction, together with lumbopelvic stabilization (“closed-loop” technique, poly-axial titanium pedicle screw, with 5.5 mm diameter titanium rod, CD Horizon©LEGACY™ 5.5, Medtronic Sofamor Danek, Memphis, Tennessee, United States) was performed to remove the tumor *via* a posterior-only approach. Artificial bone substitute (ACTIFUSE®, Baxter International Inc., Deerfield, Illinois, United States) was placed between the L5 vertebral body and the iliac crest bilaterally, after refreshing and preparing well bleeding trabecular bony host surfaces (**Figure 1C**). The large defect of the body wall between the L5 vertebral body and the coccygeal ligamentous complex was covered by Dacron mesh (anchored to the bony landmarks: L5 vertebral body, tuber ossis ischii, and iliac bone). Finally, wound closure was performed by creating bilateral m. gluteus maximus rotational flaps. During surgery, the lumbosacral intervertebral disc was resected, and the dural sac (together with the cauda equina) was cut through immediately below the L5 origins. Cranial and ventral ligaments of the SI joints, and nerve roots (below the S1 segment) were both cut through bilaterally at the lateral aspect of the tumor (16). However, the patient was able to walk with crutches at the 3rd month FU, and without any assisting device at the 12th month FU. In order to quantify and evaluate the gait of the patient at the 6th year FU, gait analysis was performed, see **Supplementary Material (Supplementary Study I)**.

Postoperative Computed Tomography Scan Acquisition

Analysis of retrospectively collected postop CT data was performed. The study was approved by the National Ethics Committee of Hungary, the National Institute of Pharmacy and Nutrition (reference number: OGYÉI/163-4/2019). Informed consent was obtained from the participant. The data set consisted of 12 CT scans, covering a 6-year FU period (**Table 1**). The CT scans were performed with the same CT machine (Hitachi Presto, Hitachi Medical Corporation, Tokyo, Japan) with an intensity of 225 mA and a voltage of 120 kV. CT slice distance and resolution were 3.75 mm and 512 by 512 pixels, respectively. The data were exported from the hospital PACS in DICOM file format. To comply with the ethical approval for patient data protection, deidentification of the DICOM data was performed using the freely available Clinical Trial Processor software (Radiological Society of North America, <https://www.rsna.org/ctp.aspx>) (17).

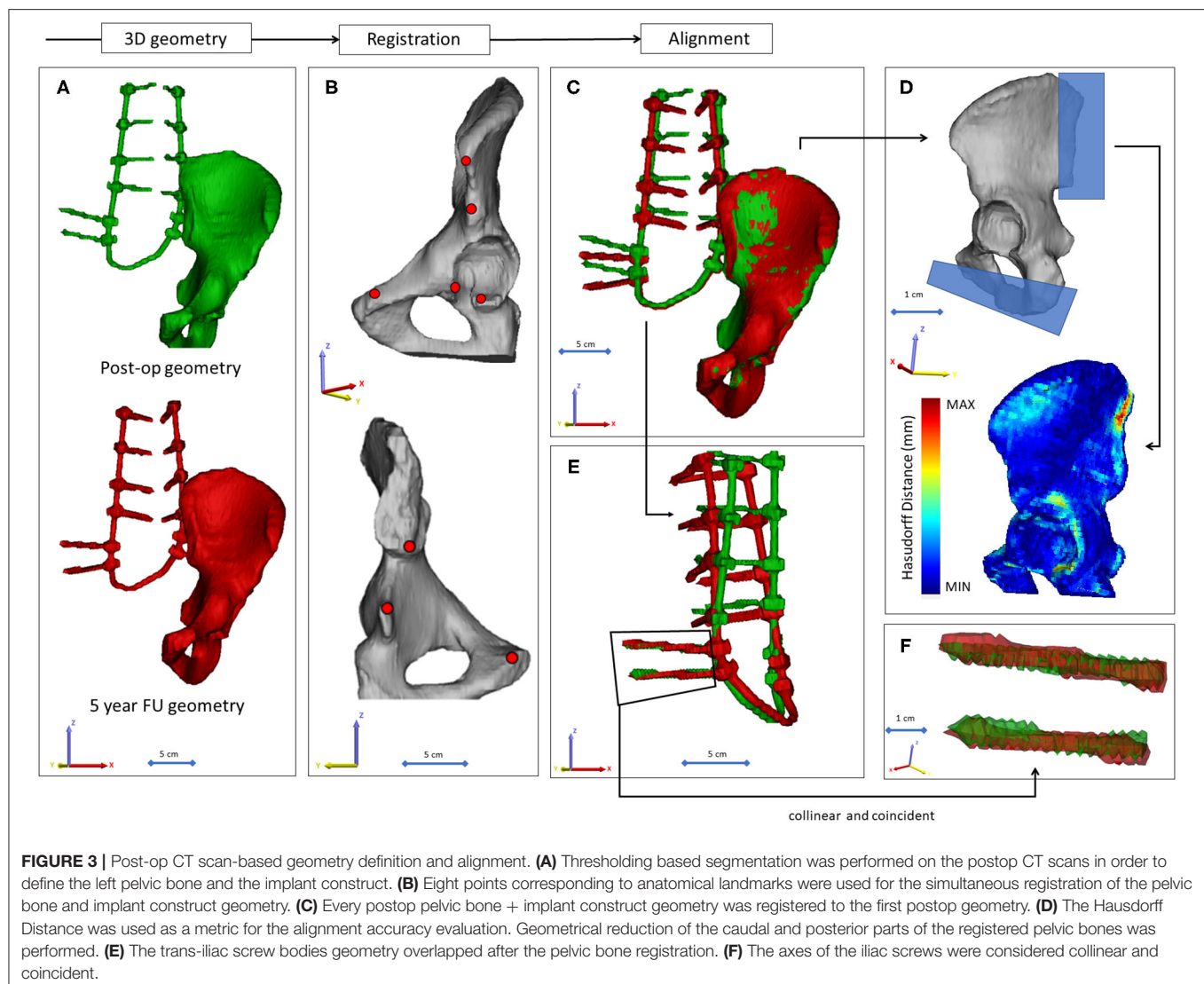
Image Processing, 3D Geometry Definition

The 3D geometry of the closed-loop implant and the left pelvic bone were defined in every CT data set. No radiological sign of implant failure (screw loosening, screw or rod breakage,

screw/rod disconnection) was registered in the 12 CT scans. The segmentation process was performed on the CT images (18) in the Mimics® image analysis software (Mimics Research, Mimics Innovation Suite v21.0, Materialise, Leuven, Belgium) (**Figure 3A**). The left pelvic bone was isolated, and then the implant geometry was separated. The resulting masks (groups of voxels) were homogeneously filled by preserving the outer contour of the geometrical border in 2D. From the masks, a triangulated surface mesh was automatically generated for the pelvic bone and the implant construct (**Figure 3A**). To evaluate the accuracy of the segmentation process, Dice Similarity Index (DSI) (19, 20) was calculated in each case. DSI values range between 0 and 1, with 1 denoting a perfect match. The implant geometry and the pelvic bone geometry were segmented 12 times by two investigators: I_1 and I_2 . The DSI was calculated by comparing the segmentation of I_2 to I_1 (21).

Alignment of the Implant Construct Geometries

To determine the implant construct's contour deformation, the 12 segmented (I_1) implant geometries were aligned with the pelvic bone in the same coordinate system. The left pelvic bone in the first postop CT scan was used as a reference geometry. A control points-based rigid registration algorithm was used in Mimics®. The 8 control points corresponded to easily identifiable anatomical landmarks on the left pelvic bone (**Figure 3B**). During registration, the implant construct moved together with its corresponding pelvic bone (**Figure 3C**). At the fusion site, after the alignment, a symmetrical geometry reduction was performed using cuboid subtraction, in order to exclude the geometrical difference (**Supplementary Figure 2**). A second geometry subtraction was performed for all pelvic bone geometries at the ischial ramus, where the last axial CT slice ended in the first postop scan (**Figure 3D**; **Supplementary Figure 2**). The uniformly reduced pelvic bone surface geometry was considered constant. To evaluate the accuracy of the registration and alignment procedure, and to demonstrate that the reduced pelvic bone surface geometry can be considered constant, Hausdorff Distance (HD) was measured with the MeshLab 1.3.2 software's (22) (<http://www.meshlab.net>) Metro tool (23) (**Figure 3D**) at the level of the aligned pelvic bones. The alignment of the 12 geometries was performed by the first investigator (I_1), and the HD measurements were performed on each postop CT scan, where the geometries derived from the 2nd–12th CT scans were compared to the first postop scan-based geometry. After registration of the pelvic bones, the trans-iliac screw bodies' geometries overlapped. The axes of the iliac screws were



collinear and coincident (**Figures 3E,F**). To test this hypothesis, HD values were calculated for the screw bodies by comparing the geometries to the first postop CT scan geometry after the alignment.

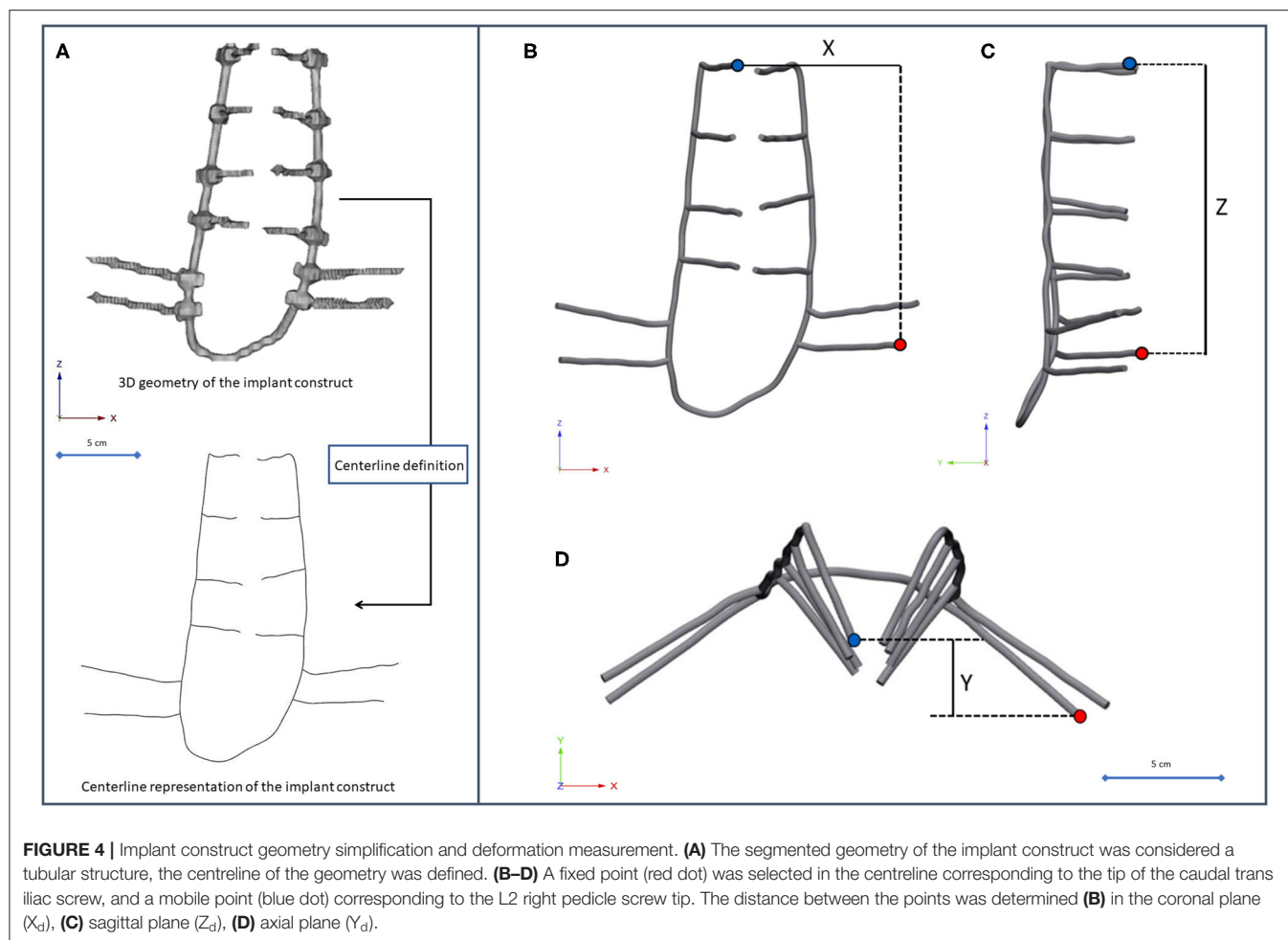
Implant Deformation Measurements

The implant construct geometry was considered a tubular structure, and the centreline of the geometry was defined with Mimics® (**Figure 4A**). A mobile point, corresponding to the L2 right pedicle screw tip, and a fixed point, corresponding to the tip of the caudal iliac screw, were selected in the centreline. The distances between the points were measured in three anatomical planes (**Figures 4B–D**) using 3-matic® (Mimics Innovation Suite v21.0, Materialise, Leuven, Belgium). The segmentation of the implant construct, the centreline definition, and the distance measurement in the three planes were performed by three investigators (I_1 , I_2 , I_3) at two different time points (T_1 , T_2). In order to test the repeatability

and reliability of the measurements, three-dimensional distance ($3D_d$) was calculated based on the X_d (coronal plane), Y_d (axial plane), and Z_d (sagittal plane), using the formula $3D_d = \sqrt{X_d^2 + Y_d^2 + Z_d^2}$.

Mapping of the Bony Fusion

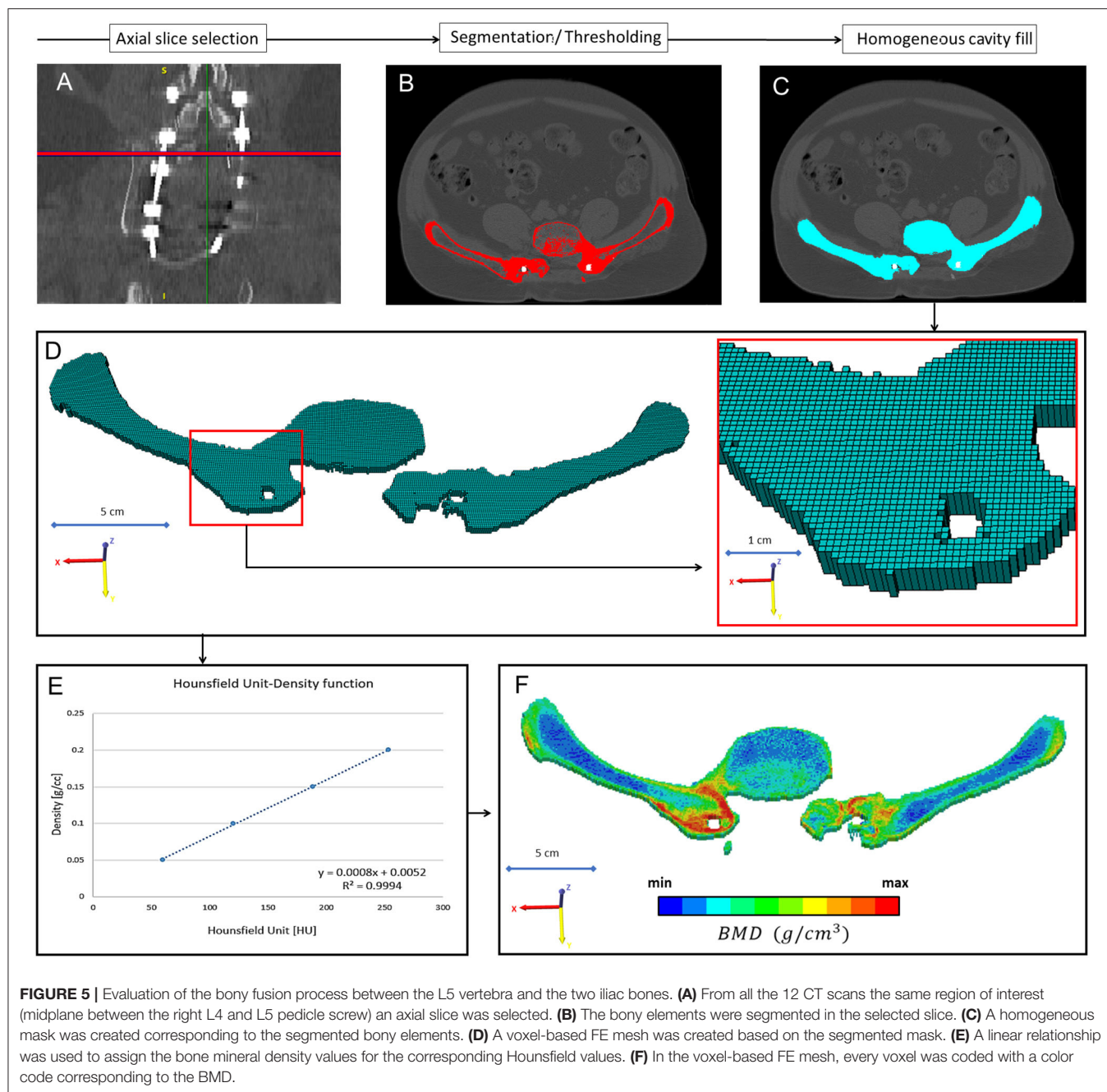
In every CT scan, from the same anatomical region (midplane between the right LIV and LV pedicle screw), a single axial slice was selected (**Figure 5A**) as a region of interest (ROI). The bone tissue was segmented based on a thresholding algorithm (left and right iliac bone, and LIV vertebra) (**Figure 5B**). The masks' internal part contained voxels representing adipose tissue (BMD close to 0). From this mask, a voxel-based finite element (FE) mesh was created with Mimics® (**Figures 5C,D**). CT scans from the FU were acquired without a densitometric calibration phantom. From the institutional PACS database, QCT scans were selected with the same acquisition protocol and machine (**Table 1**). The dates of the scans were selected



to be in the same months as the postop CT scans. The male subjects also had similar body mass indices ($BMI = 28 \pm 2$) as the presented patient ($BMI = 28$). The Hounsfield unit (HU) values of the QCT images were converted into BMD equivalent values by using a densitometric calibration obtained with an inline phantom (Hitachi Presto, Hitachi Medical Corporation, Tokyo, Japan) consisting of five cylindrical insertions with known mean equivalent BMD values (0, 0.5, 0.1, 0.15, and 0.2 g/cm^3). Based on the 12 QCTs, a mean conversion curve was defined and assumed to be linear [$BMD = \rho_{QCT} = a + b * HU$, where ρ_{QCT} (g/cm^3) is bone density] according to prior studies (24, 25) (Figure 5E). In the voxel-based FE mesh, every element was color-coded, using 10 colors, corresponding to BMD values as shown in Figure 5F. The changes in the distribution of the sets of FE mesh voxel elements over the FU were analyzed. The volumes of the voxels in every BMD category were calculated (voxel dimensions * number of elements) and visualized using a 3D surface plot (Figure 9) created with SigmaPlot 12 (SSI, San Jose, California, United States).

STATISTICAL ANALYSIS

The reliability and repeatability of our method was tested in order to demonstrate the reproducibility of the study. Due to the small sample size, we used non-parametric tests. Inter-rater (I_1 vs. I_2 vs. I_3) reliability was determined by intraclass correlation coefficient (ICC) estimates, and their 95% confidence intervals (CI) were calculated based on a mean-rating ($k = 3$), absolute-agreement, 2-way mixed-effects model. Intra-rater (I_1T_1 vs. I_1T_2 , I_2T_1 vs. I_2T_2 , I_3T_1 vs. I_3T_2) reliability was determined by ICC estimates, and their 95% confidence intervals were calculated based on a single measurement, absolute-agreement, 2-way mixed-effects model. The relationships between the implant deformation in the anatomical planes and the number of postop days, and between the volume change in the different BMD categories were analyzed using the Spearman's rank correlation (Figures 8, 10). The interpretation of the correlation was based on the work of Evans et al. (26). All statistical tests were performed with SPSS® Statistics 23 software (SPSS Inc, Chicago, IL).



RESULTS

Evaluation of the Segmentation Procedure

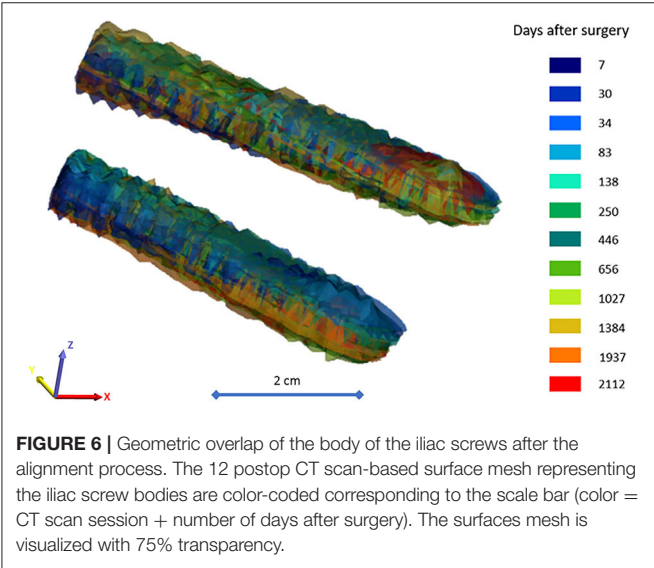
The obtained DSI values (**Supplementary Table 1**) for the implant construct geometries were very high 0.97 ± 0.02 ($n = 12$) as well as for the pelvic bone 0.96 ± 0.05 ($n = 12$) and showed negligible variance, indicating high accuracy of the segmentation method for all segmented geometries (27).

Alignment Evaluation

A mean HD of 0.63 ± 0.14 mm was obtained (**Supplementary Table 2**) from the reduced pelvic bone

geometries. The HD determined for the iliac screw bodies had a mean value of 0.95 ± 0.10 mm (**Supplementary Table 3**). These values are considered by the field to be indicative of adequate fitting (28). The colinear and coincident position of the iliac screw axes, and the geometric overlap of the bodies were visualized in **Figure 6**. The figure and the HD values (**Supplementary Table 3**) demonstrate that the screw body does not deform or change its position in the common coordinate system. Theoretically, any point in these two screw body geometries can be used as a reference point in a measurement process. The right pelvic bone could be selected for the analysis

as well, with the right iliac screw bodies, as demonstrated in **Supplementary Study II**.



	ICC	95% confidence interval	
		Lower bound	Upper bound
Intra-rater reliability			
I ₁ T ₁ vs. I ₁ T ₂	0.768	0.362	0.928
I ₂ T ₁ vs. I ₂ T ₂	0.980	0.934	0.994
I ₃ T ₁ vs. I ₃ T ₂	0.949	0.838	0.985
Inter-rater reliability			
I ₁ vs. I ₂ vs. I ₃	0.980	0.948	0.994

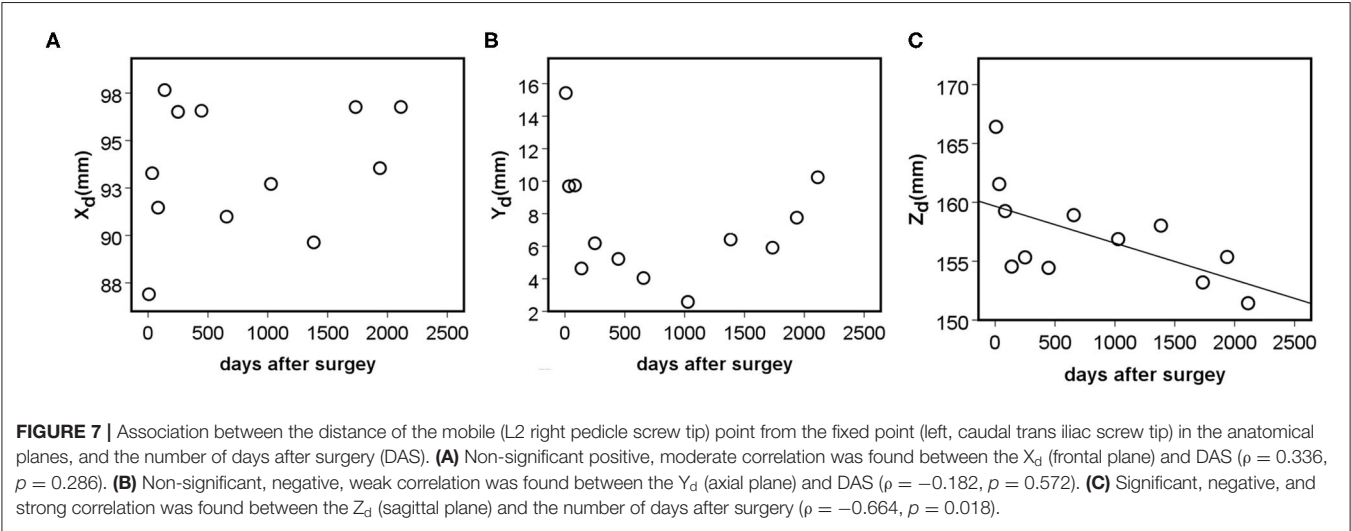
ICC, intraclass correlation; I, investigator; T, time point.

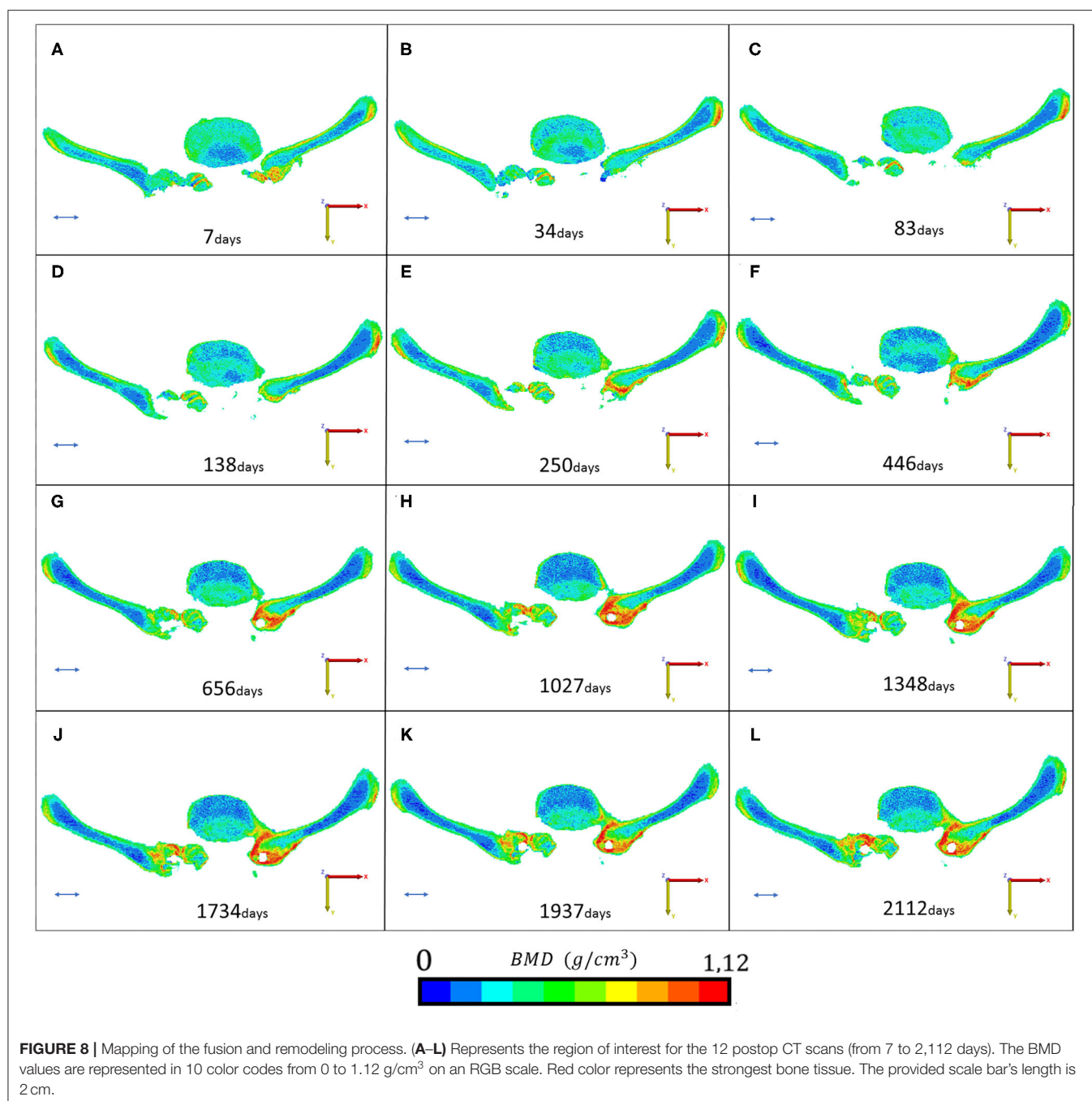
Implant Deformation

The implant deformation measurements are summarized in **Supplementary Tables 4, 5, and 6**. The mean displacement relative to the first postop CT scan was $\Delta X_d = 7.27 \pm 2.80$ mm in the frontal plane, $\Delta Y_d = 8.24 \pm 2.51$ mm in the coronal plane, and $\Delta Z_d = 10.15 \pm 2.97$ mm in the sagittal plane. To test the accuracy and reproducibility of these measurements, inter- and intra-rater reliability tests were performed by calculating the intraclass correlation coefficient (ICC) based on the 3D_d values, presented in **Table 2**. The ICC values show excellent reliability, with the exception of the I₁T₁ vs. I₁T₂ intra-rater reliability, where the ICC was 0.768, which corresponds to good reliability (29). The association between the average X_d/Y_d/Z_d measurement and the number of days after surgery is shown in **Figure 7**. The implant construct's deformation can be registered in the anatomical planes over the postop FU period. However, the deformation was only significant in the sagittal plane, showing a strong negative correlation between the Z_d and the number of days after surgery ($\rho = -0.664$, $p = 0.018$). This result demonstrates the forward bending tendency of the construct.

BMD Mapping at the Fusion Site

The bone material density distribution in the region of interest for the fusion process was measured over the FU period (**Figure 8, Table 3**). The color map captures the bone remodeling process in the ROI. After the second year FU, a solid fusion was detected between the lumbar spine, the L4 vertebra and the two iliac bones. However, due to the cyclical loading, the bone remodeling represented by the change in the element distribution in the color-coded BMD categories continued. The change in the volume of the BMD categories over the days after surgery is presented in **Figure 9**. The obtained 3D contour plot demonstrates an increase in the high BMD category volume after the second year FU. The association between the 10 BMD categories' volumetric change and the days after surgery was significantly positive, with very strong associations ($\rho > 0.800$,





$p < 0.050$) in the highest 5 BMD categories (Figure 10A). From the 10 BMD categories, no significant correlation was found between volumetric change and Y_d (axial plane). In the frontal plane (X_d), only for the third BMD category was found to have significant, strong correlation ($\rho = 0.678$, $p = 0.015$) (Figure 10B). Significant negative correlation ($\rho > -0.600$, $p < 0.050$) was found only between 3 high-value BMD categories and the Z_d (sagittal plane) measurements (Figure 10C).

DISCUSSION

In the presented study, we investigated the hypothesis that the CLT method provides a non-rigid fixation of the lumbopelvic junction after sacrectomy. We aimed to develop a method for the investigation of implant deformation and bony fusion using the postop CT scans collected over the 6-year FU period of a patient who underwent sacrectomy and closed-loop reconstruction. We were able not only to demonstrate the non-rigidity of the

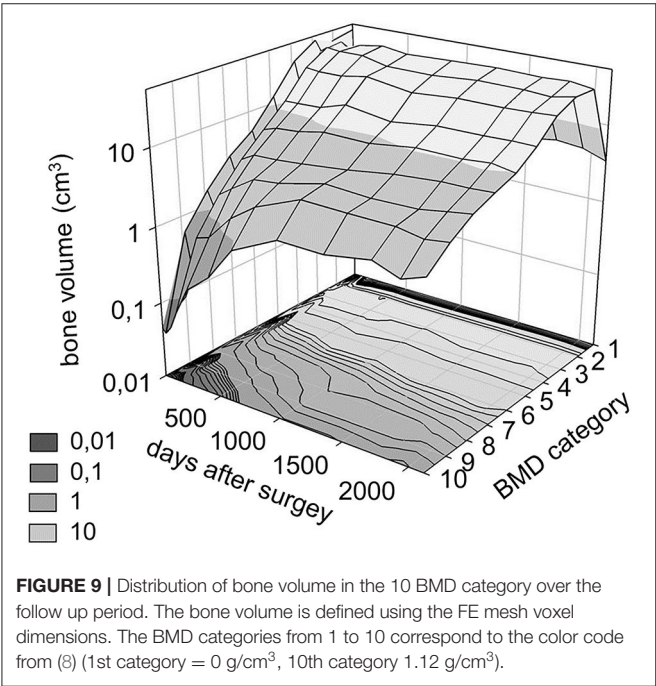
TABLE 3 | Volumetric change of the voxel groups corresponding to the BMD categories.

No.	Days after surgery	Volume of the different BMD category's during the FU (cm³)									
1	7	41.70	36.36	21.55	9.59	6.46	4.16	1.76	0.43	0.09	0.05
2	34	0.41	17.96	45.77	29.79	12.76	5.81	3.50	1.66	0.64	0.04
3	83	17.96	36.52	33.79	13.93	6.27	3.33	2.04	1.07	0.21	0.05
4	138	1.10	31.22	39.06	26.28	12.03	6.50	3.46	1.60	0.60	0.08
5	250	2.50	36.33	37.25	25.14	12.16	7.42	4.34	2.11	0.68	0.20
6	446	3.43	40.58	37.42	25.22	12.50	7.85	4.45	3.32	1.45	0.35
7	656	3.04	36.20	31.18	28.78	15.85	9.15	4.76	3.61	2.47	0.98
8	1,027	3.22	38.04	30.87	23.40	12.87	8.97	5.53	5.01	4.34	1.94
9	1,384	3.89	39.48	34.27	25.99	15.22	10.69	6.74	4.65	4.21	1.90
10	1,734	4.73	38.00	33.79	25.83	15.32	10.51	7.54	4.81	4.17	2.38
11	1,937	4.38	39.47	32.04	26.55	15.70	11.24	7.59	5.49	3.63	1.79
12	2,112	3.45	35.72	36.63	27.69	15.52	9.97	7.92	6.10	4.01	2.31

BMD category's (g/cm³)

0.000.120.250.370.500.620.750.871.001.12

BMD, bone mineral density; FU, follow up; No, Number of CT scans.

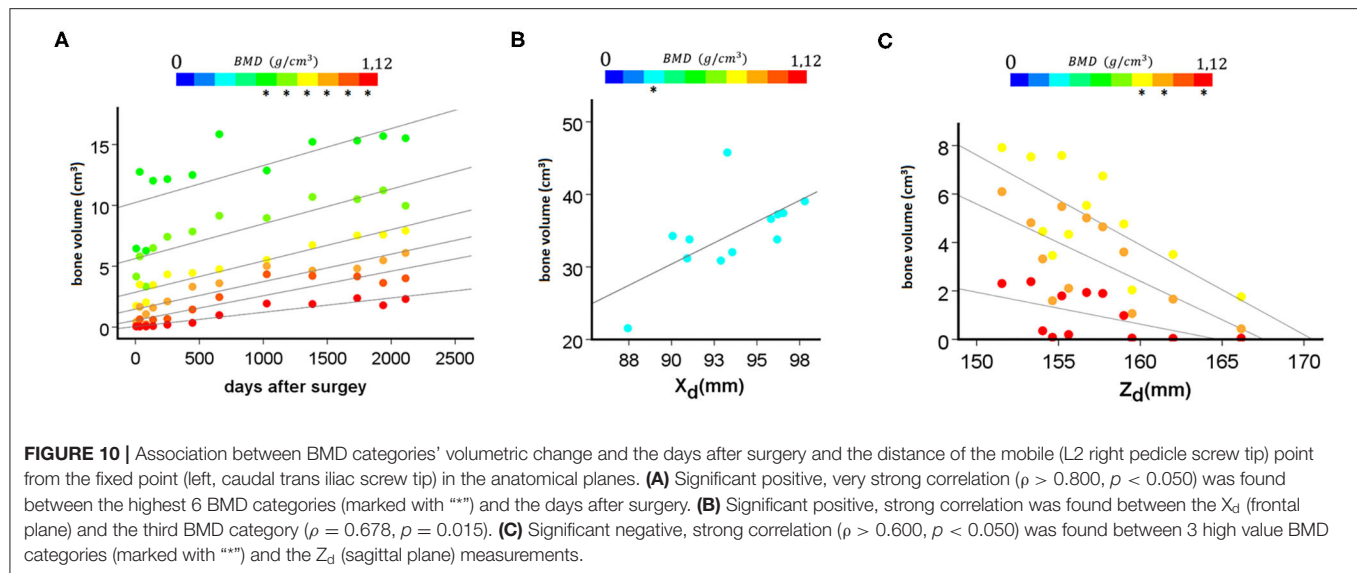


construct by measuring the geometrical deformation over the FU period, but to map the bony remodeling at the fusion site (lumbar spine and two iliac bones) as well. Significant correlation was found between deformation in the sagittal plane and postop days, denoting the forward bending tendency of the construct. The closed-loop reconstruction technique can provide excellent locomotor outcomes after total sacrectomy; a similar result was demonstrated by Smith et al. (30). The fact that the presented

patient was able to walk resulted in a periodic cyclical loading of the construct. Clark et al. (31) compared three spinopelvic reconstruction techniques under gait-simulating fatigue loading and sagittal alignment failure on cadaveric specimens. Despite the complex gait-like loading experiment, due to its limitations (cadaveric specimen), it does not take into consideration the bony fusion process, only focusing on the primary stability of the construct. We introduced the centrelines to avoid artifacts in the CT scans, even so, the resolution of the clinical CT affects the straightness of the centreline. In the future, after applying the method to a larger patient cohort, we plan to perform a curvature analysis methodologically similar to Hay et al.'s work (32), in which the centreline would be a technical advantage.

According to Frost's *mechanostat* theory (33, 34), bone growth and bone loss are stimulated by the local mechanical elastic deformation of bone. Effects of the implant construct's stiffness on the healing of fractures in the case of long bones stabilized by internal fixation has been widely investigated (35, 36), and it is known that constructs that are too stiff lead to non-union (37–40). In the case of posterior spinal fixation, the stiffness of implant rods (titanium alloys, stainless steel, cobalt-chromium-based alloys) can differ (13). Load sharing that occurs with the use of spinal implants results in a decreased load and thus reduced strain throughout the stabilized vertebral body, which leads to bone mineral density loss (13, 41).

Based on our results, the correlation between the high-value BMD categories and the forward bending tendency of the construct highlights the importance of rod stiffness (exp. diameter, material: cobalt-chrome or titanium) in the fusion process. Implant deformation *in vivo* due to upper body weight and muscle forces is rather well-known in cases of deformity correction. Several biomechanical studies have already investigated implant failure, mainly due to upper body flexion,



especially in adult spine deformities and unbalanced patients (42–44). However, it has not been investigated in lumbopelvic reconstructions. The developed method showed high accuracy and repeatability.

The quantification of bone formation uses the voxel dimensions and the Hounsfield values of the voxel-based FE element mesh in the regions of interest. The application of the mapping method on a large patient group would be desirable for other reconstruction techniques as well. The optimal, expert opinion-based, consensual reconstruction technique is not currently defined. The retrospective investigation of different methods based on CT scans over long FU periods (≥ 2 years) would be important for a better understanding of these complex surgical problems and the development of new solutions. The data obtained *via* this method could be used for the validation of FE models by identifying the regions of the construct where the highest deformation occurred during the FU, and by comparing the effect of the construct's stiffness/rigidity on the fusion process (45). Nevertheless, the data collected with the presented method could be used in implant design, especially for 3D printed patient-specific solutions (46).

We would like to highlight the limitations of our study. Three months were dedicated to the project. The study was designed as a "method" article, however, implementation on a larger patient cohort would be desirable. The study only reported on the distance between a specific point of the implant construct and the fixed iliac screw bodies. Based on this result, it is not possible to distinguish the mechanical factors involved (axial/shear load, sagittal/lateral bending, or axial torsion) in the permanent deformation. Due to the retrospective nature of the study, it was not possible to perform a repeatability test at the same follow-up time after repositioning of the patient to assess the accuracy in the BMD assessment or the construct contour deformation measurement.

CONCLUSION

The presented clinical image analysis-based computational method (segmentation, rigid registration, BMD assessment at the voxel level based on HU values) can provide accurate information about the implant construct's deformation after sacrectomy, following reconstruction with the closed-loop technique. We recommend the application of our measurement method for the scientific and clinical analysis of other surgical procedures as well, and other clinical scenarios where large constructs are needed, such as idiopathic or degenerative deformity corrections, growing rods systems, etc.

The BMD mapping at the fusion site may help in the future to evaluate the effect of the implant's (rod) diameter, or material, (titanium vs cobalt-chromium) on the fusion process.

The identification of regions where the constructs undergo the highest deformation may be useful in the surgical planning and in implant-related failure prevention.

DATA AVAILABILITY STATEMENT

The original contributions presented in the study are included in the article/**Supplementary Material**, further inquiries can be directed to the corresponding author.

ETHICS STATEMENT

The study was approved by the National Ethics Committee of Hungary, the National Institute of Pharmacy and Nutrition (reference number: OGYÉI/163-4/2019). The patients/participants provided their written informed consent to participate in this study. Written informed consent was obtained from the individual(s) for the publication of any potentially identifiable images or data included in this article.

AUTHOR CONTRIBUTIONS

PE, DL, PV, and AL contributed to the conception and design of the study. PE, MT, FB, and JF did the CT based image analyses and the visualizations. The gait assessment was performed by JF, GS, and TT. PV and AL performed the surgery described in this case report. PE wrote the first draft of the manuscript and prepared the pictures together with MT. All authors contributed to manuscript revision, read and approved the submitted version.

FUNDING

The project leading to the scientific results was supported by the Hungarian Scientific Research Fund Grant, Budapest,

Hungary (Award Number: OTKA FK123884) and by the European Commission (766012-SPINNER-H2020-MSCA-ITN-2017), and by the Doctoral Student Scholarship Program of the Co-operative Doctoral Program of the Ministry of Innovation and Technology, Hungary, financed from the National Research, Development and Innovation Fund (C1014064). The financial support from these funding bodies are gratefully acknowledged.

SUPPLEMENTARY MATERIAL

The Supplementary Material for this article can be found online at: <https://www.frontiersin.org/articles/10.3389/fsurg.2021.698179/full#supplementary-material>

REFERENCES

- Varga PP, Bors I, Lazary A. Sacral tumors and management. *Orthop Clin North Am.* (2009) 40:105–123. doi: 10.1016/j.ocl.2008.09.010
- Disler DG, Miklic D. Imaging findings in tumors of the sacrum. *AJR Am J Roentgenol.* (1999) 173:1699–706. doi: 10.2214/ajr.173.6.10584822
- Jo VY, Fletcher CDM. WHO classification of soft tissue tumours: an update based on the 2013 (4th) edition. *Pathology.* (2014) 46:95–104. doi: 10.1097/PAT.0000000000000050
- Fourney DR, Rhines LD, Hentschel SJ, Skibber JM, Wolinsky J-P, Weber KL, et al. En bloc resection of primary sacral tumors: classification of surgical approaches and outcome. *J Neurosurg Spine.* (2005) 3:111–22. doi: 10.3171/spi.2005.3.2.0111
- Zoccali C, Skoch J, Patel AS, Walter CM, Maykowski P, Baaj AA. Residual neurological function after sacral root resection during en-bloc sacrectomy: a systematic review. *Eur Spine J.* (2016) 25:3925–31. doi: 10.1007/s00586-016-4450-3
- Varga PP, Szövérfi Z, Fisher CG, Boriani S, Gokaslan ZL, Dekutoski MB, et al. Surgical treatment of sacral chordoma: prognostic variables for local recurrence and overall survival. *Eur Spine J.* (2015) 24:1092–101. doi: 10.1007/s00586-014-3728-6
- Varga PP, Szoverfi Z, Lazary A. Surgical resection and reconstruction after resection of tumors involving the sacropelvic region. *Neurol Res.* (2014) 36:588–96. doi: 10.1179/1743132814Y.0000000370
- Zileli M, Hoscoskun C, Brastianos P, Sabah D. Surgical treatment of primary sacral tumors: complications associated with sacrectomy. *Neurosurg Focus.* (2003) 15:E9. Available online at: <http://www.ncbi.nlm.nih.gov/pubmed/15323466> (accessed November 26, 2019).
- Lim S-H, Jo D-J, Kim S-M, Lim Y-J. Reconstructive surgery using dual U-shaped rod instrumentation after posterior en bloc sacral hemiresection for metastatic tumor: case report. *J Neurosurg Spine.* (2015) 23:630–4. doi: 10.3171/2015.2.SPINE14702
- Choi MK, Jo DJ, Kim SB. Pelvic reconstruction surgery using a dual-rod technique with diverse U-shaped rods after posterior en bloc partial sacrectomy for a sacral tumor: 2 case reports and a literature review. *World Neurosurg.* (2016) 95:619–e11. doi: 10.1016/j.wneu.2016.08.022
- Cidambi KR, Glaser DA, Bastrom TP, Nunn TN, Ono T, Newton PO. Postoperative changes in spinal rod contour in adolescent idiopathic scoliosis: an *in vivo* deformation study. *Spine.* (2012) 37:1566–1572. doi: 10.1097/BRS.0b013e318252ccbe
- Ohrn-Nissen S, Dahl B, Gehrchen M. Choice of rods in surgical treatment of adolescent idiopathic scoliosis: what are the clinical implications of biomechanical properties?—A review of the literature. *Neurospine.* (2018) 15:123. doi: 10.14245/ns.1836050.025
- Yoshihara H. Rods in spinal surgery: a review of the literature. *Spine J.* (2013) 13:1350–8. doi: 10.1016/j.spinee.2013.04.022
- Le Navéaux F, Aubin C-E, Parent S, Newton PO, Labelle H. 3D rod shape changes in adolescent idiopathic scoliosis instrumentation: how much does it impact correction? *Eur Spine J.* (2017) 26:1676–83. doi: 10.1007/s00586-017-4958-1
- Aebi M, Gunzburg R. OOT: the open operating theatre. *Eur Spine J.* (2011) 20:825–825. doi: 10.1007/s00586-011-1832-4
- Varga PP, Lazary A. Chordoma of the sacrum: “en bloc” total sacrectomy and lumbopelvic reconstruction. *Eur Spine J.* (2010) 19:1039–40. doi: 10.1007/s00586-010-1460-4
- Aryanto KYE, Oudkerk M, van Ooijen PMA. Free DICOM de-identification tools in clinical research: functioning and safety of patient privacy. *Eur Radiol.* (2015) 25:3685–95. doi: 10.1007/s00330-015-3794-0
- Bozic KJ, Keyak JH, Skinner HB, Bueff HU, Bradford DS. Three-dimensional finite element modeling of a cervical vertebra: an investigation of burst fracture mechanism. *J Spinal Disord.* (1994) 7:102–10. doi: 10.1097/00002517-199407020-00002
- Zou KH, Warfield SK, Bharatha A, Tempany CMC, Kaus MR, Haker SJ, et al. Statistical validation of image segmentation quality based on a spatial overlap index. *Acad Radiol.* (2004) 11:178–89. doi: 10.1016/S1076-6332(03)00671-8
- Bharatha A, Hirose M, Hata N, Warfield SK, Ferrant M, Zou KH, et al. Evaluation of three-dimensional finite element-based deformable registration of pre- and intraoperative prostate imaging. *Med Phys.* (2001) 28:2551–60. doi: 10.1118/1.1414009
- Eltes PE, Kiss L, Bartos M, Gyorgy ZM, Csakany T, Bereczki F, Lesko V, Puhl M, Varga PP, Lazary A. Geometrical accuracy evaluation of an affordable 3D printing technology for spine physical models. *J Clin Neurosci.* (2020) 72:438–446. doi: 10.1016/j.jocn.2019.12.027
- Cignoni P, Callieri M, Corsini M, Dellepiane M, Ganovelli F, Ranzuglia G. Meshlab: an open-source mesh processing tool. In: *Eurographics Italian Chapter Conference*, p. 129–136.
- Cignoni P, Rocchini C, Scopigno R. Metro: measuring error on simplified surfaces. *Comput Graph Forum.* (1998) 17:167–74. doi: 10.1111/1467-8659.00236
- Couteau B, Hobatho M-C, Darmana R, Brignola J-C, Arlaud J-Y. Finite element modelling of the vibrational behaviour of the human femur using CT-based individualized geometrical and material properties. *J Biomech.* (1998) 31:383–6. doi: 10.1016/S0021-9290(98)00018-9
- Rho J-Y, Hobatho MC, Ashman RB. Relations of mechanical properties to density and CT numbers in human bone. *Med Eng Phys.* (1995) 17:347–55. doi: 10.1016/1350-4533(95)97314-F
- Evans JD. *Straightforward Statistics for the Behavioral Sciences.* Thomson Brooks/Cole Publishing Co. (1996).
- Yao J, Burns JE, Forsberg D, Seitel A, Rasoulouian A, Abolmaesumi P, et al. A multi-center milestone study of clinical vertebral CT segmentation. *Comput Med Imaging Graph.* (2016) 49:16–28. doi: 10.1016/j.compmedimag.2015.12.006
- Hayashi T, Chen H, Miyamoto K, Zhou X, Hara T, Yokoyama R, Kanematsu M, Hoshi H, Fujita H. A computerized scheme for localization of vertebral bodies on body CT scans. In: *Medical Imaging 2011:*

- Image Processing* (International Society for Optics and Photonics), p. 796238. doi: 10.1117/12.877511
29. Koo TK, Li MY, A. Guideline of selecting and reporting intraclass correlation coefficients for reliability research. *J Chiropr Med.* (2016) 15:155–63. doi: 10.1016/j.jcm.2016.02.012
 30. Smith JA, Tuchman A, Huoh M, Kaiser AM, Schooler WG, Hsieh PC. Locomotor biomechanics after total sacrectomy: a case report. *Spine.* (2014) 39:E1481–E1487. doi: 10.1097/BRS.0000000000000594
 31. Clark AJ, Tang JA, Leasure JM, Ivan ME, Kondrashov D, Buckley JM, et al. Gait-simulating fatigue loading analysis and sagittal alignment failure of spinal pelvic reconstruction after total sacrectomy: comparison of 3 techniques. *J Neurosurg Spine.* (2014) 20:364–70. doi: 10.3171/2013.12.SPINE13386
 32. Hay O, Dar G, Abbas J, Stein D, May H, Masharawi Y, et al. The lumbar lordosis in males and females, revisited. *PLoS ONE.* (2015) 10:e0133685. doi: 10.1371/journal.pone.0133685
 33. Frost HM. From Wolff's law to the mechanostat: a new "face" of physiology. *J Orthop Sci.* (1998) 3:282–6. doi: 10.1007/s007760050054
 34. Frost HM. The Utah paradigm of skeletal physiology: an overview of its insights for bone, cartilage and collagenous tissue organs. *J Bone Miner Metab.* (2000) 18:305–16. doi: 10.1007/s007740070001
 35. Perren SM. Evolution of the internal fixation of long bone fractures: the scientific basis of biological internal fixation: choosing a new balance between stability and biology. *J Bone Joint Surg Br.* (2002) 84:1093–110. doi: 10.1302/0301-620X.84B8.0841093
 36. Bottlang M, Doornink J, Lujan TJ, Fitzpatrick DC, Marsh JL, Augat P, et al. Effects of construct stiffness on healing of fractures stabilized with locking plates. *J Bone Jt Surgery Am Vol.* (2010) 92:12. doi: 10.2106/JBJS.J.00780
 37. Potter BK. From bench to bedside: How stiff is too stiff? Far-cortical locking or dynamic locked plating may obviate the question. *Clin Orthop Relat Res.* (2016) 474:1571–3. doi: 10.1007/s11999-016-4885-1
 38. Henderson CE, Lujan TJ, Kuhl LL, Bottlang M, Fitzpatrick DC, Marsh JL. 2010 mid-America Orthopaedic Association Physician in Training Award: healing complications are common after locked plating for distal femur fractures. *Clin Orthop Relat Res.* (2011) 469:1757–65. doi: 10.1007/s11999-011-1870-6
 39. Holzman MA, Hanus BD, Munz JW, O'Connor DP, Brinker MR. Addition of a medial locking plate to an in situ lateral locking plate results in healing of distal femoral nonunions. *Clin Orthop Relat Res.* (2016) 474:1498–505. doi: 10.1007/s11999-016-4709-3
 40. Rodriguez EK, Zurakowski D, Herder L, Hall A, Walley KC, Weaver MJ, et al. Mechanical construct characteristics predisposing to non-union after locked lateral plating of distal femur fractures. *J Orthop Trauma.* (2016) 30:403–8. doi: 10.1097/BOT.0000000000000593
 41. Craven TG, Carson WL, Asher MA, Robinson RG. The effects of implant stiffness on the bypassed bone mineral density and facet fusion stiffness of the canine spine. *Spine.* (1994) 19:1664–1673. doi: 10.1097/00007632-199408000-00003
 42. Luca A, Ottardi C, Sasso M, Prosdocimo L, La Barbera L, Brayda-Bruno M, et al. Instrumentation failure following pedicle subtraction osteotomy: the role of rod material, diameter, and multi-rod constructs. *Eur Spine J.* (2017) 26:764–70. doi: 10.1007/s00586-016-4859-8
 43. La Barbera L, Brayda-Bruno M, Liebsch C, Villa T, Luca A, Galbusera F, et al. Biomechanical advantages of supplemental accessory and satellite rods with and without interbody cages implantation for the stabilization of pedicle subtraction osteotomy. *Eur spine J.* (2018) 27:2357–66. doi: 10.1007/s00586-018-5623-z
 44. La Barbera L, Wilke H-J, Liebsch C, Villa T, Luca A, Galbusera F, et al. Biomechanical in vitro comparison between anterior column realignment and pedicle subtraction osteotomy for severe sagittal imbalance correction. *Eur Spine J.* (2020) 29:36–44. doi: 10.1007/s00586-019-06087-x
 45. Anderson DD, Thomas TP, Marin AC, Elkins JM, Lack WD, Lacroix D. Computational techniques for the assessment of fracture repair. *Injury.* (2014) 45:S23–31. doi: 10.1016/j.injury.2014.04.005
 46. Huang S, Ji T, Guo W. Biomechanical comparison of a 3D-printed sacrum prosthesis versus rod-screw systems for reconstruction after total sacrectomy: a finite element analysis. *Clin Biomech.* (2019) 70:203–8. doi: 10.1016/j.clinbiomech.2019.10.019

Conflict of Interest: The authors declare that the research was conducted in the absence of any commercial or financial relationships that could be construed as a potential conflict of interest.

Publisher's Note: All claims expressed in this article are solely those of the authors and do not necessarily represent those of their affiliated organizations, or those of the publisher, the editors and the reviewers. Any product that may be evaluated in this article, or claim that may be made by its manufacturer, is not guaranteed or endorsed by the publisher.

Copyright © 2022 Eltes, Turbucz, Fayad, Bereczki, Szóke, Terebessy, Lacroix, Varga and Lazary. This is an open-access article distributed under the terms of the Creative Commons Attribution License (CC BY). The use, distribution or reproduction in other forums is permitted, provided the original author(s) and the copyright owner(s) are credited and that the original publication in this journal is cited, in accordance with accepted academic practice. No use, distribution or reproduction is permitted which does not comply with these terms.



Surgical Process Modeling for Open Spinal Surgeries

Fabio Carrillo^{1†}, Hooman Esfandiari^{1*†}, Sandro Müller¹, Marco von Atzigen^{1,2}, Aidana Massalimova¹, Daniel Suter¹, Christoph J. Laux³, José M. Spirig³, Mazda Farshad³ and Philipp Färnstahl^{1,3}

¹ Research in Orthopedic Computer Science, Balgrist University Hospital, University of Zurich, Zurich, Switzerland,

² Laboratory for Orthopaedic Biomechanics, Institute for Biomechanics, Swiss Federal Institute of Technology (ETH), Zurich, Switzerland, ³ Department of Orthopaedics, Balgrist University Hospital, University of Zurich, Zurich, Switzerland

OPEN ACCESS

Edited by:

Ralph Jasper Mobbs,
University of New South
Wales, Australia

Reviewed by:

Ziya Levent Gokaslan,
Brown University, United States
Tamas Haidegger,
Óbuda University, Hungary

*Correspondence:

Hooman Esfandiari
hooman.esfandiari@balgrist.ch;
hooman.esfandiari@gmail.com

[†]These authors share first authorship

Specialty section:

This article was submitted to
Orthopedic Surgery,
a section of the journal
Frontiers in Surgery

Received: 14 September 2021

Accepted: 30 December 2021

Published: 25 January 2022

Citation:

Carrillo F, Esfandiari H, Müller S, von
Atzigen M, Massalimova A, Suter D,
Laux CJ, Spirig JM, Farshad M and
Färnstahl P (2022) Surgical Process
Modeling for Open Spinal Surgeries.
Front. Surg. 8:776945.
doi: 10.3389/fsurg.2021.776945

Modern operating rooms are becoming increasingly advanced thanks to the emerging medical technologies and cutting-edge surgical techniques. Current surgeries are transitioning into complex processes that involve information and actions from multiple resources. When designing context-aware medical technologies for a given intervention, it is of utmost importance to have a deep understanding of the underlying surgical process. This is essential to develop technologies that can correctly address the clinical needs and can adapt to the existing workflow. Surgical Process Modeling (SPM) is a relatively recent discipline that focuses on achieving a profound understanding of the surgical workflow and providing a model that explains the elements of a given surgery as well as their sequence and hierarchy, both in quantitative and qualitative manner. To date, a significant body of work has been dedicated to the development of comprehensive SPMs for minimally invasive baroscopic and endoscopic surgeries, while such models are missing for open spinal surgeries. In this paper, we provide SPMs common open spinal interventions in orthopedics. Direct video observations of surgeries conducted in our institution were used to derive temporal and transitional information about the surgical activities. This information was later used to develop detailed SPMs that modeled different primary surgical steps and highlighted the frequency of transitions between the surgical activities made within each step. Given the recent emersion of advanced techniques that are tailored to open spinal surgeries (e.g., artificial intelligence methods for intraoperative guidance and navigation), we believe that the SPMs provided in this study can serve as the basis for further advancement of next-generation algorithms dedicated to open spinal interventions that require a profound understanding of the surgical workflow (e.g., automatic surgical activity recognition and surgical skill evaluation). Furthermore, the models provided in this study can potentially benefit the clinical community through standardization of the surgery, which is essential for surgical training.

Keywords: surgical process modeling, open spinal surgery, spinal fusion, spinal instrumentation, pedicle screw, top-down modeling, bottom-up modeling

INTRODUCTION

With the advent of new medical technologies, surgical interventions are increasingly becoming sophisticated and specialization of physicians is more abundant (1). As projected in (2), with the introduction of Computer Assisted Surgery (CAS) (3), robotic surgery (4), medical augmented reality (5), and medical Artificial Intelligence (AI) (6), the average Operating Room (OR) today involves different types of digital equipment, information, staff, and processes that collectively aim at improving the patient outcome. As a newly emerging field, “Surgical Data Science,” has been recently defined that aims at “improving the quality of interventional healthcare and its value through capturing, organization, analysis, and modeling of data” (7).

Although surgeries are complex processes, which involve numerous steps, tasks, and actions, surgeries of the same kind are commonly performed with a rather similar and reproducible workflow (8). Many of the modern surgical technologies rely on a proper understanding of the aforementioned surgical workflow and appropriate “models” that highlight the relationships between different interactions within the workflow. Deep understanding of the surgical workflow is crucial when designing context-aware medical technologies that can adapt to the underlying surgical action at any given time. Context-awareness of medical technologies has been noted as a criteria that can increase the operational efficiency (9). Furthermore, standardized models that accurately depict the surgical workflow are essential for surgical training and education (10, 11), OR management (12), and treatment quality evaluation (13).

There is a notable body of literature dedicated to the derivation of models that can capture the surgical workflow based on different sensory observations (i.e., Surgical Process Modeling, SPM). As stated in (14), a surgical process model can be defined as “a set of sequential and parallel activities, executed by clinical and technical team members with different expertise, through preparing and using equipment and tools with the ultimate goal of high-quality treatment of a patient without complications.” In general, the SPM of a given operation can be acquired through a bottom-up or a top-down approach (15). In a top-down modeling strategy, the entire operation is observed and later broken down into different steps. Contrary, the bottom-up approach starts by first defining the individual steps and then finding the inter-connections between them, and linking them until the entire operation is represented. Extensive prior work exists on surgical process modeling and surgical activity recognition that are tailored to minimally invasive laparoscopic surgeries given the readily available endoscopic camera feed that can be used for activity recognition purposes. Dynamic time warping methods were used in (16, 17) to detect the usage of laparoscopic tools visible in the endoscopic camera videos. Feature-based surgical action recognition methods have also been introduced that rely on hand-crafted features extracted from the video feed [e.g., (18)]. More recently, deep learning methods have been proposed that can identify the surgical tasks and phases based on Convolutional Neural Network (CNN) principles in

an end-to-end fashion without the need for derivation of hand-crafted features, which can provide superior accuracies (19–21).

Despite the recent technological advances that are tailored to orthopedic surgeries [e.g., (22–25)], to the best of our knowledge, there is a general scarcity of publications that focus on delivering SPMs for such interventions, specifically for ubiquitous open operations. Hence the primary objective of the herein study is to develop a method for creation of a standard SPM for such surgeries.

Compared to other orthopedic pathologies, low back pain can be noted as one of the most prevalent conditions that is present in two thirds of adults once in their life (26) and is among the leading causes of years lived with disability (27–29) associated with prominent socio-economic impacts (30) such as decreased quality of life (31) and early retirement (32). While conservative treatment options exist for patients with mild symptoms (33, 34), instrumented spinal fusion remains the baseline method of treatment for more severe cases of degenerative disk disease with failed conservative treatment (35). Additionally, spinal fusion is the preferred surgical treatment for selected spinal fractures (36), spinal infections (37), and spinal deformity corrections (38) and congenital spinal anomalies (39).

Spinal instrumentation (i.e., spondylodesis) is a common intervention during which pedicle screw implants are placed within the pedicle corridor of each vertebra to provide anchoring support for the interconnecting longitudinal rods (40). Due to the proximity of the anatomy to spinal cord, nerves and blood vessels, this is a technically demanding procedure involving a complex range of surgical actions (41). Screw breaches can happen and are associated with potential complications such as dural lesions, irritation of the nerve root, and other neurological damages in as high as 2, 4, and 3% of the inserted pedicle screws in the thoracolumbar region respectively (42). Such misplacements can result in up to a 6% rate of revision surgeries as previously reported (43).

Although different open spinal interventions achieve the desired patient outcome through different means (e.g., decompression of neural structures, intervertebral cage insertion for spinal fusion, osteotomy for deformity correction, fracture reduction, and tumor debulking or resection) spinal instrumentation can be noted as the underlying process that is utilized mostly in the aforementioned surgeries.

With the adoption of newer surgical techniques, the perioperative complication rate associated with spinal instrumentation has decreased; however, challenges such as dural tears and neurological deficits can still occur (44) due to the complexity of the procedure. Despite the recent advent of modern computer assisted navigation systems for the aforementioned interventions, it was reported in a worldwide survey that only 11% of the surgeries make use of such systems and the majority of the procedures are performed in an “free-hand” fashion (45) (in contrast to operations performed through the use of computer assisted surgery). Non-navigated open procedures are proven to be associated with a low rate of pedicle screw insertion accuracy, with a median accuracy of 86.6% (46).

Considering the abovementioned lack of comprehensive SPMs for orthopedic surgery and the ubiquity of open spinal surgeries, the focus of this work is to develop a SPM that can capture the common surgical elements performed in such interventions and the inter-connections between the events. To that end, we provide first the theoretical basis and ontological background on which our work is built on. Afterwards, we describe the data collection process, and we elaborate on the model creation steps followed for the generation of the SPMs. The SPMs will be developed in a way that they are capable of encompassing not only different granularity levels and event frequencies, but also the possibility of including unexpected deviations in the surgical workflow. The end goal of the resulting SPMs is to serve as the basis for development of future automatic assistive technologies specific to open spine surgeries (e.g., surgical activity recognition and phase detection based on the emerging AI algorithms). Furthermore, the proposed SPMs can be used for surgical training, activity monitoring, and procedure standardization.

METHODS

The following sections will provide a detailed overview into the development of the SPMs for open spinal fusion surgery. First, in Ontology and Deductive Modeling of SPM for Open Spinal Surgeries, we provide the theoretical basis and ontological background of the SPMs developed in our work, including the nomenclature and the terminology used throughout the paper. Afterwards, in Data Collection and Annotation we explain the data collection and analysis process of the surgical workflow for the open spinal surgeries, and finally, in Creation and Refinement of the SPM for Spinal Surgery we describe the model creation and refinement process of the SPM based on the collected data.

Ontology and Deductive Modeling of SPM for Open Spinal Surgeries

There exist several works that focus on the definition and the implementation of SPMs (14). While efforts have been made for standardization of SPM ontology definition (47), there exist a wide range of techniques that are tailored to a specific type of intervention [e.g., (48–50)]. Furthermore, as stated in (51), there are multiple definitions of modeling granularity levels available in the prior-art with no consensus across different domains. To this end, we have chosen a combination of recognized modeling schemes presented in (15, 52, 53), which are among the most widely used approaches to date that describe a SPM based on 6 granularity levels (μ) that correspond to different hierarchical elements, with $\mu \in [0,5]$. The highest granularity level ($\mu = 5$) encompasses the surgical procedure itself, therefore SPM will often have only one element at this granularity level. In the model described by (52), surgical procedures are further divided into steps ($\mu = 4$), sub-steps ($\mu = 3$), tasks ($\mu = 2$), sub-tasks ($\mu = 1$) and down to the lowest hierarchical level ($\mu = 0$), which describes each motion performed by the surgeon. This model provides information about the granularity level and hierarchy but does not provide other important parameters,

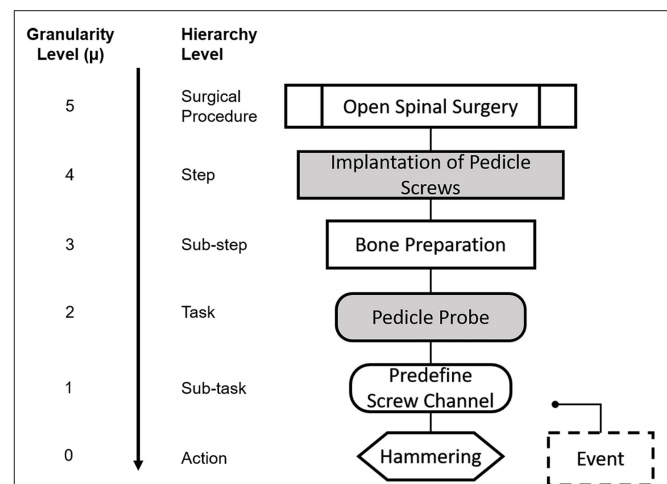


FIGURE 1 | Nomenclature for the Granularity and Hierarchy Levels used in our SPMs. Each element is depicted with a distinctive geometrical shape throughout the manuscript. We show here an example case for each of the given granularity levels. The higher granularity level ($\mu = 5$) corresponds to the surgical procedure itself and is depicted as a marked rectangle. $\mu = 4$ and $\mu = 3$ correspond to steps and substeps and are denoted by a filled and a non-filled rectangle, respectively. $\mu = 2$ and $\mu = 1$ correspond to tasks and sub-tasks and are denoted by a filled and non-filled rounded rectangle, respectively. Actions ($\mu = 0$) are denoted by hexagon and events are represented by a dashed rectangle.

such as temporal information, technologies used, structures involved, and participants. The SPM technique developed in (53) presented a model, which includes such missing information and is focused on integrating the control systems in the operation room. However, the granularity level used in (53) does not allow for an easy clinical description of the surgical workflow, as the processes are described in a rather technical manner and are not intuitive for clinical setup. Thus, in the herein study we used a modified version of the model presented in (52), with enhancements inspired from (15) and (53).

Hierarchical Decomposition and Nomenclature of Surgical Process Models

We propose a SPM with specific shapes and shadings for each hierarchical level as shown in **Figure 1**, so that we can easily identify different levels of granularity. This is required in order to capture the highly dynamic changes of surgeries within the SPM. During the normal surgical workflow, the surgeon often revisits one of the previous tasks or subtasks while still focusing on the same surgical step, meaning that the surgeon could complete elements of different granularity levels. For example, the surgeon might decide to cement the bone ($\mu = 0$) while inserting a pedicle screw ($\mu = 3$), because the quality of the bone is not as expected and the screw purchase might be otherwise compromised. In order to capture these changes throughout hierarchical levels, we needed to allow for our SPMs to operate at different granularity levels.

As indicated in **Figure 1**, granularity level $\mu = 5$ corresponds to the surgical procedure itself, open spinal surgery (e.g., spinal

fusion surgery), as presented also in (52). This surgical procedure is subsequently decomposed into surgical steps ($\mu = 4$). In our model, the surgical steps correspond to the set of standardized steps in the clinical literature of each procedure, with the purpose of maximizing compatibility with the clinical workflow, and to facilitate the identification of the different steps during the surgical process analysis. Thus, granularity level $\mu = 4$ is associated to each of the steps that define the spinal fusion procedure from a high-level perspective.

In order to include a more dynamic representation of the real workflow of the surgery, steps must be further divided into lower levels of granularity. Hence, in our model, surgical steps are further decomposed into sub-steps ($\mu = 3$). These sub-steps are defined as the collection of smaller units that can be associated to surgical checkpoints during the intervention. To this end, technical manuals provided by spinal fusion implant manufacturers (USS Universal Spine System, OPAL, MATRIX Spine System, Synthes GmbH, Oberdorf, Switzerland) were a valuable source that allowed a better insight into the definition of the sub-steps and tools used in the surgical procedure. For instance, in the example case presented in **Figure 1**, for the step “Implantation of pedicle screws”, there are two surgical sub-units or sub-steps that must be executed for the overarching step to be completed. In a first sub-step, the bone must be prepared for the screw insertion, and in a second sub-step the insertion of the screw itself is performed. This level of granularity also has the attribute of repetition, meaning that a sub-step could be done several times before moving on to the next one.

Subsequently, sub-steps can be further split into surgical tasks and sub-tasks with $\mu = 2$ and $\mu = 1$, respectively. Surgical tasks and sub-tasks are smaller workflow elements that are needed for the completion of a sub-step and that can be associated to specific techniques or tools during the surgery. The difference between a task and a sub-task, is that tasks are directly related to a specific sub-step in the hierarchy, whereas the same sub-task can be found across different sub-steps. Using again the example of **Figure 1**, for the sub-step “Bone preparation,” the task “Pedicule probe” is needed, which entails predefining the screw channel and performing hemostasis to stop bleeding (sub-tasks, $\mu = 2$). The latter is not exclusive to the bone preparation step, and it is in fact performed across different steps and sub-steps throughout the surgical procedure. The lowest hierarchical level “Action” with granularity $\mu = 0$ included in our model defines the surgical actions, which refer to specific workflow units related to the action performed by the surgeon, i.e., hammering, cementing, cutting, etc.

We have also included some enhancements to our SPM analysis inspired by the model in (15): First, the surgical tool used is indicated within the name of the “Action” when appropriate. Second, we have included an additional element with granularity levels $\mu \leq 1$, denominated “Event” and it is used to represent unexpected deviations in the standard surgical protocol that might happen more than once.

Deductive SPM for Open Spinal Surgeries

The systematic analysis of a surgical process required an in-depth insight into the surgical procedure and a sufficient understanding

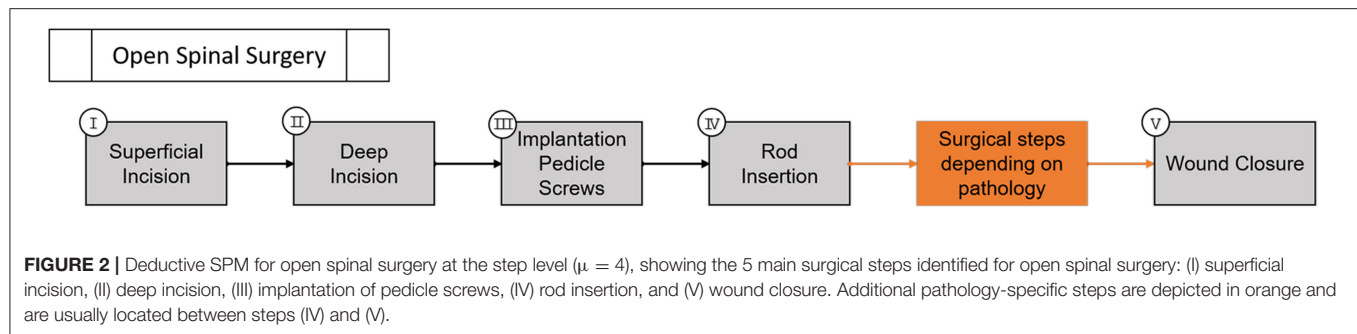
of the main steps, the used instruments, and technical aspects of the surgeries. Therefore, before the analysis and creation of the SPMs from empirical data, a deductive SPM of the surgical procedure was created at the step level ($\mu = 4$) and is shown in **Figure 2**. Five surgical steps were identified from the available clinical literature: (I) superficial incision, (II) deep incision, (III) implantation of pedicle screws, (IV) rod insertion, and (V) wound closure. Considering the variations amongst different surgical techniques that are dedicated to specific conditions (e.g., trauma, deformity correction, tumor surgery, etc.) an intermediate step between steps (IV) and (V) was identified and highlighted in a different color in **Figure 2**. Given that almost all open spinal interventions share the steps (I)–(V) in common, this work only focuses on providing detailed SPMs for those steps. These steps were proposed based on orthopedic textbooks (54) and online resources with process descriptions and surgical guidelines of spinal fusion procedures (www.orthobullets.com). Furthermore, consultations with surgery specialists were made to ensure the adequacy of the initial deductive model (See **Appendix**). This deductive SPM at the step level was validated using two video recordings of spinal fusion surgery, recorded at our institution as part of the standard clinical procedure (see Data Collection and Annotation). In particular, the workflow at the hierarchical level of surgical steps is conceived as successive, meaning that the steps are expected to follow a forward direction from the first step, up to the last one.

As stated before, in our SPM, the connection between elements can happen across different hierarchical levels and this evolution between different elements of the SPM is denominated as “Transition” and is represented with a solid arrow. These transitions indicate the standard or expected workflow. Transitions that occur due to repetition, or that happen as consequence of deviations of the standard workflow are depicted with a dashed arrow.

Through iterative top-down analyses of surgical procedures and bottom-up analyses of tool motions, we provided detailed decomposition of the procedures down to the level of actions. From observable surgical elements based on the data collection (Data Collection and Annotation), we have operationally defined the beginnings and endings of surgical steps, sub-steps, tasks, sub-tasks and actions. We have recorded the process from the main surgeon’s perspective, therefore the target participant was always the same. In terms of the anatomy, as the SPM is specific for the spine, the body part was always the vertebrae.

Data Collection and Annotation

We collected videos from open spinal operations performed at our clinic on 24 patients, between April and July 2019. We included videos captured from spinal fusion operations performed mainly in the lower thoracic and lumbosacral region (Th11-S1), which are performed more commonly. The included operations were performed to account for the following pathologies (some patients had multiple pathologies): fracture, degenerative disc disease, foraminal stenosis, spinal canal stenosis and spondylolisthesis. Each operation was performed by two surgeons and data from a total of 5 surgeons were included.



A total of 157 pedicle screws and 30 interconnecting longitudinal rods were inserted.

Given the practical limitations in recording the entire duration of the surgeries, we identified the step “implantation of pedicle screws” to have the highest priority given its inherent surgical complexity. Therefore, we ensured that all the recordings at least included the entirety of this step and possibly more of the surgical steps.

We collected intraoperative video recordings of the aforementioned spinal operations using 3 different camera systems: a flexible crane camera (custom-made model for our hospital; Medical-Polecam, Apoint Film GmbH, Switzerland), a fixed camera integrated into the operation room’s surgical light (truvidia wireless camera, 3.8–38 mm focal length, 1,080p resolution; Trumpf Medical, Germany) and an eye-tracking head-mounted camera (SMI eye tracking glasses; iMotions GmbH, Bern, Switzerland). The intraoperative videos acquired from the crane and fixed camera were previously recorded for training or quality control purposes in the frame of the standard surgical procedure. The videos captured using the eye-tracking camera were acquired within the frame of a related project within our group (BASEC No. 2018-00533). In total, we collected the video data from 24 spinal fusion surgeries performed at our institution resulting in roughly 40 h and 30 min of video footage. Information about screw insertion and fluoroscopy times was obtained from the operation protocol of each corresponding surgery. We also noted auxiliary information about the relevant intraoperative events, which could not be inferred from the video recordings, namely: the position of the two main surgeons (which surgeon was on which side of the patient and who performed which surgical steps), and unexpected events leading to deviations in the surgical procedure.

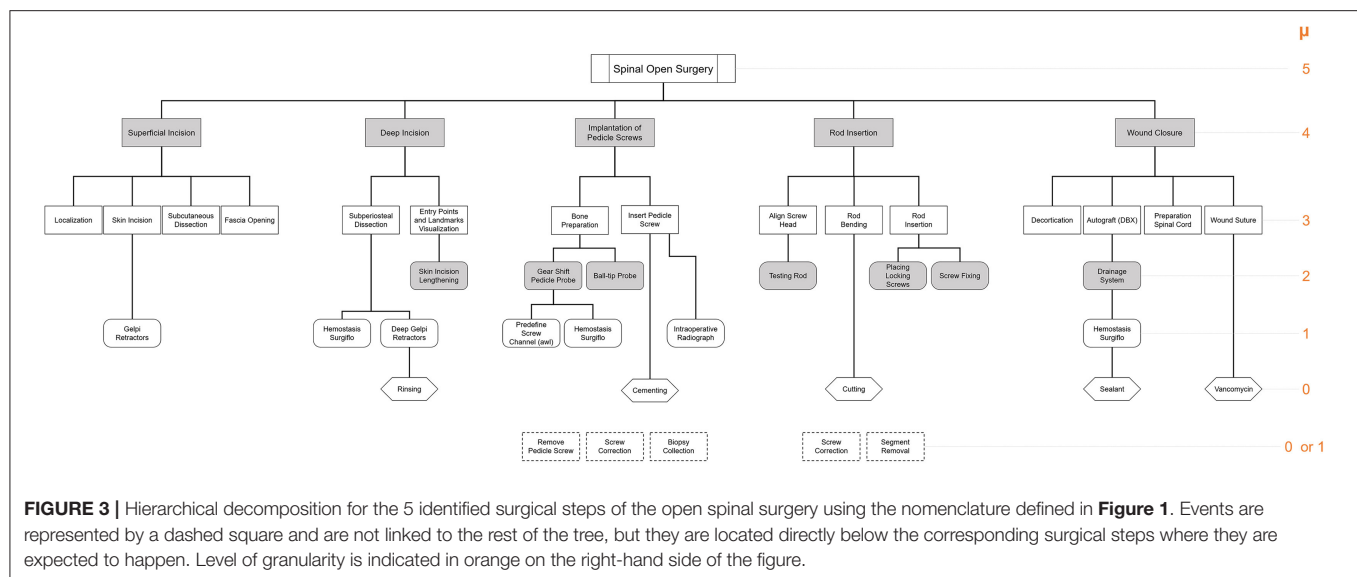
We investigated all the recordings to find the starting and the ending points in which all the primary surgical elements took place. The starting point of a video was set at the localization of the target spine levels and the dorsomedial skin incision; thereafter, the ending point was set at the wound closure. Later, we temporally annotated all of the events that were observable in the video data up to granularity level $\mu = 0$ (if necessary for the respective surgical step). For each operation, all the transitions between the observed elements were recorded in a spreadsheet, which allowed to keep track of their frequency.

Creation and Refinement of the SPM for Spinal Surgery

Having a set of recordings for the surgical procedures is one of the first steps for the analysis and generation of the SPMs. Manual labeling of the videos data and tracking of the transitions between the different states of the surgery allowed for working out the relationship between all the elements of the surgical workflow. For the exploration of several recorded processes and general overview of all the elements of the intervention under analysis, the hierarchical decomposition of the procedure is needed. Based on the surgical steps of the deductive SPM presented in **Figure 2**, and the aforementioned ontology, we generated the hierarchical decomposition for spinal fusion surgeries, and its graphical representation is presented in **Figure 3**. The upper most level ($\mu = 5$) is dictated by the surgical procedure itself, which is then branched into the identified surgical steps ($\mu = 4$). Subsequently, the hierarchical tree was iteratively refined using the information of the spreadsheet generated based on the annotated videos, the temporal information about the surgical task ($0 \leq \mu \leq 4$), and the transitions between the elements.

In a first iteration, each surgical step was extended into their corresponding sub-steps ($\mu = 3$). In case the sub-step level was not sufficient to describe the corresponding workflow of the surgery, it was further decomposed into tasks ($\mu = 2$). The iterative process was performed until the granularity level was sufficient to describe the surgical element in question (from a clinical perspective), or until the lowest granularity level was reached ($\mu = 0$). If an unexpected event happened during one of the surgical recordings, which is not normally part of the operation or which had to be performed because of a deviation of a surgical element, the event was noted and the number of transitions to that event was measured; however, the element was not linked to the rest of the hierarchical tree. These events are represented by a dashed square and are located directly below the corresponding surgical steps where they have been identified. The hierarchical decomposition of **Figure 3** is used as a guide to generate the individual SPM of each of the surgical steps of the spinal fusion procedure shown in **Figure 2**.

The final SPMs presented in this study have a granularity level $\mu \leq 3$, which includes sub-steps, tasks, sub-tasks, and actions. For the generation of each SPM, an iterative approach was followed. In a first phase and for each surgical step, all



surgical elements with $\mu = 3$ were identified from the hierarchical tree (**Figure 3**). Subsequently, the transition between the sub-steps was set using the annotated information in the spreadsheet. After each iteration, the number of transitions between the same sub-steps among all recorded operations was updated. The total number of transitions between every two elements is indicated with an integer above the connecting arrows. As stated previously, transitions that occur due to repetition, or that happen as consequence of deviations of the standard workflow were depicted with a dashed arrow. Iteratively, the transitions between all the workflow elements were updated for each granularity level, down to the level of actions. The final SPMs are given in the form of digital diagrams and were generated using the diagramming software Microsoft Visio (Creative Cloud, Microsoft Corporation, Redmond, Washington, U.S., 2020) and the tools for workflow drawing provided by Microsoft Power Point (Microsoft Office 2020, Microsoft Corporation, Redmond, Washington, U.S.). Finally, all of the generated SPMs were presented to one of the chief spine surgeons at our institution, who evaluated the quality and accuracy of the models and confirmed their validity.

RESULTS

Based on our collected data, the operations took an average of 2.5 h and were performed on an average of 3–4 spinal segments. For each of the 5 steps, we have generated individual SPMs with a minimum granularity level of $\mu = 0$ wherever it was needed. Each step was further divided according to the process described in the methodology.

As stated earlier, the *implantation of pedicle screws* step was included in all of the 24 recordings of the surgeries; however, a lower number of case recordings were present for the rest of the steps. An overview of the total number of cases for which a given surgical step was recorded is presented in **Table 1**.

TABLE 1 | Overview of the total number of cases recorded for a given surgical step.

Surgical step	Number of cases recorded
Superficial incision	11
Deep incision	22
Screw Implantation	24
Rod-Insertion	15
Wound Closure	12

The first step was the superficial incision of the tissue over the vertebral segments to be fused. The resulting SPM for this step is shown in **Figure 4**.

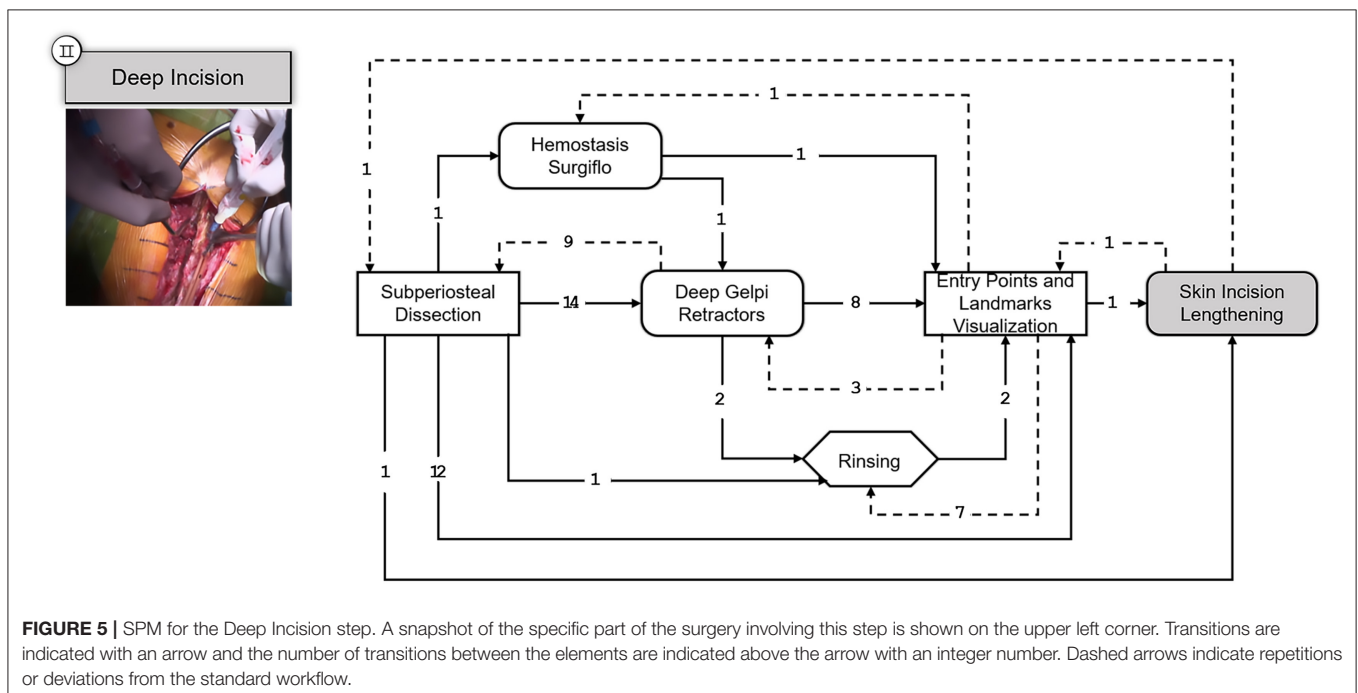
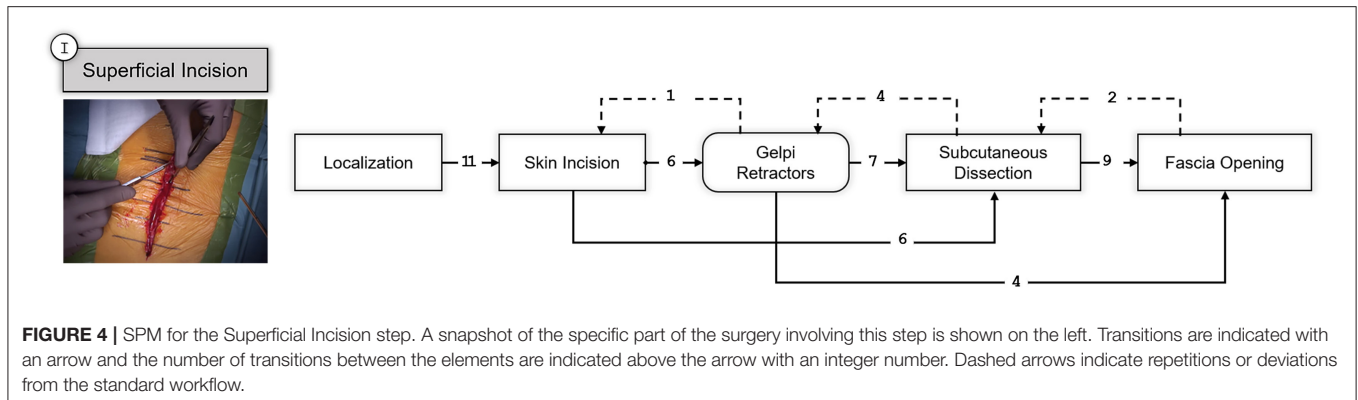
The following step, corresponds to the deep incision of the musculature after opening the muscle fascia so that the vertebral bodies are visualized. The obtained SPM is depicted in **Figure 5**.

In the third and fourth step, the intended instrumentation of the pedicle screw system and the insertion of the connecting rods takes place, **Figures 6, 7** respectively. As stated before, these two steps are optionally followed by various procedures depending on the underlying conditions. Depending on the operation, procedures for decompression of the spinal canal or spinal nerves via various techniques can be performed and cages can be inserted for anterior stabilization of the spinal column (TLIF and PLIF). Also, pedicle subtraction osteotomies (PSO) might be performed at this point. However, such condition-specific steps are excluded in this work to provide SPMs that can generalize to a wider range of open spinal surgeries.

Finally, the SPM of the last step of the surgical procedure is shown in **Figure 8**, corresponding to the wound closure.

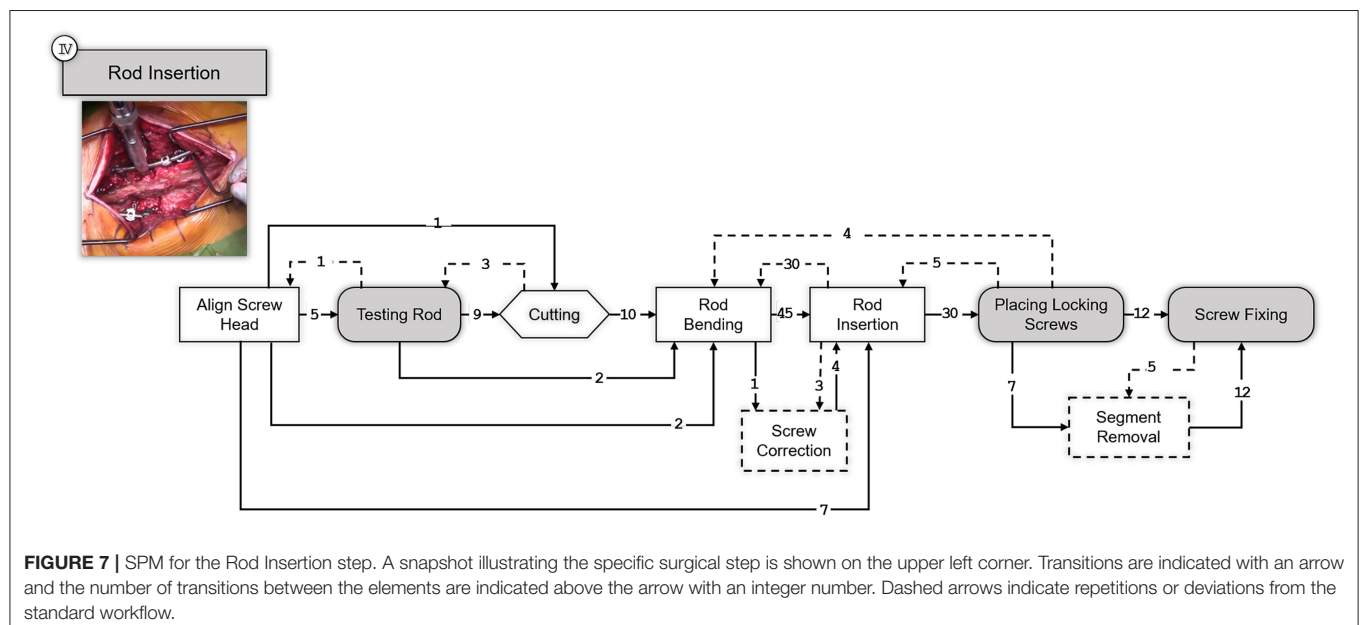
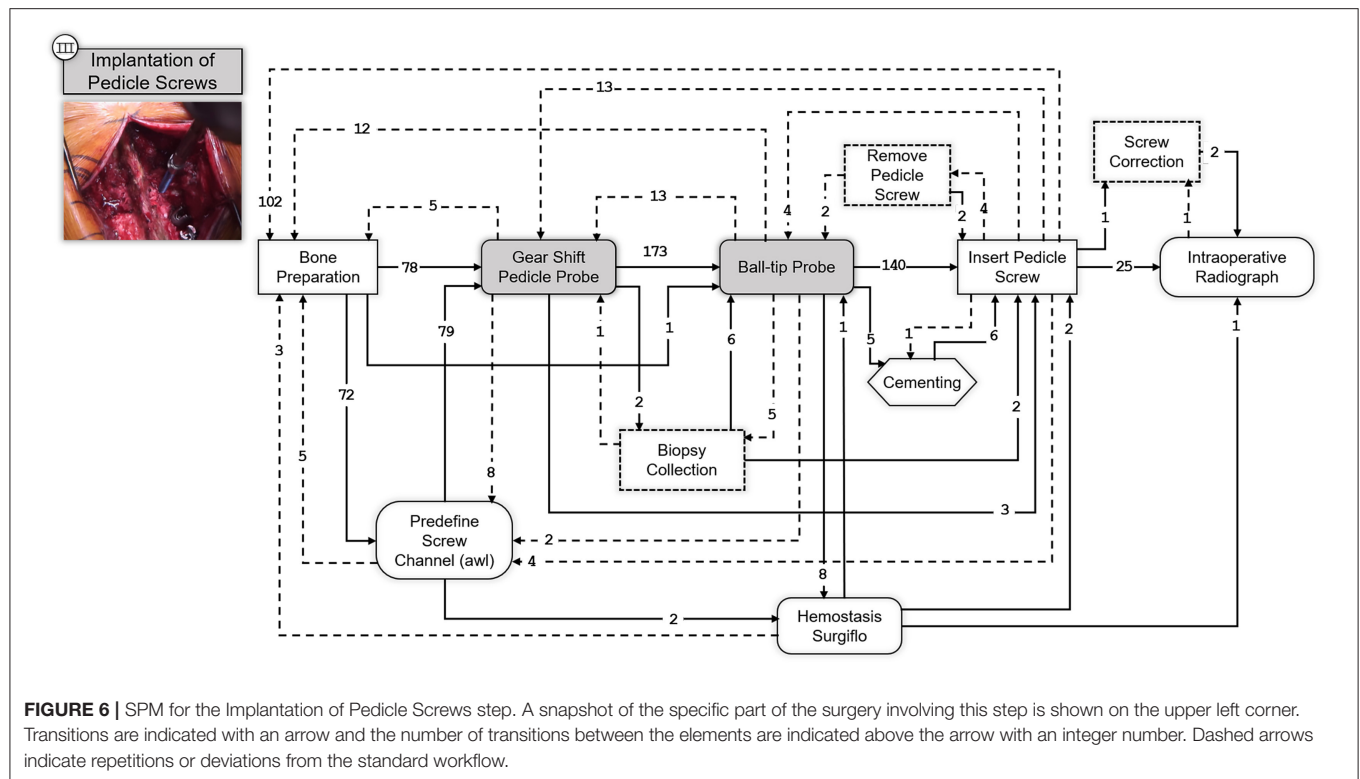
DISCUSSION

With the recent advent of advanced medical technologies and the ever-increasing surgical workflow complexity, it is



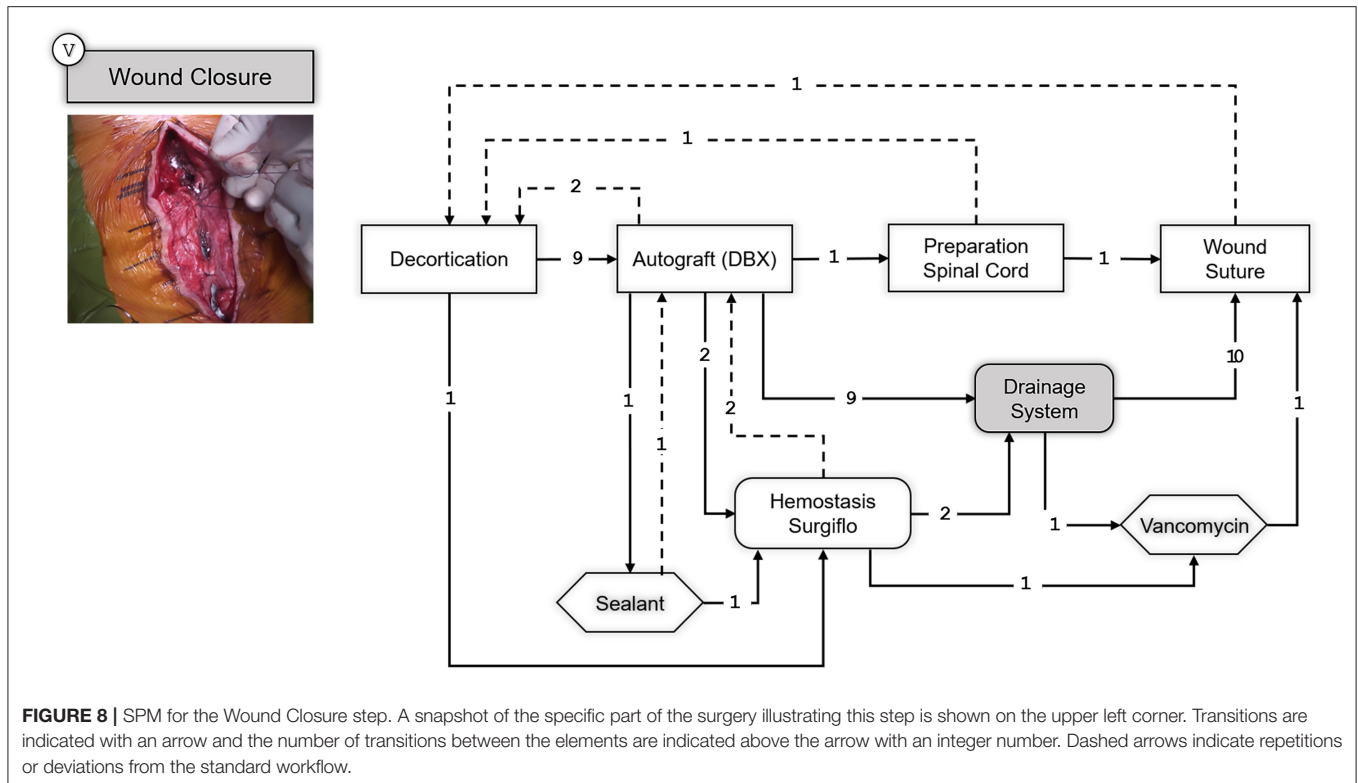
important to derive comprehensive surgical process models that can capture the activities conducted in a common surgical intervention and the inter-relationships between the events. Such models are of utmost importance for objectives such as: standardization of the interventions, surgical training and communication, surgical team workload analysis and operating room management, and development of algorithms that are focused on applications such as: surgical activity recognition [e.g. (55)], surgical skill evaluation [e.g. (56)], prediction of next surgical tasks [e.g. (57)], intervention time prediction [e.g. (58)]. Despite the abundance of methods and algorithms for generating SPMs for laparoscopic and endoscopic procedures [e.g. (49)], modeling of open spinal interventions remains an underrepresented task. Therefore, in this study, we provided an SPM dedicated to spinal fusion surgery through annotation and analysis of direct video observations captured during such operations.

An analogy similar to (52) was used to classify the hierarchy of the surgical elements. In the pre-modeling phase, we relied on the available intervention-specific literature [e.g., (54)] to derive a high-level model of the surgeries up to granularity level $\mu = 4$. The process models were then further expanded up to the action level ($\mu = 0$) based on manual annotation and analysis of the captured video observations. We encountered challenges when analyzing recordings captured by the fixed OR light camera. First, the view was often obscured by the surgeons' heads or due to the moving of the operating light. This resulted in difficulty in assessing the position of the anatomy only based on the static two-dimensional video feed provided by this camera assembly. In addition, most operations were performed within a large operating area, and the operating table was often moved up and down, making it harder to observe the surgical elements based on the fixed OR light camera feed. We overcame these challenges by using the recordings that were available from the



two other camera modalities. The crane camera footage provided more viewing angles since it was manually placed at a position to provide a view with a low level of obscurity, usually at an angle between the OR lights, or at an oblique angle from cranial or caudal directions, as well as from oblique lateral direction. Using the control unit on the embedded 3-axis remote camera head of the crane camera, the position was altered in the recordings to

achieve a clear view on to the anatomy. Additionally, the zoom function on this camera platform provided both wide-range overview shots and close-up views. The video recordings from the crane camera provided a more reliable view of the operating area, the anatomy at which the operation was performed, the forearms of the surgeon, and the instruments used. However, those videos provided limited information about events that



occurred outside the surgical area (e.g., cutting and bending of connecting rods) and interactions between the surgeons and the assistants. Using the video recordings from the eye-tracking head-mounted camera we were able to address these limitations. The first-person view provided additional information about the surgeon's line of sight, which captured many auxiliary surgical elements that were happening outside the operating area (e.g., fluoroscopy, interaction with the team, viewing the MRI/CT images).

We provided detailed SPMs for each major surgical step that are common in most open spinal surgeries and highlighted the transitions between different surgical elements and the frequencies associated with those transitions. During the analysis of the videos, we noticed some deviations from the expected surgical workflow, and we included those as events into the generated SPMs. Even though these unexpected events are rather common during surgery, they cannot be classified as a part of a surgical step and are currently difficult to predict. For instance, during spine surgeries, it might be necessary to correct the position of a pedicle screw or to change its length intraoperatively, due to low bone density in the pedicle or to a slight deviation from the afore planned surgery. These events are unavoidable but could be reduced to a minimum with an improved surgical guidance. Therefore, creating SPMs which accounts also for these deviations could eventually allow surgeons to anticipate such errors during the specific steps where they are more prompt to occur.

Knowing beforehand the possible transitions between the surgical steps, sub-steps, task, sub-task, and motions could not only improve the surgical workflow, but it could also assist novice surgeons and less experienced surgical scrub technicians to be better prepared during the surgery.

Following, we would like to discuss some of the limitations of this work. Firstly, it should be noted that although the inter-institution variability was taken into account in the developed SPMs (given that we have analyzed the data from five different spine surgeons), further data is required to improve the generalizability of the developed model to other institutions and surgeons. This is because the herein presented SPMs are closely linked to the clinical setting and to the surgical technique utilized at our clinical institution. If, for instance, a different pedicle screw supplier would be used, this might modify or introduce additional elements into the surgical workflow, which our SPMs do not currently account for. In other words, the inter-clinical variability of the generated SPMs highly depends on the adopted surgical techniques of each operating room. Another limitation of our work was the manual labeling of the video recordings, which is very time consuming and requires surgical and orthopedic knowledge. The quality of the manual video annotations is also subjective to the quality of the video and to the different perspectives available. A possible solution could be the use of a specialized software such as the SWAN-Suite (59), which has proven to be highly accurate when registering and analyzing surgical workflows in several institutions. There exist other video-based algorithms

(60–62) that could help in improving the labeling accuracy of the SPM creation process. However, most of the recent data-driven surgical activity recognition methods rely on a proper understanding of a model that describes the underlying surgical 'process'; therefore, the presented SPMs in this study can serve as the basis for the development of such algorithms that can be used in open spinal surgery applications. Finally, the generated SPM in this study was only validated based on the feedback from one surgeon.

Similar validation methods that are based on structured interviews with surgeons have been previously introduced [e.g., (63)]. A more extensive evaluation and validation protocol will contribute to refinement and standardization of the developed SPMs through follow-up studies based on input from multiple surgeons and multiple centers, as well as a technical validation through additional surgery observations with a dedicated SPM Ontology software [e.g., (55, 59, 60)].

CONCLUSION

The herein study presents the methodological process through which we generated a series of SPMs corresponding to the most common surgical steps required for open spinal surgeries. For this, we followed a top-down modeling approach for the first theoretical model of the SPM, and a bottom-up granularization approach derived from the video analysis. Combining these two development directions ensured a thorough description of the entire surgical procedure. The resulting SPMs represent a first step into digitizing surgery information and can help to improve the current intraoperative guidance methods, as well as easing the future integration of augmented reality and machine learning approaches into the daily clinical practice.

REFERENCES

- Stitzenberg KB, Sheldon GF. Progressive specialization within general surgery: adding to the complexity of workforce planning. *J Am Coll Surg.* (2005) 201:925–32. doi: 10.1016/j.jamcollsurg.2005.06.253
- Cleary K, Kinsella A, Mun SK. OR 2020 workshop report: operating room of the future. *Int Congr Ser.* (2005) 1281:832–8. doi: 10.1016/j.ics.2005.03.279
- Joskowicz L. Computer-aided surgery meets predictive, preventive, and personalized medicine. *EPMA J.* (2017) 8:1–4. doi: 10.1007/s13167-017-0084-8
- Herrell SD. Robotic surgery: past, present, and future. In: Su L-M, editor. *Atlas of Robotic Urologic Surgery*. Cham: Springer International Publishing (2017). p. 459–72.
- Negrillo-Cárdenas J, Jiménez-Pérez JR, Feito FR. The role of virtual and augmented reality in orthopedic trauma surgery: from diagnosis to rehabilitation. *Comput Methods Programs Biomed.* (2020) 191:105407. doi: 10.1016/j.cmpb.2020.105407
- Hashimoto DA, Ward TM, Meireles OR. The role of artificial intelligence in surgery. *Adv Surg.* (2020) 54:89–101. doi: 10.1016/j.yasu.2020.05.010
- Maier-Hein L, Vedula SS, Speidel S, Navab N, Kikinis R, Park A, et al. Surgical data science for next-generation interventions. *Nat Biomed Eng.* (2017) 1:691–6. doi: 10.1038/s41551-017-0132-7
- Padoy N, Blum T, Feussner H, Berger M-O, Navab N. On-line recognition of surgical activity for monitoring in the operating room. In: *Proceedings of the 20th national conference on Innovative applications of artificial intelligence, Vol.3*. Chicago, IL: AAAI Press (2008).
- Padoy N, Blum T, Ahmadi SA, Feussner H, Berger MO, Navab N. Statistical modeling and recognition of surgical workflow. *Med Image Anal.* (2012) 16:632–41. doi: 10.1016/j.media.2010.10.001
- Riffaud L, Neumuth T, Morandi X, Trantakis C, Meixensberger J, Burgert O, et al. Recording of surgical processes: a study comparing senior and junior neurosurgeons during lumbar disc herniation surgery. *Neurosurgery.* (2010) 67(2 Suppl Operative):325–32. doi: 10.1227/NEU.0b013e3181f741d7
- Nakawala H, Ferrigno G, De Momi E. Development of an intelligent surgical training system for thoracentesis. *Artif Intell Med.* (2018) 84:50–63. doi: 10.1016/j.artmed.2017.10.004
- Liebmann P, Neumuth T. Model driven design of workflow schemata for the operating room of the future. In: *INFORMATIK 2010 Service Science–Neue Perspektiven für die Informatik*. Bonn: GI (2010). p. 419.
- Driessen SRC, Van Zwet EW, Haazebroek P, Sandberg EM, Blikkendaal MD, Twijnstra ARH, et al. A dynamic quality assessment tool for laparoscopic hysterectomy to measure surgical outcomes. *Am J Obstet Gynecol.* (2016) 215:754.e1–754.e8. doi: 10.1016/j.ajog.2016.07.004
- Gholinejad M, Loeve AJ, Dankelman J. Surgical process modelling strategies: which method to choose for determining workflow? *Minim Invasive Ther Allied Technol.* (2019) 28:15. doi: 10.1080/13645706.2019.1591457
- Neumuth T. Surgical process modeling. *Innov Surg Sci.* (2017) 2:123–37. doi: 10.1515/iss-2017-0005

DATA AVAILABILITY STATEMENT

The datasets presented in this article are not readily available because according to our institutional guidelines, no patient data can be shared with third parties outside the umbrella of our organization. Requests to access the datasets should be directed to <https://rocs.balgrist.ch/en/open-access/>.

ETHICS STATEMENT

Ethical review and approval was not required for the study on human participants in accordance with the local legislation and institutional requirements. Written informed consent for participation was not required for this study in accordance with the national legislation and the institutional requirements.

AUTHOR CONTRIBUTIONS

PF, MF, JS, CL, HE, FC, MA: conceptualization. MF, JS, PF: resources. HE, FC, SM, AM, DS: methodology. SM, MA: data collection. SM: data annotation. FC, HE: data curation. SM, HE, FC: process model derivation. HE, FC: writing (original draft preparation). PF, HE, FC, MF, JS, CL, SM, MA: writing (review and editing). PF, HE, FC, MA: supervision. DS, CL, HE, FC: project administration. All authors contributed to manuscript revision, read, and approved the submitted version.

FUNDING

The work was supported by the Functionally Accurate Robotic Surgery (FAROS) project. This project has received funding from the European Union's Horizon 2020 research and innovation program under grant agreement No 101016985.

16. Padoy N, Blum T, Essa I, Feussner H, Berger MO, Navab N. A boosted segmentation method for surgical workflow analysis. *Med Image Comput Comput Assist Interv.* (2007) 10(Pt 1):102–9. doi: 10.1007/978-3-540-75757-3_13
17. Ahmadi SA, Sielhorst T, Stauder R, Horn M, Feussner H, Navab N. Recovery of Surgical Workflow Without Explicit Models. In: Larsen R, Nielsen M, Sparring J, editors. *Medical Image Computing and Computer-Assisted Intervention – MICCAI 2006*. Berlin, Heidelberg: Springer (2006). p. 420–8. (Lecture Notes in Computer Science)
18. Zappella L, Béjar B, Hager G, Vidal R. Surgical gesture classification from video and kinematic data. *Med Image Anal.* (2013) 17:732–45. doi: 10.1016/j.media.2013.04.007
19. Twinanda AP, Shehata S, Mutter D, Marescaux J, Mathelin M de, Padoy N. EndoNet: a deep architecture for recognition tasks on laparoscopic videos. *IEEE Trans Med Imaging.* (2017) 36:86–97. doi: 10.1109/TMI.2016.2593957
20. Bodenstedt S, Wagner M, Katić D, Mietkowski P, Mayer B, Kenngott H, et al. *Unsupervised Temporal Context Learning Using Convolutional Neural Networks for Laparoscopic Workflow Analysis*. ArXiv170203684 Cs. (2017). Available online at: <http://arxiv.org/abs/1702.03684> (accessed January 12, 2021).
21. Si C, Chen W, Wang W, Wang L, Tan T. *An Attention Enhanced Graph Convolutional LSTM Network for Skeleton-Based Action Recognition*. ArXiv190209130 Cs. (2019). Available online at: <http://arxiv.org/abs/1902.09130> (accessed January 12, 2021)
22. Esfandiari H, Newell R, Anglin C, Street J, Hodgson AJ. A deep learning framework for segmentation and pose estimation of pedicle screw implants based on C-arm fluoroscopy. *Int J Comput Assist Radiol Surg.* (2018) 13:1269–82. doi: 10.1007/s11548-018-1776-9
23. Liebmann F, Roner S, von Atzigen M, Scaramuzza D, Sutter R, Snedeker J, et al. Pedicle screw navigation using surface digitization on the Microsoft HoloLens. *Int J Comput Assist Radiol Surg.* (2019) 14:1157–65. doi: 10.1007/s11548-019-01973-7
24. Maffulli N, Rodriguez HC, Stone IW, Nam A, Song A, Gupta M, et al. Artificial intelligence and machine learning in orthopedic surgery: a systematic review protocol. *J Orthop Surg.* (2020) 15:478. doi: 10.1186/s13018-020-02002-z
25. Deib G, Johnson A, Unberath M, Yu K, Andress S, Qian L, et al. Image guided percutaneous spine procedures using an optical see-through head mounted display: proof of concept and rationale. *J NeuroInterventional Surg.* (2018) 10:1187–91. doi: 10.1136/neurintsurg-2017-013649
26. Lipson SJ. Spinal-fusion surgery – advances and concerns. *N Engl J Med.* (2004) 350:643–4. doi: 10.1056/NEJMp038162
27. Vos T, Barber RM, Bell B, Bertozzi-Villa A, Biryukov S, Bolliger I, et al. Global, regional, and national incidence, prevalence, and years lived with disability for 301 acute and chronic diseases and injuries in 188 countries, 1990–2013: a systematic analysis for the global burden of disease study 2013. *Lancet.* (2015) 386:743–800. doi: 10.1016/S0140-6736(15)60692-4
28. Picavet HSJ, Schouten JSAG. Musculoskeletal pain in the netherlands: prevalences, consequences and risk groups, the DMC3-study. *Pain.* (2003) 102:167–78. doi: 10.1016/S0304-3959(02)00372-x
29. Murray CJL, Vos T, Lozano R, Naghavi M, Flaxman AD, Michaud C, et al. Disability-Adjusted Life Years (DALYs) for 291 diseases and injuries in 21 regions, 1990–2010: a systematic analysis for the global burden of disease study 2010. *Lancet.* (2012) 380:2197–223. doi: 10.1016/S0140-6736(12)61690-0
30. Raciborski F, Gasik R, Klak A. Disorders of the spine. A Major Health and Social Problem. *Reumatologia.* (2016) 4:196–200. doi: 10.5114/reum.2016.62474
31. Bailly F, Foltz V, Rozenberg S, Fautrel B, Gossec L. The impact of chronic low back pain is partly related to loss of social role: a qualitative study. *Joint Bone Spine.* (2015) 82:437–41. doi: 10.1016/j.jbspin.2015.02.019
32. Schofield DJ, Shrestha RN, Percival R, Callander EJ, Kelly SJ, Passey ME. Early retirement and the financial assets of individuals with back problems. *Eur Spine J.* (2011) 20:731–6. doi: 10.1007/s00586-010-1647-8
33. Koes BW, van Tulder MW, Thomas S. Diagnosis and treatment of low back pain. *BMJ.* (2006) 332:1430–4. doi: 10.1136/bmj.332.755.1430
34. van Tulder MW, Koes BW, Bouter LM. Conservative treatment of acute and chronic nonspecific low back pain: a systematic review of randomized controlled trials of the most common interventions. *Spine.* (1997) 22:2128–56. doi: 10.1097/00007632-199709150-00012
35. Deyo RA, Nachemson A, Mirza SK. Spinal-fusion surgery—the case for restraint. *Spine J.* (2004) 4:S138–42. doi: 10.1016/j.spinee.2004.08.001
36. Heini PF. The current treatment—a survey of osteoporotic fracture treatment. osteoporotic spine fractures: the spine surgeon's perspective. *Osteoporos Int.* (2005) 16:S85–92. doi: 10.1007/s00198-004-1723-1
37. Hee HT, Majd ME, Holt RT, Pienkowski D. Better treatment of vertebral osteomyelitis using posterior stabilization and titanium mesh cages. *J Spinal Disord Tech.* (2002) 15:149–56; discussion 156. doi: 10.1097/00024720-200204000-00010
38. Maruyama T, Takeshita K. Surgical treatment of scoliosis: a review of techniques currently applied. *Scoliosis.* (2008) 3:6. doi: 10.1186/1748-7161-3-6
39. Mackel CE, Jada A, Samdani AF, Stephen JH, Bennett JT, Baaj AA, et al. A comprehensive review of the diagnosis and management of congenital scoliosis. *Childs Nerv Syst.* (2018) 34:2155–71. doi: 10.1007/s00381-018-3915-6
40. Esfandiari H. *An Intraoperative Position Assessment System for Pedicle Screw Insertion Surgeries* (PhD Thesis). The University of British Columbia, Vancouver, Canada (2020).
41. Katonis P, Christoforakis J, Aligizakis AC, Papadopoulos C, Sapkas G, Hadjipavlou A. Complications and problems related to pedicle screw fixation of the Spine. *Clin Orthop.* (2003) 411:86–94. doi: 10.1097/01.blo.0000068761.86536.1d
42. Gautschi OP, Schatlo B, Schaller K, Tessitore E. Clinically relevant complications related to pedicle screw placement in thoracolumbar surgery and their management: a literature review of 35,630 pedicle screws. *Neurosurg Focus.* (2011) 31:E8. doi: 10.3171/2011.7.FOCUS11168
43. Nevzati E, Marbacher S, Soleman J, Perrig WN, Diepers M, Khamis A, et al. Accuracy of pedicle screw placement in the thoracic and lumbosacral spine using a conventional intraoperative fluoroscopy-guided technique: a national neurosurgical education and training center analysis of 1236 consecutive screws. *World Neurosurg.* (2014) 82:866–71.e2. doi: 10.1016/j.wneu.2014.06.023
44. Mummaneni PV, Dhall SS, Ondra SL, Mummaneni VP, Berven S. Pedicle subtraction osteotomy. *Neurosurgery.* (2008) 63(suppl_3):A171–6. doi: 10.1227/01.NEU.0000325680.32776.82
45. Hartl R, Lam KS, Wang J, Korge A, Kandziora F, Audigé L. Worldwide survey on the use of navigation in spine surgery. *World Neurosurg.* (2013) 79:162–72. doi: 10.1016/j.wneu.2012.03.011
46. Kosmopoulos V, Schizas C. Pedicle screw placement accuracy: a meta-analysis. *Spine.* (2007) 32:E111–20. doi: 10.1097/01.brs.0000254048.79024.8b
47. Gibaud B, Forestier G, Feldmann C, Ferrigno G, Gonçalves P, Haidegger T, et al. Toward a standard ontology of surgical process models. *Int J Comput Assist Radiol Surg.* (2018) 13:1397–408. doi: 10.1007/s11548-018-1824-5
48. Jannin P, Morandi X. Surgical models for computer-assisted neurosurgery. *Neuroimage.* (2007) 37:783–91. doi: 10.1016/j.neuroimage.2007.05.034
49. Katić D, Julliard C, Wekerle AL, Kenngott H, Müller-Stich BP, Dillmann R, et al. LapOntoSPM: an ontology for laparoscopic surgeries and its application to surgical phase recognition. *Int J Comput Assist Radiol Surg.* (2015) 10:1427–34. doi: 10.1007/s11548-015-1222-1
50. Perrone R, Nessi F, Momi E, Boriero F, Capiluppi M, Fiorini P, et al. Ontology-based modular architecture for surgical autonomous robots. In: *The Hamlyn Symposium on Medical Robotics*. London, UK: Imperial College (2014).
51. Nagy TD, Haidegger T. A DVRK-based framework for surgical subtask automation. *Acta Polytech Hung.* (2019) 16:61. doi: 10.12700/APH.16.8.2019.8.5
52. MacKenzie L, Ibbotson JA, Cao CGL, Lomax AJ. Hierarchical decomposition of laparoscopic surgery: a human factors approach to investigating the operating room environment. *Minim Invasive Ther Allied Technol.* (2001) 10:121–7. doi: 10.1080/136457001753192222
53. Neumuth T. *Surgical Process Modeling Theory, Methods, and Applications* (Habilitation Thesis). University of Leipzig, Leipzig, Germany (2012).
54. Stein G, Eysel P, Scheyerer MJ. Expertise orthopädie und unfallchirurgie wirbelsäule. *Georg Thieme Verlag.* (2019) 1:2216. doi: 10.1055/b-006-149533
55. Wang J, Chen Y, Hao S, Peng X, Hu L. Deep learning for sensor-based activity recognition: a survey. *Pattern Recognit Lett.* (2019) 119:3–11. doi: 10.1016/j.patrec.2018.02.010

56. Uemura M, Jannin P, Yamashita M, Tomikawa M, Akahoshi T, Obata S, et al. Procedural surgical skill assessment in laparoscopic training environments. *Int J Comput Assist Radiol Surg.* (2016) 11:543–52. doi: 10.1007/s11548-015-1274-2
57. Forestier G, Petitjean F, Riffaud L, Jannin P. Automatic matching of surgeries to predict surgeons' next actions. *Artif Intell Med.* (2017) 81:3–11. doi: 10.1016/j.artmed.2017.03.007
58. Franke S, Meixensberger J, Neumuth T. Intervention time prediction from surgical low-level tasks. *J Biomed Inform.* (2013) 46:152–9. doi: 10.1016/j.jbi.2012.10.002
59. Neumuth T, Mudunuri R, Jannin P, Meixensberger J, Burgert O. SWAN-Suite: the tool landscape for surgical workflow analysis. In Paris; Berlin; Boston, MA: De Gruyter (2007). p. 199–204.
60. Lalys F, Riffaud L, Morandi X, Jannin P. Automatic phases recognition in pituitary surgeries by microscope images classification. In: Navab N, Jannin P, editors. *Information Processing in Computer-Assisted Interventions*. Berlin, Heidelberg: Springer (2010). p. 34–44. (Lecture Notes in Computer Science).
61. Bhatia B, Oates T, Xiao Y, Hu P. Real-time identification of operating room state from video. In: *Proceedings of the 19th national conference on Innovative applications of artificial intelligence - Volume 2*. Vancouver, British Columbia, Canada: AAAI Press (2007). p. 1761–6. (IAAI'07).
62. Nagy DÁ, Rudas IJ, Haidegger T. OntoFlow, a software tool for surgical workflow recording. In: *2018 IEEE 16th World Symposium on Applied Machine Intelligence and Informatics (SAMI)* Herlany, Slovakia (2018). p. 000119–24.
63. Katić D, Wekerle AL, Görtler J, Spengler P, Bodenstedt S, Röhl S, et al. Context-aware augmented reality in laparoscopic surgery. *Comput Med Imaging Graph.* (2013) 37:174–82. doi: 10.1016/j.compmidimag.2013.03.003

Conflict of Interest: The authors declare that the research was conducted in the absence of any commercial or financial relationships that could be construed as a potential conflict of interest.

Publisher's Note: All claims expressed in this article are solely those of the authors and do not necessarily represent those of their affiliated organizations, or those of the publisher, the editors and the reviewers. Any product that may be evaluated in this article, or claim that may be made by its manufacturer, is not guaranteed or endorsed by the publisher.

Copyright © 2022 Carrillo, Esfandiari, Müller, von Atzigen, Massalimova, Suter, Laux, Spirig, Farshad and Fürnstahl. This is an open-access article distributed under the terms of the Creative Commons Attribution License (CC BY). The use, distribution or reproduction in other forums is permitted, provided the original author(s) and the copyright owner(s) are credited and that the original publication in this journal is cited, in accordance with accepted academic practice. No use, distribution or reproduction is permitted which does not comply with these terms.

APPENDIX

Surgical Step	Description
Superficial incision	Preparation until the thoracolumbar fascia is reached.
Preoperative marking	Check if patient has been preoperatively marked at the planned level.
Identification of landmarks	Mark bony prominences (posterior superior iliac spine, iliac crest, spinous processes, inter spinal window) and draw incision line. Ensure with fluoroscopy that correct levels are identified.
Skin incision over the target segments	Incision over the entire planned instrumentation length and through the full thickness of the skin.
Dissection of subcutaneous tissue	Preparation of subcutaneous fat until the thoracolumbar fascia is reached. Insertion of retractors is performed.
Opening of the thoracolumbar fascia	Opening of the thoracolumbar fascia and exposure of spinous process.
Deep incision	Exposure of bony landmarks
Detach paraspinous muscles	Subperiosteal detachment of the paraspinous musculature with electrocautery/Cobb Elevator. Remain strictly subperiosteal.
Insertion of deep retractors	Insert Deep retractors.
Implantation screw system (Pedicule screws)	Metal implants are placed in the pedicles so that on the one hand they provide optimal stability and on the other hand they do not injure critical soft tissues.
Bone preparation	Various options to prepare the pedicle for screw insertion (tagged as A,B and C).
Localization of the screw entry point	Localization of the screw entry point using anatomical landmarks. (Pars interarticularis, mamillary process, lateral border of the superior articular facet, mid transverse process).
A.Drilling	Definition of screw trajectory with drill (detailed in the following points).
A.1. Pre-drilling	Direct drilling of the screw channel with a drill.
A.2. Check the screw canal	Use ball tip probe to check for perforations and confirm length of pedicle screw.
B. Insertion of K-wire	Direct drilling of a K-wire as a guide for a cannulated screw.
C. Conventional method	Definition of screw trajectory with awl (detailed in the following points).
C.1. Opening of cortex	Opening the cortex with luer or pointed awl.
C.2. Pre-define screw channel with surgical bone awl (optional)	Use the awl to predefine the screw channel.
C.3. Insert gear shift pedicle probe / pedicle deepening awl	Determine the length and diameter of the required screw using the attached marking and imaging information.
C.4. Check the screw canal	Use ball tip probe to check for perforations and confirm length of pedicle screw.
Insert Pedicle Screw	Insert pedicle screw into predefined channel and maintain the trajectory.
Check screw purchase	Check insertional torque and pull-out resistance.
Check Screw position	Check screw position with intraoperative radiograph.



An Innovative Prone Position Using a Body-Shape Plaster Bed and Skull Traction for Posterior Cervical Spine Fracture Surgeries

Zhiyu Ding¹, Yijun Ren², Hongqing Cao¹, Yuezhan Li¹, Shijie Chen¹, Jinglei Miao¹ and Jinsong Li^{1*}

¹ Department of Spine Surgery, The Third Xiangya Hospital, Central South University, Changsha, China, ² Department of Neurology, Xiangya Hospital, Central South University, Changsha, China

OPEN ACCESS

Edited by:

Jaimo Ahn,
University of Michigan, United States

Reviewed by:

Konstantinos Markatos,
Salamina Medical Center, Greece
Ajoyshetty Shetty,
Ganga Hospital, India
Takeo Furuya,
Chiba University, Japan

*Correspondence:

Jinsong Li
Jinsongli@csu.edu.cn

Specialty section:

This article was submitted to
Orthopedic Surgery,
a section of the journal
Frontiers in Surgery

Received: 04 January 2021

Accepted: 26 January 2022

Published: 10 March 2022

Citation:

Ding Z, Ren Y, Cao H, Li Y, Chen S,
Miao J and Li J (2022) An Innovative
Prone Position Using a Body-Shape
Plaster Bed and Skull Traction for
Posterior Cervical Spine Fracture
Surgeries. *Front. Surg.* 9:649421.
doi: 10.3389/fsurg.2022.649421

Background: An innovative prone cervical spine surgical position using a body-shape plaster bed with skull traction (BSPST) was compared with the traditional prone surgical position with horseshoe headrests.

Methods: A total of 47 patients, undergoing posterior cervical spine surgery for cervical spine fracture, were retrospectively classified into two groups, the BSPST group ($n = 24$) and the traditional group ($n = 23$), and underwent a posterior instrumented fusion with or without decompression. Multiple indicators were used to evaluate the advantages of the BSPST compared with the traditional position.

Results: All the operations went smoothly. The mean recovery rate was 56.30% in the BSPST group and 48.55% in the traditional group ($p = 0.454$), with no significant difference. The intraoperative blood loss (177.5 ml vs. 439.1 ml, $p = 0.003$) and the total incidence of complications (8.3 vs. 47.8%, $p = 0.004$) were significantly less in the BSPST group than in the traditional group. In addition, the BSPST position provided a greater comfort level for the operators and allowed convenient intraoperative radiography.

Conclusions: This is the first study to describe a combined body-shape plaster bed and skull traction as an innovative cervical spine-prone surgical position that is simple, safe, and stable, intraoperative traction direction adjustable, reproducible, and economical for posterior cervical spine fracture surgery, and potentially other cervical and upper dorsal spine surgeries in the prone position. Additionally, this position provides the surgeons with a comfortable surgical field and can be easily achieved in most orthopedic operation rooms.

Keywords: innovative prone position, cervical spine surgery, body-shape plaster bed, skull traction, posterior approach

INTRODUCTION

The prone position is widely used globally for posterior cervical and dorsal spine surgeries (1). To date, the traditional posterior approach to the surgical stabilization of the head and the cervical spine is usually achieved by the horseshoe headrest (2). This system, however, has many shortcomings, such as being unavailable and unstable

for position adjustment during surgery. Additionally, inappropriate pressure from the horseshoe headrest over the eyeballs and facial skin may cause damage to patients, especially during long-duration cervical spine surgery in the prone position (3–5).

According to our experience, a good patient surgical position is essential for smooth surgery and should be safe, stable, and adjustable during surgery to reduce postoperative complications. The authors present a modification of the prone surgical position for posterior cervical spine surgeries using a cervical tong for skull traction and a body-shape plaster bed for fixing the patients' bodies. We named this innovative prone surgical position the "body-shape plaster bed with skull traction" (BSPST). This innovative system using a body-shape plaster bed avoids a localized pressure associated with the horseshoe headrest and allows free access to anesthetists for better endotracheal tube management. Additionally, the body-shape plaster bed and skull traction support a reliable stable fixation at any time during surgery and can also be available for intraoperative position adjustment and radiography.

Based on our previous experiences in posterior cervical and dorsal spine surgeries, we used the BSPST position for 24 patients with unstable cervical spines; i.e., traumatic cervical cord injury caused by cervical spine fracture, undergoing surgical treatment in the prone position. There have been no previous reports of the combination of a body-shape plaster bed and cervical tong used in cervical spine surgery. To evaluate the effectiveness and safety of the BSPST position in posterior cervical spine surgeries, comparisons in perioperative events including positioning time, surgical time, intraoperative blood loss, complications, neurological improvement, and comfort of surgeons between cases using the BSPST position and traditional prone surgical position were performed.

MATERIALS AND METHODS

Patient Population

A total of 205 patients, who underwent prone position cervical spine surgery from June 2017 to February 2018 in our institute, were included and were retrospectively reviewed. All procedures performed in the studies involving human participants were in accordance with the ethical standards of the institutional and national research committee (The IRB of the Third Xiangya Hospital, Central South University. Reference number: No. 2019-S036) and with the 1964 Helsinki declaration and its later amendments or comparable ethical standards. All the participants and any identifiable individuals consented to the publication of his/her images. After excluding cases with the degenerative cervical syndrome ($n = 62$), degenerative cervical spinal stenosis ($n = 20$), ossification of the cervical spine yellow ligament ($n = 9$), ossification of the cervical spine posterior longitudinal ligament ($n = 33$), intraspinal occupying lesion of the cervical spine ($n = 26$), and other cervical spine diseases ($n = 7$), a total of 47 patients with cervical spine fracture were included and divided into a BSPST group (using the BSPST position, $n = 24$) and a traditional position group (using horseshoe headrest position, $n = 23$) as shown in **Table 1**. None of the

TABLE 1 | General preoperative information in two groups.

	Traditional position ($n = 23$)	BSPST position ($n = 24$)	<i>p</i> value
Age (year)	52.09 \pm 12.76	52.67 \pm 15.89	0.891
Gender (M\F)	21\2	20\4	0.413
Diabetes (n)	3	5	0.478
Hypertension (n)	4	4	0.947
BMI	23.22 \pm 4.30	23.30 \pm 4.05	0.949
Surgery levels of cervical spine of patients			0.885
2 levels	3	5	
3 levels	8	6	
4 levels	7	9	
5 levels	4	3	
6 levels	1	1	

included patients had other diseases related to the cervical spine fracture, and coagulation function test results were normal for every patient. All patients received regular outpatient visits or telephone follow-up every 3 months, and the final follow-up was defined as the 12-months postoperative follow-up. Informed consent was obtained from all individual participants included in the study.

The Body-Shape Plaster Bed

Six different sizes (XS, S, M, L, XL, and XXL) of the body-shape plaster bed was made by our doctors and can be used repeatedly. We used the bandage and cotton pad to cover the body-shape plaster bed surface every time before surgery so that the bed can keep clean. Doctors must choose the most suitable body-shape plaster bed for each patient before surgery. According to our experience, the distance between the patients' forehead and lower jaw must match the diameter of the plaster bed head-ring, while the total length and width of the plaster bed have no strict requirements because of the use of soft cotton pad and surgical drapes.

The Innovative BSPST Position

All surgeries were performed by a senior surgeon with the same standard. The patients were placed in the supine position after general anesthesia on a surgical transfer trolley, and after the body-shape plaster bed was buckled onto the patient's head and chest (see **Supplementary File 1**), the whole body and the body-shape plaster bed were turned over together and placed in the prone position; then, an anesthesia tube was attached and a surgical drape or bandage was used to bind the patient, body-shape plaster bed, and operation table together to ensure stability (see **Supplementary File 2**). The skull traction was assembled in the appropriate direction and placed on a conventional operating table (here an Alphastar bed, MAQUET GmbH & Co. KG, Sweden) as shown in **Figures 1, 2**. Subsequently, surgeons and assistants can adjust the posture of the cervical spine and head by putting a soft cotton pad between the patient's shoulder and the body-shape plaster bed before surgery. Together, the

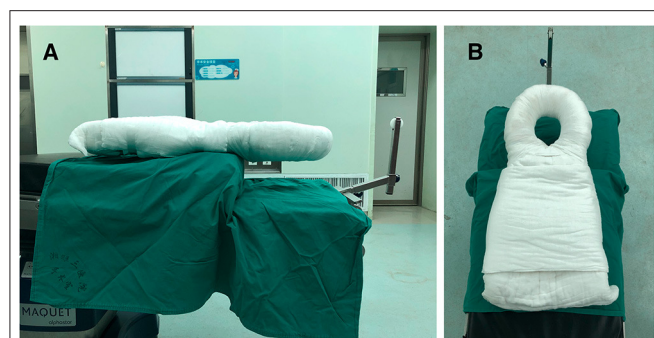


FIGURE 1 | The assembly of traction system set on a conventional operating table and the body-shape plaster bed as seen from different positions (A,B). The body-shape plaster bed with skull traction (BSPST) position system can provide enough space for managing anesthesia tube.

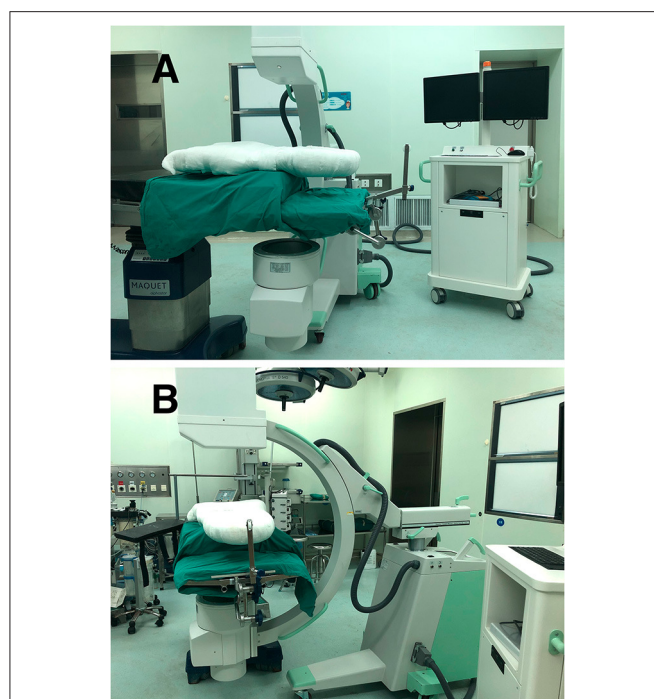


FIGURE 2 | The BSPST system and C-arm digital radiography machine from different positions (A,B), which can make anterior-posterior interoperative radiography available.

body-shape plaster bed and traction system provide stability to the patient during the adjustment of the operating table and can provide enough space for intraoperative anesthesia tube management (Figure 3 and Supplementary Files 2, 3). Additionally, this system allows the intraoperative adjustment of the traction direction and weight by the traction system. At the end of the surgery, the patient was turned supine, and the tong was removed (see Supplementary File 4). The pin sites were dressed with band-aids.

The Limit of Usage

Patients with severe cervical and thoracic kyphosis.

Data Statistics and Clinical Assessments

All the patients underwent radiologic examinations, including CT and MRI of the cervical spine before surgery. The modified Japanese Orthopedic Association (JOA) scores were used to assess neurological function, and the neurological recovery rate was calculated as $\text{rate} = (\text{final JOA} - \text{preoperative JOA}) / (11 - \text{preoperative JOA}) \times 100\%$. The neurological recovery rate of 75–100% was designated as excellent; 50–74%, good; 25–49%, fair; and <25%, poor. According to our experience in cervical spine surgeries and cervical spine anatomy, we described an assessment of intraoperative surgeon comfort. The angle between the C7 spinous process-external occipital protuberance line and the horizontal line (C7SP-EOP angle) was categorized into four levels from -5° to 15° (Figure 4). Level 4 was defined as the most comfortable position for surgeons with a C7SP-EOP angle between 10° and 15° , while Level 1 was defined as a difficult process to finish the surgery for surgeons with a C7SP-EOP angle between -5° and 0° . Intraoperative blood loss, operation time, and positioning time (the time required after induction of anesthesia until positioning the patient prone on the operating table), perioperative complications, C7SP-EOP angle, and possibility for intraoperative radiography were recorded and compared between the two groups.

Statistical Analysis

All the data were analyzed by PASW Statistics 18.0 (SPSS Inc., Chicago, IL, USA). Intragroup or intergroup comparisons were performed by independent samples *t*-test or Pearson's χ^2 test, and data were presented as means and SD unless otherwise indicated. $P < 0.01$ were defined as statistically significant.

RESULTS

The differences in general preoperative information between the two groups were not significant, as shown in Table 1. A total of 169 segments (traditional position group, $n = 84$; BSPST group, $n = 85$) were involved. The distribution of the surgical levels was not significantly different between the two groups ($p = 0.885$).

As shown in Table 2, the intraoperative blood loss in the BSPST group was significantly less than that in the traditional position group (177.5 ml vs. 439.1 ml, $p = 0.003$), while the operation time (3.755 h vs. 4.400 h, $p = 0.144$) and position time (16.25 min vs. 15.96 min, $p = 0.184$) have no significant differences. Although the mean JOA scores in the BSPST group and traditional position group significantly increased at the final follow-up, differences in the preoperative JOA score (7.875 vs. 7.913, $p = 0.979$), 6-months follow-up JOA score (12.46 vs. 11.09, $p = 0.353$), final JOA score (12.46 vs. 11.09, $p = 0.353$), and neurological recovery rate (56.30 vs. 48.55%, $p = 0.454$) were not significant. There were six patients in the traditional position group, but no patients in the BSPST group, who experienced facial skin necrosis ($p = 0.007$), and these patients completely recovered after a consultation in the department of dermatology with regular dressing changes for 1 week. Only two cases in

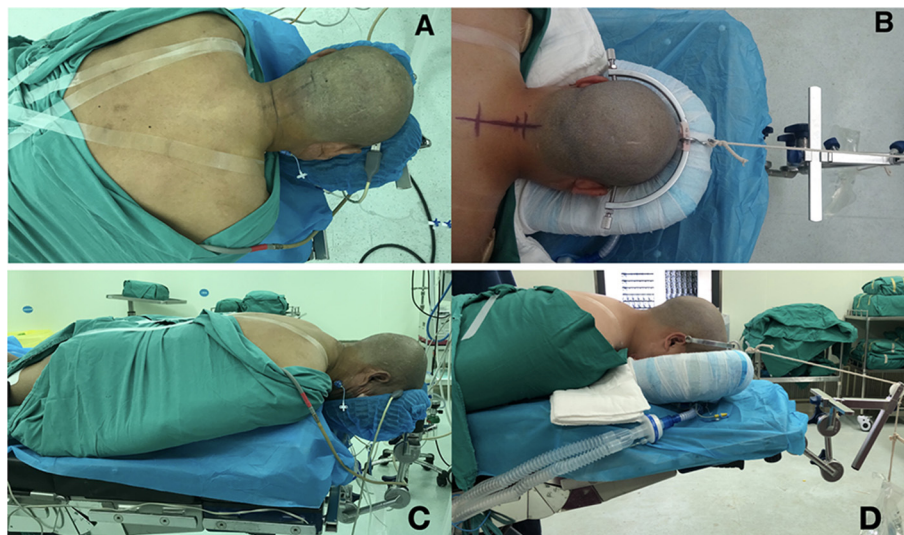


FIGURE 3 | The patients undergoing surgical treatment in the prone position. The patients in the traditional position with a horseshoe headrest (A,C) and in the BSPST position with a cervical tong for skull traction and body-shape plaster bed for fixation (B,D) as seen from a vertical and horizontal angle. The BSPST position can provide enough space for managing the anesthesia tube and reliable intraoperative steadiness with the usage of body-shape plaster bed and skull traction.

the traditional position group received conjunctival and corneal abrasions but recovered without treatment within several days ($p = 0.140$). The leakage of cerebrospinal fluid occurred with one patient in the traditional position group, but no patient in the BSPST group, and this patient experienced an incision healing without infection ($p = 0.302$). Both groups had one patient with C5 palsy after the operation that healed on its own ($p = 0.976$). The traditional position group had one patient with wound infection ($p = 0.302$), and this patient was completely healed after regular dressing changes and the use of intravenous antibiotics within one postoperative week. There was only one patient with a cervical tong pin site complication in the BSPST position group ($p = 0.322$). The patient was bleeding under galea aponeurotica because of the use of low molecular weight heparin in the intensive care unit, and the blood was gradually absorbed after stopping the use of low molecular weight heparin. The total incidence of perioperative complications in the BSPST group was significantly less than that in the traditional position group ($p = 0.004$).

There were 20 patients in the BSPST position group but only one patient in the traditional position group who were assessed at level 4 or level 3 in the evaluation system for the degree of comfort of the surgeon during the operation as shown in **Table 3** ($p < 0.01$). The BSPST position allowed for both anterior-posterior and lateral intraoperative radiography, while the traditional position did not allow them ($p < 0.01$).

DISCUSSION

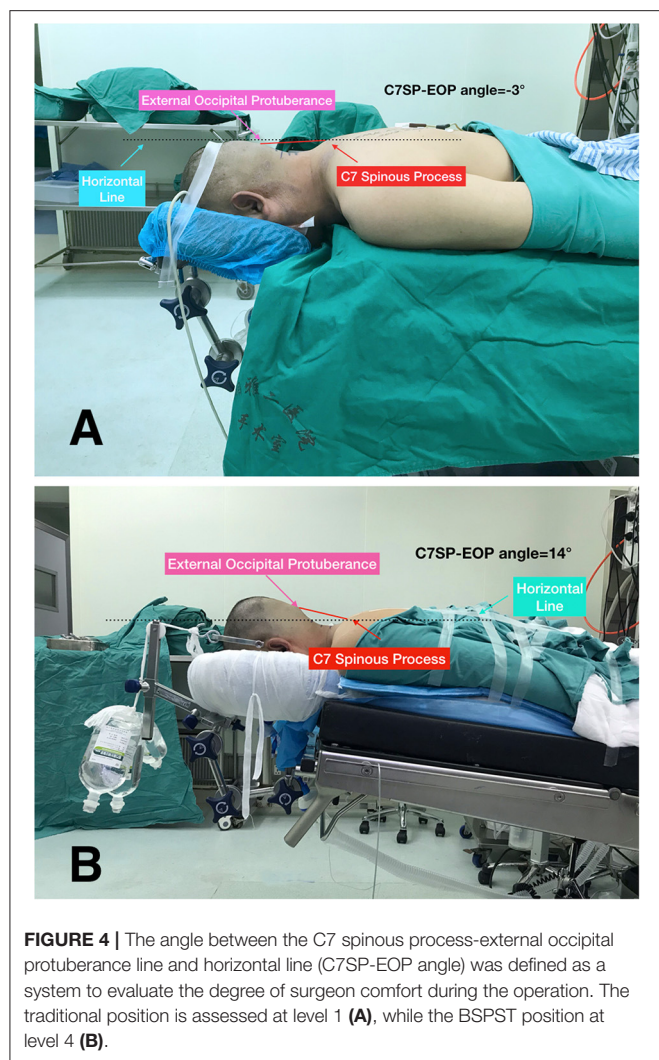
According to lots of research, many complications have been reported due to the disadvantages of the traditional posterior approach position, such as postoperative visual loss (POVL), skin necrosis, venous air embolism, etc. (3, 6). These complications

may have serious consequences to the patients, but researchers have only sporadically attempted to modify the traditional prone surgical position.

Improper pressure over the eyeballs and facial skin for a long time is a common cause of visual loss and skin necrosis. Several studies have discussed a postoperative vision loss due to the prone position (3). They conclude that the inappropriate pressure from the horseshoe headrest led to direct pressure over the eyeball, which may cause intraocular pressure and visual loss (7, 8). In addition, there have been many documented cases of facial pressure sores and ischemic orbital compartments related to the prone position and horseshoe headrest (3). It has been reported that the long-term localized pressure on the face in the prone position is, on average, below 30 mmHg, but can be higher than 50 mmHg in certain areas, such as the chin and forehead above the supraorbital ridge, which may cause facial edema and pressure sores (9–11).

According to our experience, surgeons may need intraoperative readjustment of patients' positions for a better surgical field. The traditional prone position has no fixation of the patients' head, body, and operating table, so it is impossible to ensure the stability of patients when adjusting the operating table and the traction direction during the operation, which may lead to a respiratory passage compression and asphyxia. Additionally, Kadam et al. (2) proposed a modified prone position for posterior cervical spine surgeries using a cervical tong for traction and two lateral brace attachments on an operating table, which can avoid a localized pressure over the eyeballs and the face skin associated with the horseshoe headrest. However, this modified prone position has the inability to intraoperatively readjust the position and tilt the table beyond 30° to either side.

Immobilization by a cervical collar to protect the patient from secondary damage is a standard procedure in patients



with cervical spine trauma (12, 13). However, more studies have pointed out that applying a cervical collar, in general, will cause an immense three-dimensional movement, and extrication collars can result in abnormal movement within the upper cervical spine in the presence of a severe injury (14–16). We believe that an absolute restriction of the cervical spine cannot be only achieved by the cervical collar during preoperative positioning and may cause secondary dislocation in those with spinal cord injury, especially in the presence of a dissociative injury (17).

The BSPST position can protect the facial skin and the eyes from skin necrosis and ocular complications with the use of protective macromolecular material. The body-shape plaster bed can decrease the vertical direct pressure by distributing the pressure equally across the facial skin, while the round head holder has no direct contact with the patients' eyes. In our analysis of the traditional and BSPST positions, we identified 10 patients (47.8%) with postoperative complications in the traditional position group and three patients (8.3%) with postoperative complications in the BSPST group ($p =$

0.004). This result showed that the incidence of postoperative complications was relatively high when cervical spine surgery incorporated a traditional prone surgical position compared with the BSPST prone surgical position.

As for the adjustment of the surgical position, the BSPST position can maintain a stable position even when the table exceeds 35° to either side. Additionally, the traction direction can be intraoperatively adjusted to expose the operation fields for obese and short-neck patients. This method also allows the patients to be stably positioned in the reverse Trendelenburg's position because the traction can balance with part of the patients' own gravity (see **Supplementary File 3**), which can reduce venous congestion and bleeding, as well as reduce orbital pressure to diminish the occurrence of postoperative vision loss (6, 18). It was obvious in our research that only one patient in the traditional position group, but 20 patients in the BSPST group, provided the surgeon the comfort levels of 1 and 2 ($p < 0.01$), and intraoperative blood loss in the BSPST position group was significantly less than that in the traditional position group ($p = 0.003$). Since the plaster bed extends to the abdominal region, we think that the part of the plaster bed in contact with the abdomen may compress the soft tissues and increase the abdominal pressure; to avoid this situation, we put cotton and soft gel pads around the contact part to reduce the direct pressure on the abdomen. All these results indicated that the BSPST position may provide the surgeons with a more comfortable surgical position and reduce intraoperative blood loss.

To maintain safety during the preoperative positioning, the surgeon and assistants can create a situation in which the patient and body-shape plaster bed stay together so that the patients' head, whole cervical spine, and body can turn around at the same time by using the body-shape plaster bed. The BSPST position also facilitated an easy access to the anesthesia tube, which could be removed from either side below the body-shape plaster bed (**Figures 1, 2 and Supplementary File 2**).

Intraoperative radiography is necessary for spine surgery, especially cervical spine surgery, and it can help surgeons conform to surgical segments and guide, as well as conform to pedicle screw placement (19). However, the anterior-posterior interoperative radiography is unavailable in the traditional position because of the material of the headrest, which may create difficulties for the surgeons (**Figures 2, 5**). Although carbon fiber headrest is a good choice, most hospitals and patients in developing countries cannot afford it. The BSPST position system is X-ray penetrable, easy to assemble and inexpensive, and can be acceptable for patients in many hospitals in developing countries compared with other innovations of prone position for cervical spine surgeries (20–22).

For patients with obesity, the soft tissues of the cervicothoracic transition can cause wrinkling of the cervical skin incision. To solve this problem, we put a soft cotton pad between the shoulder and the plaster bed to slightly change the kyphosis of the cervical spine. We also use a shoulder strap or tape to pull the fat tissue to the tail end at the same time, and the skinfold can be solved when fixed with the head.

The positioning time was 16.250 ± 6.835 min in the BSPST group and 15.960 ± 6.832 min in the traditional group, which

TABLE 2 | Comparisons in outcomes and complications between two groups.

	Traditional position (n = 23)	BSPST position (n = 24)	p value
Operation time (h)	4.400 ± 1.752	3.755 ± 1.136	0.144
Positioning time (min)	15.960 ± 6.832	16.250 ± 6.835	0.184
Intraoperative blood loss (ml)	439.1 ± 369.0	177.5 ± 105.2	0.003*
JOA score			
Before surgery	7.913 ± 5.017	7.875 ± 4.675	0.979
6-months follow-up	9.736 ± 5.268	11.040 ± 4.506	0.366
12-months follow-up	11.090 ± 5.468	12.460 ± 4.520	0.353
Neurological recovery rate (%)	48.550 ± 35.770	56.300 ± 34.690	0.454
Grading of neurological recovery rate (n)			
Excellent	7	9	0.176
Good	2	7	
Fair	7	3	
Poor	7	5	
Complication, number of patients			
Face skin necrosis	6	0	0.007#
Conjunctival and corneal abrasions	2	0	0.140
POVL	0	0	—
Injury to spinal cord (Leakage of CSF)	1	0	0.302
C5 palsy	1	1	0.976
Wound infection	1	0	0.302
Cervical tong pin sites complications	0	1	0.322
Difficult access to anesthesia tubes	0	0	—
Total incidence of complications (%)	47.8	8.3	0.004§

JOA, Japanese Orthopedic Association.

*Statistically different from the intraoperative blood loss ($p < 0.01$).

#Statistically different from the face skin necrosis cases ($p < 0.01$).

§Statistically different from the total incidence of complications ($p < 0.01$).

TABLE 3 | C7SP-EOP angle (comfort level for surgeons) and intro-op radiography.

	Traditional position (n = 23)	BSPST position (n = 24)	p value
Comfort level for surgeons			0*
Level 4	0	15	
Level 3	1	5	
Level 2	10	4	
Level 1	12	0	
Intro-op radiography			0#
A-p (unable\able)	23\0	0\24	
Lateral (unable\able)	0\23	0\24	—

*Statistically different from the comfort level of surgeons ($p < 0.01$).

#Statistically different from the anterior-posterior intro-operation radiography ($p < 0.01$).

were not significantly different ($p = 0.144$). Although cervical tong application may appear to require additional time, it is a relatively quick procedure, and the time consumed is well-compensated by the reduced time required to reduce skin necrosis and ocular complications. In addition, the BSPST position can be used not only in cervical spine fracture surgeries but also in other posterior cervical spine surgeries.

In this research and our clinical work, the BSPST position and traditional position almost have the same effect in prone cervical spine decompression and fixation surgeries to treat cervical spine fracture. However, the body-shape plaster bed may provide a better choice to some hospitals in developing countries because of the lower prices.

All techniques have downsides, and there are still several limitations of this study and of the BSPST position. First, retrospective results from a single-center should be prospectively verified by multicenter and randomized controlled studies. Second, the patient sample was relatively small, and the follow-up was relatively short in this study. Besides, this position is not available for patients with advanced deformity, and has some disadvantages that are directly related to the prone position. In addition, the measurement of the C7SP-EOP angle may show significant deviations in patients with obesity due to the thick fat tissue around the neck and back. Finally, further studies are required to conclusively establish the efficacy and the safety of the BSPST position to put it into use and improve upon it.

CONCLUSION

This is the first study to describe a combined body-shape plaster bed and skull traction as an innovative prone surgical

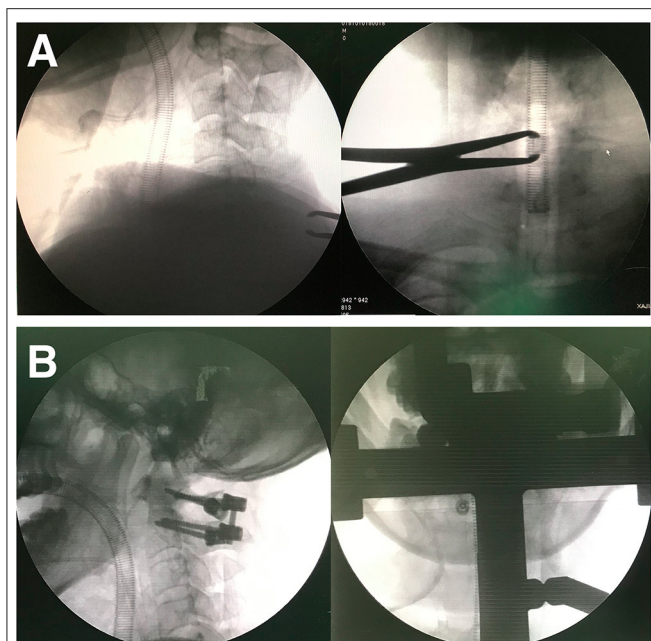


FIGURE 5 | Anterior-posterior intra-operation radiography is available in BSPST position benefit from X-ray penetrable characteristics of plaster (A,B).

position that has characteristics of simple construction, safe and stable, intraoperative traction direction adjustable, reproducible, and economical for posterior cervical spine fracture surgery and potentially other cervical and upper dorsal spine surgeries in the prone position. Additionally, this position can be easily achieved in most operating rooms and provides a comfortable surgical field for surgeons. However, further studies are required to conclusively establish the efficacy and safety of this innovative method.

DATA AVAILABILITY STATEMENT

The raw data supporting the conclusions of this article will be made available by the authors, without undue reservation.

ETHICS STATEMENT

The studies involving human participants were reviewed and approved by the IRB of the Third Xiangya Hospital, Central South University. The patients/participants provided their written informed consent to participate in this study.

REFERENCES

- Schonauer C, Bocchetti A, Barbagallo G, Albanese V, Moraci A. Positioning on surgical table. *Eur Spine J.* (2004) 13:S50. doi: 10.1007/s00586-004-0728-y
- Kadam AB, Jaipuria AS, Rathod AK. Modified prone position using lateral brace attachments for cervico-dorsal spine surgeries. *Eur Spine J.* (2013) 22:1474–9. doi: 10.1007/s00586-012-2653-9

AUTHOR CONTRIBUTIONS

Material preparation was performed by ZD and YR, data collection and analysis were performed by HC, YL, JM, and SC. The first draft of the manuscript was written by ZD and JL and all the authors commented on previous versions of the manuscript. All the authors read, approved the final manuscript, and contributed to the study's conception and design.

FUNDING

This study was partially supported by the National Natural Science Foundation of China (Grant Nos. 81502331 and 81772866) and the Natural Science Foundation of Hunan Province (Grant Nos. 2016JJ3176, 2018JJ2602, and 2018JJ2617). The study supporters played no role in the study design, collection, analysis, and interpretation of data, in the writing of the manuscript, and in the decision to submit the manuscript for publication.

ACKNOWLEDGMENTS

We thank Dr. Qingming Peng, Dr. Haoming Feng, and Dr. Dongbiao Liu who helped make the simulated videos as the additional files, and Dr. Song Wu for his expertise in spine surgery.

SUPPLEMENTARY MATERIAL

The Supplementary Material for this article can be found online at: <https://www.frontiersin.org/articles/10.3389/fsurg.2022.649421/full#supplementary-material>

Supplementary File 1 | The model was placed in the supine position after “general anesthesia” on a surgical transfer trolley, and the body-shape plaster bed was buckled onto the model's head and chest (This is an illustrative video, and not an actual patient).

Supplementary File 2 | The model's whole body and the body-shape plaster bed were turned over together by the surgeon and the assistants and placed in the prone position; then, an anesthesia tube was attached. The head, whole cervical spine, and body can turn around at the same time with the use of the body-shape plaster bed (This is an illustrative video and not an actual patient).

Supplementary File 3 | The body-shape plaster bed and skull traction support a reliable stable fixation at any time during surgery, even in reverse Trendelenburg position (This is an illustrative video and not an actual patient). The C7SP-EOP angle is 11.3° in the BSPST position during the surgery which provides the most comfortable position for surgeons (Practical surgery).

Supplementary File 4 | At the end of the surgery, the model and the body-shape plaster bed were turned supine, the tong and body-shape plaster bed were removed (This is an illustrative video and not an actual patient).

- Kwee MM, Ho YH, Rozen WM. The prone position during surgery and its complications: a systematic review and evidence-based guidelines. *Int Surg.* (2015) 100:292–303. doi: 10.9738/INTSURG-D-13-00256.1
- Jain V, Bithal P, Rath G. Pressure sore on malar prominences by horseshoe headrest in prone position. *Anaesth Intensive Care.* (2007) 35:304–6.
- Bekar A, K Türeyen, K Aksoy. Unilateral blindness due to patient positioning during cervical syringomyelia surgery: unilateral blindness

- after prone position. *J Neurosurg Anesthesiol.* (1996) 8:227–9. doi: 10.1097/00008506-199607000-00007
6. Stambough JL, Dolan D, Werner R, Godfrey E. Ophthalmologic complications associated with prone positioning in spine surgery. *J Am Acad Orthop Surg.* (2007) 15:156–65. doi: 10.5435/00124635-200703000-00005
 7. Slocum H, O'neal K, Allen C. Neurovascular complications from malposition on the operating table. *Surg Gynecol Obstet.* (1948) 86:729–34.
 8. Kasodekar V, Chen J. Monocular blindness: a complication of intraoperative positioning in posterior cervical spine surgery. *Singapore Med J.* (2006) 47:631–3.
 9. Leibovitch I, Casson R, Laforest C, Selva D. Ischemic orbital compartment syndrome as a complication of spinal surgery in the prone position. *Ophthalmology.* (2006) 113:105–8. doi: 10.1016/j.ophtha.2005.09.025
 10. Atwater BI, Wahrenbrock E, Benumof JL, Mazzei WJ. Pressure on the face while in the prone position: proneview™ versus prone positioner™. *J Clin Anesth.* (2004) 16:111–6. doi: 10.1016/j.jclinane.2003.06.001
 11. Shamshery C, Haldar R, Srivastava A, Kaushal A, Srivastava S, Singh PK. An unusual cause of unilateral facial injuries caused by horseshoe headrest during prone positional craniocervical junction surgery. *J Craniocervical Junction Spine.* (2016) 7:62–4. doi: 10.4103/0974-8237.176629
 12. ATLS Subcommittee, Tchorz KM, I.A.W Group. Advanced trauma life support (ATLS®): the ninth edition. *J Trauma Acute Care Surg.* (2013) 74:1363. doi: 10.1097/TA.0b013e31828b82f5
 13. Walters BC, Hadley MN, Hurlbert RJ, Aarabi B, Dhall SS, Gelb DE, et al. Guidelines for the management of acute cervical spine and spinal cord injuries: 2013 update. *Neurosurgery.* (2013) 60:82–91. doi: 10.1227/01.neu.0000430319.32247.7f
 14. Ben-Galim P, Dreianel N, Mattox KL, Reitman CA, Kalantar SB, Hipp JA. Extrication collars can result in abnormal separation between vertebrae in the presence of a dissociative injury. *J Trauma Acute Care Surg.* (2010) 69:447–50. doi: 10.1097/TA.0b013e3181be785a
 15. Liao S, Schneider NR, Hüttlin P, Grützner PA, Weilbacher F, Matschke S, et al. Motion and dural sac compression in the upper cervical spine during the application of a cervical collar in case of unstable craniocervical junction—a study in two new cadaveric trauma models. *PLoS ONE.* (2018) 13:e0195215. doi: 10.1371/journal.pone.0195215
 16. Prasarn ML, Conrad B, Del Rossi G, Horodyski M, Rehtine GR. Motion generated in the unstable cervical spine during the application and removal of cervical immobilization collars. *J Trauma Acute Care Surg.* (2012) 72:1609–13. doi: 10.1097/TA.0b013e3182471d9f
 17. Horodyski M, DiPaola CP, Conrad BP, Rehtine GR II. Cervical collars are insufficient for immobilizing an unstable cervical spine injury. *J Emerg Med.* (2011) 41:513–9. doi: 10.1016/j.jemermed.2011.02.001
 18. Carey TW, Shaw KA, Weber ML, DeVine JG. Effect of the degree of reverse Trendelenburg position on intraocular pressure during prone spine surgery: a randomized controlled trial. *Spine J.* (2014) 14:2118–26. doi: 10.1016/j.spinee.2013.12.025
 19. Abumi K, Shono Y, Ito M, Taneichi H, Kotani Y, Kaneda K. Complications of pedicle screw fixation in reconstructive surgery of the cervical spine. *Spine.* (2000) 25:962–9. doi: 10.1097/00007632-200004150-00011
 20. Moon AS, Cignetti CA, Isbell JA, Weng C, Manoharan SRR. Traumatic hyperextension-distraction injuries of the thoracolumbar spine: a technical note on surgical positioning. *Eur Spine J.* (2019) 28:1113–20. doi: 10.1007/s00586-019-05917-2
 21. Kolb B, Large J, Watson S, Smurthwaite G. An innovative prone positioning system for advanced deformity and frailty in complex spine surgery. *J Neurosurg Spine.* (2019) 32:229–34. doi: 10.3171/2019.7.SPINE19161
 22. Gupta N. A modification of the Mayfield horseshoe headrest allowing pin fixation and cranial immobilization in infants and young children. *Oper Neurosurg.* (2006) 58:ONS-E181–ONS-E181. doi: 10.1227/01.NEU.0000193929.11266.87

Conflict of Interest: The authors declare that the research was conducted in the absence of any commercial or financial relationships that could be construed as a potential conflict of interest.

Publisher's Note: All claims expressed in this article are solely those of the authors and do not necessarily represent those of their affiliated organizations, or those of the publisher, the editors and the reviewers. Any product that may be evaluated in this article, or claim that may be made by its manufacturer, is not guaranteed or endorsed by the publisher.

Copyright © 2022 Ding, Ren, Cao, Li, Chen, Miao and Li. This is an open-access article distributed under the terms of the Creative Commons Attribution License (CC BY). The use, distribution or reproduction in other forums is permitted, provided the original author(s) and the copyright owner(s) are credited and that the original publication in this journal is cited, in accordance with accepted academic practice. No use, distribution or reproduction is permitted which does not comply with these terms.

Frontiers in Surgery

Explores and improves surgical practice and clinical patient management

A multidisciplinary journal which explores surgical practices - from fundamental principles to advances in microsurgery and minimally invasive techniques. It fosters innovation and improves the clinical management of patients.

Discover the latest Research Topics

[See more →](#)

Frontiers

Avenue du Tribunal-Fédéral 34
1005 Lausanne, Switzerland
frontiersin.org

Contact us

+41 (0)21 510 17 00
frontiersin.org/about/contact



Frontiers in Surgery

